REGULATION AND DYMANIC BEHAVIOR OF THE HEAT SHOCK TRANSCRIPTION FACTOR HSF-1 IN *C. ELEGANS*

Elizabeth A. Morton

A DISSERTATION

in

Cell and Molecular Biology

Presented to the Faculties of the University of Pennsylvania

in

Partial Fulfillment of the Requirements for the

Degree of Doctor of Philosophy

2013

Supervisor of Dissertation

_____

S. Todd Lamitina, PhD, Assistant Professor of Physiology

Graduate Group Chairperson

_____

Daniel S. Kessler, PhD, Associate Professor of Cell and Developmental Biology

Dissertation Committee

Morris J. Birnbaum, MD, PhD, Professor of Medicine

Nancy M. Bonini, PhD, Professor of Neuroscience

David M. Raizen, MD, PhD, Assistant Professor of Neurology

John I. Murray, PhD, Assistant Professor of Genetics

DEDICATION

This work is dedicated to my parents.

ACKNOWLEDGMENTS

I would first like to thank my thesis advisor, Todd Lamitina. He always made it easy to discuss problems and ideas (as evidenced by the many, many hours we have spent in conversation about my project). Under his guidance, I have learned not only how to design experiments and think about research, but also how to be critical and persistent (especially when things are not going well). I would also like to thank my undergraduate research advisor, Scott Samuels, for first introducing me to the world of molecular biology.

I would like to give special thanks to the current and former members of the Lamitina lab, whose friendship was instrumental in seeing me through graduate school. Thank you to: Predrag, for sharing all of his hard-earned wisdom; Lorenza, for encouraging me to explore the world; Jen, for her efforts cheering me up; Rosemary, for being naturally so cheerful; Liping, for her kindness and empathy; Jess, for always encouraging rebellion; and Tim, for being naturally not so cheerful, but always the most fun to talk to. I also thank former lab members Anne-Katrin and Yana, for their technical support and instruction when I was a young grad student. Everyone in the lab has taught me something, and I could not have succeeded without their encouragement, advice, and companionship.

I need to thank Bob Kalb, David Raizen, and John Murray for being so generous with their time and advice. My committee members – David, John, Morrie Birnbaum and Nancy Bonini, as well as former member Aaron Gitler – have been invaluable in focusing and refining my project. The entire worm community at Penn has been from

the beginning a source of valuable feedback and suggestions. I especially thank Vinnie Mancuso, Ishmail Abdus-Saboor, Kelly Howell, Ria Lim, and Jean Parry for their individual help and support. I would also like to acknowledge the kind aid of the Khurana, Raizen, Sundaram, Murray, and Kalb labs, all of whom have been generous in the lending of materials and reagents.

Lastly, and most importantly, I would like to thank my family: my parents, brother and sister. I would have never gotten this far without their love and encouragement.

ABSTRACT

REGULATION AND DYMANIC BEHAVIOR OF THE HEAT SHOCK TRANSCRIPTION FACTOR HSF-1 IN *C. ELEGANS*

Elizabeth A. Morton

S. Todd Lamitina, PhD

Eukaryotic cells respond to heat stress by activating the transcription factor HSF1. In addition to its role in stress response, HSF1 also functions in protein homeostasis, aging, innate immunity, and cancer. Despite prominent HSF1 involvement in processes pertinent to human health and disease, there are still gaps in our understanding of HSF1. For example, controversy exists regarding the localization of HSF1, the identity of HSF1 regulators, and the function and conservation of heat-induced HSF1 stress granules. Many of the physiological roles for HSF1 have been defined using the model organism *Caenorhabditis elegans*, yet little is known about how the molecular and biological properties of HSF-1 in *C. elegans* compare to HSF1 in other organisms, including humans. To address these questions, we generated animals expressing physiological levels of a GFP-tagged *C. elegans* HSF-1 protein. We studied the localization of HSF-1::GFP *in vivo* and observed its behavior upon heat shock in *C. elegans*. Furthermore, we conducted a genome-wide, RNAi-based screen for regulators of an HSF-1-dependent, heat shock-inducible transcriptional reporter. We found that in live *C. elegans*, HSF-1 localizes predominantly to the nucleus before and after heat shock. Following heat shock, HSF-1 redistributes into subnuclear puncta that share many characteristics with human nuclear stress granules, including rapid formation, reversibility, and colocalization with markers of active transcription. Granule formation in worms was affected by

growth temperature, implying physiological regulation of this process. From our RNAi screen, we identified 44 regulators of HSF-1 target gene expression, the majority of which were positive regulators. One RNAi clone, encoding the worm homolog of the post-translational modifier SUMO, resulted in hyper-induction of the HSF-1 target after heat shock. Our findings from the screen suggest that basal repression of HSF-1 under low-temperature conditions may be very strict, and that sumoylation may be involved in downregulation of the activated heat stress response pathway. Our data also support a model of constitutively nuclear *C. elegans* HSF-1 and present evidence that HSF-1 nuclear stress granule formation may be an evolutionarily conserved phenomenon.

TABLE OF CONTENTS

LIST OF TABLES

LIST OF FIGURES

1. Introduction

Summary

The heat shock transcription factor HSF1 is highly evolutionarily conserved among eukaryotes, with a several functional domains throughout the protein. In the nearly thirty years since its identification as a major factor involved in the heat shock response, model systems have also revealed roles for HSF1 in development, innate immunity, cancer, and aging. Our understanding of the regulation of this critical transcription factor is yet incomplete. HSF1 clearly has a complex, multi-step activation process involving post-translational modification and inter- and intra-molecular interactions, but many questions about these interactions are unanswered. Properties as straightforward as its localization are still debated, and it likely has many regulators not yet identified. Despite many years of study, we still have much to learn about HSF1.

Discovery of heat shock response

The heat shock response was discovered in *Drosophila* by Ferruccio Ritossa in 1962, when an unintended increase in incubator temperature changed the pattern of nucleic acid puffs in fly salivary glands (De Maio et al., 2012; Ritossa, 1962). In these puffs, Ritossa observed rapid synthesis of new RNA with heat shock (Ritossa, 1996; Ritossa, 1964). The induced genes encoded heat shock proteins (HSPs), of various molecular weights (Lindquist, 1986; Schedl et al., 1978). HSPs were latter linked to protection against stress, and many were determined to be molecular chaperones (Beckmann et al., 1990; Ellis, 1993; Huot et al., 1991; Kang et al., 1990; Parsell and Lindquist, 1993; Pelham, 1986). This reaction to heat stress is now known as the heat shock response. The heat shock-induced upregulation specifically of HSPs is also

accompanied by a global downregulation of general gene expression (McKenzie et al., 1975; Spradling et al., 1977; Tissieres et al., 1974).

Heat shock-induced target genes were found to have a conserved regulatory sequence involving inverted repeats of nucleotides GAA (Amin et al., 1988; Bienz and Pelham, 1982; Mirault et al., 1982; Pelham, 1982; Shuey and Parker, 1986). A protein factor that bound to these upstream elements of heat shock genes and had increased activity with heat shock was eventually identified (Kingston et al., 1987; Parker and Topol, 1984; Wu, 1984a), and heat shock factors (HSFs) were soon cloned from yeast (Sorger and Pelham, 1988), flies (Clos et al., 1990), and human cells (Rabindran et al., 1991).

HSFs

Vertebrates now have four major described HSFs. The primary mammalian HSFs are HSF1, HSF2 and HSF4 (Nakai et al., 1997; Rabindran et al., 1991; Schuetz et al., 1991). The fourth factor, HSF3, was long thought to be avian-specific, but was recently observed in mice and is functionally able to induce some gene expression in HSF1-null embryonic fibroblasts (Fujimoto et al., 2010; Nakai and Morimoto, 1993). HSF1 is the best studied mammalian HSF and activates the heat shock response via inducible trimerization, DNA binding and transactivation (Baler et al., 1993; Sarge et al., 1993). HSF2, the second-best studied, has constitutive DNA binding when transcribed *in vitro* or expressed in *Escherichia coli* (Anckar et al., 2006; Manuel et al., 2002; Sarge et al., 1991) but in some *in vivo* circumstances exhibits inducible DNA binding (Sistonen et al., 1994; Sistonen et al., 1992). HSF2 has primarily been implicated in differentiation and development in mice (Mezger et al., 1994; Murphy et al., 1994; Rallu et al., 1997;

Sistonen et al., 1992), along with being active in adult mouse testes (Sarge et al., 1994). More recently, it has been proposed that HSF2 does have a role during stress, interacting with HSF1 (forming heterotrimers) and binding some *hsp* promoters and repeat DNA (Östling et al., 2007; Sandqvist et al., 2009). HSF4 is important in the mammalian lens, where its absence results in cataract formation (Fujimoto et al., 2004; Somasundaram and Bhat, 2004). Additionally, studies have identified two more potential mammalian HSFs on the X and Y chromosomes (termed HSFX and HSFY), which remain to be fully characterized (Bhowmick et al., 2006; Shinka et al., 2004; Tessari et al., 2004).

While mammals have a handful of HSFs and plants even more (21 HSFs have been cloned from *Arabidopsis,* for instance (Nover et al., 2001)), many invertebrate models have only a single, essential HSF. These include *Drosophila melangaster*, *Saccharomyces cerevisiae*, *Schizaosaccharomyces pombe,* and *Caenorhabditis elegans* (Clos et al., 1990; Gallo et al., 1993; Garigan et al., 2002; Jedlicka et al., 1997; Morton and Lamitina, 2013; Sorger and Pelham, 1988) (Note that an HSF-1 paralog in the *C. elegans* genome, HSF-2, has recently been proposed (Barna et al., 2012)). Fewer HSFs simplifies study in these systems, making them useful tools in the study of HSF function.

HSF1 Domains

DNA binding domain. The DNA binding domain (DBD) of HSF1 is the most highly conserved region of the protein, forming a winged helix-turn-helix structure at the N-terminus (Åkerfelt et al., 2010; Anckar and Sistonen, 2011; Harrison et al., 1994; Vuister et al., 1994). Target promoters contain multiple copies of a DNA motif known as the heat shock element (HSE), which consists of three or more inverted repeats of nGAAn (where "n" is any nucleotide) (Amin et al., 1988; Pelham and Bienz, 1982; Xiao

and Lis, 1988). One DBD contacts one nGAAn (Kim et al., 1994), and the number and arrangement of repeats influences the strength of HSF1 binding (Bonner et al., 1994; Xiao et al., 1991). The "wing" of the DBD is proposed to be involved in protein-protein interactions in the HSF1 trimer (Ahn et al., 2001; Littlefield and Nelson, 1999).

Heat shock induces protein binding to HSEs in humans, *Drosophila*, and *C. elegans* (Chiang et al., 2012; Kingston et al., 1987; Sarge et al., 1993; Sorger et al., 1987; Wu, 1984a, b). In *S. cerevisiae*, HSF is constitutively bound to DNA (Jakobsen and Pelham, 1988; Sorger et al., 1987; Sorger and Pelham, 1988), whereas regulation in *S. pombe* has more similarity to humans and flies, with heat shock-induced DNA binding (Gallo et al., 1991).

Trimerization domain. HSF1 forms trimers in human (Baler et al., 1993; Zuo et al., 1994), mouse (Sarge et al., 1993), *Drosophila* (Westwood et al., 1991; Westwood and Wu, 1993), yeast (Sorger and Nelson, 1989), and *C. elegans* (Chiang et al., 2012). With the exception of constitutively trimerized *S. cerevisiae* HSF, trimerization is induced by heat shock. Trimerization is mediated by a sequence of hydrophobic heptad repeats (HR-A/B), or leucine zipper motifs, that follow the DBD (Peteranderl and Nelson, 1992; Rabindran et al., 1991; Rabindran et al., 1993; Sorger and Nelson, 1989; Zuo et al., 1994). The sequence is proposed to form an α-helix in which hydrophobic residues (like leucine) form a surface that will interact with similar helices, thus promoting intermolecular interaction (Sorger and Nelson, 1989). This domain is capable of inducing DNA binding of a heterologous DNA binding domain that requires dimerization (Zuo et al., 1994).

Regulatory domain. HSF1 contains a regulatory domain, located between the trimerization and transactivation domains, that is not present in HSF2 or HSF3 (Green et al., 1995). In chimeric proteins of HSF-1 and the GAL4 DNA binding domain, the HSF1 activation domain conferred constitutive transcriptional activity, whereas proteins with both the activation and regulatory domains were active only after heat shock (Green et al., 1995). The regulatory domain is rich in serines and subject to many post-translational modifications that modulate activity (Holmberg et al., 2001; Hong et al., 2001; Kline and Morimoto, 1997; Murshid et al., 2010).

HR-C domain. HSF1 possesses another hydrophobic heptad repeat motif near its C-terminus, termed the HR-C region. HSF1 mutated in this motif displays increased binding activity and constitutive trimerization (Rabindran et al., 1993). This domain is thought to interact with the HR-A/B trimerization domain in monomeric HSF1 in order to inhibit trimerization, keeping the molecule inactive (Farkas et al., 1998; Rabindran et al., 1993; Zuo et al., 1994). Avian HSF3 and *Drosophila* HSF also contain HR-C regions (Nakai and Morimoto, 1993; Rabindran et al., 1993). *S. cerevisiae* HSF and human HSF4, both of which appear to constitutively trimerize and bind DNA, lack the HR-C domain (Nakai et al., 1997; Rabindran et al., 1991; Sorger et al., 1987; Sorger and Nelson, 1989).

Transactivation domain. The transactivation (TA) domain of HSF1 is located at the C-terminus of the protein, capable of activating transcription when fused to a heterologous DNA binding domain (Green et al., 1995; Wisniewski et al., 1996; Yuan et al., 1997). Yeast HSF differs slightly in that it has two transactivation domains, at the N

and C termini (Chen et al., 1993; Sorger, 1990). Figure 1-1 presents a visual summary of the domains in human HSF1.

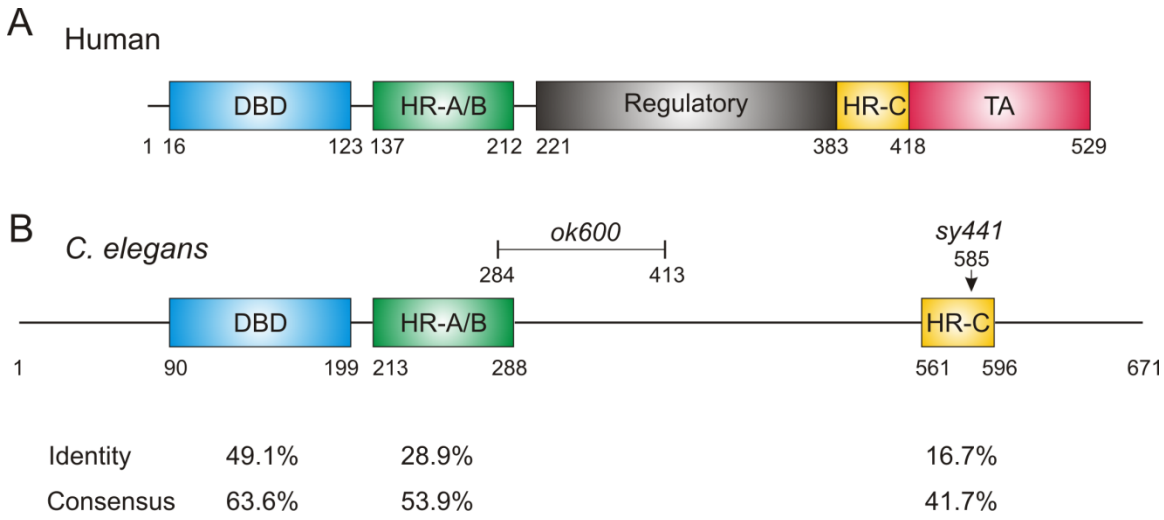

Figure 1-1. HSF1 domains

(A) Human HSF1 domains, including DNA binding domain (DBD), trimerization leucine zipper domain (HR-A/B), regulatory domain, trimerization repression domain (HR-C), and transactivation domain (TA), with amino acid residue positions below (Åkerfelt et al., 2010; Green et al., 1995; Pirkkala et al., 2001; Rabindran et al., 1991; Rabindran et al., 1993; Zuo et al., 1994). (B) Putative *C. elegans* HSF-1 domains. Above are locations of the two alleles available for *C. elegans* HSF-1: *sy441*, a nonsense mutation at W585, and *ok600*, a frame shifting deletion starting at amino acid 284 (Hajdu-Cronin et al., 2004; Morton and Lamitina, 2013). Sequence comparison places potential DNA binding and trimerization domains near the N-terminus, while a possible HR-C domain occurs at near the C-terminus. Identity and consensus position percentages from the human domains aligned to *C. elegans* HSF-1 are below (BLOSUM62mt2 alignment). The exact location of the transactivation domain in *C. elegans* HSF-1 is unclear, as the *sy441* allele retains some transactivation ability.

HSF1 Regulation

Localization

Localization of a protein has substantial implications for its potential interaction partners and regulation. The role localization plays in the activation of HSF1 has been long debated. Human cells and *Drosophila* are two of the most prominent systems used to study early stages of HSF1 activation, but both have produced multiple conflicting reports on the location of HSF1 under non-stress conditions.

Cytoplasmic extracts from control human HeLa cells contained inactive HSF1 (Larson et al., 1995; Mosser et al., 1990). Early studies describe nuclear localization as a step in the activation of HSF1 (Baler et al., 1993; Sarge et al., 1993). Baler *et al*. report exclusive localization of HSF1 to cytosolic fractions obtained after lysis and centrifugation of unstressed HeLa cells, and Sarge *et al*. report unstressed HSF1 as diffuse in both the nucleus and the cytoplasm of HeLa and 3T3 cells by immunofluorescence (Baler et al., 1993; Sarge et al., 1993). Two later immunofluorescence experiments, however, showed predominantly nuclear HSF1 in unstressed HeLa, 3T3 (mouse), and COS-7 (monkey) cells (Martinez-Balbas et al., 1995; Vujanac et al., 2005), with only an estimated 5% of HSF1 in enucleated cytosol of HeLa cells (Vujanac et al., 2005). Vujanac *et al*. report that the predominantly nuclear localization of HSF1 is due to strong nuclear import of HSF1, opposing weak nuclear export, which stress inactivates (Vujanac et al., 2005). Several other studies using both immunofluorescence and GFP tagging also visualized constitutive nuclear localization of HSF1 (Cotto et al., 1997; Jolly et al., 2002; Jolly et al., 1997).

Drosophila HSF was also present in cytosolic extracts from unstressed SL2 cells by biochemical fractionation (Clos et al., 1990; Zimarino et al., 1990), but constitutively nuclear by immunofluorescence (Westwood et al., 1991). Another immunofluorescence study, however, disagreed and saw primarily cytoplasmic HSF in SL2 cells and stress-induced nuclear entry (Zandi et al., 1997). Still other studies describe constitutively nuclear HSF, both by immunofluroescence and by fluorescent tagging of HSF (Orosz et al., 1996; Yao et al., 2006).

The preponderance of fractionation studies that place HSF1 in the cytoplasm are most likely responsible for early models of cytoplasmic to nuclear transitioning of HSF1, and yet are prone to artifacts, such as fraction contamination. The first immunofluorescence study in *Drosophila* observed nuclear HSF in unstressed cells, but also reproduced the earlier results of HSF present in unstressed isolated cytoplasmic fractions (Westwood et al., 1991). The authors performed immunofluorescence on nuclear fractions of homogenized cells with and without heat shock and found reduced nuclear staining in the unstressed fractions, even though staining of intact unstressed cells showed high nuclear HSF, thus suggesting that the homogenization process may permit leakage of inactive HSF from non-heat shocked nuclei (Westwood et al., 1991). Mercier *et al.* attempted to examine the discrepancies in HSF1 localization and also found that the fractionation procedure heavily influenced the amount of HSF1 observed in the cytosol (Mercier et al., 1999). They further speculate that the variation in antibodies used by different studies, perhaps possessing different affinities for the various forms of HSF1, could explain some immunofluorescence discrepancies (Mercier et al., 1999). Despite strong contradiction in the literature, the dogma of cytoplasmic HSF1 persists. Because

experiments had primarily been done in cell culture or *Drosophila* salivary glands, there were no reports of HSF1 localization in a whole animal until 2012. Chiang *et al*. attempted to determine HSF-1 localization in *C. elegans* by overexpressing HSF-1::GFP, reporting that it had diffuse nucleo-cytoplasmic fluorescence before heat shock and weak nuclear accumulation after heat shock (Chiang et al., 2012). However, as HSF is a low abundance protein compared to typical transcription factors (Biggin, 2011; Fritsch and Wu, 1999; Mivechi et al., 1994a; Wu et al., 1987), high levels of the protein are far from its native state and may interfere with its regulation. We have thus recently examined localization of physiological levels of HSF-1 in a live organism. Our studies suggest that HSF-1 is indeed a nuclear protein even in the absence of stress (Morton and Lamitina, 2013).

Trimerization

Mammalian HSF1 exists predominantly as a monomer before stress activation, and trimerization appears to be a step in gaining competence to bind HSE promoters (Baler et al., 1993; Sarge et al., 1993). Trimerization and DNA binding can be separated from transcriptional activation, however, as some activators (like salicylate) lead to trimerization and promoter binding but no subsequent transcription (Cotto et al., 1996; Jurivich et al., 1995).

S. cerevisiae HSF forms a trimer both when bound to DNA and in solution (Sorger and Nelson, 1989). Human HSF2, which constitutively trimerizes in yeast, complements HSF-deficient yeast, while hHSF1 does not (Liu et al., 1997). Interestingly, mutated forms of hHSF1 that constitutively trimerize do, in fact, rescue function in yeast, hinting at the importance of trimerization in HSF1 regulation (Liu et

al., 1997). Furthermore, mutations that enhance human HSF1 oligomerization enhance binding to certain varieties of HSE sequences (those that are discontinuous, with gaps between repeat arrays), prompting the hypothesis that oligomerization may have a role in promoter-binding specificity (Takemori et al., 2009).

Trimerization is often thought to be the regulatory step controlled by interaction with other factors, including chaperones and RNA, discussed below.

Chaperones

Because the primary known targets of HSF1 are molecular chaperones (HSPs), it has long been hypothesized that the protein state of the cell may play a role in regulating HSF1 activity. Amino acid analogues, which can cause misfolding when incorporated into proteins, activate the heat shock response, suggesting that disruption of protein folding may be a key factor in HSF1 activation (Kelley and Schlesinger, 1978; Mosser et al., 1988). Furthermore, injection of denatured proteins into *Xenopus* oocytes induces the heat shock response (Ananthan et al., 1986; Mifflin and Cohen, 1994). One group, notably, only observed this response when the denatured proteins were injected directly into the nucleus of the oocytes (Mifflin and Cohen, 1994).

Evidence arose that HSF1 may be regulated directly by HSPs, particularly HSP70 and HSP90. These two chaperones were separately found *in vitro* to inhibit heat-induced activation (trimerization and DNA binding) of HSF1 (Abravaya et al., 1992; Zou et al., 1998). HSP70 and HSP90 weakly associate with HSF1 from unstressed HeLa cells; in both cases the interaction required very specific conditions to be detected and was described as “unstable” (Baler et al., 1996; Zou et al., 1998). Overexpression of HSP70 in human cells reduced heat shock-induced HSF1 DNA binding and repressed

transactivation by a GAL4-HSF1(TA domain) fusion (Mosser et al., 1993; Shi et al., 1998). Injection of antibodies against HSP90 into *Xenopus* oocyte nuclei caused HSF1 to gain HSE-binding activity even in the absence of heat shock (Ali et al., 1998; Bharadwaj et al., 1999).

The above evidence has led to a commonly held model that HSF1 is kept inactive by association with HSPs. Heat shock denatures proteins, competing chaperones away from HSF1, allowing it to trimerize, bind DNA, and activate target transcription. However, it is clear that HSPs do interact with activated HSF1 (Ali et al., 1998; Bharadwaj et al., 1999; Rabindran et al., 1994). It is possible that in some cases, HSPs may be less involved in the maintenance of inactive basal HSF1 and have a greater role in the deactivation of HSF1 after heat shock. Westwood and Wu found that before activation, HSF1 in flies is monomeric and does not appear to be in a stable complex with chaperones (Westwood and Wu, 1993), and Abravaya *et al*.'s 1992 study only reported association of HSP70 with activated (DNA-bound) HSF1 (Abravaya et al., 1992). Another group found that elevated HSP70 could not inhibit DNA binding of HSF1 in rat cells, nor did HSP70 have a higher affinity to the inactive form of HSF1 than the active form, but elevated HSP70 could increase the loss of DNA binding during heat shock recovery (Rabindran et al., 1994). Mosser *et al*. reported that HSP70 overexpression *in vivo* increased the rate of HSF1 release from DNA (Mosser et al., 1993). Multi-chaperone complex constituents HSP90, p23 and immunophilin FKBP52 associate with trimeric DNA-bound HSF1 in *Xenopus* and seem to repress transcriptional activity (Bharadwaj et al., 1999; Guo et al., 2001), while injection of antibodies against these proteins delayed HSF1 attenuation (defined as trimer disassembly and DNA release) (Ali

et al., 1998; Bharadwaj et al., 1999). Microinjection of purified HSP90 into oocyte nuclei also increased HSF1 release from HSEs (Bharadwaj et al., 1999). These studies indicate that HSP interaction with HSF1 is likely a step in its deactivation during recovery after heat shock, but do not in every case support involvement in routine repression of HSF1 during basal growth or in derepression during activation. Many factors that mediate the latter may yet be unidentified.

One question, in light of the studies on HSF1 localization, is how cytoplasmic chaperones might be regulating a nuclear transcription factor. A simple explanation is that some of the chaperones localize to the nucleus. HSP70, though cytoplasmic before heat shock, was localized to the nucleus of HeLa cells after heat shock (Sarge et al., 1993), and small amounts of HSP90 were detected in nuclear extracts from both stressed and unstressed *Xenopus* oocytes (Bharadwaj et al., 1999). Immunotargeting experiments that activated HSF1 using HSP90 antibodies did so via direct nuclear injection (Bharadwaj et al., 1999). Nevertheless, the majority of HSP90 is cytoplasmic (Ali et al., 1998; Bharadwaj et al., 1999). It has also been proposed that shuttling of HSF1 from the nucleus into the cytoplasm and back allows interaction with cytoplasmic factors (Vujanac et al., 2005), though the fact that the vast majority of HSF1 is nuclear at any given time would argue that the bulk of its repressive regulation must occur in the nucleus.

RNA

An RNA has also been proposed to regulate HSF1 trimerization. Shamovsky *et al.* discovered that heat shocked mammalian HSF1 coimmunoprecipitated with translation factor eEF1A and an RNA termed heat shock RNA 1 (HSR1) (Shamovsky et al., 2006). These two components were capable of inducing *in vitro* trimerization and

DNA binding of HSF1, and siRNA against HSR1 decreased the *in vivo* heat shock response (Shamovsky et al., 2006). The authors propose that the general downregulation of translation that occurs with heat shock could make eEF1A available to bind HSF1. A putative RNA-binding protein was recently found to negatively regulate most of the 21 HSFs in *Arabidopsis* (Guan et al., 2012). A precedent exists in bacteria for RNA to act as a molecular thermometer, folding into a secondary structure at low temperature that heat shock relieves, permitting protein-binding to the RNA (Morita et al., 1999). Certainly the potential for RNA-based regulation of HSF1 warrants much further investigation.

Post-translational modification

Phosphorylation. Human HSF1 is both constitutively and inducibly phsophorylated, with as many as 20 potential phosphoylation sites identified. The purpose of these modifications varies. Some residues (S303 and S307) are constitutively phosphorylated and act to keep HSF1 activity repressed (Kline and Morimoto, 1997). Other residues are inducibly phosphorylated and enhance activity (S320, S326), while others still are inducibly phosphorylated and reduce activity (S363) (Dai et al., 2000; Guettouche et al., 2005; Murshid et al., 2010). The mechanism of function has been determined for some of these modifications and includes such actions as affecting nuclear localization, DNA binding, transactivation (independent of DNA binding), and recovery from granule formation. Table 1-1 summarizes proposed roles of phosphorylation sites and their identified kinases. Mass spectrometry has detected phosphorylation at many other sites in human HSF1 that have not been further experimentally confirmed: S292, S314, S319, T323, T328, T367, S368, T369, S344, and S444 (Guettouche et al., 2005; Mayya et al., 2009; Olsen et al., 2010).

Most of the identification of phosphorylation sites and kinases was done *in vitro* and through overexpression, perhaps leading to the occasional conflicting reports on specific modifications. For instance, Kline and Morimoto found S303 to be constitutively phosphorylated, while Hietakangas *et al*. observed heat shock-induced phosphorylation and gradual dephosphorylation during attenuation (Hietakangas et al., 2003; Kline and Morimoto, 1997). Residue S363 has been proposed to have two different primary kinases: c-Jun N-terminal kinase (JNK) and protein kinase C (PKC) (Chu et al., 1998; Dai et al., 2000). Though one explanation for contradictory results is artifacts in kinase overexpression assays, they may also be an indication that phosphorylation states and kinases of HSF1 have previously unsuspected cell- or condition-specific complexity.

S. cerevisiae HSF is phosphorylated with heat stress, the degree of which correlates with transcriptional activity (Sorger et al., 1987; Sorger and Pelham, 1988). Because *S. cerevisiae* HSF is constitutively trimerized and bound to DNA, it has been proposed that this phosphorylation is a major step in converting HSF to a strong activator of transcription (Sorger et al., 1987); although, as with human HSF1, phosphorylation of some residues has been reported as deactivating (Høj and Jakobsen, 1994). In contrast, *Drosophila* HSF total phosphorylation load is unchanged with heat shock, and phosphorylation does not seem to affect DNA binding, though different residues are phorsphorylated before and after stress (Fritsch and Wu, 1999). Recently, *C. elegans* HSF-1 has also been reported to undergo heat stress-induced phosphorylation, but the exact effect of this modification has not been explored (Chiang et al., 2012).

Modification	Residue	Domain	Kinase	Activity	Affected Process
Phosphorylation	S121	DBD	MK2 (Wang et al., 2006)	Repressive (Wang et al., 2006)	DNA binding
Phosphorylation	T142	HR-A/B	CK2 (Soncin et al., 2003)	Activating (Soncin et al., 2003)	DNA binding
Phosphorylation	S216	Linker	Plk1 (Lee et al., 2008)	Repressive (Lee et al., 2008)	Degradation (during mitosis)
Phosphorylation	S230	Regulatory	CaMKII (Holmberg et al., 2001)	Inducible, activating (Holmberg et al., 2001)	Transactivation
Phosphorylation	S303	Regulatory	GSK-3β (Chu et al., 1998)	Constitutive, repressive (Kline and Morimoto, 1997); inducible, repressive (Hietakangas et al., 2003)	Transactivation, granule recovery, priming for sumoylation
Phosphorylation	S307	Regulatory	ERK (He et al., 1998)	Constitutive, repressive (Kline and Morimoto, 1997)	Priming for S303 phosphorylation
Phosphorylation	S320	Regulatory	PKA (Murshid et al., 2010)	Inducible, activating (Murshid et al., 2010)	Nuclear localization
Phosphorylation	S326	Regulatory	mTOR? (Chou et al., 2012)	Inducible, activating (Guettouche et al., 2005)	
Phosphorylation	S363	Regulatory	JNK (Dai et al., 2000) or PKC (Chu et al., 1998)	Inducible, repressive (Dai et al., 2000)	Granule recovery
Phosphorylation	S419	TA	PLK1 (Kim et al., 2005)	Activating (Kim et al., 2005)	Nuclear localization
Acetylation	K80	DBD		Inducible, repressive (Westerheide et al., 2009)	DNA binding
Sumoylation	K298	Regulatory		Activating (Hong et al., 2001) or repressive (Hietakangas et al., 2006)	

Table 1-1. Post-translational modifications to human HSF1
DBD = DNA binding domain, HR-A/B = trimerization domain, TA = transactivation domain.

Acetylation. After stress, human HSF1 is acetylated at residue K80 as well as eight other lysines (Westerheide et al., 2009). K80 is in the DNA binding domain, and a

mutant at this residue was found to be non-functional, localizing to the nucleus but unable to form nuclear stress granules or induce target gene expression (Westerheide et al., 2009). SIRT1 is the deacetylase proposed to aid in HSF1 activity by removing acetylation, as SIRT1 siRNA or sirtuin inhibitors reduce the production of HSF1-target mRNAs in HeLa cells (Westerheide et al., 2009). SIRT1 siRNA reduced the amount of HSF1 bound to the *hsp70* promoter over the whole course of a six-hour heat shock, and overexpression of SIRT1 enhanced DNA binding, indicating that acetylation regulates HSF1 through its ability to bind DNA (Westerheide et al., 2009).

Sumoylation. SUMO is a small (11 kDa), ubiquitin-like protein modifier originally identified conjugating to RanGTPase activating protein (Matunis et al., 1996). Sumoylation of a protein can influence many different processes, including protein localization, protein-protein interactions, protein-DNA interactions, and protein ubiquitination (Desterro et al., 1998; Duprez et al., 1999; Goodson et al., 2001; Hirano et al., 2003; Kim et al., 2002; Mahajan et al., 1997; Ross et al., 2002). One of the best-studied roles of SUMO is as a regulator of transcriptional activity. Sumoylation may inhibit (Bies et al., 2002; Hirano et al., 2003; Muller et al., 2000; Ross et al., 2002; Subramanian et al., 2003) or activate activity (Kim et al., 2002; Muller et al., 2000). In mammals, there are three SUMOs, SUMO-1, SUMO-2 and SUMO-3. SUMO-2 and -3 contain sumoylation motifs in their N-terminal regions, and form poly-SUMO chains *in vitro*, while SUMO-1 does not (Tatham et al., 2001). SUMO conjugation is a process very similar to ubiquitination: an E1 activating enzyme (SAE1/SAE2 in humans) bonds first to SUMO in an ATP-dependent manner, followed by transfer to an E2 conjugating enzyme (UBC9) which, with the aid of an E3 ligase, conjugates the C-terminus of SUMO

to a lysine residue in its target protein (Anckar and Sistonen, 2007; Dye and Schulman, 2007). SUMO-1 does not absolutely require an E3 enzyme, however, and can be conjugated *in vitro* with only the E1, E2 and ATP (Duprez et al., 1999). The canonical consensus site for sumoylation is the motif ΨKXE (where Ψ is a large hydrophobic amino acid), though this exact sequence is not present in every case of sumoylation (Rodriguez et al., 2001; Sentis et al., 2005).

In humans, both HSF1 and HSF2 are SUMO-1 targets (Goodson et al., 2001; Hietakangas et al., 2003; Hong et al., 2001). In both of these cases, however, controversy exists on the role of this modification. For HSF2, sumoylation occurs in the DNA binding domain (residue K82) and was initially reported to activate mammalian HSF1 DNA binding (Goodson et al., 2001). The proposed mechanism of this activation was that sumoylation stabilized the HSF1 timer, a model based on the location of K82 within a "wing" region of the DNA binding domain that in yeast appears to form protein-protein contracts rather than protein-DNA contacts (Littlefield and Nelson, 1999). This conclusion was supported by the observation that *Xenopus laevis* expresses an HSF2 homologue that is also sumoylated on K82A in a way that promotes DNA binding (Hilgarth et al., 2004). A later study by Anckar *et al*., however, found that sumoylation of the mammalian HSF2 impaired DNA binding and did not affect oligomerization (Anckar et al., 2006). This study concludes that the majority of HSF2 is unsumoylated and bound to DNA (Anckar et al., 2006). One way Anckar *et al*. proposed to reconcile the results was the possibility of differences between the HSEs used to determine DNA binding capacity, in which case, sumoylation may serve more as a promoter specificity regulator than a regulator of general activity.

Sumoylation of HSF1 tells a similar story. All reports agree that sumoylation of human HSF1 occurs inducibly with stress in the regulatory domain, on residue K298 (Hietakangas et al., 2003; Hong et al., 2001). In the first report of this modification, mutation of this residue to arginine eliminated *in vitro* DNA binding and decreased heat-induced *in vivo* activity of an HSE reporter, indications that sumoylation serves to enhance DNA binding of HSF1 (Hong et al., 2001). Subsequent reports found that phosphorylation of S303 (a repressive modification) was required for sumoylation and that nonsumoylated HSF1 was still capable of binding DNA, contradicting Hong *et al*. (Hietakangas et al., 2003). Hietakangas *et al*. later reported that K298R had increased activity in a GAL4-HSF1 chimera system as well as in *Hsf-1-/-* MEFs stressed with MG132 (a proteasome inhibitor), arguing that sumoylation of HSF1 represses activity (Hietakangas et al., 2006). The exact role of sumoylation in HSF1 regulation remains uncertain. The later model – that SUMO represses stress-induced activity – is supported by our recent screen for regulators of heat stress gene expression. We found that in *C. elegans*, inhibition of SUMO led to hyperexpression of an HSF-1-dependent reporter after heat shock. This result is in agreement with Hietakangas *et al*., placing SUMO as a repressor of HSF-1 activity (Morton and Lamitina, unpublished data).

Granule formation

In their studies of HSF1 localization in HeLa cells, Sarge *et al*. noted that heat shocked HSF1 seemed to stain in distinct puncta within the nucleus (Sarge et al., 1993). A pair of papers in 1997 characterized these granules and revealed that they are present in heat shocked primary fibroblasts, epithelial cells and several transformed human cell lines (Cotto et al., 1997; Jolly et al., 1997). In HeLa cells, they fall into two different

populations based on size, 0.5-1.5 µm and 1.5-2.5µm, with approximately 7 granules per nucleus (fewer in primary cells) (Cotto et al., 1997). They were declared a novel subnuclear structure because they do not colocalize with sites of DNA replication, kinetochores, splicing factor SC35, coiled bodies (marked by p80-coilin), promyelocytic leukemia bodies, nuclear lamins, or nucleoli (detected by a marker of the dense fibrillar center) (Cotto et al., 1997). Surprisingly, they also do not colocalize with transcript foci of either *HSP70* or *HSP90*, leading to the conclusion that HSF1 granules are not forming at target gene loci (Jolly et al., 1997).

HSF1 granules form rapidly, starting to appear after only 30 sec of 42°C heat shock, and are highly dynamic: fluorescence recovery after photobleaching (FRAP) shows full recovery of HSF1-GFP granule fluorescence within 3 minutes (Jolly et al., 1999). Granules are also reversible, dispersing again after as little as 8 min (recovery time is longer if exposure time to the initial heat shock is increased) (Jolly et al., 1999). This dispersal is facilitated by overexpression of kinases JNK or GSK-3β (Dai et al., 2000; He et al., 1998). A second heat shock following recovery causes granules to re-form in the same location as in the original heat shock, suggesting an underlying nuclear structure may be involved (Jolly et al., 1999). The number of granules per nucleus seems to show a degree of correlation to cell ploidy, implicating DNA in their formation (Cotto et al., 1997; Jolly et al., 1997).

Granules can be induced without heat stress via other reagents, indicating that it is not heat as a physical property that causes them (Cotto et al., 1997). The heavy metal stressor cadmium and the amino acid analogue azetidine induced granule formation in the absence of heat (Cotto et al., 1997). Both of these stressors are known to induce HSF1

DNA binding and transcriptional activation (Mosser et al., 1988). Salicylate is a non-steroidal anti-inflammatory drug that induces HSF1 trimerization and DNA binding and yet does not induce transcription (Cotto et al., 1996; Jurivich et al., 1995). Interestingly, salicylate does not induce granule formation (Cotto et al., 1997). This suggests that granule formation correlates with the active HSF1. However, a truncated form of HSF1 containing only the DBD and trimerization domain does form constitutive granules (at either 37°C or 42°C) (Jolly et al., 2002). HSF1 granules have also been observed after heat shock in non-transcribing mitotic cells, as well as cells treated with actinomycin D, indicating that transcriptional activity is not necessary for granules to exist (Jolly et al., 1997; Jolly et al., 1999).

Eventually, other granule components were detected. Nuclear SUMO transiently colocalizes with HSF1 granules (Hietakangas et al., 2003; Hong et al., 2001). This may indicate that granule-localized HSF1 is sumoylated, since Hong *et al*. report HSF1(K298R) is incapable of forming granules while Hietakangas *et al*. report HSF1(K298R) still forms granules but no longer colocalizes with SUMO (Hietakangas et al., 2003; Hong et al., 2001). HSF2 is also present in most (but not all) granules, in hetero-oligomers with HSF1 (Alastalo et al., 2003).

The most intriguing components identified in granules, however, are RNA binding proteins and splicing factors. Approximately an hour after HSF1 granules form, heterogeneous nuclear ribonucleoprotein (hnRNP) A1 associated protein (HAP) forms overlapping granules (Weighardt et al., 1999). This recruitment depends on RNA synthesis, and HAP remains in these granules well after HSF1 has dispersed again in recovery (Weighardt et al., 1999). Serine/arginine rich (SR) proteins are a family of

splicing factors involved in both constitutive and alternative splicing; two prototypical members are SF2/ASF and SC35 (Long and Caceres, 2009). SC35 does not colocalize with either HSF1 or HAP after heat shock, but SF2/ASF strongly colocalizes with stress-induced HAP granules (Cotto et al., 1997; Denegri et al., 2001). Two other SR proteins, SRp30c and 9G8, and the RNA processing factor Sam68, also colocalize with HAP after stress (Denegri et al., 2001). A subset of HAP granules colocalize with hnRNP M as well (Chiodi et al., 2000). Thus, there is strong evidence for a role of RNA processing in nuclear granules, although alternative functions for these proteins are possible; for instance, SF2/ASF is also known to stimulate sumoylation of proteins (Pelisch et al., 2010), and HAP was first identified as a scaffold attachment factor involved in chromatin structure (Renz and Fackelmayer, 1996).

In 2002, the DNA locus underlying granule formation was finally identified. The DNA binding domain of HSF1 was shown to be necessary for granule formation, and a heterochromatic region of chromosome nine, 9q12, was linked to HSF1 granule location using FISH (Denegri et al., 2002; Jolly et al., 2002). This region consists primarily of satellite III DNA, which in turn largely consists of GGAAT repeats (Grady et al., 1992; Jolly et al., 2002; Prosser et al., 1986). These do not form perfect HSEs, but HSF1 was capable of binding the sequence *in vitro* (Jolly et al., 2002). A single locus does not account for the number of granules observed in cells, however, and HSF1 was later found to bind to pericentromeric regions of 14 other chromosomes as well, all of which contain satellite II (similarly containing GGAAT repeats) or III repeat sequences (Denegri et al., 2002; Eymery et al., 2010; Prosser et al., 1986; Tagarro et al., 1994).

Despite failure of granules to colocalize with traditional HSF1 targets, granules are associated with newly synthesized RNAs (He et al., 1998), though not poly(A)$^+$ RNAs (Weighardt et al., 1999). After identification of the granule target chromosomal locus, sat III repeats were found to be inducibly transcribed, in an HSF1-dependent manner (Jolly et al., 2004; Rizzi et al., 2004). The sat III transcripts are stable and remain associated with the 9q12 locus long after HSF1 has dispersed (Jolly et al., 2004). Sat III transcripts also contain putative binding sites for SF2/ASF (Chiodi et al., 2004), and recruitment of SF2/ASF and SRp30c to granules requires sat III transcripts (Metz et al., 2004). HSF1 transcription in granules may be in part regulated by HSF2, as depleting HSF2 leads to increased stress-induced sat III transcription, but HSF2 overexpression results in sat III transcription in the absence of stress (Sandqvist et al., 2009).

Sarge *et al*. observed by immunofluroescence that HSF1 in HeLa (human) cells formed granule structures after heat shock, but that HSF1 in 3T3 (mouse) cells was diffuse within the nucleus (Sarge et al., 1993). The authors state that they observed granules in a number of other human cell lines, but never in mouse lines. From this they posit that granules might be a distinctly human phenomenon. Two other groups likewise failed to see granules in murine cells (mouse 3T3 or hamster B14-150 or HA-1 cells) (Denegri et al., 2002; Mivechi et al., 1994b). The discovery that sat III repeats are granule targets firmly reinforced the belief that granules are a human characteristic, because satellite III DNA is specific to primates (Jarmuz et al., 2007). This assumption has been challenged, however, by our very recent discovery that *C. elegans* HSF-1 redistributes into nuclear puncta after stress (Morton and Lamitina, 2013). *C. elegans*

HSF-1 granules share many properties with human granules, though their target DNA locus has not yet been identified.

Physiological roles of HSF1

Stress resistance

As discussed earlier, the best-studied function of HSF1 is that in stress-inducible gene transcription. HSF1 has been well defined in its ability to be activated by a wide variety of stresses, including heat, heavy metals, amino acid analogues, energy depletion, oxidative stress, and many different chemicals (including proteasome and protease inhibitors) (Hahn and Thiele, 2004; Holmberg et al., 2000; Jacquier-Sarlin and Polla, 1996; Massie et al., 2003; Mosser et al., 1988; Rossi et al., 1998; Sarge et al., 1993; Westerheide and Morimoto, 2005; Westerheide et al., 2012; Zhong et al., 1998). HSF1 is an essential part of the heat shock response. *Hsf1-/-* mice grow to adulthood, but induce no HSP production with heat shock (Xiao et al., 1999). Mutations in HSF1 also prevent robust heat shock gene expression in flies, yeast, and worms (Hajdu-Cronin et al., 2004; Jedlicka et al., 1997; Smith and Yaffe, 1991). Interestingly, in both mouse cells and *C. elegans*, HSF1 loss does not seem to affect survival during an initial heat shock. Instead, HSF1 is required for the acquisition of increased thermotolerance after a preconditioning stress (McColl et al., 2010; McMillan et al., 1998).

Development

Although HSF1 is most strongly associated with stress in the literature, it is an essential gene in many organisms under non-stress conditions. Both *S. cerevisiae* and *S. pombe* require HSF for growth at normal temperatures (Gallo et al., 1993; Sorger and Pelham, 1988). HSF-1 is also essential for growth beyond an early larval stage in *C.*

elegans (Hajdu-Cronin et al., 2004; Morton and Lamitina, 2013). In *Drosophila*, HSF is required for oogenesis and larval development, though not for general cell growth (Jedlicka et al., 1997). In mice, which have multiple HSFs, HSF1 is dispensable for viability, but deletion results in placental defects, slowed post-natal growth, and female infertility (Xiao et al., 1999). HSF1 is present at high levels in oocytes and zygotes (while HSF2 levels are very low) (Christians et al., 1997; Metchat et al., 2009), and *Hsf1-/-* oocytes exhibit meiosis defects and, if fertilized, arrest before the blastocyst stage (Christians et al., 2000; Metchat et al., 2009). HSF1 is thus not only a stress-inducible factor but is also an indispensible player in fertility and development. *Hsf1* mutant oocytes also exhibit higher levels of reactive oxygen species and show signs of oxidative damage, further supporting a role of HSF1 in redox homeostasis (Bierkamp et al., 2010).

Cancer

A great deal of recent attention has been given to the role of HSF1 in cancer promotion. HSP levels were known to be elevated in many different types of tumors (Ferrarini et al., 1992; Jameel et al., 1992; Jolly and Morimoto, 2000; Kaur and Ralhan, 1995; Ralhan and Kaur, 1995), and in fact a member of the HSP family was one of the first identified tumor antigens (Ullrich et al., 1986). The Lindquist group revealed an association between HSF1 and cancer, observing that HSF1 is involved in many processes during transformation (Dai et al., 2007), though the transcriptional network regulated by HSF1 in carcinogenesis appears to differ from that induced during heat shock (Mendillo et al., 2012). Deficiencies in HSF1 in mice reduce the degree of turmorigenesis induced by p53 or NF1 mutation or chemical carcinogens (Dai et al., 2012; Dai et al., 2007; Jin et al., 2011). High HSF1 expression is associated with poor

breast cancer prognosis (Mendillo et al., 2012; Santagata et al., 2011), and HSF1 reduction in human cancer cell lines interferes with proliferation (Dai et al., 2007; Mendillo et al., 2012; Meng et al., 2010; Sato et al., 2012). HSF1 has thus been proposed as a promising target for cancer prognositics and therapies.

Innate immunity

HSPs have a role in immunity in mammalian systems. Extracellular HSP60 seems to serve as a "danger signal" for innate immune cells like macrophages, signaling them to produce pro-inflammatory cytokines TNF-α, interleukin (IL) 12 and IL-15 (Chen et al., 1999). *Hsf1-/-* mice have increased susceptibility to *E. coli* lipopolysaccharide (LPS) (Xiao et al., 1999) and are deficient in LPS-triggered expression of IL-6 and chemokine CCL5 (Inouye et al., 2004). HSPs are also protectors in the innate immune response in *C. elegans*. Worms with HSF-1 reduced through either mutation or RNAi die from *Pseudomonas aeruginosa* pathogenicity more rapidly than wild type, and overexpression of HSF-1 extends survival in a manner requiring HSP production (Singh and Aballay, 2006a). Several hypothesis about the potential mechanism by which HSF1 and HSPs aid immunity have been proposed : they may regulate antimiocrobial peptide gene expression and protein folding, they may be necessary for the cell to survive stresses or toxins induced by the pathogen, they may be involved in recognizing foreign peptides, or they may serve as immune signals themselves when released during cell necrosis (Chen et al., 1999; Singh and Aballay, 2006b). The exact mechanism of the heat shock response's role in pathogen resistance is yet to be determined.

Aging

It has been known for decades that mutations in single genes can drastically increase the lifespan of *C. elegans* (Friedman and Johnson, 1988; Kenyon et al., 1993). Mutations in these genes also confer increased thermotolerance (Lithgow et al., 1995), linking stress tolerance to longevity. Stress-induced HSP expression declines with age in rats, *C. elegans*, and human fibroblasts (Ben-Zvi et al., 2009; Fargnoli et al., 1990; Kregel et al., 1995; Liu et al., 1989; Udelsman et al., 1993); and overexpression of HSPs extends lifespan in *Drosophila* and *C. elegans* (Tatar et al., 1997; Walker and Lithgow, 2003; Yokoyama et al., 2002). Pretreatment with a nonlethal heat shock will also increase worm and fly lifespan (Khazaeli et al., 1997; Lithgow et al., 1995).

HSF-1 itself was directly implicated in aging by Garigan *et al*., who found that reduction of HSF-1 accelerates aging in *C. elegans* (Garigan et al., 2002). Conversely, HSF-1 overexpression increases overall lifespan (Hsu et al., 2003). HSF-1 has also been directly linked to the insulin/insulin-like signaling pathway (Barna et al., 2012; Chiang et al., 2012; Hsu et al., 2003; Morley and Morimoto, 2004), a pathway that has been extensively studied for its role in lifespan in *C. elegans*, *Drosophila* and mice (Bluher et al., 2003; Clancy et al., 2001; Dorman et al., 1995; Giannakou et al., 2004; Holzenberger et al., 2003; Kenyon et al., 1993). Mutations of the insulin receptor *daf-2* extend *C. elegans* lifespan and protect against proteotoxicity in a manner dependent on both DAF-16 (a FOXO transcription factor) and HSF-1 (Cohen et al., 2006; Hsu et al., 2003; Morley and Morimoto, 2004). Dietary restriction, a separate longevity-inducing pathway, also protects against proteotoxicity by a mechanism dependent on HSF-1 (Steinkraus et al., 2008). One of the current models of aging is that the proteostasis

network of the cell becomes overburdened with age, accounting for the critical effect expression of molecular chaperones can have on longevity. Indeed, in *C. elegans*, aging is a determinant of protein misfolding and proteotoxicity, apparently due to a declining ability to detoxify damaging proteins (Ben-Zvi et al., 2009; Cohen et al., 2006). HSF1, as a regulator of molecular chaperones, plays a major part in proteostasis and the constituents of aging.

The integral role of HSF1 in these many areas relevant to human health illustrates the importance of gaining a full understanding of HSF1 regulation. Moreover, our knowledge of the behavior of HSF-1 in *C. elegans* specifically is surprisingly sparse, given the prevalence of the worm as a model for HSF-1-dependent processes. It was our goal to gain a greater understanding of HSF-1 activation in *C. elegans* and use this model organism to explore its regulation.

Project summary

With the aim of determining HSF-1 localization in a live, intact organism, we visualized tagged HSF-1 in *C. elegans* and concluded that in worms it is a constitutively nuclear protein. During this study, we generated many useful reporter worm strains and further characterized an *hsf-1* mutant allele in this widely used model organism. We discovered that heat stress induces *C. elegans* HSF-1 to form structures that are reminiscent of human nuclear stress granules. Comparison of a range of properties of these two structures revealed substantial implications for the evolutionary conservation of granule formation. We also used the RNAi tools available in the worm to screen for new regulators of the heat stress response pathway. In the process, we developed a MATLAB-based tool to automate analysis of quantitative fluorescent data, facilitating

future large-scale screens. One of the many genes identified in our screen encodes the small ubiquitin-like modifier SUMO. We hypothesize that this modification may be a direct regulator of HSF-1 function in worms.

2. HSF-1 is an essential nuclear protein that forms stress granule-like structures following heat shock[1]

Summary

The heat shock transcription factor (HSF) is a conserved regulator of heat shock-inducible gene expression. Physiological roles for HSF in processes such as development, aging, and immunity have been defined in great part through studies of the single *C. elegans* HSF homolog, *hsf-1*. However, the molecular and cell biological properties of *hsf-1* in *C. elegans* are incompletely understood. We generated animals expressing physiological levels of an HSF-1::GFP fusion protein and examined its function, localization, and regulation *in vivo*. HSF-1::GFP was functional as measured by its ability to rescue phenotypes associated with two *hsf-1* mutant alleles. Rescue of *hsf-1* development phenotypes was abolished in a DNA-binding-deficient mutant, demonstrating that the transcriptional targets of *hsf-1* are critical to its function even in the absence of stress. Under non-stress conditions, HSF-1::GFP was found primarily in the nucleus. Following heat shock, HSF-1::GFP rapidly and reversibly redistributed into dynamic, subnuclear structures that share many properties with human nuclear stress granules, including colocalization with markers of active transcription. Rapid formation of HSF-1 stress granules was promoted by HSF-1 DNA binding activity, and the threshold for stress granule formation was altered by growth temperature. HSF-1 stress granule formation was not induced by inhibition of IGF signaling, a pathway previously suggested to function upstream of *hsf-1*. Our findings suggest that development, stress,

---

[1] This chapter is adapted from the published work under the same title by Elizabeth A. Morton and Todd Lamitina, *Aging Cell*, **12**, 112-120 (2013).

and aging pathways may regulate HSF-1 function in distinct ways, and that HSF-1 nuclear stress granule formation is an evolutionarily conserved aspect of HSF-1 regulation *in vivo*.

Introduction

The heat shock transcription factor (HSF) plays essential and evolutionarily conserved roles in the activation of heat shock-inducible gene expression. While HSFs are best recognized as regulators of stress-induced gene expression, they also contribute to more complex organismal processes such as development, growth, aging, immunity, and reproduction. HSFs are also central to many pathophysiological processes and can contribute to tumorogenesis as well as to the pathology underlying diseases of protein misfolding, such as Huntington's and Alzheimer's diseases (Cohen et al., 2006; Dai et al., 2007; Hsu et al., 2003; Morley and Morimoto, 2004). Given the importance of HSFs to these physiological states, understanding the mechanisms that regulate HSF function could provide new insights and therapeutic strategies for a variety of diseases (Westerheide and Morimoto, 2005).

In mammals, HSF1 encodes the master regulator of the heat shock response (Åkerfelt et al., 2010). Regulation of HSF1 is thought to occur at several levels. In the absence of heat shock, the predominant model presents mammalian HSF1 as primarily a monomeric protein that is bound and repressed by chaperones such as heat shock protein 90 (HSP90) (Voellmy and Boellmann, 2007). Following an acute heat shock, these chaperones bind to misfolded client proteins, releasing HSF1 so that it can trimerize, bind sequence-specific heat shock elements (HSEs), and transactivate gene expression. In human (but not rodent) cells, HSF1 also responds to stress by localizing to subnuclear

structures termed nuclear stress granules (or nuclear stress bodies (Biamonti and Vourc'h, 2010)). HSF1 stress granules represent the binding of HSF1 to heterochromatic, pericentromeric repeat regions of DNA, leading to transcription of non-coding RNAs (ncRNAs) (Denegri et al., 2002; Eymery et al., 2010; Jolly et al., 2004; Jolly et al., 1997; Jolly et al., 1999). Stress granule formation seems to be determined by specific DNA sequences, since rodent HSF1 can be induced to form stress granules when it is in the presence of human chromosomes (Denegri et al., 2002). Despite intensive study, the functional role of HSF1 stress granules and their associated ncRNAs remains one of the most mysterious aspects of HSF1 regulation. Since HSF1 stress granule formation has only been observed in primate cells, their study has been hampered by the lack of a suitable system in which to manipulate stress granule formation and ncRNA synthesis. Moreover, while the biochemical and cell biological properties of HSF1 are well described in isolated cells, studies investigating whether similar regulation occurs in a multicellular organism are more limited.

Recent studies in *Caenorhabditis elegans* have played a major role in understanding how HSF contributes to organismal physiology. While vertebrates express four major HSFs, worms express a single HSF homolog, *hsf-1*. By sequence homology, *C. elegans* HSF-1 contains N-terminal DNA binding and trimerization domains, with a putative transactivation domain at the C-terminus (Hajdu-Cronin et al., 2004). RNAi-mediated knockdown of *hsf-1* gives rise to a progeric phenotype (Garigan et al., 2002), while *hsf-1* overexpression promotes longevity and delays age-related protein misfolding and proteotoxicity (Cohen et al., 2006; Hsu et al., 2003; Morley and Morimoto, 2004). *hsf-1* also plays important functional roles in *C. elegans* innate immunity (Singh and

Aballay, 2006a), where it helps inhibit pathogen-induced protein aggregation in the intestine (Mohri-Shiomi and Garsin, 2008). Despite these many roles, the localization pattern and dynamic regulation of the *C. elegans* HSF-1 protein expressed at physiological levels have not been reported.

Here, we generated *C. elegans* expressing a functional single-copy HSF-1::GFP transgene driven by the native *hsf-1* promoter. We find that *in vivo*, HSF-1::GFP is a ubiquitously-expressed, predominantly nuclear protein. Following heat shock, HSF-1::GFP does not exhibit further nuclear enrichment but does undergo rapid and reversible reorganization into subnuclear structures that share many characteristics with human HSF1 stress granules. The rapid formation of these structures in *C. elegans* required DNA binding activity but was not induced by inactivation of the insulin/IGF signaling. These studies are among the first to demonstrate the dynamic nuclear behavior of HSF in native tissues in a live animal setting, suggesting that nuclear stress granule formation may be an evolutionarily ancient mechanism for regulating HSF *in vivo*.

Results

HSF-1 constitutively localizes to the nucleus and forms nuclear granules upon heat shock. Many HSF-1-dependent processes have been studied in *C. elegans* and the properties of overexpressed *C. elegans* HSF-1 have recently been investigated (Chiang et al., 2012). However, overexpressed *C. elegans* HSF-1 produces gain-of-function phenotypes (Chiang et al., 2012; Hsu et al., 2003; Morley and Morimoto, 2004; Singh and Aballay, 2006a) and may not accurately reflect the physiological properties of endogenous HSF-1. To characterize these properties, we generated a fluorescent reporter that fused GFP to the C-terminus of the HSF-1 protein and integrated this transgene at

single-copy level into the *C. elegans* genome (Figure 2-1A) (Frøkjær-Jensen et al., 2008). Quantitative real-time PCR confirmed that this transgenic line expressed *hsf-1* at near physiological levels (Figure 2-1B). In contrast with previous studies of overexpressed HSF-1::GFP, single-copy HSF-1::GFP localized predominantly to the nucleus under basal conditions (20°C) (Figure 2-1C). Following heat shock (35°C for 1 min or 20 min), HSF-1::GFP did not exhibit further accumulation of fluorescence intensity within the nucleus (Figure 2-2), suggesting that during the earliest phases of heat shock, nuclear translocation of HSF-1::GFP is a minor component of its regulation in *C. elegans*. However, heat shock did result in the redistribution of HSF-1::GFP into distinct subnuclear structures (Figure 2-1C,D), a property reminiscent of human HSF1, which forms structures termed HSF1 nuclear stress granules upon heat shock (Cotto et al., 1997; Jolly et al., 1997). HSF-1::GFP granule formation also occurred in the *hsf-1(ok600)* deletion mutant, indicating that stress granule formation does not require the endogenous HSF-1 protein (data not shown). A PCR fusion-derived HSF-1::YFP extrachromosomal array containing introns and lacking the Gateway adaptor sequences also showed nuclear enrichment and stress granule formation (Figure 2-3). Quantification of the size of *C. elegans* HSF-1 stress granules revealed an average diameter of 0.6±0.2 μm, slightly smaller than human HSF1 stress granules, which distribute among two populations of structures with diameters of 0.5-1.6 μm and 1.6-3.0 μm (Figure 2-1E) (Cotto et al., 1997). The *C. elegans* HSF-1 structures were also similar in number to human HSF1 granules (7.1±2.7 granules per nucleus in *C. elegans* (Figure 2-1F) versus 6.8±2.4 granules per nucleus in HeLa cells (Cotto et al., 1997)). Stress-induced HSF-1::GFP granules were observed in all examined tissue types (Figure 2-4). Polyploid intestinal

nuclei appeared to contain more granules per nucleus than other cell types, but intestinal autofluorescence hindered precise quantification (data not shown). Granules formed within one minute during heat shock at 35°C and dispersed following an hour of recovery at 20°C (Figure 2-4). After recovery, HSF-1::GFP could re-form nuclear granules with subsequent heat shocks, although re-formation required a longer heat shock suggesting that stress granule formation exhibits adaptation (Figure 2-5). A decrease in the number of granules formed in a second heat shock after recovery has also been observed in human cells (Alastalo et al., 2003). Also like human granules, *C. elegans* HSF-1 granules from a second heat shock formed in locations similar to the initial granules, suggesting that another existing nuclear structure, such as DNA or RNA, acts as a scaffold for granule formation. When animals were grown at 16ºC, HSF-1::GFP formed granules at heat shock temperatures ≥ 28 ºC (Figure 2-6). Animals grown at 20ºC or 25ºC formed few or no granules at this temperature, but did form stress granules when exposed to ≥ 33ºC (Figure 2-6). This suggests that the induction of HSF-1::GFP granules by heat shock is adaptable and regulated by growth temperature. Together these data suggest that stress-induced HSF-1::GFP nuclear granules in *C. elegans* resemble human HSF-1 stress granules in their number, kinetics, re-formation, and reversibility.

We considered the possibility that the behavior of HSF-1::GFP may represent an artifact of the GFP tag. We therefore attempted to immunolocalize endogenous worm HSF-1 using a human antibody previously reported to recognize worm HSF-1 by immunoblot (Alavez et al., 2011; Volovik et al., 2012). Although we could detect human HSF1 expressed in worms, we were unable to immunolocalize *C. elegans* HSF-1::GFP with this antibody following heat shock (Figure 2-7). As an alternative approach, we generated

single-copy transgenic animals expressing an HA-tagged form of HSF-1. We inserted the HA tag into the HSF-1 protein between the predicted DNA binding and transactivation domains (Hajdu-Cronin et al., 2004). Like HSF-1::GFP, HSF-1::HA localized to the nucleus and re-distributed into granule-like structures following heat shock (Figure 2-1G-I). HSF-1::HA retained function, as measured by its ability to rescue an *hsf-1* mutant (Figure 2-8A). These data show that HSF-1 is a predominantly nuclear protein that undergoes rapid and reversible changes in subnuclear distribution in response to acute heat shock in *C. elegans*.

HSF-1::GFP is functional. We considered the possibility that the GFP fusion might disrupt HSF-1 protein function. We tested this by assessing the ability of HSF-1::GFP to rescue *hsf-1* mutant phenotypes. We also investigated the ability of a human HSF1::GFP protein to functionally substitute for *C. elegans* HSF-1. The *hsf-1(sy441)* allele introduces a stop codon at position 585 preceding the predicted C-terminal transactivation domain, and mutant animals exhibit temperature-sensitive growth arrest, reduced expression of HSP-16.2 after heat shock, shortened lifespan, and sensitivity to pathogens (Hajdu-Cronin et al., 2004; Singh and Aballay, 2006a). A second *hsf-1* allele, *ok600*, encodes a frameshifting deletion that eliminates potential regulatory and transactivation domains at the C-terminus of the HSF-1 protein (Figure 2-1A) and causes a 100% penetrant larval arrest phenotype at all growth temperatures, suggesting that *ok600* is a more severe allele than *sy441*. Whether the lethality of *ok600* is due to loss of *hsf-1* or another linked mutation has not been described. Single-copy worm *hsf-1p::hsf-1::GFP* rescued the temperature-dependent growth defects, temperature-dependent induction of HSP-16.2, lifespan reduction, and enhanced pathogen sensitivity of *hsf-*

1(sy441) mutants (Figure 2-8A-D). Unlike *hsf-1* overexpression transgenes, single-copy HSF-1::GFP did not cause increased longevity or enhanced pathogen resistance, suggesting that this transgene does not produce gain-of-function phenotypes like that observed for *hsf-1* overexpression (Figure 2-8C,D). HSF-1::GFP was also able to rescue the larval lethality associated with the *hsf-1(ok600)* allele, indicating that the *ok600* lethal phenotype is indeed due to loss of *hsf-1* function (Figure 2-8E,F). Human HSF1::GFP under the control of the *C. elegans hsf-1* promoter was expressed, properly localized to the nucleus, and capable of forming granules following heat shock (Figure 2-7, Figure 2-9A), albeit with substantially slower kinetics than those observed with worm HSF-1::GFP (1 hr of heat shock required for human HSF1::GFP versus 1 min for *C. elegans* HSF-1::GFP). Human HSF1::GFP behaved the same (no granule formation after 1 min, sparse granule formation after 1 hr of heat shock) when given a 42°C heat shock as with a 35°C heat shock, even though 35°C should be close to basal temperature for a human protein (data not shown). This observation is in agreement with the behavior of hHSF1 seen in other systems, where the activation temperature is determined by the host; for example, hHSF1 activates with a heat shock of 37°C when expressed in *Xenopus* (Baler et al., 1993; Zuo et al., 1994) and at 32-37°C in *Drosophila* cells (Clos et al., 1993). However, human HSF1::GFP was unable to rescue *hsf-1(sy441)* mutant phenotypes (Figure 2-9C-F), suggesting that worm and human HSF1 are not functionally interchangeable. These data show that, in addition to its roles in aging, *C. elegans hsf-1* is an essential gene required for larval development and that worm HSF-1::GFP, but not human HSF1::GFP, is functional and capable of rescuing *hsf-1*-associated mutant phenotypes in *C. elegans*.

HSF-1::GFP granules are dynamic and induced by specific environmental stressors. We next considered the possibility that HSF-1::GFP granules may simply be the result of protein aggregation caused by heat shock. We used fluorescence recovery after photobleaching (FRAP) to examine the mobility of the HSF-1::GFP protein within stress-induced nuclear granules. In contrast to protein aggregates induced by either stress or aging (Moronetti Mazzeo et al., 2012), puncta of HSF-1::GFP exhibited rapid recovery after photobleaching (Figure 2-10). Similar results have been shown for human HSF1 stress granules (Jolly et al., 1999). These data demonstrate that the HSF-1::GFP granules are not aggregates but rather are composed of dynamic HSF-1::GFP molecules.

In addition to heat shock, other environmental stressors, including cadmium and azetidine, induce the formation of HSF1 granules in human cells (Jolly et al., 1999). We asked if *C. elegans* HSF-1::GFP also forms nuclear granules in response to various environmental stressors. Exposure of HSF-1::GFP worms to osmotic stress (219 mM NaCl), heavy metals (100 μM cadmium), or ethanol (100 mM) did not induce granule formation (Figure 2-11D-F). However, exposure to sodium azide, a well known inhibitor of cytochrome oxidase and cellular ATP production and a commonly used anesthetic in the *C. elegans* field (Sulston and Hodgkin, 1988), induced robust HSF-1::GFP granule formation similar to that observed with heat shock (Figure 2-11B,C). Conditions that induced granule formation also activated *hsf-1*-dependent gene expression, as measured using a reporter transgene (*hsp-16.2p::GFP*) (Figure 2-11H-M). HSF-1::GFP granule formation can therefore be induced by elevated temperature or through azide-dependent inhibition of ATP production, demonstrating that heat shock *per se* is not required for granule formation.

Post-translational modification of HSF-1 temporally lags granule formation. Previous data from several species demonstrate that upon heat shock, HSF-1 is subject to a number of post-translational modifications (Åkerfelt et al., 2010). We asked if *C. elegans* HSF-1::GFP was similarly modified after heat shock. Consistent with other recent observations of HSF-1 in *C. elegans* (Chiang et al., 2012), HSF-1::GFP shifted towards a higher molecular weight in response to heat shock (Figure 2-12A), suggesting it is the target of stress-inducible post-translational modification (PTM). While previous studies showed that this PTM is due to phosphorylation (Chiang et al., 2012), we were unable to confirm this by phosphatase assay due to the extremely low abundance of the single-copy HSF-1::GFP protein (data not shown). The molecular weight shift was not apparent after one minute of heat shock but was detectable after 10 minutes of heat shock, thus temporally lagging the observed kinetics of HSF-1 stress granule formation (Figure 2-12B).

DNA binding promotes HSF-1 stress granule formation. Studies in human cells have established that human HSF1 nuclear stress granules do not represent the binding of HSF1 to HSEs in canonical HSF1 targets like HSP70 (Jolly et al., 1997), but rather HSF1 binding to and transcription of non-coding satellite II and III repeats, elements specific to primate genomes (Eymery et al., 2010; Jolly et al., 2002). Supporting this model, the DNA binding domain of HSF1 is required for stress granule formation in human cells (Jolly et al., 2002). To assess if DNA binding was also required for *C. elegans* HSF-1::GFP stress granules formation, we generated a point mutation (R145A, equivalent to human R71A, Figure 2-13A) in a completely conserved amino acid within the DNA binding domain that has been previously shown to be required for

HSF-1-HSE DNA binding (Inouye et al., 2004; Morley and Morimoto, 2004). We expressed this HSF-1(R145A) as a fusion with GFP under the native *hsf-1* promoter at single copy level. Like wild-type HSF-1::GFP, HSF-1(R145A)::GFP was expressed and localized to the nucleus; however, the ability of HSF-1(R145A)::GFP to form nuclear granules in response to acute heat shock was significantly reduced (Figure 2-13B-D). This suggests that DNA binding promotes HSF-1 granule formation in *C. elegans*.

As HSF-1 mutant phenotypes are probably due to an inability to transactivate target gene expression, we examined the ability of HSF-1(R145A)::GFP to rescue the *hsf-1* mutant alleles *ok600* and *sy441*. Because the *sy441* point mutation is viable and the *ok600* deletion allele lethal, *sy441* likely results in the expression of a partially functional protein, which is predicted to contain intact DNA binding and oligomerization domains but lack the putative C-terminal transactivation domain. Given that the active form of HSF-1 is thought to be a trimer (Baler et al., 1993), we hypothesized that the DNA binding-deficient HSF-1(R145A), which contains a functional transactivation domain, might be able to interact with the truncated *hsf-1(sy441*) protein and provide the missing transactivation function. Consistent with this model, *hsf-1(sy441)* animals expressing the HSF-1(R145A)::GFP transgene produced a marked increase in stress-inducible gene expression as compared to the *hsf-1(sy441)* background alone (Figure 2-13F), though quantification of this was difficult due to the very low levels of HSP-16.2 expression in *hsf-1(sy441)*. However, HSF-1(R145A)::GFP was unable to rescue the developmental functions of HSF-1 in either the *sy441* or *ok600* backgrounds (Figure 2-13E and data not shown). The ability of HSF-1(R145A)::GFP to partially rescue the stress-inducible phenotype of *hsf-1(sy441)* but not the developmental phenotype suggests that the

functional requirements for *hsf-1* in stress responses and development may be genetically separable.

HSF-1 granules in *C. elegans* colocalize with markers of active transcription. In human cells, HSF1 granules represent sites of HSF1 binding at satellite II and III repeats, colocalization with markers of active transcription such as phosphorylated RNA polymerase II and acetylated histones, and transcription of ncRNAs (Denegri et al., 2002; Jolly et al., 2002; Jolly et al., 2004; Metz et al., 2004). Because *C. elegans* contains little if any satellite repeat DNA sequences (Emmons et al., 1980; Sulston and Brenner, 1974), the putative site(s) of HSF-1 stress granule binding are unknown. Therefore, we asked whether worm HSF-1 stress granules also colocalized with general markers of active transcription. We stained control and heat shocked animals for either the phosphorylated serine 2 form of RNA polymerase II (RNA polII Ser2p) or the acetylated lysine 5 form of histone H2A (H2Aac), both of which have been used as markers of active transcription in human HSF1 stress granules (Jolly et al., 2004). Both of these markers showed colocalization with some (but not all) stress-induced HSF-1::GFP granules (Figure 2-14A-C, I-K, arrows). The overall number of H2Aac foci was significantly increased by heat shock, consistent with transcriptionally active HSF-1 granules being induced by stress (Figure 2-15). Although these data do not directly demonstrate transcriptional activity of HSF-1 within nuclear stress granules, they strongly suggest that active transcription is occurring at some sites of HSF-1 granule formation.

IGF and neuronal genetic pathways influence HSF-1 granule formation. Previous studies have shown that several genetic and physiological pathways require HSF-1 function. For example, extension of lifespan via activation of insulin signaling

requires HSF-1 activity (Hsu et al., 2003; Morley and Morimoto, 2004). Likewise, a recently described neuronal pathway regulates HSF-1-dependent gene expression (Prahlad et al., 2008; Prahlad and Morimoto, 2011). To determine if these pathways regulate HSF-1 in a way similar to that of heat shock, we examined the expression, localization, and stress-inducible behavior of HSF-1::GFP in the IGF mutant *daf-2(e1370)* and in the AIY neuron mutant *ttx-3(ks5)*. In *daf-2(e1370),* in the absence of stress, HSF-1::GFP localized to and was evenly distributed within the nucleus (of hypodermis, intestine and other cell types), as was previously observed in non-stressed wild-type animals (Figure 2-16E,F, and data not shown). Granule formation could still be induced, but quantification of granule formation revealed a statistically significant decrease in the number of granules induced by heat shock in a *daf-2(e1370)* background (Figure 2-16H) in hypodermal nuclei. The effect of *daf-2(e1370)* on granule formation in other tissues was more difficult to quantify due to the small size of the nuclei and autofluorescence, although stress-induced granule formation was observed (data not shown). Likewise, in the AIY interneuron mutant *ttx-3(ks5),* which has been previously shown to be required for non-neuronal heat shock-inducible gene expression, HSF-1::GFP remained localized to the nucleus in the absence of stress. Following heat shock of *ttx-3*, HSF-1::GFP continued to form stress granules in hypodermal nuclei (Figure 2-16D) and other cell types (data not shown). However, as with *daf-2*, the number of granules induced by heat shock in *ttx-3* animals was reduced (Figure 2-16G). These findings show that IGF and AFD signaling promote proper stress-inducible HSF-1::GFP granule formation but do not alter HSF-1::GFP nuclear localization in non-stressful

environments, suggesting that the mechanism(s) by which IGF signaling regulates HSF-1 is distinct from the mechanisms that regulate HSF-1 in response to heat shock.

Discussion

While much of the work demonstrating a functional role for HSF1 in the regulation of aging and diseases of protein aggregation has been carried out in *C. elegans,* there is still much to learn regarding the molecular properties of HSF-1 in this system or any organismal context. Our findings fill important gaps in our knowledge of HSF biology, provide new resources with which to study this conserved transcription factor, and describe insights into HSF-1 regulation in *C. elegans* that both concur with and contradict other recent studies (Chiang et al., 2012).

The major model for HSF1 regulation predicts it to be predominantly cytoplasmic under control conditions, constrained by interactions with cytoplasmic heat shock proteins (HSPs) (Voellmy and Boellmann, 2007). Following heat stress, HSPs are competed away by interactions with misfolded client proteins, allowing HSF1 to trimerize and translocate to the nucleus. While all studies agree that HSF1 is localized to the nucleus following stress, the localization of HSF1 prior to stress has been controversial. For example, *Drosophila* HSF is considered a constitutively nuclear protein (Westwood et al., 1991; Yao et al., 2006), but some studies have suggested that it is predominantly cytoplasmic and undergoes nuclear translocation with heat shock (Zandi et al., 1997). Likewise, human HSF1 has been reported both as a nuclear protein under all conditions (Martinez-Balbas et al., 1995; Mercier et al., 1999) and as a predominantly cytoplasmic protein that undergoes stress-induced nuclear translocation (Baler et al., 1993; Sarge et al., 1993). The reasons for these inconsistencies are unclear but may be

due to artifacts of overexpression or biochemical preparations that artificially place inactive HSF1 in the cytoplasm (Mercier et al., 1999). Recently, Chiang *et al*. reported that an HSF-1::GFP protein in *C. elegans* exhibited diffuse nucleo-cytoplasmic fluorescence under control conditions, converting to weak nuclear localization after heat shock (Chiang et al., 2012). This finding contrasts with our observations that HSF-1::GFP is a nuclear protein before and after stress. How can this discrepancy be explained? One possibility is that the HSF-1::GFP fusion protein differs between the two studies and these differing sequences alter localization. Both fusion proteins are derived from an HSF-1 cDNA fused with C-terminal GFP via different linker sequences. The presence of the GFP tag does not affect localization, since an HSF-1::HA protein exhibits similar nuclear localization to our HSF-1::GFP protein. Likewise, our linker sequences also do not affect localization, since an HSF-1::YFP protein lacking linkers similarly localized to the nucleus and formed granules with stress. It is possible that overexpression of HSF-1::GFP in the Chiang *et al.* study alters localization. High-level expression may overwhelm HSF-1 regulatory mechanisms, driving dysregulated HSF-1 into the cytoplasm. Such dysregulation would be unlikely to affect our HSF-1 reporter due to its physiological-level expression. This discrepancy could be best resolved by examining the localization of the endogenous HSF-1 protein, but such studies will require the generation of new antibodies that are compatible with immunofluorescence techniques in *C. elegans*.

One important new finding of our work is that heat shock induces *C. elegans* HSF-1 to form discrete subnuclear foci that are very similar to structures previously thought to occur only in primate cells. While *C. elegans* and human HSF-1 foci share

many characteristics (Table 2-1), we have not shown that all properties are shared between the two structures. For example, human HSF1 granules do not colocalize with standard HSF1 targets (Jolly et al., 1997) but rather with heterochromatic pericentromeric sat II and sat III repeats (Eymery et al., 2010; Jolly et al., 2004; Metz et al., 2004), where they promote the transcription of ncRNAs that remain associated with the stress granule. While we have shown the *C. elegans* HSF-1 granules involve DNA binding and are (in a subset) associated with transcription, we have not shown that such binding is distinct from the binding of HSF-1 to target promoters or that these binding sites are associated with the transcription of ncRNAs. Additionally, worms do not have centromeric sequences or satellite repeat DNA, so it remains possible that the specific properties of stress granule binding sites in *C. elegans* may be distinct from those in human cells. Despite these potential differences, it is also possible that the *C. elegans* stress granules are sites of centromere-independent ncRNA transcription. If so, *C. elegans* could provide important insights regarding the role of such ncRNAs in *hsf-1*-dependent processes. This is currently an important but unanswered question in the HSF1 field to which studies in *C. elegans* could make an important contribution.

Our data also suggest that the mechanisms regulating HSF-1 may not be the same in all contexts. In *C. elegans*, *hsf-1* has been primarily studied at the phenotypic level where it has roles in aging, immunity, and development. Prior to our work, it was not clear if these processes acted through mechanisms similar to those by which temperature regulates HSF-1 activity. We found that activation of HSF-1 via heat shock induces granule formation, but inactivation of insulin signaling via mutation of *daf-2* does not. It bears noting that we were able to induce granule formation with sodium azide,

demonstrating that heat shock itself is not required for granule formation. Like inhibition of insulin signaling, inhibition of AFD signaling via *ttx-3* mutation also does not constitutively induce or prevent granule formation, though it does reduce number of granules visible per nucleus. This observation could be due to a requirement of neuronal signaling for stress-induced granule formation, or possibly due to a decrease in total HSF-1, as HSF-1 levels were not quantified in this line. Altogether, our findings provide an alternative model to that proposed by Chiang *et al*. (Chiang et al., 2012) and suggest that insulin signaling and temperature might employ distinct mechanisms to control HSF-1 activity.

Consistent with the idea that multiple mechanisms may regulate HSF-1, we also found evidence that the activity of HSF-1 in development and heat shock are not two outcomes of a single activation pathway, but rather two mechanistically different activation pathways (Figure 2-17). Similar observations have been noted for *Drosophila hsf-1* (Jedlicka et al., 1997) and *C. elegans hsf-1*(Walker et al., 2003). We have built on these observations by showing that the DNA binding-deficient HSF-1(R145A) molecule could partially complement the transactivation-deficient *hsf-1(sy441)* mutant for stress-inducible gene expression but not for development. This could be explained through stress-specific oligomerization of HSF-1(R145A) and HSF-1(*sy441*) molecules, both of which possess intact putative trimerization domains, leading to an oligomer containing functional domains for both transactivation and DNA binding. An alternative possibility is that the R145A mutant may retain low levels of DNA binding activity that are sufficient to rescue *hsf-1* stress functions but not developmental functions. Regardless, the fact that HSF-1(R145A) is incapable of rescuing development strongly suggests that

HSF-1 has transcriptional targets even in the absence of stress. Such targets may even be transcribed by monomeric HSF-1, likely the predominant form in the absence of stress (Figure 2-17). Further testing of this model, using more precise deletion alleles that eliminate specific HSF-1 functional domains, is called for.

In conclusion, we have provided new *in vivo* insights into the regulation of HSF-1 in *C. elegans* and its mechanism of regulation by heat shock, including a potentially evolutionarily conserved subnuclear behavior that was previously thought to be present only in primates. Expression of epitope-tagged, physiological levels of HSF-1 *in vivo* offers new experimental opportunities to understand how this protein integrates development, stress, aging, and metabolic pathways in a live organism setting to determine condition-specific gene expression.

Materials and Methods

C. elegans strains and culture

The following strains and alleles were used in this study: N2, EG4322 *ttTi5605;unc-119(ed9)*, PS3551 *hsf-1(sy441)*, CB1370 *daf-2(e1370)*, FK134 *ttx-3(ks5)*, VC3071 *hsf-1(ok600)/hIn1[unc-101(sy241)]*, UP1459 *hDF10/hT2[bli-4(e937) let-?(q782) qIs48]*, TJ375 *gpIs1[hsp-16.2p::GFP::unc-54utr]*, OG153 *unc-119(ed3);drEx206[hsf-1p::genomic hsf-1::YFP::unc-54utr;unc-119+]*, OG497 *drSi13[hsf-1p::hsf-1::GFP::unc-54utr;Cb-unc-119+];unc-119(ed9)*, OG496 *drSi12[hsf-1p::human hsf-1::GFP::unc-54utr;Cb-unc-119+];unc-119(ed9),* OG566 *drSi28[hsf-1p::hsf-1(R145A)::GFP::unc-54utr;Cb-unc-119+];unc-119(ed9)*, OG636 *drSi41[hsfp-1p::hsf-1::HA::unc-54utr;Cb-unc-119+];unc-119(ed9)*, OG576 *hsf-1(ok600)/hT2[bli-4(e937) let-?(q782) qIs48]*, OG575 *hsf-1(ok600)/hT2[bli-4(e937) let-?(q782)*

qIs48];drSi13, OG574 *hsf-1(ok600);drSi13*, OG529 *drSi13;ttx-3(ks5)*, OG537 *drSi13;daf-2(e1370)*, OG532 *hsf-1(sy441);drSi13*, OG528 *hsf-1(sy441);drSi12*, OG584 *hsf-1(ok600)/hT2[bli-4(e937) let-?(q782) qIs48];drSi28*, OG580 *hsf-1(sy441);drSi28*, OG646 *hsf-1(sy441);drSi41*. *ok600* encodes a deletion that removes sequence from nucleotide 4212 to 5088 (marked from the A of the start codon of genomic *hsf-1*). This gives rise to an 877 bp deletion, rather than the Wormbase reported 1085 bp deletion (flanking sequences of the *ok600* deletion - 5'-AAATAAAAATTTCTTAGAA [877 bp deletion] ATGTACATGGGATCCGGTCCA-3'). The resulting cDNA is predicted to frame shift and lead to an early stop codon. The genotypes of all strains were confirmed with PCR or DNA sequencing during crosses. Worms were maintained on standard NGM medium with OP50 bacteria, except for EG4322, which was maintained on HB101.

Molecular biology methods

Four kb of genomic sequence upstream of the *hsf-1* start ATG (inclusive) was PCR amplified from *C. elegans* N2 genomic DNA with added attB sites and cloned into the Gateway promoter vector pDONRP4-P1R (primers OG371 and OG937; plasmid pOG88). *C. elegans hsf-1* cDNA was cloned from EST clone yk609a8 into Gateway entry clone pDONR221, including the start and stop codons (primers OG289, OG290, followed by PCR with attB adaptor primers OG78 and OG79; plasmid pOG37). The first base pair of the start codon and last two of the stop codon were deleted by site-directed mutagenesis (QuikChange II Kit, Cat. #200523) in order to put the clone in frame for Gateway (primers OG396, OG400, OG475, OG476; plasmid pOG34). GFP with the 3' UTR of *unc-54* was cloned from pPD95.75 (which contains synthetic introns) into

Gateway cloning vector pDONRP2R-P3 (OG949, OG950; plasmid pOG99). Human *hsf-1* was recombined from BC014638 from the human ORFeome collection (Open Biosystems). The HA tag was inserted into *C. elegans* HSF-1 between amino acids 370 and 371 (as counted from the start methionine of HSF-1) by PCR in two parts, using pOG34 as the template and primers containing the HA tag (M13 primer in the vector plus OG793, and T7 reverse primer in the vector plus OG790). These two fragments were combined by PCR fusion and attB sites were added using primers OG745 and OG746; the product was recombined into pDONR221 to create plasmid pOG142. The HSF-1(R145A) entry clone (pOG123) was created by site-directed mutagenesis (QuikChange II Kit, Cat. #200523) of pOG34. Plasmids for injection were created by Invitrogen Multisite Gateway recombination reactions of the above promoter, human or worm *hsf-1* coding sequence, and GFP tag into pCFJ150 (creating plasmids pOG113 (*C. elegans* HSF-1::GFP), pOG108 (human HSF1::GFP), or pOG124 (*C. elegans* HSF-1(R145A)::GFP) or the above promoter, HSF-1::HA entry clone, and pCM5.37 (*unc-54* 3' UTR in pDONRP2R-P3) into pCFJ150 creating pOG144 (*C. elegans* HSF-1::HA). Though translated *att* linker sequences are present in the above clones, these do not appear to affect worm HSF-1::GFP in either localization or granule formation. We confirmed this by using PCR and *in vivo* recombination to fuse 6 kb of the *hsf-1* promoter followed by the genomic version of *hsf-1* to YFP with the *unc-54* 3' UTR and expressed this as an extrachromosomal array. Six kb upstream of *hsf-1* through the first intron was amplified (OG275 and OG282) from N2 genomic DNA, as was *hsf-1* coding region after the first exon (OG280 and OG274. OG274 contains overlapping YFP sequence). YFP followed by the *unc-54* 3' UTR was amplified from pPD132.102 (OG273 and OG23) and

added to the *hsf-1* genomic product by PCR fusion. The fragments of *hsf-1* promoter and *hsf-1*::YFP were coinjected for *in vivo* recombination, along with an *unc-119*-rescuing plasmid (MM051) into an *unc-119(ed3)* mutant. Plasmids for protein expression were created by Invitrogen Gateway recombination into the expression vector pDEST17 (containing an N-terminal 6XHis tag) using human *hsf-1* cDNA BC014638 or worm *hsf-1* cDNA with an intact stop codon (creating plasmids pOG143 and pOG20, respectively). All primer sequences are available in Table 2-2.

Single-copy injection

Single-copy transgenetic strains were produced as in Frøkjær-Jensen *et al.* 2008. Strain EG4322 was maintained at 16°C on HB101. This strain contains the Mos1 insertion allele on chromosome II and the *unc-119(ed9)* allele. Young adults were injected with a mix of the single-copy insertion plasmid (*hsf-1* cDNA in pCFJ150 at 50 ng/µL), pGH8 (*rab-3p::mCherry* at 10 ng/µL), pCFJ90 (*myo-2p::mCherry* at 2.5 ng/µL), pCFJ104 (*myo-3p::mCherry* at 5 ng/µL), and pJL43.1(*glh-2p::transposase* at 50 ng/µL. In the case of *drSi41*, *eft-3p::transposase* was used instead). Injected worms were allowed to recover at 16°C for at least an hour and then individually picked to HB101 plates and put at 25°C until starved. Non-red, moving worms were selected and their progeny were singled to isolate homozygotes (no unc progeny). Only one homozygous line was selected from any single injected P0. Homozygous lines were grown to starvation on 10cm plates and genomic DNA prepared via phenol/chloroform extraction. Single-copy insertion was confirmed by PCR amplification of the region using primers just outside the recombination region (OG 967 and OG970, see Table 2-2). PCR products of the correct size were verified by restriction digest.

Microscopy

Worms were anesthetized in 1 mM levamisole in M9 unless otherwise stated and imaged on 2% agarose pads. All images (with the exception of the FRAP studies, Figure 2-8E and Figure 2-11H-M,) were collected as Z-stacks on a Leica DMI4000 with a 63X lens and deconvolved (10 iterations, 16-bit, blind, with background removed) using Leica software. Images in Figure 2-11H-M were collected on the same microscope, but with a 10X lens and not deconvolved. With the exception of Figure 2-2 (in which raw images were quantified), all quantification of granules was done after deconvolution, using hypodermal and/or seam cell tail nuclei (4-15 nuclei assessed per worm). All worms for live fluorescence imaging were grown at 20°C (unless otherwise noted) and were L4 the day before imaging. During comparisons of worms grown at different temperatures, L4s were picked at different times throughout the day (such that 16°C worms had 6-8 hours more growth than 25°C). To obtain percent of nuclei with granules, nuclei were scored as "granulated" if they had at least one granule, which is defined as fluorescent puncta that are distinguishable from surrounding fluorescence on all sides. The fraction of nuclei with at least one granule for each worm was averaged among all worms to get the mean ± SEM for each sample. For quantification of number of granules per nucleus in Figure 2-16 and quantification of percent nuclei with granules in Figure 2-6, the experimenter was blinded to genotype. Assays of *drSi13;ttx-3(ks5)* and the corresponding control *drSi13* were performed on worms grown under sparse growth conditions, as previously described (Prahlad et al., 2008; Prahlad and Morimoto, 2011), and imaged 24-25 hr after being picked as L4. Quantification of total nuclear GFP (for Figure 2-2) was done on non-deconvolved, 16-bit images, using ImageJ to take the mean

grayscale value for a nucleus before and after heat shock (1 min or 20 min at 35°C), or before and after a mock heat shock (1 min or 20 min at 20°C), to correct for photobleaching (the mean difference in fluorescence after mock heat shock was added to all of the post-heat shock values). Heat shocks for imaging were performed with worms anesthetized on slides and incubated on an aluminum heat block (at 35°C 1 minute unless otherwise stated), with the exception of heat shock for Figure 2-11, which was done on worms anesthetized in 1 mM levamisole on a watch glass slide pre-heated to 35°C and kept on an aluminum heat block for 30 min, and for Figure 2-12B, for which worms were grown at 16°C and the 10 min and 20 min heat shocks were done in 1 mM levamisole on a watch glass slide in a 35°C incubator. FRAP studies were conducted on a Zeiss LSM 510 using a 1.2NA water immersion 40X lens. Four samples were observed after 1 min 35°C heat shock, and five samples were observed after 5 min 35°C heat shock. Photobleaching utilized 50 iterations of a 488nm laser at 50% power.

Lifespan and immunity assays

For lifespan assays, worms grown at 20°C were picked as L4 and allowed to grow at 20°C until the next day, when 10 young adults were placed on five 3 cm plates. Lifespan assays were performed with concentrated OP50 spotted on NGM plates containing 50 μM FUdR at 25°C. *Pseudomonas* (PA14) survival assays were performed as previously described (Singh and Aballay, 2006a) with the addition of FUdR to the growth media and use of worms grown at 20°C. Lifespan and immunity assays were conducted at 25°C and replicated at least twice. Worms were classified as alive, dead (no movement in response to touch with a wire), or censored (lost or bagged worms) twice a day during *Pseudomonas* assays (starting on day 2) and once a day for lifespan assays.

Immunoblotting

Protein samples were obtained for HSF-1::GFP detection by washing synchronized young adult worms grown 4 days at 16°C off plates with 16°C M9. Worms were pelleted (2000 rpm 1 min) and the pellet distributed in 20-25 µL aliquots to 1.5 mL tubes, which were incubated either in a 35°C heat block (heat shock) or in a 16°C incubator (non-heat shock). After incubation, samples were flash frozen in liquid nitrogen. 2X SDS-PAGE loading buffer was added to the samples which were then boiled for >15min before loading. Samples for HSF-1::GFP molecular weight shift Westerns were run on a 7.5% SDS-PAGE gel (Figure 2-12A) or a 5% Tris-HCl gel (Bio-Rad, Figure 2-9B); both were transferred to a nitrocellulose membrane. Membranes were blocked with 2% milk in 1X TTBS for 1.5 hr, then probed with Roche anti-GFP mouse (7.1 and 13.1, 1:1000 dilution) and anti-β-actin mouse (Sigma, AC-15, 1:2000 dilution) primary antibodies overnight, followed by incubation with anti-mouse HRP-linked Cell Signaling Technology secondary antibody (1:2000 dilution). Immunoblots for HSP-16.2 expression were performed on samples of 15-25 young adult worms (grown at 16°C and picked as L4 the previous day onto 6 cm plates). One plate of each line was heat shocked for 3 hr in a 35°C incubator, followed by a 3 hr recovery at 16°C. A matching plate was left at 16°C for the full 6 hr period (no heat shock control). Plate lids were left slightly ajar for the first 5 hours of the time period for both sets of samples. Worms were collected into a 20µL volume of M9, 2X SDS-PAGE loading buffer was added, and samples were boiled ≥15 min. Samples were loaded on a 10-20% Tris-HCl gel (Bio-Rad) and transferred to a nitrocellulose membrane, which was probed simultaneously with rabbit anti-HSP-16.2 (1:5000 dilution, #5506 R120; kind gift of Chris Link, UC

Boulder) and mouse anti-β-actin (1:2000 dilution, Sigma, AC-15). Secondary antibodies used were anti-mouse HRP (as above) and anti-rabbit HRP (1:5882 dilution, Amersham). Bands were visualized with a Thermo Scientific chemiluminescent substrate detection system (Prod. #34080). Western results were replicated at least twice. Quantification of bands was performed using ImageJ software; the intensity of the HSP-16.2 band divided by the intensity of the actin band was calculated for each lane, and normalized to the WT heat shock lane.

Immunoblots of bacterial HSF-1 protein were run on lystates of BL21 cells expressing either human or worm *hsf-1* cDNA N-terminally tagged with 6XHis in pDEST17. Five milliliters cultures were inoculated with 200µL of overnight culture, allowed to grow to a density of ~ 0.6 OD_{600}, induced with 50µL 20% L-arabinose, and allowed to grow 4 more hours at 37°C. Equivalent amounts of each culture (based on final OD_{600}) were spun down, resuspended in 25µL ICB followed by addition of 25µL 2x SDS-PAGE loading dye and boiling for 10 min. Five microliters of each sample (+/- induction) were run on duplicate 7.5% SDS-PAGE gels. One gel was stained overnight with Coomassie blue and one was transferred to a nitrocellulose membrane. The membrane was blocked with milk and then probed with a commercial polyclonal anti-human HSF1 antibody overnight. The antibodies used were: Calbiochem (#385580) at 1:5000 (following a block of 5% milk for 1 hr) or Enzo Life Sciences (SPA-901) at 1:1000 (following a block of 2% milk for 1.5 hr). The secondary antibody was anti-rabbit, as above.

Immunofluorescence

Worms were dissected and stained for immunofluorescence with the following protocol: adult worms (picked as L4 the day before, grown at 25°C for Figure 2-1, 20°C for Figure 2-7) were picked to a watchglass slide of either 25°C (for no heat shock samples in Figure 2-1) or 35°C (for heat shock samples) M9, and then placed in an incubator of the corresponding temperature. Slides were kept inside a container with a moist paper towel to maintain humidity. After the heat shock interval (30 min, 1 hr, 1.5 hr, or no interval for no heat shock samples in Figure 2-7), worms were picked to 100 mM K_2HPO_4, after which a 28G syringe needle was used to dissect them, exposing their intestines. Dissected worms were picked to 3% paraformaldehyde (diluted in 100 mM K_2HPO_4), incubated in a room-temperature humid chamber 1 hr, washed five times for five minutes with BT buffer (20 mM H_3BO_3, 10 mM NaOH, 0.5% Triton X-100), permeabilized with BTB buffer (BT buffer, 2% β-mercaptoethanol), incubated in a room-temperature humid chamber 1 hr, washed once for 5 minutes with BT, twice for 5 minutes with AbA buffer (1X PBS, 0.5% BSA, 0.5% Triton X-100, 10 mM sodium azide), incubated in AbA in a room-temperature humid chamber 1 hr, and then placed in 200µL primary antibody diluted in AbA. Samples were left in primary antibody in a 4°C humid chamber overnight. Primary antibodies used were: mouse anti-HA (clone 16B12, Covance MMS-101R, 1:1000) for Figure 2-1; rabbit anti-human HSF1 (Stressgen SPA-901, 1:100 in Figure 2-7E-L, 1:2000 in Figure 2-7A-D) and mouse anti-GFP (Roche 7.1 and 13.1, 1:500) for Figure 2-7; rabbit anti-acetyl-histone H2A (Lys5) (Cell Signaling #2576, 1:150) and mouse anti-GFP (Roche 7.1 and 13.1, 1:500) for Figure 2-14A-H; mouse anti-RNA polymerase II phosphorserine 2 (clone H5, Covance MMS-129R,

1:300) and Alexa 488-conjugated rabbit anti-GFP (Invitrogen A21311, 1:500) for Figure 2-14I-P. On the second day, samples were washed five times for five minutes with AbA, incubated in the appropriate secondary antibodies (Invitrogen A21207 donkey α rabbit Alexa 594, A10680 goat anti-mouse Alexa 488, A21203 donkey anti-mouse Alexa 594) at 1:1000 in AbA in a 4°C humid chamber 2 hr, washed three times for five minutes in AbA, once for 10 minutes in AbA with 1 µg/mL Hoechst dye, and washed once again for five minutes with AbA. After the last wash, worms were picked into a drop of ProLong Gold (Invitrogen P36934), covered with a cover slip, and imaged the following day. H2Aac staining distribution was assessed by a MATLAB program that used the Hoechst staining to identify the nucleus, then binned pixels of the H2Aac stain 3x3 (in order to smooth out artifacts of pixel-to-pixel variation). The mean intensity of nuclear H2Aac staining was calculated, and anything below one standard deviation above the mean was subtracted from the image. The number of discrete objects left was counted as an approximation of the number of H2Aac puncta. The MATLAB script used in these studies is available upon request.

RNA isolation and qRT-PCR

Synchronized L1s were grown at 20°C for 3 days. Adults were washed off with M9 and counted and collected using a COPAS Biosort. Worms were centrifuged briefly and brought down to a volume of ~100µL, to which 400µL TRIzol was added (Ambion, Cat. no. 15596-018) and the samples were frozen. After three freeze-thaw cycles, 200µL TRIzol was added, followed by a 5 min room temperature incubation, addition of 140µL choloroform, vigorous shaking, and a 2 min incubation. Samples were centrifuged at 12,000 x g for 15 min at 4°C and the aqueous phase was moved to a new tube. From this

point, RNA was isolated as described by the TRIzol reagent protocol. RNA was treated with TURBO DNase (from Ambion kit AMM1340) 2 μL DNase in 40 μL RNA sample, 15 min 37°C. An equal volume of 70% ethanol was added and purification was finished using RNeasy columns (Qiagen, Cat. no. 74106), following the animal tissue RNA purification protocol. cDNA was generated using the Applied Biosystems High Capacity cDNA Reverse Transcription kit (Part no. 4368814). cDNA was diluted to 2.5 ng/μL, 9μL of which was used in each 20μL SYBR Green qPCR reaction (Qiagen, Cat. no. 330522). Primers for *act-2* and *hsf-1* are in Table 2-2. Quadruplicate technical replicates were run.

Statistical analysis

Survival studies were analyzed using the Kaplan-Meier log-rank function (GraphPad Software) (Table 2-3). Comparisons of means were analyzed with either a two-tailed Students t-test (2 groups) or ANOVA (3 or more groups) using Bonferroni post-test analysis. A paired t-test was used in Figure 2-2, others were unpaired. p-values of < 0.05 were considered significant.

Acknowledgements

We thank Aaron Gitler for the human *hsf-1* clone, Chris Link for the HSP-16.2 antibody, Peter Klein and John Murray for immunofluorescence antibodies, Meera Sundaram and the CGC for strains. This work was supported by NIH training grant T32 GM07229 (E.A.M.) and by NIH grant R01AA017580 (T.L.). Some nematode strains used in this work were provided by the Caenorhabditis Genetics Center, which is funded by the NIH National Center for Research Resources (NCRR).

HSF1 Stress Granule Property	Human	*C. elegans*
Reversible	✓	✓
Number per nucleus	6.8[1]	7.1
Size	0.5-3.0μ[1]	~0.6μ
Dynamic	✓	✓
Stressors that induce	Heat, azetidine, Cd^{2+}	Heat, azide
Reform in similar location	✓	✓
Transcriptionally active	✓	✓
Binds centromeric DNA	✓	N/A
Transcribes ncRNA	✓	?
Associates with splicing factors	✓	?

Table 2-1. Comparison of HSF-1 stress granule properties between human cells and *C. elegans*

1 - from Cotto et al, 1997

Oligo Name	Oligo Sequence	Purpose
OG23	AAGGGCCCGTACGGCCGACTAGTAGG	Reverse primer for *unc-54* 3' UTR
OG78	GGGGACAAGTTTGTACAAAAAAGCAGGCT	attB1 adapter primer
OG79	GGGGACCACTTTGTACAAGAAAGCTGGGT	attB2 adapter primer
OG275	ATTGCAATCTTCCGCTCGGTTTCC	Forward primer 6 kb upstream of *hsf-1* start
OG280	GCTGAAATTTGAAGAAAATAGCCCA	Forward after first *hsf-1* exon
OG282	GAGCCAATTCACTAGAAAAATCCGGCG	Reverse after first *hsf-1* intron
OG289	AAAAAAGCAGGCTATGCAGCCAACAGGGAATCA	*hsf-1* forward with start codon plus partial attB1
OG290	AAGAAAGCTGGGTTTAAACCAAATTAGGATCCG	*hsf-1* reverse with stop codon plus partial attB2
OG371	GGGGCAACTTTGTATAGAAAAGTTGGAATCGGCCCGGCAAGTGGTAC	*hsf-1* promoter forward plus attB4 (upstream 3998 bp from ATG)
OG396	CCAACTTTGTACAAAAAAGCAGGCTTGCAGCCAACAGG	Mutagenesis for deleting start A in *hsf-1* (sense)
OG400	CCTGTTGGCTGCAAGCCTGCTTTTTTGTACAAAGTTGG	Mutagenesis for deleting start A in *hsf-1* (antisense)
OG475	AGTCCATCGGATCCTAATTTGGTTTACCCAGCTTTCTT	Mutagenesis for deletion of stop in *hsf-1* (sense)
OG476	AAGAAAGCTGGGTAAACCAAATTAGGATCCGATGGACT	Mutagenesis for deletion of stop in *hsf-1* (antisense)
OG535	CCCAATCCAAGAGAGGTATCCTT	qRT-PCR primer for *act-2*, forward
OG536	GAAGCTCGTTGTAGAAAGTGTGATG	qRT-PCR primer for *act-2*, reverse
OG611	TATGTACGGCTTCCGAAAGATGA	qRT-PCR primer for *hsf-1*, forward
OG612	TCTTGCCGATTGCTTTCTCTTAA	qRT-PCR primer for *hsf-1*, reverse
OG745	GGGGACAAGTTTGTACAAAAAAGCAGGCTTGCAGCCAACAGGGAATCA	*hsf-1* forward without start codon plus attB1
OG746	GGGGACCACTTTGTACAAGAAAGCTGGGTAAACCAAATTAGGATCCG	*hsf-1* reverse without stop codon plus attB2
OG937	GGGGACTGCTTTTTTGTACAAACTTGTCATTTTACGAACTAGCAC	*hsf-1* promoter reverse attB1R (with ATG in frame)
OG949	GGGGACAGCTTTCTTGTACAAAGTGGCAATGAGTAAAGGAGAAGAACT	GFP plus attB2R forward
OG950	GGGGACAACTTTGTATAATAAAGTTGAAACAGTTATGTTTGGTATA	*unc-54* 3' UTR plus attB3 reverse
OG967	AGGCAGAATGTGAACAAGACTCG	Outside of left arm of MosSCI recombination site
OG970	ATCGGGAGGCGAACCTAACTG	Outside of right arm of MosSCI recombination site
OG1055	AGGCAAAGCTCAGCTGATGATATTG	Outside deletion *hsf-1(ok600)* (intronic) forward
OG1057	AAAGCCAATAATTGGGCGGAGC	Outside deletion *hsf-1(ok600)* (intronic) reverse
OG1156	CATAACAATATGAATAGCATGGTCGCTCAGTTGAATATGTACGGCTTCCGA	Mutagenesis for *hsf-1* R145A (sense)
OG1157	TCGGAAGCCGTACATATTCAACTGAGCGACCATGCTATTCATATTGTTATG	Mutagenesis for *hsf-1* R145A (antisense)

Table 2-2. Primers

Trial	Strain	Mean Lifespan*‡ (Days ± SEM)	Number of Worms	p-value vs. N2	p-value vs. *hsf-1(sy441)*
1	N2	11.3 ± 0.5	46/50		<0.0001
	hsf-1(sy441); drSi13[wormHSF-1::GFP]	9.9 ± 0.3	35/50	<0.0001	<0.0001
	hsf-1(sy441)	4.9 ± 0.3	41/50	<0.0001	
2	N2	10.5 ± 0.6	33/50		<0.0001
	hsf-1(sy441); drSi13[wormHSF-1::GFP]	10.4 ± 0.3	32/50	0.0036	<0.0001
	hsf-1(sy441)	5.2 ± 0.3	44/50	<0.0001	
1	N2	8.6 ± 0.3	49/50		<0.0001
	hsf-1(sy441); drSi12[humanHSF1::GFP]	5.0 ± 0.4	48/50	<0.0001	0.6048
	hsf-1(sy441)	5.6 ± 0.2	50/50	<0.0001	
2	N2	10.5 ± 0.3	50/50		<0.0001
	hsf-1(sy441); drSi12[humanHSF1::GFP]	5.3 ± 0.3	46/50	<0.0001	0.737
	hsf-1(sy441)	5.1 ± 0.4	41/50	<0.0001	

Table 2-3. Statistics for HSF-1::GFP rescue of *hsf-1(sy441)* lifespan

*Excludes censored worms.

‡ Lifespan assays were done at 25°C

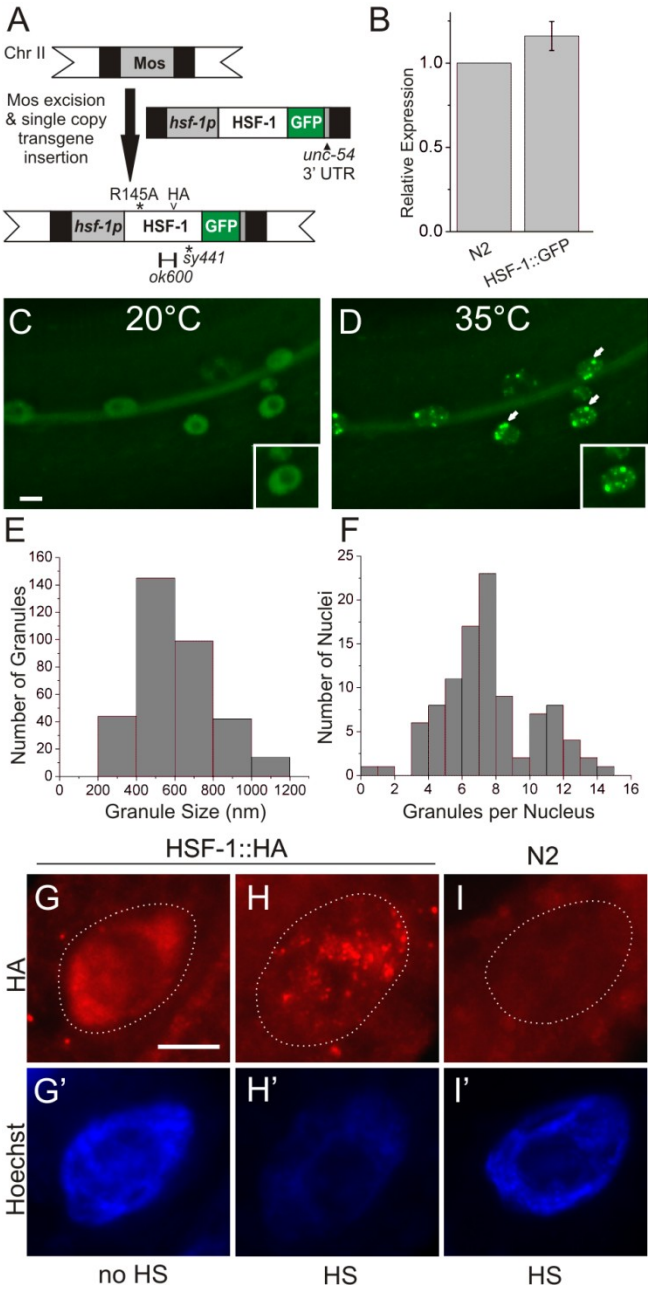

Figure 2-1. HSF-1::GFP is broadly expressed and condenses into nuclear granules following heat shock

(A) Diagram of the *hsf-1p::hsf-1(cDNA)::GFP::unc-54 3'UTR* expression construct (*drSi13*) used in this study. *hsf-1p* is 4 kb of sequence upstream of the *hsf-1* start ATG. Notations above the construct diagram indicate changes made to the transgene (R to A at residue 145 and HA insertion after residue 370); notations below indicate relative

positions of mutations in the endogenous gene (diagram not to scale.) (B) qRT-PCR comparing wild type (N2) and HSF-1::GFP *hsf-1* mRNA levels relative to actin mRNA, normalized to N2. Shown is the mean relative expression ± SEM in *drSi13* for three independent experiments. *hsf-1* mRNA in a wild-type background is less than double control wild type, suggesting compensatory mechanisms acting on *hsf-1* expression. (C) HSF-1::GFP localizes primarily to the nucleus at 20°C. (D) After 1 min of 35°C heat shock, HSF-1::GFP collects into nuclear puncta (arrows). Shown are four merged (Z-dimension) deconvolved slices depicting hypodermal nuclei. Scale bar = 5µm. (E) HSF-1::GFP granule size in hypodermal cells after 1 min 35°C heat shock (N = 349 granules). (F) Number of HSF-1::GFP granules per cell in hypodermal cells after 1 min 35°C heat shock. (N = 100 nuclei). (G-I) *drSi41*, a single-copy line expressing *hsf-1p::hsf-1::HA::unc-54 3'UTR*, in which the HA tag is inserted into the region between the putative trimerization and transactivation domains of the *hsf-1* cDNA. *drSi41* worms were either heat shocked (G, 30 min at 35°C) or not (F, 30 min at 25°C), dissected, fixed, probed for HA (red, G-I), and stained with Hoechst dye (blue, G'-I'). Heat shocked N2 worms are shown as a control (I). Shown are nine merged (Z-dimension) deconvolved slices. Dotted line indicates outline of nuclei as determined by Hoechst. Scale bar = 5 µm.

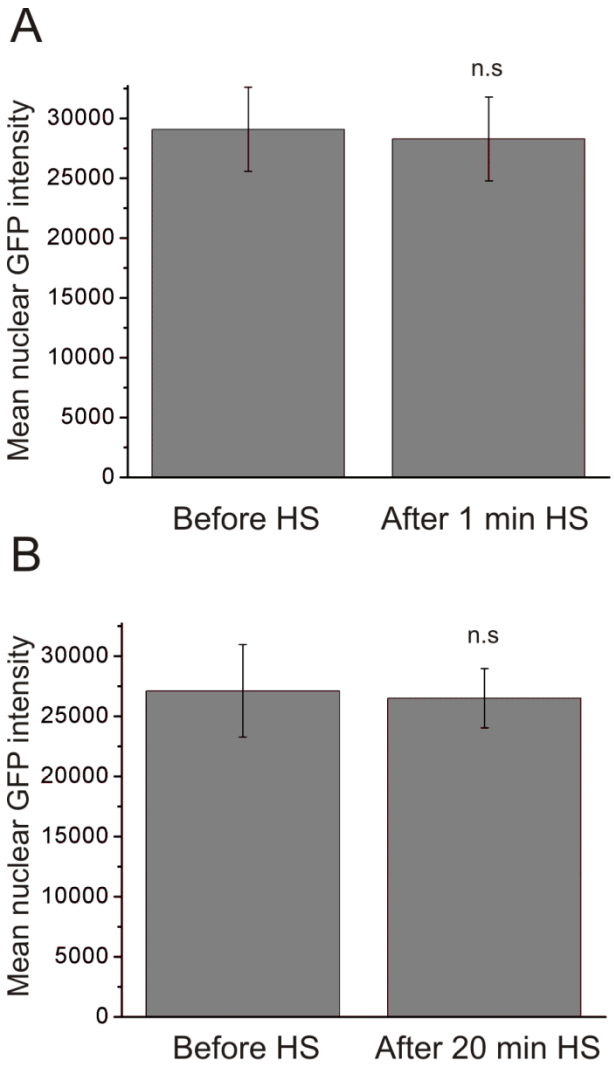

Figure 2-2. The levels of nuclear HSF-1::GFP are not significantly increased in response to heat shock

Mean intensity of HSF-1::GFP in the nucleus was quantified before and after 1 min (A, N = 40, representing 11 worms) or 20 min (B, N = 60, representing 11 worms) 35°C heat shock. Post-heat shock mean was corrected for photobleaching effect, as described in 'Methods.' (Mean ± SD, n.s. - not significant, paired t-test.)

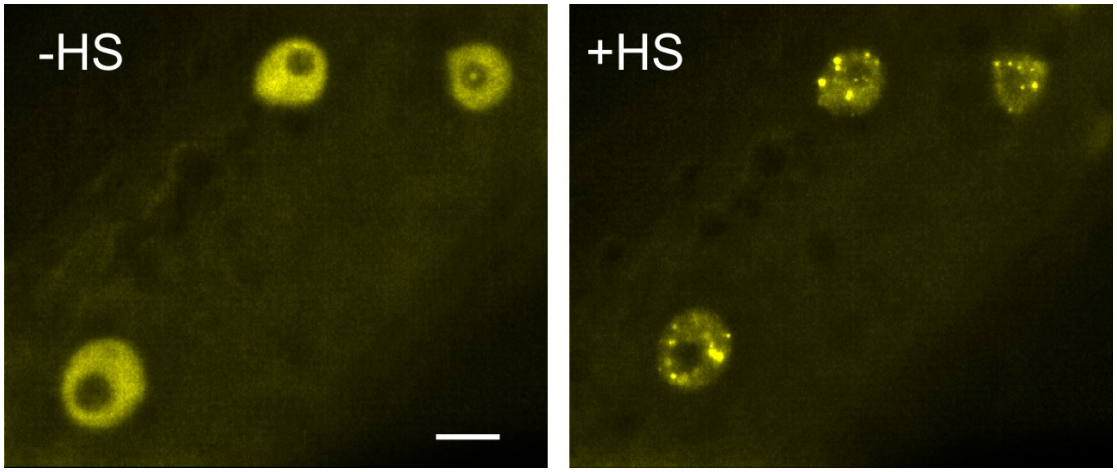

Figure 2-3. HSF-1::YFP localization is not affected by absence of Gateway *att* linker sequences

The *hsf-1* promoter (6 kb) and genomic DNA were fused to YFP and the *unc-54* 3'UTR through PCR and *in vivo* recombination to generate a multicopy array. The resulting transgenic protein utilizes the endogenous *hsf-1* start codon and fuses to YFP without any linker sequences. As with the Gateway-cloned HSF-1::GFP single-copy protein, the HSF-1::YFP protein exhibits strong nuclear localization pre-heat shock (left) and forms stress granules after 1 minute of a 35°C heat shock (right). Scale bar = 5μm.

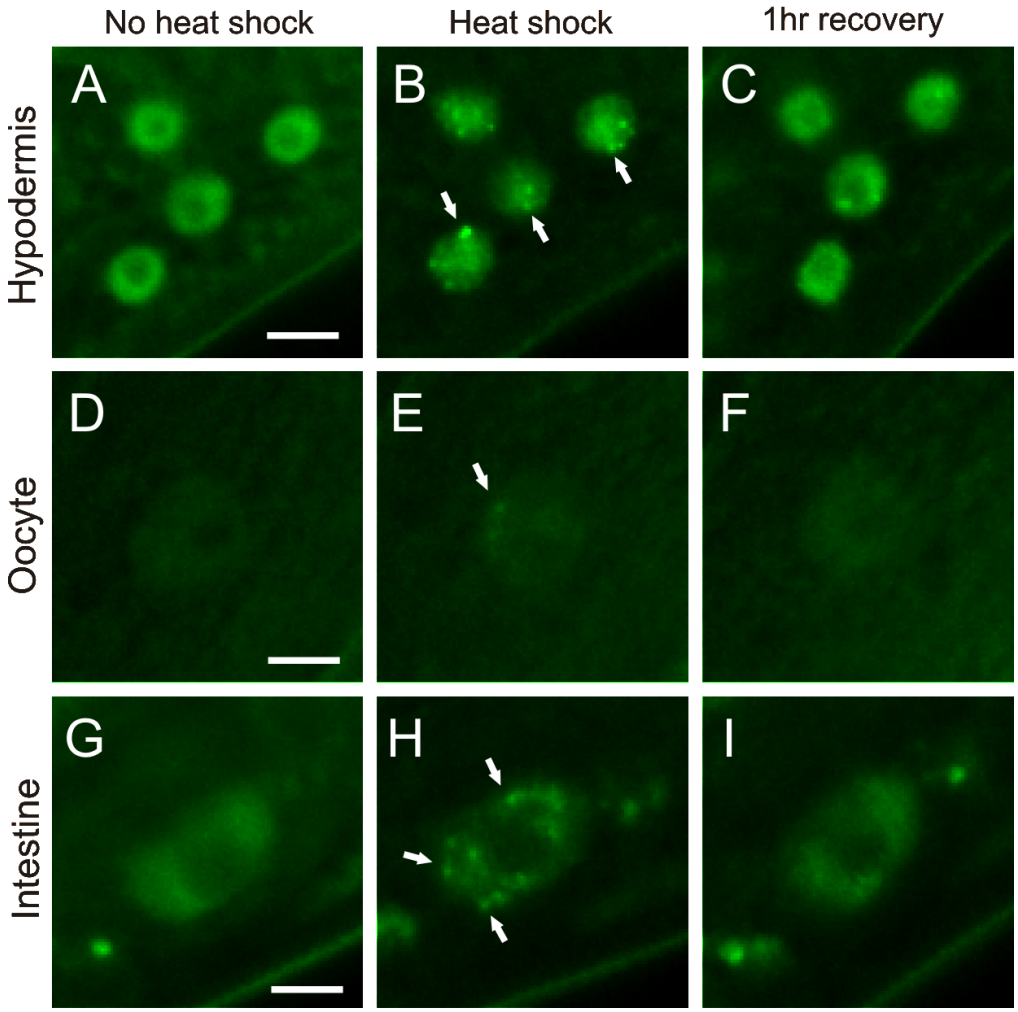

Figure 2-4. HSF-1::GFP is expressed and forms granules in multiple cell types

Images of hypodermal (A-C), oocyte (D-F), or intestinal (G-I) nuclei in *drSi13* HSF-1::GFP worms before heat shock (A,D,G), following 1 min heat shock at 35°C (B,E,H), and following recovery at 20°C for 1 hour (C,F,I). Scale bar = 5μm.

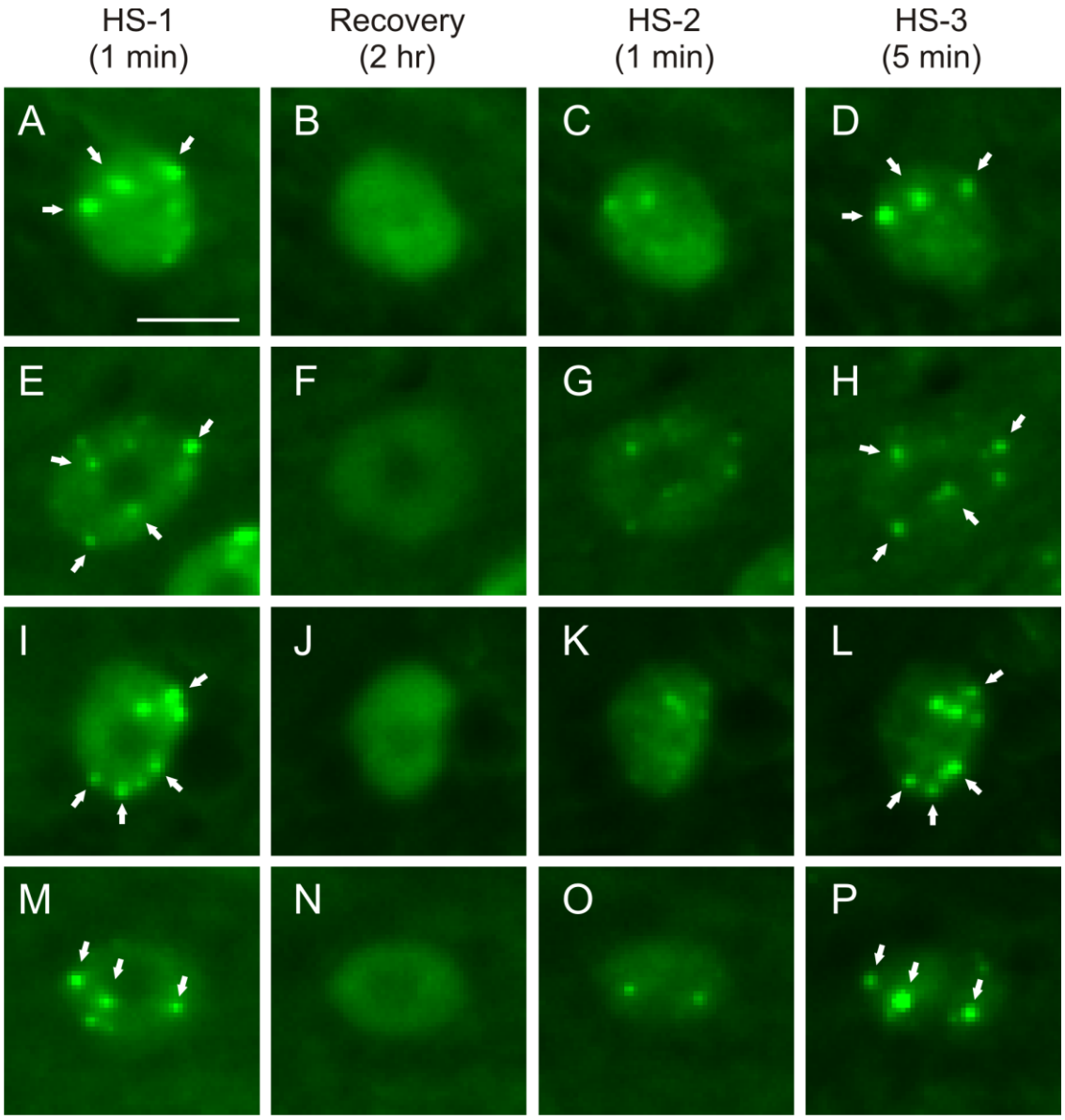

Figure 2-5. HSF-1::GFP granules re-form in similar locations with subsequent heat shocks

drSi13 HSF-1::GFP hypodermal nuclei were heat shocked for 1 min at 35°C (A,E,I,M), allowed to recover for 2 hr at 20°C (B,F,J,N), heat shocked a second time for 1 min (C,G,K,O), and then heat shocked a third time for 5 min (D,H,L,P). Panels A-H show only one (Z-dimension) deconvolved slice, I-L show two merged slices, and M-P show three merged slices. Arrows point to HSF-1 stress granules that appear to reform in the same location and pattern upon a second heat shock exposure. Scale bar = 5μm.

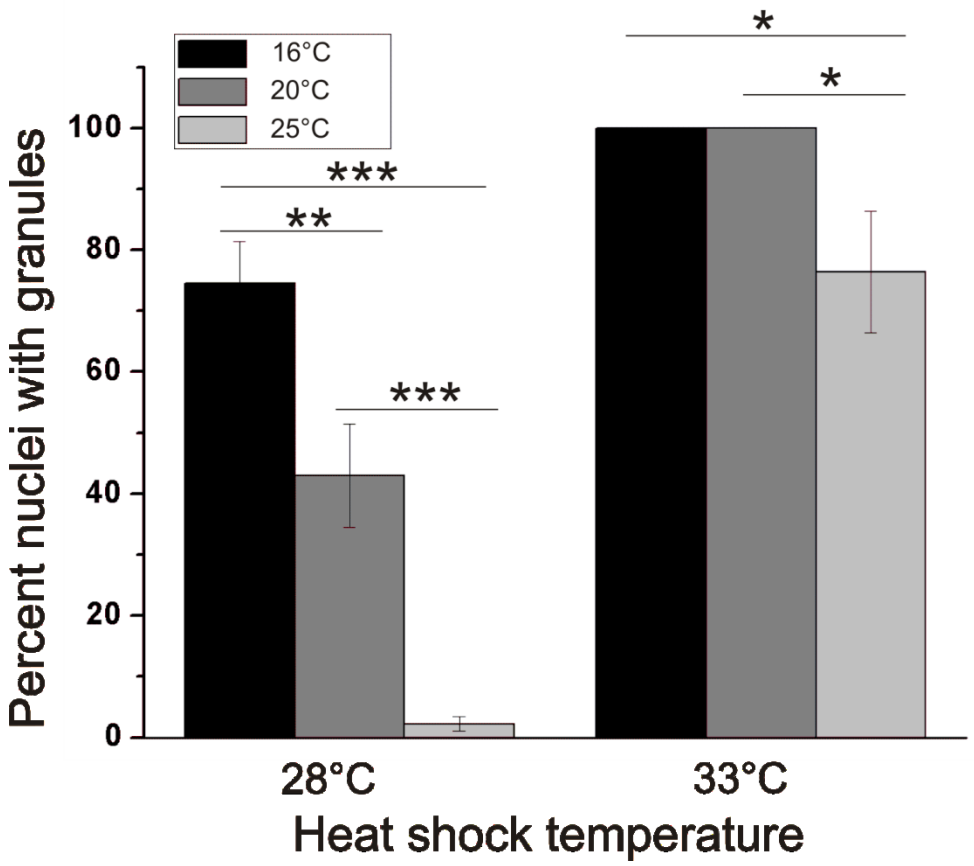

Figure 2-6. The threshold for HSF-1::GFP stress granule formation is influenced by growth temperature

HSF-1::GFP-expressing worms were grown to young adult at 16°C (black), 20°C (dark gray) or 25°C (light gray) and then subjected to a 5 minute heat shock at either 28°C or 33°C and imaged. Percent of hypodermal nuclei with at least one visible granule was quantified for each condition (N ≥ 13 worms per condition, representing ≥ 130 nuclei. Mean ± SEM, *** - $p < 0.001$, ** - $p < 0.01$, * - $p < 0.05$).

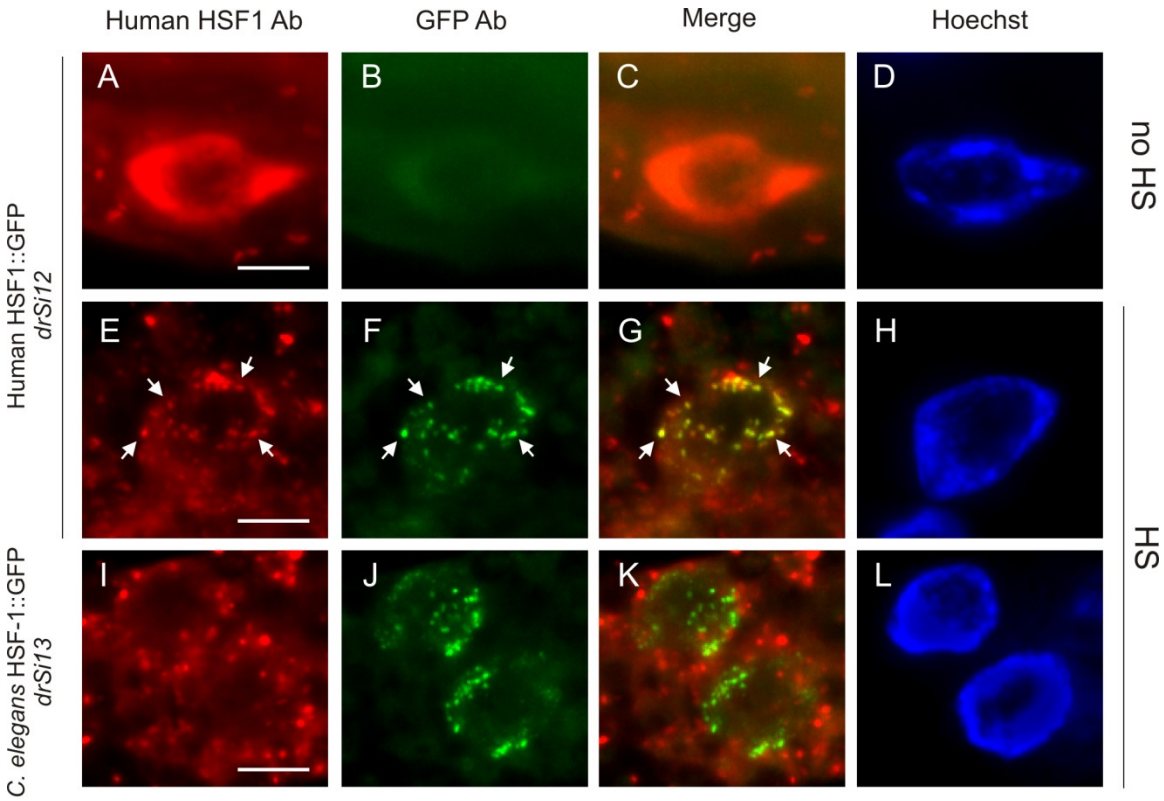

Figure 2-7. Human HSF1 antibody does not detect heat shocked worm HSF-1 by immunofluorescence

Non-heat shocked *drSi12* (human HSF1::GFP) (A-D), heat shocked *drSi12* (E-H), and heat shocked *drSi13* (worm HSF-1::GFP) (I-L) worms were dissected, fixed, and probed with a human HSF1 antibody (red, A,E,I) and an anti-GFP antibody (green, B,F,J). Heat shock was 35°C for 1 hr. GFP-positive granules are stained by the HSF1 antibody in the human HSF1::GFP-expressing line (arrows). Nuclei (intestinal) are labeled with Hoechst staining (D,H,L). Shown are 11 merged (Z-dimension) deconvolved slices. Note that the human HSF1 antibody does not co-localize with *C. elegans* HSF-1::GFP stress granules (I-L). Scale bar = 5µm.

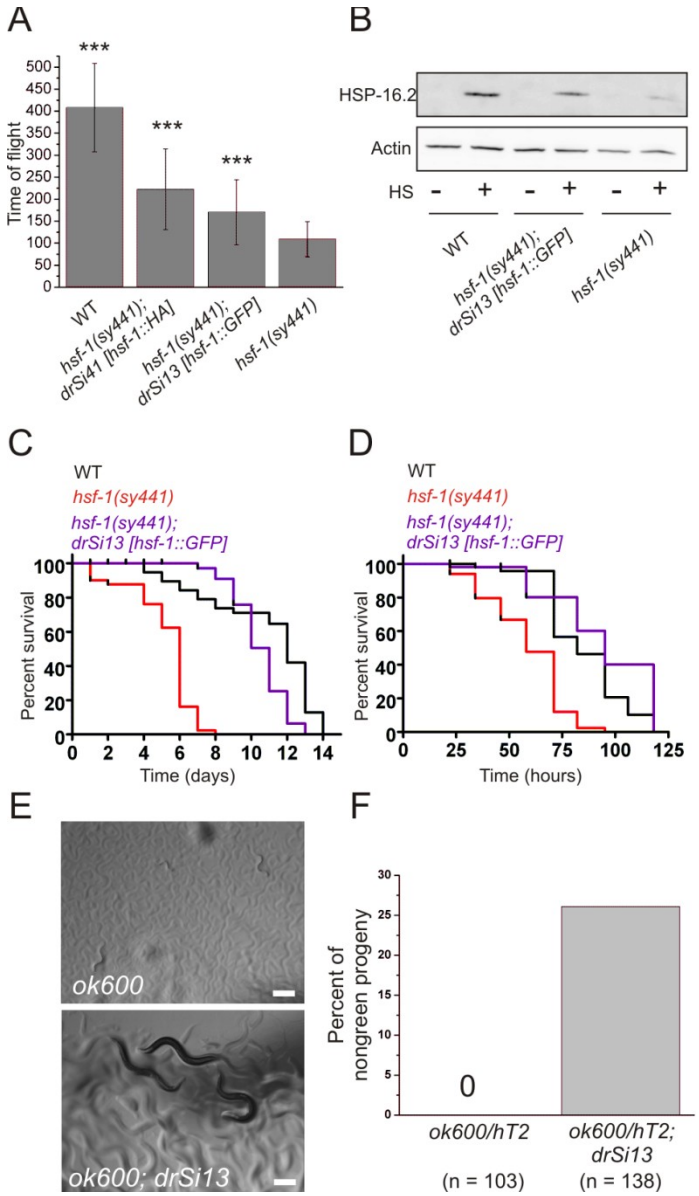

Figure 2-8. HSF-1::GFP is functional

(A) Wild type (WT), *hsf-(sy441);drSi41[hsf-1p::hsf-1::HA::unc-54 3'UTR], hsf-(sy441);drSi13[hsf-1p::hsf-1::GFP::unc-54 3'UTR]*, and *hsf-1(sy441)* eggs were placed at 25°C and allowed to grow until wild type was L4/young adult. Worms were analyzed for size (time of flight) in a COPAS Biosort (N ≥ 89 animals. Mean ± SD, *** - $p < 0.001$ as compared to *hsf-1(sy441)*). (B) Representative Western against HSP-16.2 (top panel) and β-actin (bottom panel) on WT, *hsf-1(sy441);drSi13,* and *hsf-1(sy441)* worms ±

a 35°C 3h heat shock followed by 3 hr recovery at 16°C. Relative HSP-16.2:actin ratio for WT : *hsf-1(sy441);drSi13* : *hsf-1(sy441)* is 1.0:0.67:0.22. (C) Lifespan of WT, *hsf-1(sy441)*, and *hsf-1(sy441);drSi13* animals at 25°C (N = 50 for all). ($p < 0.0001$ between *hsf-1(sy441)* and *hsf-1(sy441);drSi13*; $p = 0.0036$ between WT and *hsf-1(sy441);drSi13*) (D) Survival of WT, *hsf-1(sy441)*, and *hsf-1(sy441); drSi13* animals on *P. aeruginosa* PA14 at 25°C (N = 50 for all) ($p < 0.0001$ between *hsf-1(sy441)* and *hsf-1(sy441);drSi13*; $p = 0.498$ between WT and *hsf-1(sy441);drSi13*). (E) Images of *ok600* homozygous animals with (lower) or without (upper) the *drSi13* HSF-1::GFP transgene. Scale bar = 100µm. (F) Quantification what percent of total progeny that reach L4 stage or later within 3 days at 20°C are homozygous for *ok600,* with or without the *drSi13* HSF-1::GFP transgene.

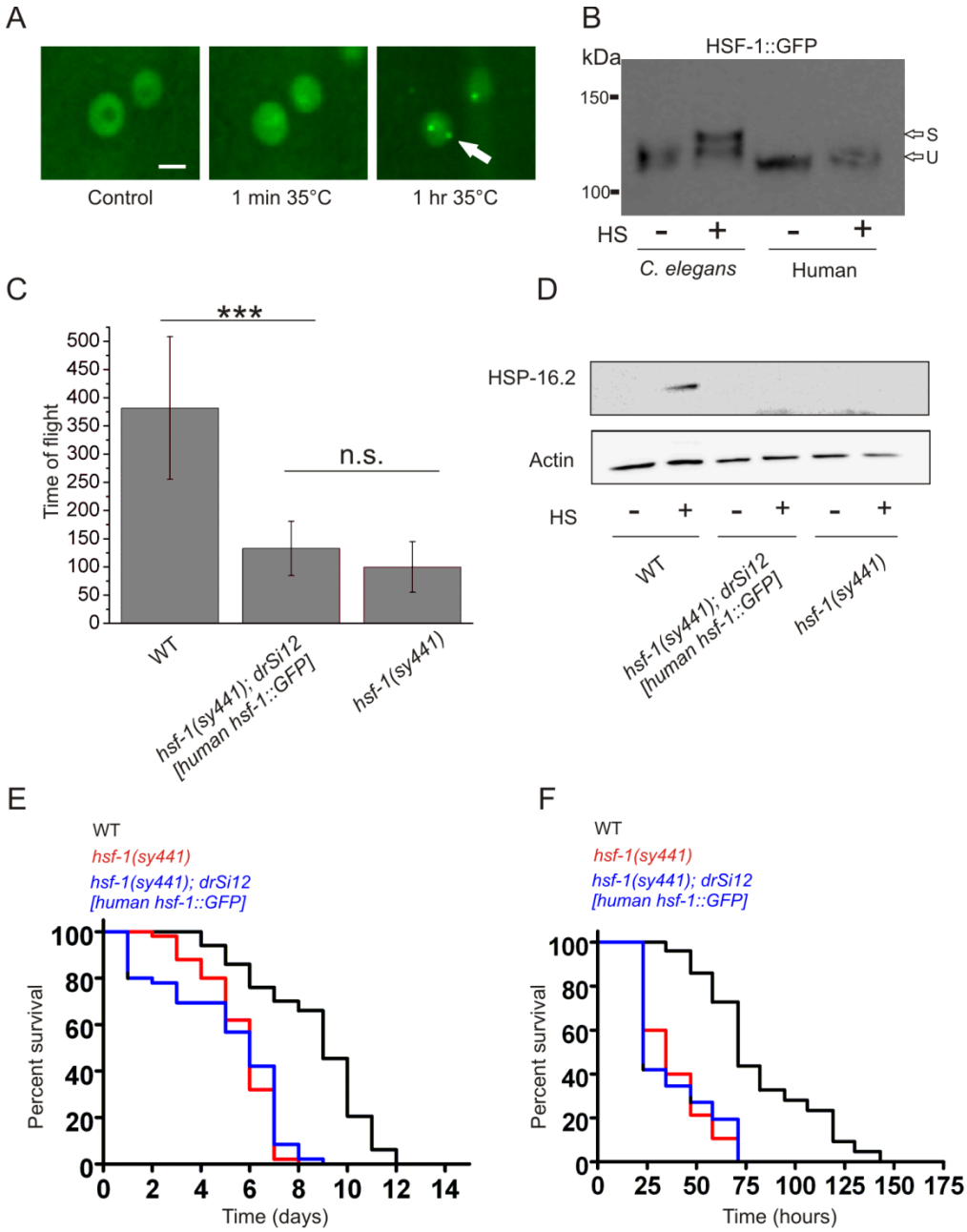

Figure 2-9. Human HSF1 is expressed and localizes to the nucleus but does not rescue *C. elegans hsf-1(sy441)* mutant phenotypes

(A) Human HSF-1::GFP (*drSi12[hsf-1p ::human hsf-1::GFP::unc-54 3'UTR]*) expressed under the *C. elegans* promoter without heat shock (control), after 1 min 35°C, or 1 hour 35°C. Arrow points to a stress granule. Scale bar = 5µm. (B) GFP Western for *C. elegans* (*drSi13*) and human (*drSi12*) HSF-1::GFP after 30 min at 16°C (-HS) or 35°C (+HS), showing shifted (S) or unshifted (U) HSF-1::GFP. Size markers are indicated to

the left. (C) Wild type, *hsf-1(sy441)*, and *hsf-(sy441);drSi12* eggs were placed at 25°C and allowed to grow until wild type was L4/young adult. Worms were analyzed for size (time of flight) in a COPAS Biosort ($N \geq 44$ animals. Mean ± SD, *** - $p < 0.001$, n.s. - not significant). (D) Representative Western against HSP-16.2 (top panel) and β-actin (bottom panel) on young adult wild type, *hsf-(sy441);drSi12,* and *hsf-1(sy441)* worms plus or minus a heat shock of 3 hr 35°C followed by 3 hr recovery at 16°C. (E) Lifespan of young adult wild-type, *hsf-1(sy441)*, and *hsf-1(sy441);drSi12* animals at 25°C ($N = 50$ for all). ($p < 0.0001$ between N2 and *hsf-1(sy441);drSi12*; $p = 0.6048$ between *hsf-1(sy441)* and *hsf-1(sy441);drSi12*) (D) Survival of young adult wild-type, *hsf-1(sy441)*, and *hsf-1(sy441);drSi12* animals on PA14 at 25°C ($N = 50$ for all) ($p < 0.0001$ between N2 and *hsf-1(sy441);drSi12*; $p = 0.9251$ between *hsf-1(sy441)* and *hsf-1(sy441);drSi12*. In the second trial, *hsf-1(sy441);drSi12* was significantly shorter lived than *hsf-1(sy441)*, $p < 0.0001$).

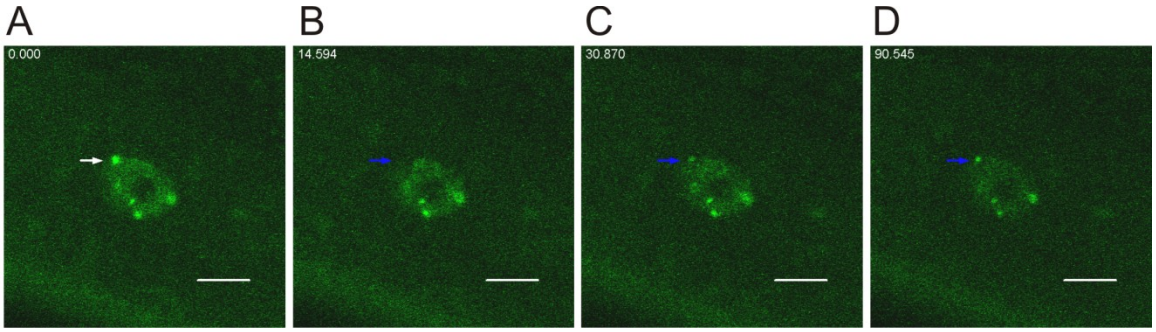

Figure 2-10. HSF-1::GFP granules are not aggregates

(A) HSF-1::GFP expression after 1 min 35°C heat shock. A granule (arrow) was photobleached (B, blue arrow) and imaged through recovery (C, ~16 sec recovery, D, ~76 sec recovery). Timestamp in the upper left corner = seconds since start of imaging. Scale bar = 5µm. This experiment was repeated in samples given a heat shock of 35°C for 1 min (N = 4 nuclei), or 5 min (N = 5 nuclei) with similar results.

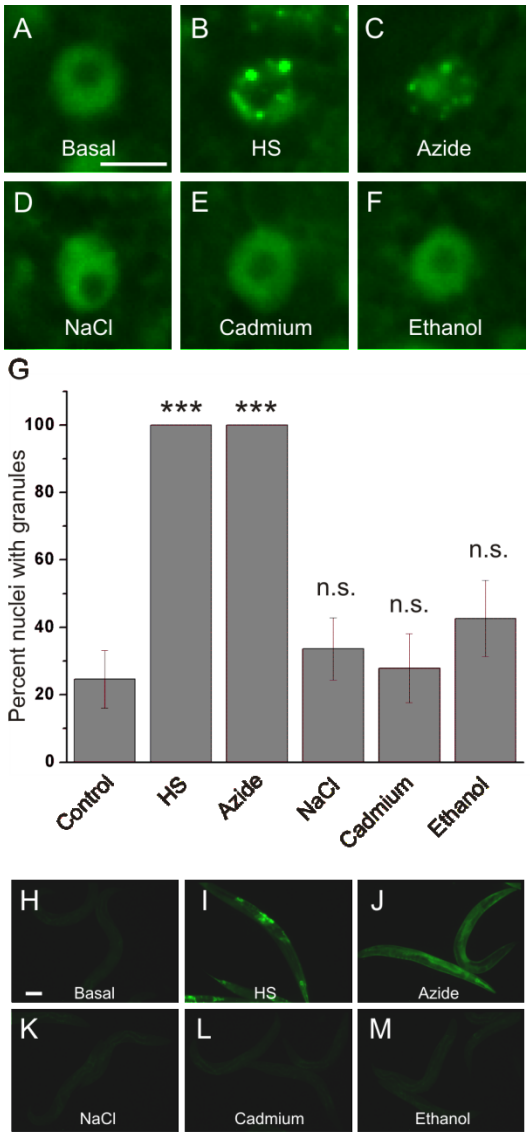

Figure 2-11. Nuclear granules form in response to heat shock and sodium azide

Worms expressing *drSi13* HSF-1::GFP were anesthetized 30 min in 1 mM levamisole at either room temperature (A), 35°C (HS) (B), 5 mM sodium azide (C), 219 mM NaCl (D), 100 µM $CdCl_2$ (E), or 100 mM ethanol (F). Scale bar = 5µm. (G) Percent of hypodermal nuclei with ≥ one visible granule were quantified for each condition (N ≥ 10 worms per condition, representing ≥ 85 nuclei. Mean ± SEM, *** - $p < 0.001$ vs. control, n.s. - not significant). (H-M) TJ375 (*hsp-16.2p::GFP*) worms were subjected to 30 min of the same conditions as in A-F, followed by recovery at 20°C for 4 hr before imaging. Scale bar = 100µm.

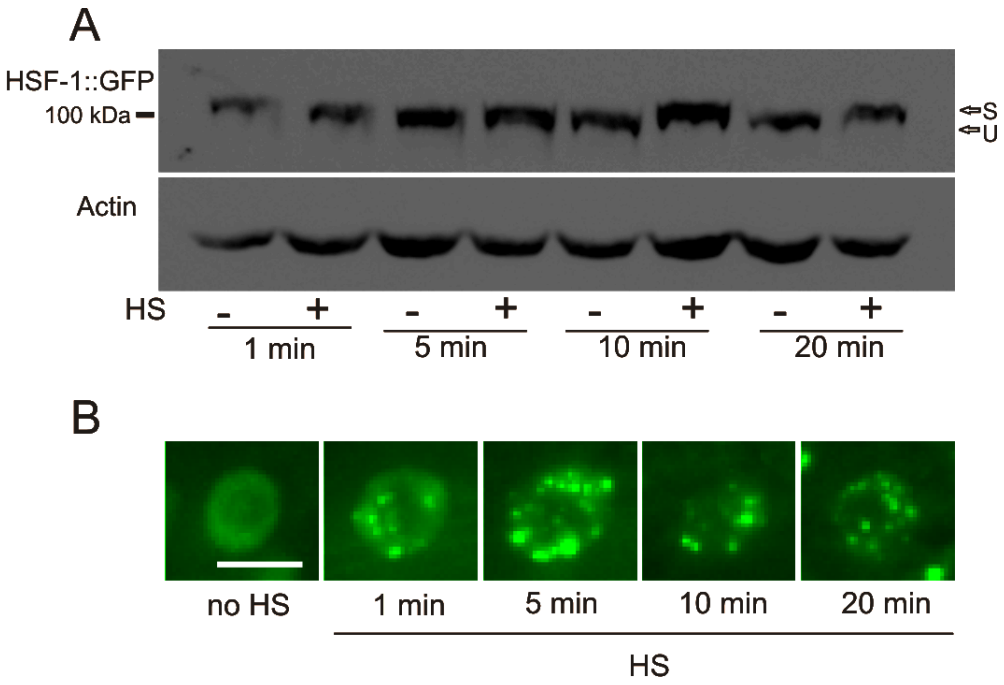

Figure 2-12. HSF-1::GFP is post-translationally modified following heat shock

(A) Immunoblot with anti-GFP and anti-β-actin antibodies against young adults worms expressing *drSi13* HSF-1::GFP. Worms were subject to 16°C (-HS) or 35°C (+HS) for the stated times. Arrows point to shifted (S) or unshifted (U) HSF-1::GFP. (B) *drSi13* HSF-1::GFP worms imaged without heat shock, or after a 35°C heat shock for 1, 5, 10 or 20 minutes. Images are from separate worms. Scale bar = 5μm.

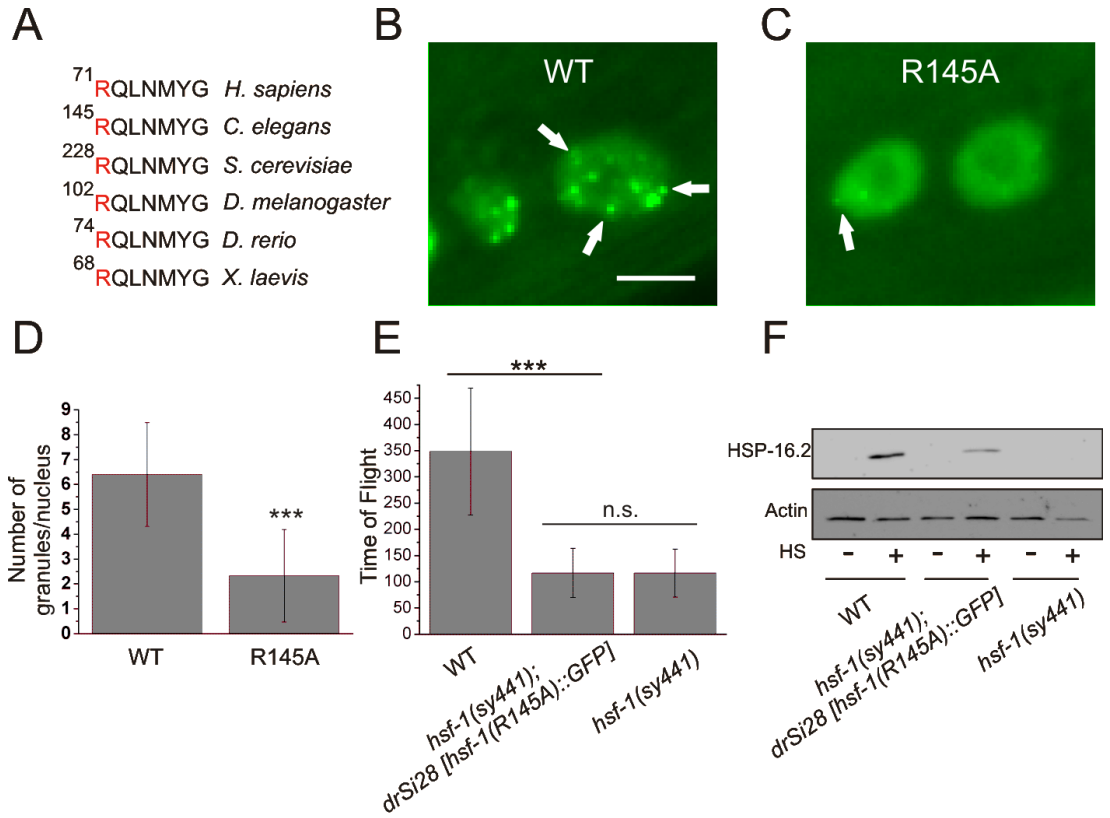

Figure 2-13. HSF-1 DNA binding promotes stress granule formation and developmental rescue of *hsf-1(sy441)*

(A) Alignment of the region of the DNA binding domain containing R145 (red) from the indicated species. (B,C) Images of *drSi13* HSF-1::GFP (WT) and *drSi28* HSF-1(R145A)::GFP (R145A) taken after a 1 min 35°C heat shock, showing granule formation (arrow). Scale bar = 5µm. Shown are four merged (Z-dimension) deconvolved slices. (D) Number of granules per nucleus was quantified for WT and R145A. (N ≥ 18 worms, representing ≥ 140 nuclei for each line. Mean ± SD, *** - $p < 0.001$). (E) N2 wild type (WT), *hsf-1(sy441)*, and *hsf-1(sy441);drSi28* eggs were placed at 25°C and allowed to grow until wild type was L4/young adult. Worms were analyzed for size (time of flight) in a COPAS Biosort (N ≥ 30 animals. Mean ± SD, *** - $p < 0.001$, n.s. - not significant). (F) Representative Western against HSP-16.2 (top panel) and β-actin (bottom panel) on young adult wild type, *hsf-1(sy441);drSi28,* and *hsf-1(sy441)* worms ± a 3 hr 35°C heat shock followed by 3 hr recovery at 16°C.

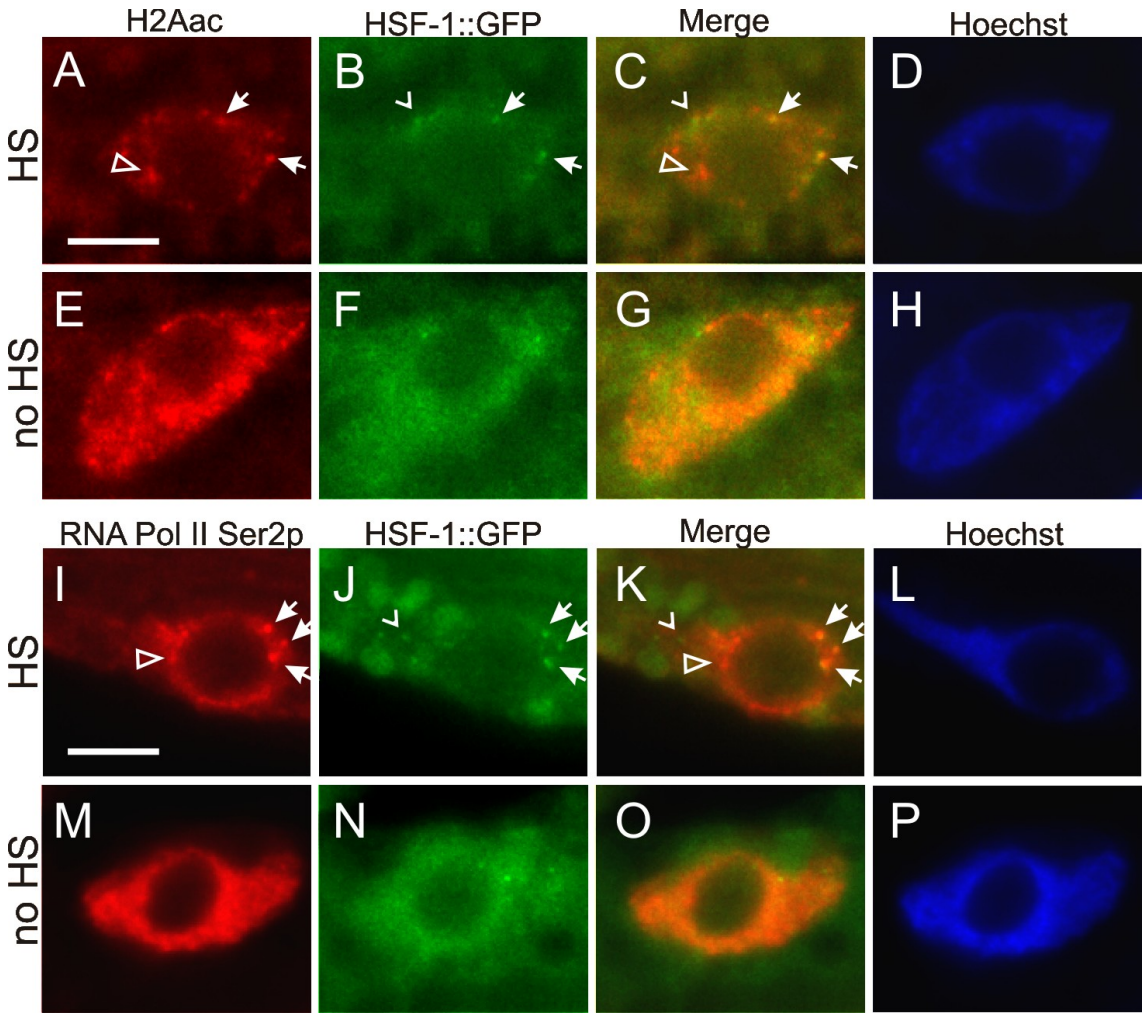

Figure 2-14. HSF-1::GFP granules colocalize with markers of active transcription

drSi13 HSF-1::GFP worms grown at 25°C were heat shocked for 1.5 hr at 35°C (HS) or put at 25°C 1.5 hr (no HS) and intestinal nuclei were probed for GFP (green, B,F,J,N) histone H2A acetylated on Lysine 5 (red, A,E), or RNA polymerase II phosphorylated on Serine 2 (red, I,M. Exposure times in I and M were different because we observed substantially reduced RNA polII Ser2p staining post-heat shock). Nuclei (intestinal) were detected by Hoechst staining (D,H,L,P). Nuclear staining showed puncta of fluorescence, some of which show colocalization of GFP and an active transcription marker (arrows). Other puncta exhibit GFP-only (carrot) or active transcription marker-only (open arrowhead) staining. Scale bar = 5μm.

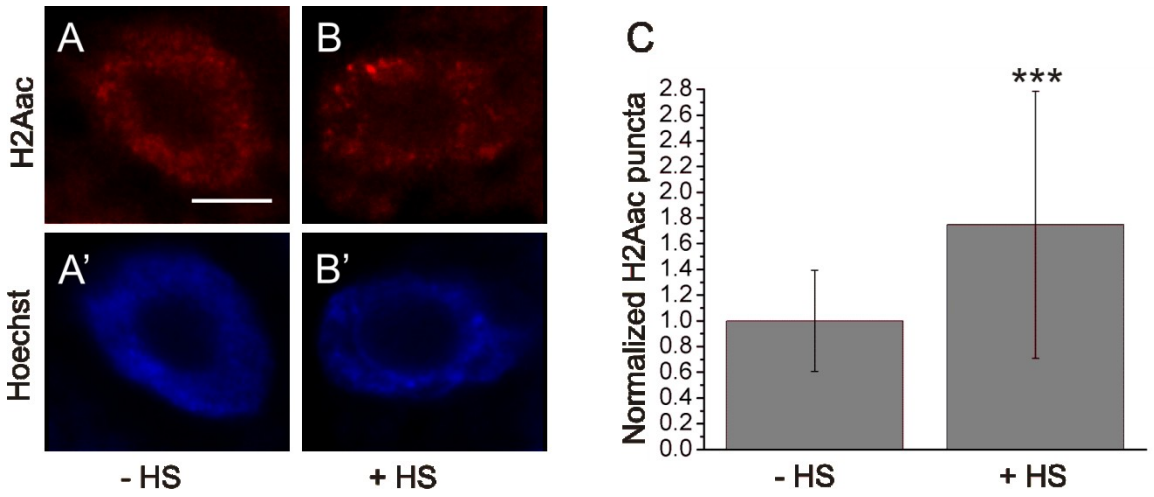

Figure 2-15. H2Aac is distributed in a greater number of discrete puncta after heat shock

(A,B) *drSi13* HSF-1 ::GFP worms grown at 25°C were fixed and probed for H2Aac after 1.5 hr at 25°C (no HS) or 1.5 hr at 35°C (HS). Nuclei (intestinal) were detected with Hoechst staining (A',B'). Scale bar = 5µm. (C) Images were deconvolved and then analyzed with MATLAB to detect number of discrete punca with an intensity of more than one standard deviation over the mean intensity. These numbers were normalized to the mean number for the no HS samples (Mean ± SD, N = 30 nuclei, *** - $p < 0.001$, Student's t-test).

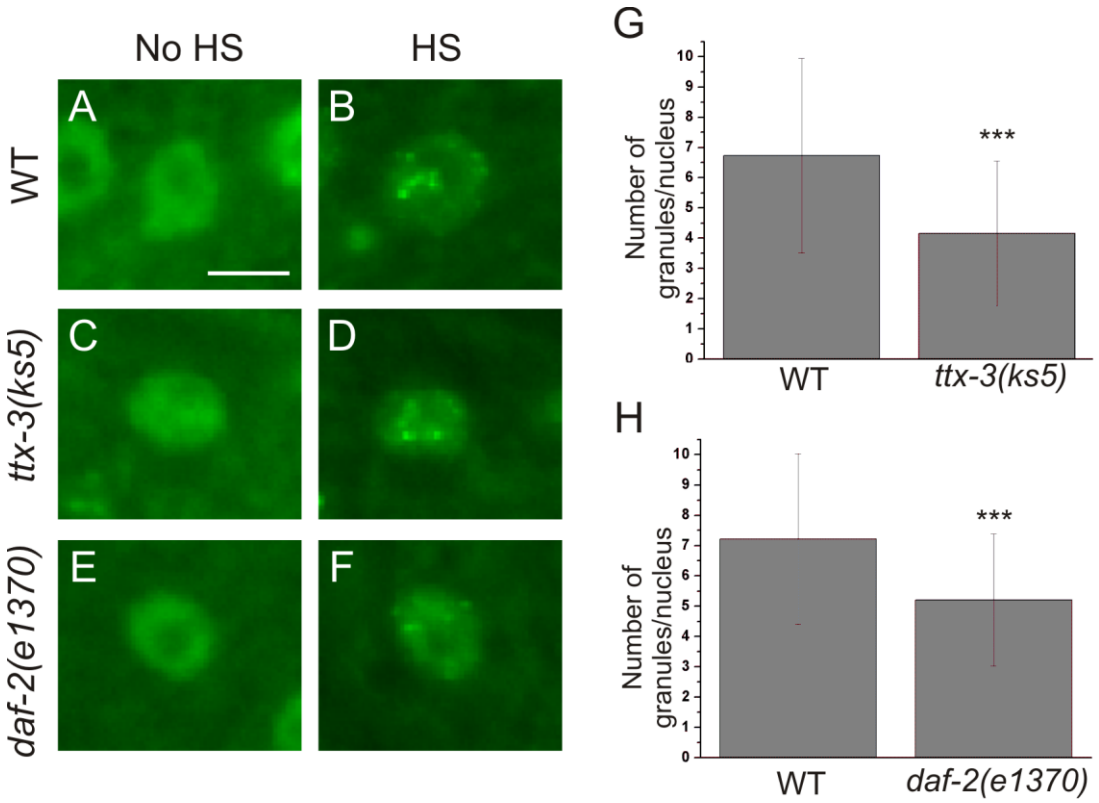

Figure 2-16. *ttx-3* and *daf-2* mutations reduce the number of HSF-1 granules

HSF-1::GFP in wild-type (A,B), *ttx-3(ks5)* (C,D) or *daf-2(e1370)* (E,F) background before (A,C,E) or after (B,D,F) 1 min 35°C heat shock. Shown are three merged (Z-dimension) deconvolved slices. Worms were grown at 20°C. Scale bar = 5μm. Average number of granules per nucleus was quantified for each of the three strains after 1 min 35°C (N ≥ 15 worms for each, representing ≥ 117 nuclei per strain. Mean ± SD, *** - $p < 0.001$, Student's t-test). Wild type (WT) and *ttx-3(ks5)* are compared in (G) and wild type and *daf-2(e1370)* in (H).

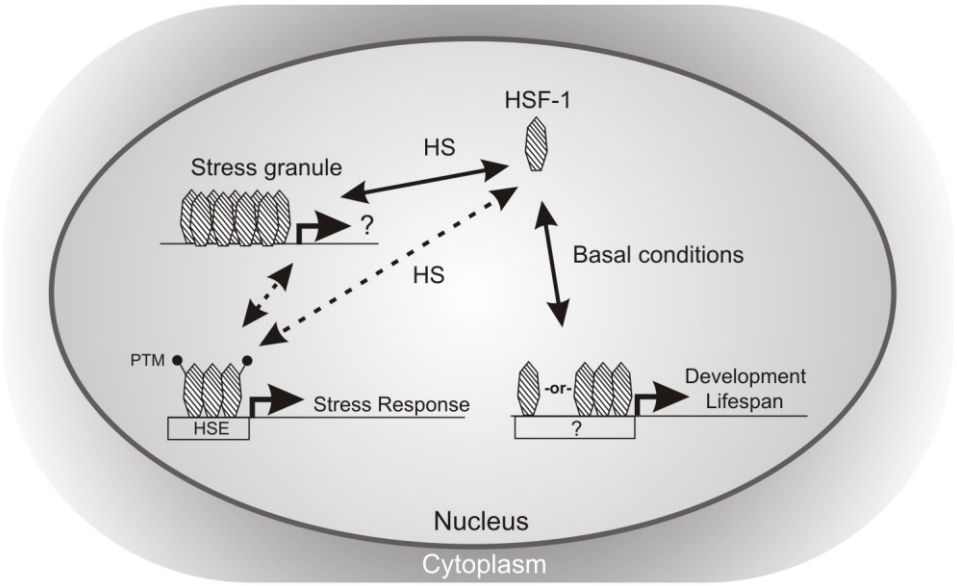

Figure 2-17. Model for HSF-1 regulation in *C. elegans*

HSF-1 is a predominately nuclear protein in *C. elegans*, and its modes of activity under basal conditions and stress conditions (HS) differ. Stress-inducible activity is distinguished by stress granule formation, oligomerization, and post-translational modification of HSF-1. Due to its oligomeric nature, we hypothesize that physiological levels of the DNA binding-deficient HSF-1(R145A) can still associate with the active HSF-1 complex and contribute transactivation function to stress-inducible targets in *trans.* The observation that HSF-1(R145A) cannot rescue developmental defects in the *sy441* transactivation-deficient background suggests that HSF-1 activity in the context of development may not operate in *trans*. Basal targets of HSF-1, including genes involved in development and possibly lifespan, require DNA binding activity, but may not involve stress granule formation or oligomerization.

3. A suite of MATLAB-based computational tools for automated analysis of COPAS Biosort data[2]

Summary

Complex Object Parametric Analyzer and Sorter (COPAS) devices are large-object, fluorescence-capable flow cytometers used for high-throughput analysis of live model organisms, including *Drosophila melanogaster*, *Caenorhabditis elegans*, and zebrafish. The COPAS is especially useful in *C. elegans* high-throughput genome-wide RNA interference (RNAi) screens that utilize fluorescent reporters. However, analysis of data from such screens is relatively labor-intensive and time-consuming. Currently, there are no computational tools available to facilitate high-throughput analysis of COPAS data. We used MATLAB to develop algorithms (COPAquant, COPAmulti, and COPAcompare) to analyze different types of COPAS data. COPAquant reads single-sample files, filters and extracts values and value ratios for each file, and then returns a summary of the data. COPAmulti reads 96-well autosampling files generated with the ReFLX adapter, performs sample filtering, graphs features across both wells and plates, performs some common statistical measures for hit identification, and outputs results in graphical formats. COPAcompare performs a correlation analysis between replicate 96-well plates. For many parameters, thresholds may be defined through a simple graphical user interface (GUI), allowing our algorithms to meet a variety of screening applications. In a screen for regulators of stress-inducible GFP expression, COPAquant dramatically accelerated data analysis and allowed us to rapidly move from raw data to hit

---

[2] This chapter is adapted from the published work under the same title by Elizabeth Morton and Todd Lamitina, *Biotechniques,* **48**, xxv-xxx (2010).

identification. Because the COPAS file structure is standardized and our MATLAB code is freely available, our algorithms should be extremely useful for analysis of COPAS data from multiple platforms and organisms. The MATLAB code is freely available at our web site (www.med.upenn.edu/lamitinalab/downloads.shtml).

Introduction

Automation has been a great boon to the field of high-throughput screening. The Complex Object Parametric Analyzer and Sorter (COPAS) platform (Union Biometrica, Holliston, MA, USA) is a tool that allows for rapid quantification of the fluorescence, size, and optical density of small biological specimens, such as *Caenorhabditis elegans*, *Drosophila*, and zebrafish. The COPAS utilizes microfluidic approaches to draw intact live organisms through a fluorescence-compatible flow cell at extremely high rates (~50 animals per second) and quantifies the size (measured as object time-of-flight (TOF)), object optical density (EXT), and fluorescence emissions from up to three separate fluorescent channels for each animal. Because of its complete optical transparency, rapid growth rates, and amenability to forward and reverse genetic approaches, *C. elegans* is an excellent model system for COPAS-based high-throughput phenotypic and genetic studies (Boyd et al., 2010; Boyd et al., 2009; Burns et al., 2006; Doitsidou et al., 2008; Lamitina et al., 2006; Smith et al., 2009; Sprando et al., 2009). In many cases, these studies are enabled by the expression of fluorescent reporter transgenes (Doitsidou et al., 2008; Lamitina et al., 2006; Pujol et al., 2008), which often exhibit significant animal-to-animal variability. Because of this inherent variability in reporter expression, quantification of fluorescence by the COPAS within a population of animals is a more accurate phenotypic assessment than subjective visual inspection of individual animals

(Pujol et al., 2008). While the COPAS excels at the rapid collection of population-based data, the number of individual samples analyzed during a large-scale screen can easily reach into the thousands. Efficient analysis of such large COPAS data sets requires the use of automated computational tools, which have so far not been developed.

Currently, the COPAS can collect data in two modes, a single-sample mode and an autosampler 96-well mode. The single-sample mode permits very large sample sizes to be analyzed, which is a tremendous advantage for assaying highly variable or subtle phenotypes. However, because samples must be loaded one at a time into the sample chamber, the throughput of this mode is slow and labor-intensive and best suited to small-scale screens. The autosampler mode, enabled by the ReFLX adapter system, allows rapid analysis of liquid-based samples from 96-well plates, which provides tremendous sample throughput. However, the small volumes of 96-well assays limit the number of events per well to sample sizes much smaller than those obtained in the single-sample mode, making the autosampler mode well suited to large-scale genome-wide RNA interference (RNAi) or drug screens that utilize phenotypes of low variability. In the single-sample mode, each file contains the data from one sample. In the autosampler 96-well mode, each file contains the data from every well within a 96-well plate, classified according to well address. In both cases, the time required to filter, extract, and normalize the data; graph the summary results of the screen; compare results among plates; and statistically identify hits is a major rate-limiting step in the screening pipeline. Tools that facilitate the analysis of such large-scale data sets would tremendously advance the throughput capability of COPAS-based assays. Such tools are currently unavailable.

Many different software environments are suitable for the analysis of large-scale COPAS data sets, including R, SAS, and Visual Basic. Another program suitable for such analyses is MATLAB (MathWorks, Natick, MA, USA). MATLAB is a computer interface program specifically designed for analysis of matrix based data sets, which is typically applied to the automation and standardization of image analysis routines. However, MATLAB can just as easily be applied to analyze any type of numerical data presented in a matrix format. Since the COPAS data file structure is a standardized $26 \times n$ matrix worksheet (where n is the number of events sorted), we reasoned that COPAS-generated data could be analyzed in the MATLAB environment. While analysis of COPAS data is possible in other programming environments, such as Microsoft Excel and Visual Basic, MATLAB offers several distinct advantages for COPAS data analyses. First, MATLAB is an interpreted language, making it very easy to learn, use, and modify. It is compatible with many different operating systems (Windows, Linux, Macintosh, etc.) and is therefore accessible to almost all users, regardless of platform. Second, MATLAB can receive user input through custom graphical user interfaces (GUIs); end-users need not have any experience with MATLAB to execute prewritten MATLAB functions. Third, MATLAB provides access to a library of common data handling methods, graphical representations, and statistical tools that can be visualized in highly flexible ways using plotting and imaging commands integrated within the MATLAB program. Such commands must often be written *de novo* in other programming languages. Since MATLAB is written for science and engineering applications, this library is tailored for analysis of scientific data. Finally, MATLAB is widely used throughout the biomedical research community, providing access to a strong user base for

teaching, implementation, and code sharing. These advantages strongly support the use of MATLAB as the software of choice for analysis of COPAS data sets.

Herein, we describe a suite of MATLAB algorithms—COPAquant, COPAmulti, and COPAcompare—which extract, filter, normalize, graph, statistically analyze, and compare intra- and interplate values from COPAS Biosort data files acquired with the Advanced Acquisition Software Package (Union Biometrica). COPAquant analyzes data generated in the single-sample mode, whereas COPAmulti and COPAcompare analyze data obtained in the 96-well autosampling ReFLX mode. Automation of this step within the context of a high-throughput RNAi screen allowed us to rapidly move from secondary validations to hit identification. Although we have used it primarily for screens in *C. elegans*, the standard file format of COPAS data files, our simple GUI for multiwell plate analyses, and the freely available nature of the algorithms make it widely useful for analysis of any type of COPAS-generated data.

Results and Discussion

Many RNAi screens performed in *C. elegans* are based on the *in vivo* expression of GFP reporters. One such screen under investigation in our laboratory involves the temperature-dependent regulation of an *hsp-16p::GFP* reporter. In this strain, GFP expression within young adult hermaphrodites (TOF = 400–1000) is negligible under basal conditions (Figure 3-1A), but is highly induced in almost all cells after a brief heat shock and recovery period (Figure 3-1B) (see the "Materials and Methods" section for a more detailed description of the experiment). Quantification of this induction among young adult animals revealed a wide distribution of GFP expression levels between individuals (Figure 3-1C), as has been previously reported (Link et al., 1999; Rea et al.,

2005). However, the population means accurately reflect expression of the transgene (Figure 3-1D). In order to identify regulators of the heat-shock response pathway in *C. elegans*, we conducted a genome-wide RNAi screen for suppressors and enhancers of heat shock-dependent *hsp-16.2p::GFP* expression (see Chapter 4). GFP reporter expression was initially quantified by visual inspection. After the secondary validation screen, RNAi treatments were quantified using the COPAS Biosort in the single-sample mode of screening.

To facilitate analysis of the numerous COPAS data files generated by our RNAi screen, we wrote an algorithm, using the programming platform MATLAB, to automatically extract desired values from COPAS *.txt data files (one file per RNAi condition) (Table 3-1). The COPAS exports data in a 26-column format, in which each row represents data from a single worm. The basic function of our COPAquant algorithm, COPASFun, imports numerical values from a COPAS data file. After data import, COPAquant queries the user as to whether the data to be analyzed should be filtered based on gating criteria, which are a unique combination of COPAS parameters (TOF, EXT, Ch1, Ch2, and Ch3) that are user-defined during data acquisition. COPAquant can be instructed to analyze gated data only, nongated data only, or all data. Using our *hsp-16.2p::GFP* screen data as an example, we chose to extract gated values for TOF, EXT, and fluorescence for each of the three fluorescent channels. Because COPAS-measured GFP fluorescence is related to object size (unpublished data), COPASFun can correct for this bias by normalizing to the object TOF. These ratio values (Ch1/TOF, Ch2/TOF, Ch3/TOF) are entered into new columns. The resulting columns for our values of interest (TOF, EXT, Ch1, Ch2, and Ch3, as well as their

associated ratios) are then summarized with mean and standard deviation (SD). In the current screen for *hsp-16.2::GFP* regulators, meaningful yellow (Ch2) and red (Ch3) data were not obtained, since this strain does not express reporters in either of these fluorescent channels. These statistics, as well as the number of events in the sample (N), are then exported to the function COPASImp (Figure 3-2A).

The COPASImp function sends multiple COPAS *.txt files to COPASFun for analysis (Figure 3-2A). Once the MATLAB directory is set to the appropriate folder, COPASImp recognizes and reads all *.txt files within the folder (Figure 3-2A). Once all the files in the folder have been analyzed, the results are presented in a table titled Results (which is automatically saved as the tab-delimited text file Results.txt for analysis outside of MATLAB) as well as in a structure labeled ImStruc (in which each cell contains the results for one sample). Following analysis, COPASImp queries the user as to which parameter should be represented in graphical format. The user-selected parameter is then plotted and displayed (Figure 3-2B).

In addition to the form of normalization discussed above, COPAquant V2 will also normalize all samples to a negative control sample to produce a relative fold-change value (Table 3-1). The program presents data in both the raw form (Figure 3-2B, C) and in various normalized forms (Figure 3-2D, E), using the lowest numbered file as the negative control reference. The mean of the reference sample is calculated for each parameter, and each event within subsequent samples is divided by this value, creating a new, normalized column of values. The means of the normalized values, as well as their SD values, are exported back to COPASImp (Figure 3-2D, E).

Using COPAquant, we dramatically enhanced the rate of data analysis in our screen for regulators of *hsp-16.2p::GFP* expression using the single-sample mode of COPAS screening. We were able to rapidly identify hits that affect GFP expression but not worm growth by analyzing both normalized GFP, as well as normalized TOF values (i.e., normalized to the negative control sample—empty vector RNAi in this case). Prior to implementation of COPAquant, the time required for manual analysis of a single day's worth of COPAS data obtained using the single-sample acquisition mode frequently exceeded 8 hr. Using COPAquant, data from one day of sorting are now analyzed, normalized, and graphed within 10 sec, which represents a ~3000-fold increase in data analysis efficiency.

In addition to the single-sample sorting mode described above, some labs also employ an autosampling device called the ReFLX system. ReFLX-equipped COPAS systems sort and quantify events from individual wells of 96-well plates using the optional ReFLX sampler. Data from each well are stored within a single 26-column format file according to their row and column address. To make our MATLAB program applicable to ReFLX screening platforms, we modified our existing single-sample MATLAB code to read ReFLX files. The modified programs, COPAmulti and COPAcompare (Figure 3-3 and Table 3-1), read raw *.txt files generated by the ReFLX, filter and extract matrices for each well, and summarize useful parameters. Data from one or more 96-well files (COPAmulti) or a replicate pair of 96-well files (COPAcompare) are analyzed, and the data for each plate is stored in a separate cell of a Results Structure within MATLAB. For each plate analyzed, the raw data (N and well mean ± SD for each of eight different parameters for every well) are exported to a Results

Structure, which can be accessed for export to other programs. To make COPAmulti as user-friendly as possible, we implemented a GUI within MATLAB that allows users to define several criteria for data analysis, including filtering cutoffs, the parameter to be utilized for analysis, and statistical criteria and thresholds used to identify hits (Figure 3-4A). Since these criteria can be adjusted through the GUI and the data are rapidly reanalyzed, the effects of altered filtering and statistical criteria are easily determined.

Since ReFLX files offer unique analysis challenges and opportunities not present in single-sample data collection modes, we implemented several additional features common to high-throughput multiwell-based RNAi screening for ReFLX file analysis. First, the mean of a user-selected parameter from each well is plotted in an 8 × 12 matrix heat map that is color-coded by well value (Figure 3-3B). This visualization strategy is a useful way to compare the data across a plate and often helps in the identification of plate edge effects, a common confounder in high-throughput RNAi screening (Birmingham et al., 2009). Second, instead of normalizing to a single negative control sample (as we do for single-sample data analysis), COPAmulti takes advantage of the large number of samples and uses the plate mean (calculated from the median 80% of nonzero value samples to remove effects of outliers) as the negative control value. This approach is a well-accepted data normalization strategy for multiwell plate assays that can be uniformly applied across all plates (Birmingham et al., 2009). In addition to this normalization strategy, we also implemented a second approach (COPAmulti V2) that allows users to define the well(s) that contain negative control data through the COPAmulti GUI (Figure 3-4B). Using these calculated negative control reference values, we implement three common statistical tests for hit identification that have been

previously utilized in RNAi screening formats: 1) mean ± *k* SD; 2) median ± *k* MAD; and 3) the multiple-comparisons *t*-test with Bonferroni correction. The specific significance test and threshold for each test is set within the user-adjustable GUI. Each test has specific strengths and weaknesses and in some cases may not represent the best statistical approach for data analysis. Nonetheless, these methods are among the most commonly used approaches for analysis of high-throughput RNAi screening data (Birmingham et al., 2009), and the best approach is usually to compare results obtained with each statistical method. In general, the mean ± *k* SD test is the most commonly used hit identification technique for RNAi screening, due to its ease of calculation (Bard et al., 2006; DasGupta et al., 2005). Most screeners utilize a 3(SD) cutoff with this approach. However, this method is sensitive to outlier data and frequently misses weaker positives. Decreasing the SD cutoff usually increases false positives to an unacceptably high rate. An alternative approach is the median ± *k* MAD test. Like the mean ± *k* SD test, MAD is relatively easy to calculate but is much less sensitive to outlier data. MAD also does a good job of identifying weak hits while controlling false positives (Chung et al., 2008). A shortcoming of MAD is that it is not easily linked to probability distributions and p-values. Despite this shortcoming, others have recommended MAD as the method-of-choice for hit selection in high throughput RNAi screens (Chung et al., 2008). MAD values of ≥ 2 are commonly used for hit identification in genome-wide RNAi screens (Chung et al., 2008). A final common statistical test for RNAi screening is the multiple-comparison *t*-test. This statistic is easy to calculate (due to the large number of events in each well), but is extremely sensitive to outliers and requires multiple-comparison correction (Birmingham et al., 2009). For multiple comparison *t*-tests, the simplest form

of correction is the Bonferroni correction, which scales the desired p-value by the number of samples to obtain an equivalent multiple comparison p-value. In general, users should analyze their data with each statistical approach and utilize the method or combination of methods that most frequently identifies known positive controls. A major advantage of our software is that it allows users to rapidly adjust and test each of these statistical methods for hit identification through the simple GUI. For users that wish to perform statistical analysis of their data using other approaches, COPAmulti automatically exports both summarized and raw data to delimited text files for further analysis.

Following statistical analysis, hits meeting user-determined thresholds are binarized in an 8 × 12 matrix, with hits plotted in white and non-hits plotted in black (Figure 3-3C). We also visualize all data from all plates using a well index plot (Figure 3-3D). Such plots are useful indicators of screen phenotypic behavior among plates and can help identify plates with phenotypic drift or substantial variance. For example, data in Figure 3-3 demonstrate lower values toward the end of the plate as compared with the beginning of the plate. Finally, since some users may screen in duplicate, we implemented a separate algorithm, COPAcompare, that allows users to compare results between two plates (Figure 3-5). COPAcompare plots a user-selected parameter for each well between two user-selected plates. The degree of overall plate-to-plate correlation is determined by calculating the Pearson correlation coefficient (R), where an R value of 1 equals perfect correlation among all wells and -1 equals perfect opposite correlation among all wells.

We developed a suite of MATLAB-based programs to process large COPAS file data sets such as those associated with *C. elegans* RNAi screens. We implemented one

program, COPAquant, for comparisons among data collected in the single-sample format, which is useful for small-scale screens with larger populations. We also implemented two additional programs, COPAmulti and COPAcompare, that use more advanced filtering, analysis, normalization, and statistical analysis of data from 96-well plates obtained using the COPAS ReFLX system. Both programs allow users to rapidly move from raw COPAS data to graphical data representation, replicate plate comparison, and hit identification without extensive knowledge of or experience with the programming environment. Our software greatly simplifies the analysis of COPAS data and fills a major gap in our need for data analysis tools for high-throughput screening using this platform. While we used this program in the validation steps of an RNAi screen for regulators of a heat shock–inducible reporter in *C. elegans*, the program is customized to the standard data format output by COPAS Biosort instruments and thus can be used in any type of COPAS application, including data obtained from other organisms.

Materials and Methods

Strains

The *C. elegans* strain TJ375 (*hsp-16.2p::GFP*) was used in this study and was obtained from the *Caenorhabditis* Genetics Center (University of Minnesota, Minneapolis, MN, USA). RNAi was conducted as described (Lamitina et al., 2006). Worms were dispensed to wells as L1s and given 4 days to grow to adulthood at 16°C. Worms were visually screened for basal GFP fluorescence, heat-shocked at 35°C for 3 hr, allowed to recover at 16°C for 3 hr, and then visually screened again for wells whose RNAi treatment prevented activation of the heat shock promoter. Clones identified as hits from the primary screen were rescreened in quadruplicate and compared with an

empty vector control by quantitative analysis on the COPAS. Hits were considered verified if their normalized values were ≤ 60% of the empty vector.

COPAS Biosort

A COPAS Biosort with Advanced Acquisition Software Version 5.2.69 was utilized. Systems without Advanced Acquisition Software or earlier versions of the COPAS software that do not output data in 26-column format are not compatible with the software as written. Young adult animals fed either empty vector RNAi or gene-specific RNAi were sorted through the COPAS for quantification of GFP fluorescence. Worms were washed from plates with 5–10 mL deionized water, placed in the COPAS sample cup, and analyzed in the single-sample format. COPAS settings were as follows: gain ext, 1; green, 5; yellow, 1; red, 1; threshold signal, 30; TOF minimum, 1; photomultiplier tube (PMT) settings control green, 600; yellow, 0; red, 0. Worms were gated based on TOF to select for adults, and MATLAB analysis was performed specifically on this gated population. Although we prefiltered our data during screening, COPAquant allows users to filter raw data files based on gating status (gated, nongated, or all data). COPAmulti also filters based on gating status and will additionally filter on any COPAS measured parameter (TOF, EXT, fluorescent channel 1 (Ch1), fluorescent channel 2 (Ch2), or fluorescent channel 3 (Ch3)).

MATLAB

MATLAB version 7.0.1.24704 was used in the creation of this program. MATLAB M-files for COPAquant, COPAmulti, and COPAcompare, as well as sample data files and instructional documentation are freely available through our web site (www.med.upenn.edu/lamitinalab/index.shtml).

Statistics

Bar graphs indicate mean values ± SD. In COPAmulti, we implement the mean ± *k* SD method for hit identification by calculating the plate mean ± plate SD and then determining which wells exceed this minimum SD threshold. The median absolute deviation (MAD) test was conducted using the MAD function in the MATLAB library. Multiple comparison *t*-tests were conducted using the *t*-test function in the MATLAB library. It should be noted that user-defined *P* values must be corrected for multiple comparisons by dividing the selected *P* value by the number of samples analyzed (Bonferroni correction).

Acknowledgements

This work was supported by a grant from the National Institutes of Health (NIH; grant no. 1R01AA017580 to T.L.) and an NIH training grant in Cell and Molecular Biology [no. T32 GM-07229 to E.M. (principle investigators Richard Schultz and Marisa Bartolomei)]. The authors wish to thank Hernan Garcia and Michael Springer for helpful training in MATLAB-based analysis, Weon Bae and Rock Pulak for providing sample ReFLX data, and the suggestions of four anonymous reviewers that greatly improved the manuscript.

Program	Purpose	Filtering capability	Parameters analyzed	Data normalization
COPAquant	Analysis of single-file data	Gating status	TOF, Ext, Ch1, Ch2, Ch3	None
COPAquant V2	Anlysis of single-file data	Gating status	TOF, Ext, Ch1, Ch2, Ch3	File 1
COPAmulti	Analysis of 96-well plate data	Gating status, TOF, Ext, Ch1, Ch2, Ch3	TOF, Ext, Ch1, Ch2, Ch3	Plate mean
COPAmulti V2	Analysis of 96-well plate data	Gating status, TOF, Ext, Ch1, Ch2, Ch3	TOF, Ext, Ch1, Ch2, Ch3	User-selected well(s)
COPAcompare	Pair-wise comparison of replicate plates	Gating status, TOF, Ext, Ch1, Ch2, Ch3	TOF, Ext, Ch1, Ch2, Ch3	Plate mean
COPAcompare V2	Pair-wise comparison of replicate plates	Gating status, TOF, Ext, Ch1, Ch2, Ch3	TOF, Ext, Ch1, Ch2, Ch3	User-selected well(s)

Table 3-1. Analysis properties of the COPAS MATLAB analysis software

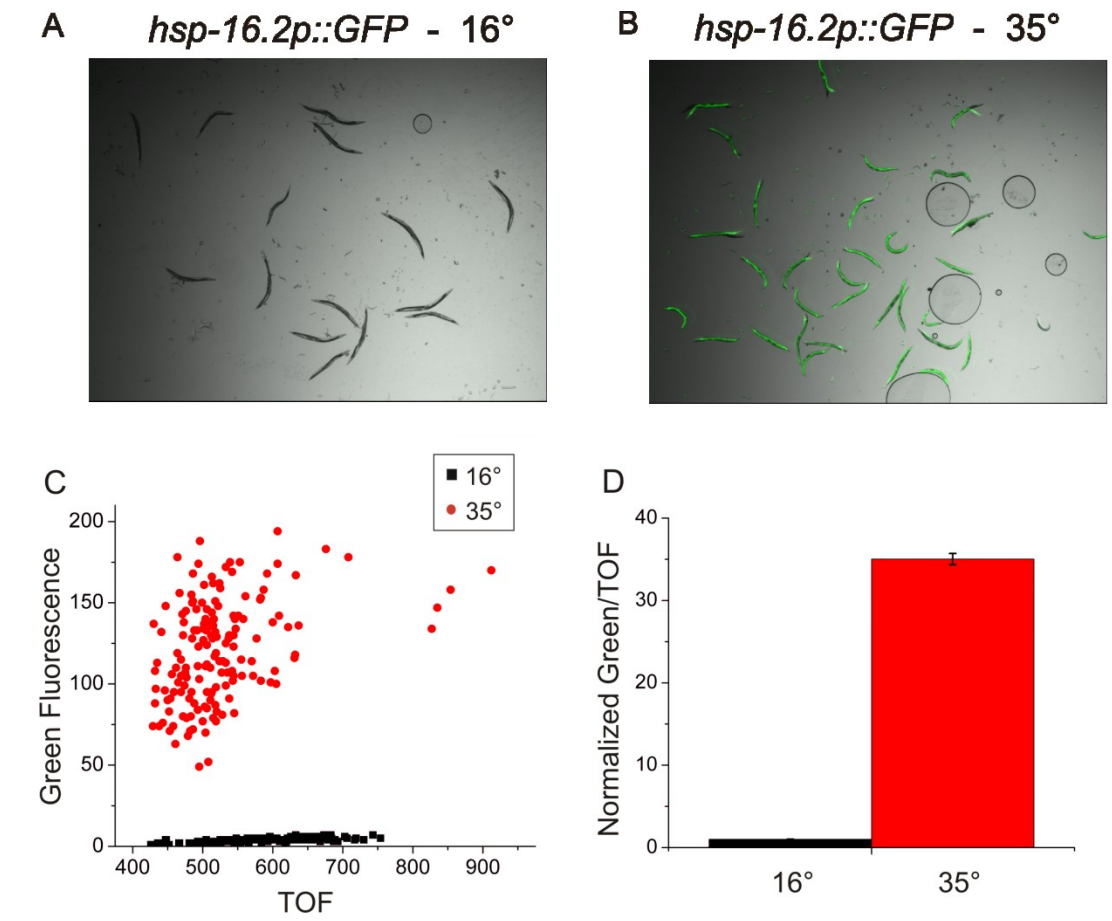

Figure 3-1. COPAS quantification of a heat shock–inducible GFP reporter

(A) Photomicrographs of *hsp-16p::GFP* at 16°C or (B) after 3 h of heat-shock at 35°C and 3 h of recovery at 16°C. (C) Values of TOF and green fluorescence were recorded for each individual adult worm using the COPAS Biosort. (D) The reporter expression in each population was summarized by mean ± SD GFP expression normalized to the TOF and displayed here as the fold-change increase of heat-shocked worms over non–heat-shocked worms. N = 149 for each.

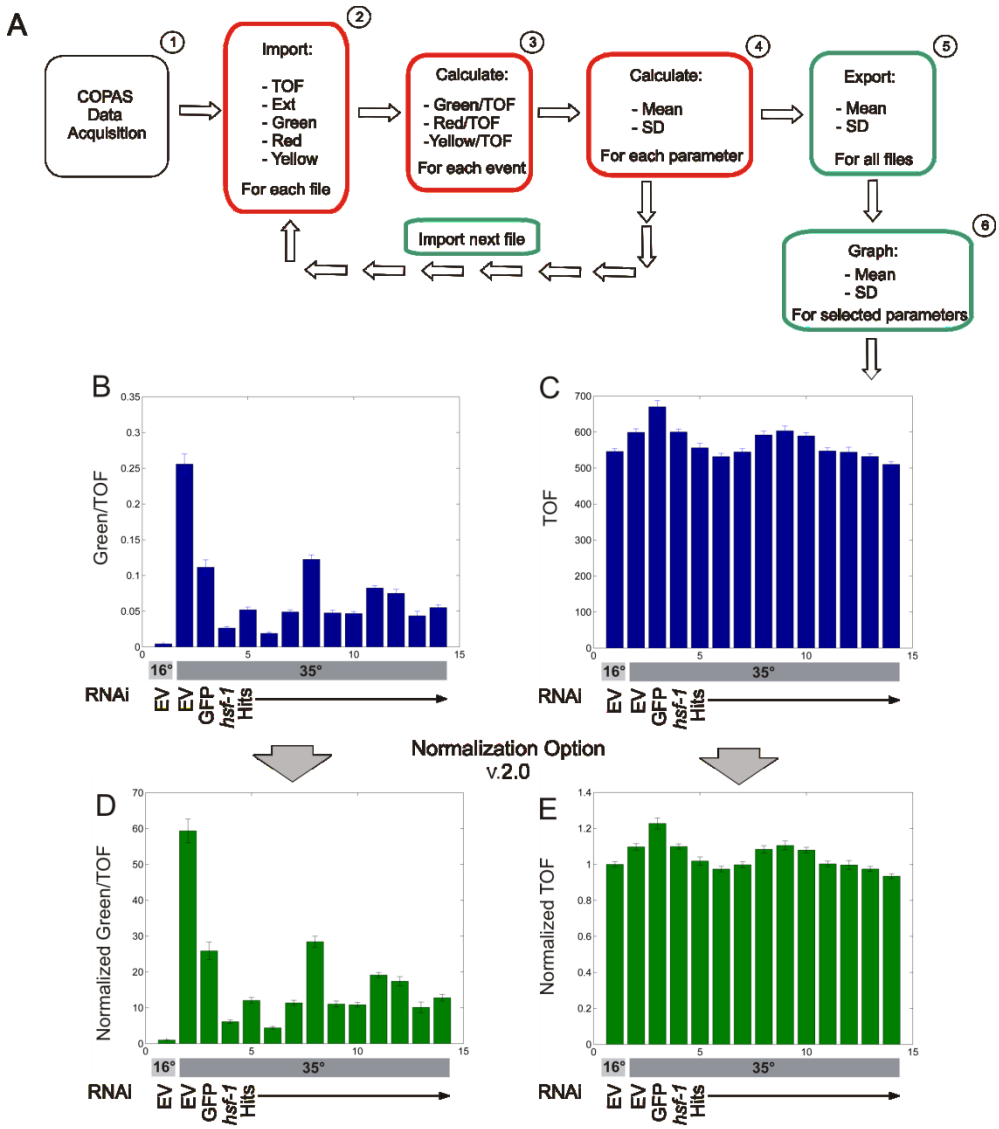

Figure 3-2. Data analysis flowchart for COPAquant analysis of single-sample mode data

(A) Data flow is diagrammed for extraction of mean and SD of particular parameters from COPAS files. Red boxes represent tasks completed by the function COPASFun, while green boxes represent COPASImp tasks. (B) MATLAB was used to quantify fluorescence in an RNAi screen for suppressors of *hsp-16p::GFP* expression after heat-shock (35°C). Empty vector (EV) RNAi represents the negative control before and after heat shock. GFP and *hsf-1* RNAi represent the positive controls for clones that decrease expression. HSF-1 is a transcription factor that promotes *hsp-16.2* expression. Hits are

RNAi clones identified as repressing reporter expression in our screen. Values were normalized to TOF. (C) TOF values for the same samples as in panel B were graphed. (D and E) COPASFun version 2.0 normalizes each event value to the mean of the 16°C EV control and returns the new means and standard deviations. Shown are the normalized graphs for the data in panels B and C. For all conditions, $N \geq 41$.

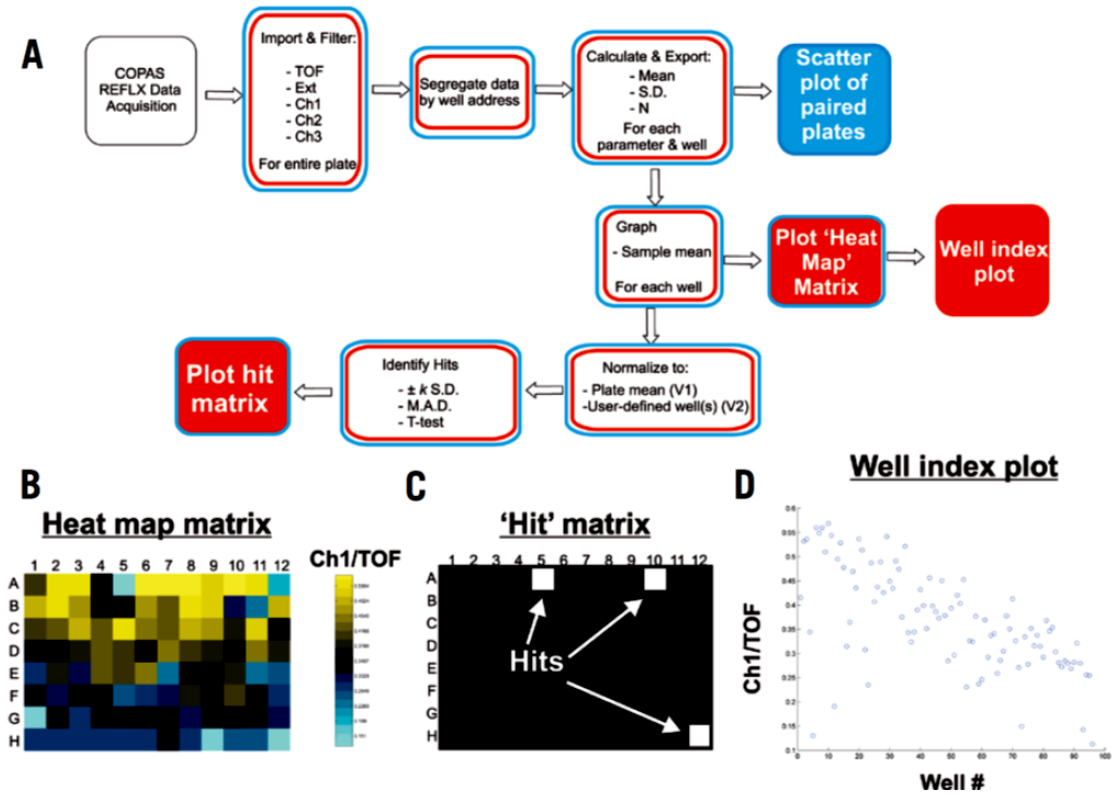

Figure 3-3. Data analysis flowchart for COPAmulti and COPAcompare analysis of ReFLX multiwell mode data

(A) Data flow is diagrammed for extraction of well mean and SD of user-defined parameters from COPAS ReFLX files. Red boxes represent tasks completed by COPAmulti. Blue boxes indicate specific tasks completed by COPAcompare. Solid boxes indicate plots generated by COPAmulti or COPAcompare. (B) Heat map plot for the well means of Ch1/TOF data from a hypothetical 96-well ReFLX file. Note that the coloring is autoscaled according to the specific data for each plate. (C) Hit matrix plot indicating wells that passed a user-defined statistical threshold (in this case, MAD > 3 for Ch1/TOF). Hits are plotted in white, and non-hits are plotted in black. (D) Well index graph plotting the GUI-selected parameter for each well. If multiple 96-well plates are analyzed, all wells from all plates are plotted (i.e., plate 1, wells 1–96; plate 2, wells 97–192; plate 3, wells 193–278; etc.).

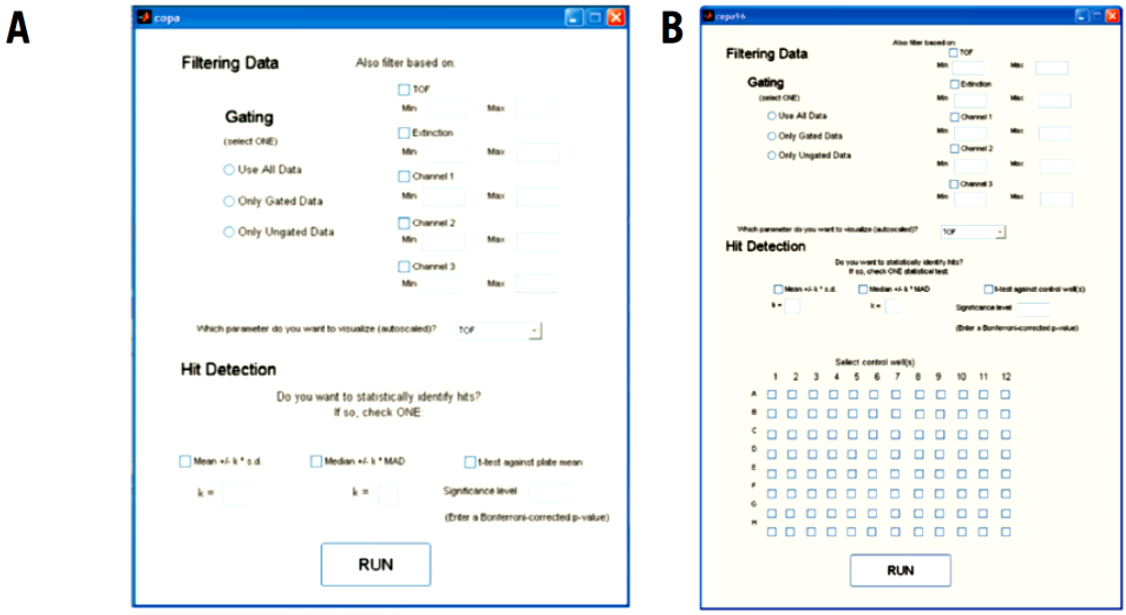

Figure 3-4. Graphical user interface for COPAmulti

(A) Screen shot of the COPAmulti GUI demonstrating user-configurable parameters for multiwell plate analyses. Ch1, Ch2, and Ch3 refer to the respective fluorescence channel (green, yellow, and red on most, but not all, COPAS systems). The parameter to be analyzed is selected from the drop-down menu in the middle of the GUI. Hit identification is accomplished via selection of one statistical test and associated threshold criteria. (B) Screen shot of the COPAmulti GUI that allows users to select negative control normalization well(s).

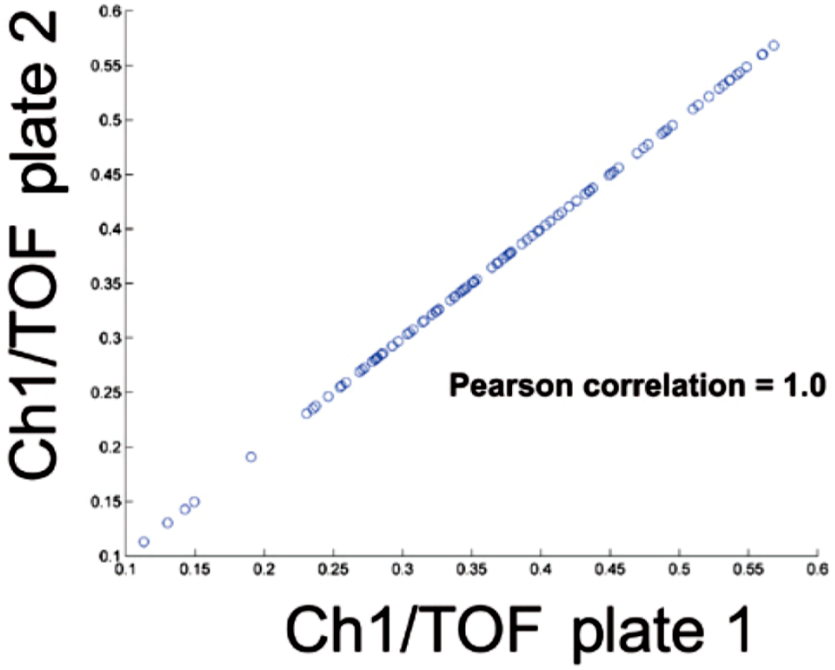

Figure 3-5. Two plate comparison using COPAcompare

Screen shot of the results from a hypothetical COPAcompare two plate comparison. Two identical hypothetical ReFLX files were compared with one another, resulting in a calculated Pearson correlation coefficient of 1. The calculated Pearson Correlation is displayed within the MATLAB command console, as illustrated in our online tutorials (www.med.upenn.edu/lamitinalab/downloads.shtml). Each point on the graph represents a single well, with the x-coordinate representing data from plate 1 and the y-coordinate representing data from plate 2. Overall correlation was determined using the Pearson Correlation function within the MATLAB library.

4. A genome-wide RNAi screen for regulators of HSF-1

Summary

The eukaryotic heat shock factor HSF1 is an evolutionarily conserved transcription factor with functions in stress response, protein homeostasis, aging, innate immunity, and cancer. Its critical role in these organismal processes makes its regulation potentially of great interest in the understanding and management of human health and disease, yet many questions persist concerning the specifics of HSF1 activation. One such question is the identity of its upstream regulators. The nematode *Caenorhabditis elegans* is an established model for studying HSF1-dependent biological processes, and the tools available in worms, as well as the similarity between worm HSF-1 and human HSF1, make *C. elegans* an excellent system for identifying new regulators of this transcription factor. We used a bacterial RNAi feeding library to screen the *C. elegans* genome for regulators of a heat shock-inducible fluorescent reporter and identified 44 genes. Knockdown of 42 of these genes resulted in decreased reporter expression after heat shock. Knockdown of one resulted in limited reporter expression in the absence of heat shock, and knockdown of another resulted in hyper-induced reporter expression after heat shock. The hyper-inducer of reporter expression was *smo-1*, a gene encoding the worm homolog of the post-translational modifier SUMO. We hypothesized that SUMO modification may directly affect HSF-1 activity after heat shock, as a mechanism of activation-dependent feedback regulation. Mutation of four potential sumoylation sites on the HSF-1 molecule itself resulted in some phenotypes that support this hypothesis and others that suggest a different role for SUMO in heat shock-inducible gene regulation.

Introduction

HSF1 is a highly evolutionarily conserved eukaryotic transcription factor with roles promoting not only response to heat stress, but also innate immunity, development, and longevity (Hsu et al., 2003; Sarge et al., 1993; Singh and Aballay, 2006a; Xiao et al., 1999). It has been implicated in protection against proteotoxicity and protein aggregation in models of human neurodegenerative diseases like Huntington's, Machado-Joseph, and Alzheimer's (Cohen et al., 2006; Nollen et al., 2004; Teixeira-Castro et al., 2011). More recently, it was identified as a possible therapeutic or prognostic target in several types of cancer (Dai et al., 2007; Mendillo et al., 2012; Santagata et al., 2011; Sato et al., 2012). The regulation of this transcription factor, therefore, is of great interest in human health and disease.

When activated by stress, HSF1 upregulates transcription of its target genes, heat shock proteins (HSPs), to re-establish proteostasis after stress-triggered disruption of protein folding. The process leading to activation of HSF1 is complex. HSF1 is believed to be kept in an inactive state under routine growth. Activation upon stress exposure involves inter- and intra-molecular interaction release, trimerization, post-translational modification, and DNA binding (Baler et al., 1993; Green et al., 1995; Sarge et al., 1993). A common model of HSF1 suppression proposes that its inactive form is cytoplasmic, repressed primarily by binding to cytoplasmic chaperones. Release from chaperones and translocation to the nucleus are major components of its activation in this model (Baler et al., 1996; Zou et al., 1998). An increasing number of reports argue, however, that HSF1 is constitutively nuclear (Mercier et al., 1999; Morton and Lamitina, 2013; Westwood et al., 1991), questioning the importance of cytoplasmic chaperones in its direct regulation.

In light of the tight and rapid regulation of the activation process, there are likely many other yet unidentified factors involved in control of HSF1 activity.

C. elegans has many advantages as a tool in the study of HSF1 regulation. It is an established model for several of the above HSF1-dependent processes (aging, immunity, proteotoxicity). It is genetically tractable and optically transparent to fluorescent reporters, allowing localization of tagged proteins or visualization of reporter gene expression. Quantification of fluorescent reporter expression is rapid and straightforward through the use of a small object sorter (COPAS Biosort, Union Biometrica) and computational analysis tools (Morton and Lamitina, 2010). Finally, commercially available libraries of bacterial clones expressing double-stranded RNA allow specific knockdown of target genes through RNA interference (RNAi) and permit rapid genome-wide screening in *C. elegans*.

The *C. elegans* HSF homolog, HSF-1, shares approximately 32% sequence similarity overall with human HSF1, with much greater homology in the predicted DNA binding and trimerization domains (Figure 1-1). It is also predicted to contain a C-terminal transactivation domain, like human HSF1 (Hajdu-Cronin et al., 2004). Worm HSF-1 has recently been shown to exhibit subnuclear redistribution upon heat shock into structures very similar to the HSF1 stress granules once thought to be primate-specific (Morton and Lamitina, 2013). Similarity between worm and human HSF1s suggests that regulators might be conserved between the two species.

Here we describe a genome-wide RNAi-based screen for regulators of an inducible HSF-1-dependent transcriptional reporter. We identified many genes whose downregulation resulted in decreased expression from the target promoter, classifying

them as positive regulators of heat shock reporter expression. The predicted functions of these screen hits span many ontological classes, including ribosome structure and translation, mitochondrial function, and post-translational modification. Many fewer negative regulators or attenuators were identified. The latter category consisted solely of the gene *smo-1*, encoding the worm homolog to SUMO, a small ubiquitin-like protein modifier. SUMO is a known direct post-translational modification of human HSF1, but its function is debated. We present evidence that in worms, SUMO may be a regulator involved in deactivation of HSF-1 after transient stress exposure, but that, like in human cells, the full effect of this modification on regulation may be complex.

Results

A genome-wide RNAi screen identified 44 regulators of heat shock-inducible gene expression. To screen for regulators of a heat shock-induced reporter, we took advantage of the RNAi tools available in *C. elegans*. Ingestion of double stranded RNA (dsRNA) by *C. elegans* is capable of drastically reducing expression of a homolgous gene throughout most, but not all, tissues in the organism (Timmons and Fire, 1998). *Escherichia coli* clones that target *C. elegans* genes are commercially available in libraries that cover approximately 90% of the ~19,000 predicted protein-coding genes. In our screen, worms were grown from L1 to adult (4 days) at 16°C on induced RNAi bacterial clones, in order to maximize repression of target genes.

Our screen assay utilized strain TJ375, a reporter strain expressing a heat shock-inducible, HSF-1-dependent promoter driving GFP, *hsp-16.2p::GFP*. Expression of this reporter is tightly regulated, with virtually undetectable expression under growth conditions but very high expression following heat shock (Figure 4-1). Unless otherwise

stated, all references herein to heat shock (HS) or 35°C treatment of TJ375 refer to 3 hr exposure on NGM agar plates in a 35°C incubator followed by 3 hr recovery at 16°C (Figure 4-1A). Worms were screened for four different phenotypes: 1) expression of GFP without heat shock, 2) moderately reduced GFP expression following heat shock, 3) severely reduced GFP expression following heat shock, and 4) hyperexpressed GFP following heat shock. A list of 722 primary hits (genes visually selected as having a phenotype during the initial screen) is given in Table 4-1.

Hits from the primary screen were subjected to secondary screening. Secondary screening involved visual examination of the primary hits in quadruplicate, using the same heat shock protocol. Clones with a visible phenotype in 3 of the 4 quadruplicate wells were considered verified by the rescreen. Hits were eliminated if they also reduced expression of a *col-12p::dsRed* reporter (strain OG119) that was examined visually in a paired screen, on the assumption that knockdown of that gene interfered with general transgene expression. Clones that passed this secondary screen (see Table 4-2, column 1) were then quantified for fluorescence expression using the COPAS Biosort. This has the advantage of allowing the highly variable phenotype of heat-induced gene expression to be assessed at a population level (Figure 4-1F). Additional criteria were implemented at this step to cull genes into a final hit list. Reasons hits were eliminated (or re-annotated) at this juncture included 1) COPAS quantification of post-heat shock *hsp-16.2p::GFP* expression (normalized for animal size as measured by time of flight (TOF)) for positive regulators was ≥ 60% of EV, 2) RNAi reduced expression of a non-heat stress-induced reporter, the osmotically activated *gpdh-1p::GFP*/TOF, 3) RNAi clone could not be recovered, or 4) sequencing revealed a different RNAi clone than reported (sequencing

primer in Table 4-3). Roughly 10% of clones within the RNAi library are incorrectly annotated. Reasons for elimination and the final gene list are given in Table 4-2.

It should be noted that our validation procedure was stringent, and RNAi efficiency is variable, making false negatives in our final screen results a near inevitability. The primary list of non-validated 'hits' is given in Table 4-1 and contains several additional putative heat shock protein and chaperonin genes (*dnj-16*, *dnj-3*, *cct-1*, *cct-4*, and *cct-5*) and 16 predicted kinases, including MAP kinase kinase *jkk-1*, and insulin/insulin-like signaling pathway kinase *age-1*. The Ras-like GTPase *rab-1* is also on the list, a gene whose described RNAi phenotype is acceleration of protein aggregation, a process known to involve HSF-1 function (Nollen et al., 2004). There are therefore many hits on this list that might prove valid regulators given further investigation.

hsf-1 itself was blindly identified as a hit during two different primary screens of chromosome I. It was rescreened in quadruplicate twice, but in only one of these did it meet the 3 of 4 minimum rescreen criteria. *hsf-1* RNAi clones were also included as known controls during heat shock on each day of screening, exhibiting reduction of GFP expression ~90% of the time during the primary screen. Thus, *hsf-1* exemplifies both the general reliability and occasional fallibility of RNAi.

Of the 44 verified final hits, 42 genes were identified whose knockdown reduced heat shock-induced gene expression. The predicted functions of these putative positive regulators varied. The largest class consisted of ribosomal and translational genes. Other classes of positive regulators include genes involved in transcription, post-translational modification, mitochondria, and development, among others (Table 4-4). Of the two

remaining hits, one hit, *smo-1*, resulted in overexpression of GFP only after initial activation, and one hit, *his-63*, had weak constitutive GFP expression. Figure 4-2 presents quantification of fluorescence for the 43 post-heat shock hits. The exact quantification values are given in Table 4-5.

Constitutive *hsp-16.2p::GFP* expression was observed with knockdown of chaperone genes only at higher growth temperature. It is notable that only one hit, the histone H3 gene *his-63*, was identified with constitutive (very localized) GFP expression during our screen (Figure 4-3). The current model of HSF-1 regulation states that it is kept inactive by interaction with chaperones, making it surprising that knockdown of chaperone genes did not induce constitutive GFP expression. To explore this result, we selectively screened a chaperone RNAi sub-library at three different growth temperatures: 16°C, 20°C, and 25°C. We found that growth temperature greatly influenced the effect of chaperone RNAi on *hsp-16.2p::GFP* expression. Expression without heat shock was visually determined after growth on RNAi for 2 days at 25°C, 3 days at 20°C, and 4 days at 16°C. Of the 97 different genes screened, only one was capable of inducing constitutive GFP at 16°C, the temperature at which our original screen was conducted. Many chaperone clones, however, induced higher basal levels of GFP when animals were grown at 25°C (Table 4-6). GFP expression was assessed again the following day, before heat shock of the samples. Genes that exhibited a phenotype are summarized in Table 4-6. It should be noted that in nearly every case, GFP expression on these clones was extremely localized and appeared tissue-specific.

The only RNAi clone to produce weak basal GFP at 16°C was *hsp-1*. Only 2 of ~30 worms on this clone showed this expression, explaining why this clone failed to be

detected as a constitutive GFP hit in the original screen. *hsp-1* was identified in the original screen, however, as having reduced heat shock-induced expression (Figure 4-2). The contradictory phenotype of increased basal GFP and decreased post-heat shock GFP was also observed for several of the clones when worms were grown at 25°C (Table 4-6, last column). While this seems counterintuitive, one possible explanation is that upregulation of the stress response pathway before heat shock protects animals, such that induction of the pathway is not as robust when they are exposed to acute stress. In other words, inducing basal expression of the heat shock response may be analogous to preconditioning the animals to heat shock. Ultimately, we conclude that knockdown of single chaperones is insufficient to activate *hsp-16.2p::GFP* expression unless worms are already subject to the mild stress of high growth temperatures.

***smo-1* RNAi increased expression of the *hsp-16.2p::GFP* reporter only after heat shock.** One screen hit was verified with the phenotype of increased levels of GFP post-heat shock. *smo-1* encodes the sole worm homolog of SUMO, a small, 11 kDa, ubiquitin-like peptide that covalently modifies proteins. SUMO is an essential gene in *C. elegans*, *Saccharomyces cerevisiae*, and *Drosophila melanogaster* (Broday et al., 2004; Johnson et al., 1997; Johnson and Hochstrasser, 1997; Jones et al., 2002; Talamillo et al., 2008). Modification by SUMO affects many different aspects of protein regulation, including localization (Dobreva et al., 2003), stability (Desterro et al., 1998), protein-protein interaction (Lin et al., 2006), and protein conformation (Steinacher and Schar, 2005). Sumoylation is known to occur on many nuclear proteins, often regulating activity of transcription factors (Gill, 2005).

RNAi against *smo-1* had an unusual phenotype: hyperexpression of heat shock-induced GFP (Figure 4-4). Knockdown of *smo-1* had no effect on the reporter in the absence of stress. Before heat shock, worms had no visible GFP (Figure 4-4C), indicating that *smo-1* is not a simple essential negative regulator of gene expression. Expression post-heat shock, however, displayed a marked increase in GFP expression compared to heat shocked empty vector controls (Figure 4-2, Figure 4-4B, D). This is true not only for the transgenic *hsp-16.2p::GFP* reporter, but also for the endogenous HSP-16.2 protein (Figure 4-4E). This observation led us to hypothesize that *smo-1* is involved in activation-dependent suppression of the heat stress pathway, possibly via direct modification of the HSF-1 protein.

***smo-1* RNAi affects inducible expression of *gpdh-1p::GFP*.** As part of the rescreening process, RNAi hits were screen for a phenotype on another stress-inducible reporter: the osmotically-induced *gpdh-1p::GFP*. *smo-1* RNAi was also found, in most trials, to increase post-stress expression of this reporter (Figure 4-5B). This suggests that effects of SUMO are not restricted to the heat stress pathway. *smo-1* RNAi does not affect all transgene expression, as demonstrated by the unaltered expression of the constitutive reporter *unc-54p::YFP* (Figure 4-5A). Our original aim being to identify heat stress-specific regulators, we eliminated RNAi clones from the positive regulator hit list if they reduced expression of both *hsp-16.2p::GFP* and *gpdh-1p::GFP*. A literature search revealed that human HSF1 is a known SUMO target (Hong et al., 2001), and shortly after our screen was completed, Kaminsky *et al.* found that *C. elegans* HSF-1 is a SUMO conjugate, though the function of the modification was unclear (Kaminsky et al.,

2009). On the basis of these observations, we continued to explore our hypothesis that SUMO is a direct regulator of HSF-1 and retained it in the final RNAi hit list.

***gei-17* RNAi decreased expression of *hsp-16.2p::GFP* reporter.** If SUMO attenuates the heat stress response pathway, downregulation of enzymes that promote sumoylation should phenocopy *smo-1* RNAi. Like ubiquitin conjugation, SUMO conjugation involves multiple enzymes: an E1 activating enzyme (a heterodimer of Aos1 and Uba2), E2 conjugating enzyme (Ubc9), and E3 ligases (facilitating SUMO conjugation to targets). *gei-17*, the SUMO E3 ligase in *C. elegans* (Holway et al., 2005), was a verified hit in our screen, but its phenotype was the opposite of the one predicted based on *smo-1* RNAi. While *smo-1* RNAi increased heat shock-induced GFP, *gei-17* RNAi decreased it (Figure 4-2, Figure 4-6). One quality of SUMO conjugation, however, is the capacity of the E2 enzyme to directly interact with target protein sequences (Buschmann et al., 2001; Sampson et al., 2001), and sumoylation has been demonstrated to occur in the absence of an E3 *in vitro* (Hietakangas et al., 2003; Okuma et al., 1999). Thus, knockdown of the E3 does not necessarily preclude a role for sumoylation.

We hypothesized that the effects of *smo-1* and *gei-17* RNAi were through the transcription factor HSF-1 and thus should translate to other transcriptional targets of HSF-1. Using qRT-PCR, we examined mRNA levels of *hsp-70* (C12C8.1) after heat shock. *hsp-70* expression is reduced on *hsf-1* RNAi and *gei-17* RNAi, and hyper-induced on *smo-1* RNAi (Figure 4-7), the same expression pattern seen with *hsp-16.2p::GFP*. The regulatory effects of SUMO and GEI-17 therefore apply to at least two different HSF-1 targets.

Though no other SUMO conjugation enzymes were pulled out during our screen, these results prompted us to do directed screening on other members of the sumoylation pathway. RNAi clones against the E1 enzyme were unavailable, but RNAi against the E2, *ubc-9*, showed significantly greater *hsp-16.2::GFP* expression than EV, suggesting a phenocopying of *smo-1* (Figure 4-6F).

The effect of *smo-1* RNAi is independent of growth temperature and development, but dependent on HSF-1. SUMO has a role in development in worms (Broday et al., 2004; Jones et al., 2002; Rytinki et al., 2011). In order to eliminate complicating developmental factors in the *smo-1* RNAi phenotype, we exposed *hsp-16.2p::GFP* worms to *smo-1* RNAi post-developmentally (plated as L4s) and quantified their GFP expression after 1, 2, or 3 days of knockdown at 16°C (Figure 4-8). After 2 days, we saw increased GFP expression of the *smo-1* RNAi worms compared to their EV counterparts, indicating that the phenotype is independent of the developmental role of SUMO.

As evidenced by the chaperone knockdown results above, growth temperature can influence response to heat stress. We examined *smo-1* RNAi on worms grown at 16°C, 20°C, and 25°C. At all temperatures, post-heat shock *hsp-16.2p::GFP* expression was increased by exposure to *smo-1* RNAi (Figure 4-9). Reporter hyperexpression on *smo-1* RNAi is not specific to growth temperature.

We asked if the effect of *smo-1* RNAi was dependent on HSF-1 activity. The allele *hsf-1(sy441)* contains a nonsense mutation just before the predicted transactivation domain at the C-terminus of the protein. These mutants are viable (unlike *hsf-1* nulls), but exhibit deficiencies in lifespan, immunity, development, and stress-inducible gene

expression. Expression of the *hsp-16.2p::GFP* reporter in this background demonstrated that heat shock no longer induced high levels of GFP on *smo-1* RNAi (Figure 4-10A). Heat-induced HSP-16.2 expression is not completely abolished in the *hsf-1(sy441)* hypomorph, however, and the very low levels of GFP induced trended toward further reduction on *hsf-1* RNAi and slight increase on *smo-1* RNAi, though neither to a significant extent (Figure 4-10B). We concluded that the very high levels of GFP seen with heat shock on *smo-1* RNAi are the result of an HSF-1-dependent pathway.

HSF-1(K4xR)::GFP rescues *hsf-1* mutant phenotypes. It is to be expected that global knockdown of SUMO will affect more aspects of physiology than just heat-induced gene expression. Kaminsky *et al*. identified 248 proteins conjugated to SUMO in worms of mixed developmental stages (Kaminsky et al., 2009). Consistent with our hypothesis that HSF-1 is one of the direct targets of sumoylation, mass spectrometry revealed worm HSF-1 as a SUMO conjugate (Kaminsky et al., 2009). We approached the problem of parsing the effects of SUMO on HSF-1 regulation specifically by attempting to generate a non-sumoylatable form of HSF-1.

SUMO modification occurs on a lysine residue, and most frequently at a consensus motif (ΨKXE, where Ψ is a hydrophobic residue and X is any amino acid) (Rodriguez et al., 2001). Human HSF1 is sumoylated at lysine 298 (Hong et al., 2001). Unfortunately, this residue is in the poorly-conserved regulatory domain, and there is no equivalent lysine in worm HSF-1. We used computational methods to predict potentially sumoylated lysines based on sequence analysis of worm HSF-1 (Ren et al., 2009). The program used identified potential sites based both on the consensus motif as well as predicted non-cannonical sumoylation sites. Four residues were identified as potential

targets of sumoylation in the HSF-1 protein: lysines K24, K192, K239, and K434 (Figure 4-11A). We used site-directed mutagenesis to mutate these lysines to arginines in *hsf-1* cDNA, maintaining the positively charged residue while eliminating potential targets for sumoylation.

We expressed this mutated construct as an integrated, single-copy transgene, under 4 kb of the native *hsf-1* promoter and with a C-terminal GFP tag (HSF-1(K4xR)::GFP). This construct was as capable of rescuing development as the wild-type version of the construct (HSF-1::GFP) (Morton and Lamitina, 2013) in two different mutant backgrounds (*hsf-1(sy441)* and the more severe allele, *hsf-1(ok600)*) (Figure 4-11B,C). Mutation of these lysines, therefore, did not interfere with activity of HSF-1 in a developmental context.

smo-1 RNAi decreases worm lifespan (Figure 4-11D). As HSF-1 activation and overexpression are known to extend worm lifespan (Hsu et al., 2003; Lithgow et al., 1995), our *hsp-16.2p::GFP smo-1* RNAi result would predict knockdown of *smo-1* to either increase lifespan or more likely (given that the effect of *smo-1* in our screen was only seen after heat shock) have no effect on lifespan. HSF-1(K4xR)::GFP and HSF-1::GFP were equally capable of rescuing the lifespan phenotype of *hsf-1(sy441)* (Figure 4-11E), though HSF-1(K4xR)::GFP did have statistically reduced survival in a single trial of pathogen resistance (Figure 4-11F). Absence of a phenotype with the lysine mutant could be interpreted to mean we have not successfully interfered with sumoylation, or that HSF-1 is not the relevant target of sumoylation, but it is also consistent with the model that SUMO is a repressor only of stress-induced HSF-1 activity, and short lifespan on *smo-1* RNAi is due to effects of sumoylation on proteins other than HSF-1.

On the prediction that the effect of SUMO on HSF-1 is stress-dependent, we asked if HSF-1(K4xR)::GFP displays resistance phenotypes in assays of induced stress. In our test for thermotolerance (survival at continuously high temperature) we again failed to observe increased survival with HSF-1(K4xR)::GFP (Figure 4-11G). However, the mutant *hsf-1(sy441)* alone also failed to display a phenotype in this assay. This observation has been made before (Kourtis et al., 2012; McColl et al., 2010), leading to a current model that HSF-1 is not involved in defense against a primary heat shock, but rather in acquisition of increased tolerance against subsequent heat shocks (an assay in which *hsf-1(sy441)* does display a phenotype).

Based on these results, the better assay to use is one that might involve post-heat shock gene expression. A recently published paper described an assay for survival after an acute heat stress with or without a preconditioning heat stress (Kourtis et al., 2012). Unlike the published work, we were unable to detect reduced survival of *hsf-1(sy441)*; and survival of both wild-type and mutant controls was inconsistent (Figure 4-12). The lack of control consistency prohibits reliable interpretation of the results, but we do note that preconditioned HSF-1(K4xR)::GFP repeatedly showed the highest survival rates.

HSF-1(K4xR)::GFP exhibits normal stress behavior. Formation of nuclear stress granules is a behavior of HSF-1 associated with stress activation in *C. elegans* (Morton and Lamitina, 2013). We hypothesized that HSF-1(K4xR)::GFP might be altered in its ability to form granules, recovery from them, or re-form them after a second stress. However, HSF-1(K4xR)::GFP showed no defect in nuclear localization, and exhibited the same granule formation behavior as HSF-1::GFP (Figure 4-13A-H). The same result was seen for HSF-1::GFP grown on *smo-1* RNAi (data not shown). HSF-

1(K4xR)::GFP also appeared to undergo a heat-induced increase in molecular weight (Figure 4-13I). The molecular weight increase immediately following heat shock has been shown to be the result of phosphorylation, not sumoylation (Chiang et al., 2012).

HSF-1(K4xR)::GFP expression phenocopies *smo-1* RNAi in some genetic backgrounds. *smo-1* RNAi causes an increase in HSP-16.2 expression after heat shock. If the mechanism for this involves sumoylation of one of our identified lysines, the lysine mutant HSF-1(K4xR) should phenocopy *smo-1* RNAi in its expression of HSP-16.2. We compared rescue of HSP-16.2 induction with HSF-1::GFP and HSF-1(K4xR)::GFP in two different *hsf-1* mutant backgrounds. In the background of *hsf-1(sy441)*, rescue with HSF-1(K4xR)::GFP showed hyperexpression of HSP-16.2 after heat shock compared to wild-type HSF-1::GFP, phenocopying *smo-1* RNAi (Figure 4-14A). Rescue in the *hsf-1(ok600)* background, surprisingly, did not display this phenotype (Figure 4-14B).

These conflicting results led us to question whether the HSP-16.2 hyperexpression phenotype was really due to lack of HSF-1 sumoylation. If mutation of the potential target lysines abolished sumoylation of HSF-1, and if sumoylation of HSF-1 is responsible for the HSP-16.2 phenotype, *smo-1* RNAi on HSF-1(K4xR)::GFP worms should result in no further increase of HSP-16.2 expression (i.e. depletion of SUMO should have no effect if the relevant target already cannot be sumoylated). Increase of HSP-16.2 on *smo-1* RNAi would indicate that sumoylation is still capable of repressing HSP-16.2 expression even in the absence of the potential sumoylation sites on HSF-1, suggesting the action is through a different target (or target site). Examination of HSP-16.2 expression after heat shock in *hsf-1(ok600)* HSF-1(K4xR)::GFP-rescued lines on empty vector or *smo-1* RNAi showed a decrease in HSP-16.2 on *smo-1* RNAi (Figure

4-14C). Paradoxically, HSF-1::GFP on *smo-1* RNAi did not show the increase in HSP-16.2 expression previously seen with wild-type HSF-1, even though control TJ375 on matching RNAi plates did display the *smo-1* RNAi phenotype (data not shown). Whether this could be the result of a deficiency in the strain background or a characteristic of the rescuing transgene is unclear.

In this set of experiments, HSF-1(K4xR)::GFP induced HSP-16.2 expression higher than HSF-1::GFP when both were on empty vector (compare lanes 1 and 4, Figure 4-14C). The only apparent difference between the experimental conditions in which *hsf-1(ok600):hsf-1(K4xR)::GFP* shows the hyperexpression phenotype and those in which it does is the food source used. This could potentially account for the inconsistent results, as the RNAi-expressing strain of bacteria used in Figure 4-14C, HT115, contributes to stress preconditioning differently than OP50, the standard strain used in Figure 4-14A and B (LaRue and Padilla, 2011). Clearly, further investigation is needed to reconcile the results shown here and fully understand the role of SUMO in the heat shock response.

Discussion

We describe here an RNAi-based screen for regulators of heat shock-inducible gene expression. We identified 44 genes that affected expression of an HSF-1-dependent reporter, the majority of which exhibited reduced reporter expression after heat shock. One gene was identified as a potential feedback regulator: the worm's SUMO homolog. Knockdown of SUMO caused no change in basal phenotype but resulted in hyperexpression of HSF-1 target genes after an initial heat shock. This was dependent on HSF-1 but independent of growth temperature and developmental effects of SUMO knockdown. From this observation, we hypothesized that sumoylation may be involved

in deactivation of the induced heat stress response pathway via modification of HSF-1. We mutated four potentially sumoylated lysines in the HSF-1 protein and phenocopied *smo-1* RNAi effect on HSP-16.2 expression, but only in certain genetic backgrounds.

Surprisingly, our screen identified no chaperones whose depletion constitutively activated HSP expression. This was unexpected in light of the model that chaperones bind to HSF1 and maintain it in an inactive form (Baler et al., 1996; Zou et al., 1998). One explanation is redundancy in the repression of HSF-1, such that depletion of a single chaperone is not sufficient for activation. Another possibility is that specific single chaperones do repress HSF-1, and our failure to detect them was a false negative, due either to the inefficiency of RNAi or a lack in library coverage (for instance, the chaperone DAF-21 is not present in our libraries). In combination with our published observation that worm HSF-1 is constitutively nuclear (Morton and Lamitina, 2013), we feel the simplest explanation is that cytoplasmic chaperones simply do not have a major repressive role in the acute stress response. This would contradict the long-standing model, but others have also proposed inconsistencies with chaperone-repression of HSF-1 (Rabindran et al., 1994; Westwood and Wu, 1993). We did find that RNAi against chaperone genes induced localized basal *hsp-16.2p::GFP* expression when worms were cultured at 25°C. This suggests that downregulation of a single chaperone is enough to activate target gene expression in certain tissues when in conjunction with a mild degree of stress.

The largest class of genes in the final hit list was ribosomal components and other genes involved in translation. Because knockdown of these genes did not reduce expression in another transgenic reporter, it is unlikely that the reduced *hsp-16.2p::GFP*

expression is simply due to globally reduced protein translation. Instead, this result may suggest a role for translation in regulation of the heat shock response. A recent screen for HSF1 regulators using a library of *Saccharomyces cerevisiae* loss of function alleles similarly identified many translational mutations with reduced HSF1 activity (Brandman et al., 2012). These components of translation may be involved in sensing problems with nascent protein folding and signaling to the stress response pathway. The yeast mutant screen also identified many mitochondrial mutants, another class of genes present in our hit list, suggesting that roles for these processes in HSF-1 regulation may be evolutionarily conserved.

The worm homolog for SUMO was identified in our screen with a unique phenotype: activation-dependent repression of HSF-1 target gene expression. HSF-1 itself is a promising target for sumoylation. Human HSF1 is inducibly modified by SUMO-1 on lysine 298 in the regulatory domain (Hong et al., 2001). Heat shock-induced phosphorylation is a prerequisite for this sumoylation (Hietakangas et al., 2003). The effect of sumoylation on HSF1 activity is debated. Some report that sumoylation of HSF1 promotes granule formation, DNA binding and target gene transactivation (Hong et al., 2001). Others argue that non-sumoylatable HSF1 is still capable of DNA binding and forming nuclear granules, but sumoylation represses inducible gene expression (Hietakangas et al., 2003; Hietakangas et al., 2006). Our data on SUMO depletion in worms are in general agreement with this latter report. We hypothesized that worm HSF-1 was inducibly sumoylated and that sumoylation was an activation-dependent repressor of HSF-1 activity. This hypothesis was supported by observations that *smo-1* RNAi increased post-heat shock expression of two different HSF-1 target genes, mutation of

potential sumoylation sites in HSF-1 phenocopied this in at least one genetic background, and the literature reports that worm HSF-1 is a SUMO conjugate (Kaminsky et al., 2009). We have encountered several discrepancies with our model, however, discussed below.

Although we did not show here that *C. elegans* HSF-1 is directly sumoylated, proteomics for SUMO conjugates have been done on unstressed, mixed stage worms (Kaminsky et al., 2009). HSF-1 was identified as a SUMO conjugate in this screen, confirming that it is a direct target of sumoylation, but contradicting our hypothesis that sumoylation is stress-induced. There are many possible explanations for this. *C. elegans* HSF-1 may be constitutively sumoylated (unlike human HSF1), and the heat shock-specific phenotype we see is due to interaction with other regulators. Alternatively, HSF-1 may be subject to both constitutive and inducible sumoylation, or the samples in the study were stressed in some way during the extraction procedure, inducing sumoylation. Finally, early developmental stages may differ from the adults used in our RNAi screen in their HSF-1 sumoylation properties. Since SUMO has a role in development, and HSF-1 in worms has recently been shown to be expressed at the highest levels during the earliest stages of development (Volovik et al., 2012), it is not a stretch to propose that the interaction between SUMO and HSF-1 may be different during development than it is in adulthood.

We predicted that mutation of four lysines in potential sumoylation sites in HSF-1 would phenocopy the *smo-1* RNAi-induced overexpression of HSP-16.2 seen after heat shock. These sites were selected solely on sequence analysis, so it is possible that HSF-1 is sumoylated on a non-canonical sequence that we did not mutate. Unfortunately, we were unable to biochemically confirm sumoylation of HSF-1. As a result, the

inconsistencies seen with the HSF-1 lysine mutant in this work could be due to mutation of incorrect lysines, or to HSF-1 not being the relevant direct SUMO target at all.

Rescue with HSF-1(K4xR) reproduced the *smo-1* RNAi phenotype, but only in a background of a hypomorphic allele of *hsf-1* (*sy441*), and not in a null (*ok600*). This could be due to unknown genetic differences in the backgrounds of these strains, failure to have mutated the correct lysines, or compromised protein function conferred by mutation of multiple lysines. We speculate that mutation of the four lysines may have a detrimental impact on HSF-1 outside of the proposed effect on sumoylation. If so, expression in the presence of a partially functional HSF-1 protein (i.e. *hsf-1(sy441)*) may rescue this function where expression in a null background does not. We have previously reported that a functionally deficient HSF-1 transgene is capable of rescuing some *hsf-1* phenotypes in the presence of *sy441*, which has intact DNA binding and trimerization domains (Morton and Lamitina, 2013). One of the mutated lysines in HSF-1(K4xR) is within the DNA binding domain and another is within the trimerization domain – mutations within either of these domains might interfere with function. K192 is also a potential acetylation site, based on sequence alignment with human HSF1 acetylation sites (Westerheide et al., 2009). Proteins with residues that are targets of both acetylation and sumoylation have been described in other systems – p300 (Bouras et al., 2005), estrogen receptor (Sentis et al., 2005), and MEF2A (Shalizi et al., 2006) – and a model has been proposed of a SUMO-acetyl trade-off paradigm in which one modification represses and one activates (Anckar and Sistonen, 2007). In such a case, mutation of the target lysine may well muddle the transcriptional consequences of eliminating sumoylation versus acetylation.

HSF-1(K4xR) induced greater HSP-16.2 levels in the *ok600* background when worms were cultured on the RNAi-producing *E. coli* strain, HT115(DE3). This was not true for worms grown on the standard *E. coli* strain, OP50. HT115 is known to influence stress response, and can contribute to anoxic stress preconditioning where OP50 does not (LaRue and Padilla, 2011). Attempts to use RNAi bacteria to understand the lack of phenotype of HSF-1(K4xR) in *ok600* were unsuccessful. Inconsistencies in the phenotype suggest that HSF-1 regulation by SUMO may be a complex process, much like it is for mammalian HSF1 and HSF2 (Anckar et al., 2006; Goodson et al., 2001; Hietakangas et al., 2006; Hong et al., 2001).

gei-17 RNAi reproducibly caused a reduction of *hsp-16.2p::GFP* expression, a phenotype contrary to what we would expect based on its proposed role in SUMO conjugation. In the ubiquitin pathway, E3 ligases are responsible for substrate specificity. There are over 600 human ubiquitin E3 ligases (Li et al., 2008), but only approximately 11 described vertebrate SUMO E3 ligases (Wang and Dasso, 2009), suggesting that their role in SUMO conjugation may not be specificity. SUMO E3 ligases do seem to facilitate SUMO transfer to target proteins, but the E2 enzyme UBC-9 is capable of conjugating SUMO to certain targets without an E3 (Buschmann et al., 2001; Okuma et al., 1999; Reindle et al., 2006). Therefore, even though GEI-17 is so far the only described SUMO E3 in *C. elegans* (Holway et al., 2005; Rytinki et al., 2011), depleting it may not eliminate sumoylation of proteins. It is even conceivable that knockdown of *gei-17* may simply shift the profile of sumoylated proteins, resulting in increased sumoylation of proteins that do not rely on an E3. Whether *gei-17* affects HSF-

1 directly or indirectly, or if this phenotype is yet another example of the variable nature of the SUMO modification, remains to be determined.

In human cells, SUMO-1 transiently colocalizes with HSF1 granules (overlapping after 15 min of heat shock, but not after 30 min) (Hietakangas et al., 2003). We did attempt to express a fluorescently-tagged SUMO to look for colocalization with HSF-1::GFP, but were unable to functionally rescue a *smo-1* mutant with this mCherry::SUMO (data not shown). Reports conflict on whether or not non-sumoylatable human HSF1 is capable of forming nuclear granules (Hietakangas et al., 2003; Hong et al., 2001), but it should be noted that in the study that found lysine-mutated HSF1 retained granule formation ability (Hietakangas et al., 2003), as well as in our own lysine mutant study, endogenous wild-type HSF-1 was present in the background. This could be a confounding factor due to the oligomeric nature of induced HSF-1.

In human cells, splicing factors are recruited to HSF-1 stress granules in a manner dependent on HSF-1 transcription (Denegri et al., 2001; Metz et al., 2004). Our RNAi screen identified some predicted splicing factors as positive regulators of the heat shock response. Future investigation should determine if these or other spicing factors are recruited to HSF-1 granules in worms, and what their role might be in stress response regulation.

We have described here identification of many potential regulators of the heat shock response. Much work remains in exploring the mechanisms by which these candidates might influence stress responsive gene expression. Unraveling the function of SUMO, specifically, may be a challenging process. As has been observed in studies of human HSF1 (Hietakangas et al., 2003), it does not appear that characterization of the

role of sumoylation in HSF1 regulation is straightforward. Nevertheless, there is encouraging evidence of its possibility as a feedback regulator of HSF-1.

Materials and Methods

C. elegans strains

The following strains and alleles were used in this study: N2, EG4322 *ttTi5605;unc-119(ed9)*, PS3551 *hsf-1(sy441)*, TJ375 *gpIs1[hsp-16.2p::GFP::unc-54utr]*, AM134 *rmIs126[unc-54p::YFP]*, OG233 *hsf-1(sy441);gpIs1*, OG119 *drIs4[col-12p::dsRed;gpdh-1p::GFP]*, OG497 *drSi13[hsf-1p::hsf-1::GFP::unc-54utr;Cb-unc-119+];unc-119(ed9)*, OG565 *drSi27[hsf-1p::hsf-1(K4xR)::GFP::unc-54utr;Cb-unc-119+];unc-119(ed9)*, OG576 *hsf-1(ok600)/hT2[bli-4(e937) let-?(q782) qIs48]*, OG575 *hsf-1(ok600)/hT2[bli-4(e937) let-?(q782) qIs48];drSi13*, OG593 *hsf-1(ok600)/hT2[bli-4(e937) let-?(q782) qIs48];drSi27*, OG532 *hsf-1(sy441);drSi13*, OG586 *hsf-1(sy441);drSi27.* Single-copy strains were created as described in Chapter 2. The *hsf-1(sy441)* point mutation background was confirmed by sequencing a 613bp PCR product (primers OG1054 and OG130. OG1054 is intronic, preventing amplification of cDNA transgenes. See Table 4-3). Strains were maintained on standard NGM (Brenner, 1974) seeded with OP50. EG4322 was maintained on HB101 bacteria.

RNAi screen

Two commercially available RNAi libraries were employed in the screen. The MRC library (MRC Geneservice, Cambridge, England) was screened in its entirety, supplemented by additional genes from the ORFeome-based library (Open Biosystems Inc., Huntsville, Alabama). The bacterial clones in these libraries contain plasmids with T7 promoters driving expression of a region homologous to a *C. elegans* gene, creating

double-stranded RNA. Expression of the T7 RNA polymerase is regulated by a lac operon-based promoter, which can be induced by lactose or its analog IPTG (isopropyl-β-D-thiogalactopyranoside). The RNAi screen was done in 24-well format, on standard NGM containing 25 μg/mL carbenicillin and 10 mM β-lactose (for the primary screen) or 1 mM IPTG (for repeated primary screening of chromosome I and II and additional RNAi experiments). RNAi bacteria (HT115(DE3)) was cultured from the frozen libraries on LB plates containing 25 μg/mL carbenicillin and 12.5 μg/mL tetracycline. Cultures were grown overnight in liquid LB and 25 μg/mL carbenicillin and spotted 30-50μL per well, followed by a day of growth at room temperature. L1 worms, synchronized by post-bleach developmental arrest via overnight incubation in M9 at 20°C, were seeded to each well and grown at 16°C for 4 days. Approximately 30 L1s per well were seeded on IPTG RNAi plates, and approximately 100 L1s per well were seeded on lactose RNAi plates. In the primary screening stage, chromosomes I and II were screened on both IPTG and lactose RNAi plates, while the remaining chromosomes were screened only on lactose. Standard heat shock of *hsp-16.2p::GFP* consisted of 3 hr in a 35°C incubator followed by 3 hr of recovery in a 16°C incubator. To facilitate temperature change, plate lids were kept ajar for the entire heat shock period and most of the recovery period (lids were closed between hours 1-2 of the 3 hr recovery period). Controls with lids left ajar at 16°C for the same period of time showed no GFP expression. Plates were screened visually before and after heat shock. Each gene identified as a primary hit was rescreened in quadruplicate. A confirmed hit showed a phenotype in at least 3 of 4 replicates and had quantified GFP expression that was ≤ 60% EV expression (for positive regulators). During rescreening, control EV RNAi was included on every 24-well plate.

Fluorescence was quantified using a COPAS Biosort (Union Biometrica, Holliston, MA, USA). Worms were washed off plates with ~10-30 mL dH_2O, placed in sample cup, and run through the machine, from which size (time of flight (TOF)) and GFP fluorescence were determined. A threshold for TOF was set to eliminate eggs and very young larvae (mean and minimum TOF values for each RNAi clone in Figure 4-2 are presented in Table 4-5). The fluorescence value for each individual was divided by its TOF value to normalize to size (GFP/TOF). For normalization to a control, individual GFP/TOF values were divided by the mean value of GFP/TOF for the control sample. The mean of these normalized values is presented in the bar graphs. The identity of the final RNAi clones were confirmed by DNA sequencing.

Molecular biology methods

Site-directed mutagenesis (QuikChange Multi Site kit, Cat. #200515-5) was used to create HSF-1(K4xR)::GFP (pOG116) from *hsf-1* cDNA (pOG34). The primers used, OG1095, OG1054, OG1097 and OG1029, can be found in Table 4-3. pOG34 contains a silent valine→valine mutation compared to the canonical WormBase sequence; this mutation was unintentionally fixed by primer OG1095 and then reinstated with primer OG1098, generating plasmid pOG119. An Invitrogen Multisite Gateway reaction was performed using plasmids pOG119, pOG88 (4 kb of *hsf-1* promoter in pDONRP4-P1R), pOG99 (*GFP::unc-54 3' UTR* in pDONRP2R-P3), and pCFJ150 (chromosome II single-copy insertion vector) to make plasmid pOG121. See Morton and Lamitina 2013 for creation of pOG34, pOG88 and pOG99. Single-copy insertion (Frøkjær-Jensen et al., 2008) of pOG121 into strain EG4322 was performed as described in Chapter 2.

Immunobloting

HSP-16.2 and GFP reporter expression was assessed using samples of 100 worms grown at 16°C on RNAi plates and collected in 25 µL dH_2O. An equal volume of 2x SDS-PAGE loading dye was added after collection, followed by 15 min boiling. Samples (15µL, approximately 30 worms) were run on a 10-20% TrisHCl gel (Bio-Rad) after another 15 min boiling, followed by transfer to nitrocellulose and blocking in 2% milk in 1X TTBS (1M Tris, 150 mM NaCl, 0.1% Tween 20). Membranes were probed simultaneously for HSP-16.2 (1:5000, rabbit, #5506 R120; kind gift of Chris Link, UC Boulder), GFP (1:1000, mouse, Roche 7.1 and 13.1) and β-actin (1:2000, mouse, Sigma AC-15) overnight at 4°C. Membranes were washed in 0.1% milk 1X TTBS three times and then probed with secondary antibodies, anti-mouse HRP and anti-rabbit HRP (1:5882 dilution both, Amersham). Immunoblots were visualized with Amersham ECL Western Blotting System (RPN2108). Westerns for HSP-16.2 expression in *hsf-1(sy441)* and *hsf-1(ok6000)* backgrounds used 20 young adults grown at 16°C on OP50, collected in M9, and boiled ≥15 min in an equal volume of 2x SDS-PAGE loading dye. These samples were run as above with the following exceptions: no GFP antibody was present in the primary antibody solution, secondary antibodies were anti-rabbit HRP (1:5882, Amersham) and anti-mouse HRP (1:2000, #7076 Cell Signaling), and blots were visualized with Thermo Scientific chemiluminescent substrate detection system (Prod. #34080). In the *hsf-1(ok600)* background, strains were maintained over the hT2 GFP balancer and thus non-green adult progeny of heterozygotes were selected for immunoblotting. Westerns on *hsf-1(ok600)* worms exposed to RNAi were performed as above, with the exception that samples consisted of 16 worms grown on RNAi plates

(HT115 bacteria) and collected in 30 µL total volume, though only 25 µL of each sample was loaded in a 15% polyacrylamide gel. Immunoblot detection of molecular weight of HSF-1::GFP (Figure 4-13) were performed on samples collected and run on a 7.5% gel as described for HSF-1::GFP westerns in Morton and Lamitina, 2013.

Rescue assays

In lifespan, *Pseudomonas* survival, and thermotolerance assays, worms were grown at 20°C and picked as L4 the day before the assay. For *P. aeruginosa* PA14 assays, 20 µL of 11-hour PA14 culture was spotted on 3 cm plates containing 50 µM FUdR and 0.35% peptone and let grow overnight. The next day, 10 young adults were placed on each PA14 plate, totaling 5 plates for most strains and 7 plates for *sy441*. For lifespan assays, 10 young adults were picked to 5 OP50 plates containing 50 µM FUdR. Both lifespan and *P. aeruginosa* assays were conducted at 25°C. In thermotolerance assays, 4 plates of 10 worms each (or 2 plates of 25 worms in trial 1) were put at 35°C in a box with a wet paper towel to prevent desiccation. Thermotolerance trials 2-4 were scored blindly. Worms were classified as alive, dead (no movement in response to touch with a wire), or censored (lost or bagged worms) twice a day starting on day 2 for *Pseudomonas* assay, once a day for lifespan, and every 1-2 hr for thermotolerance.

For developmental rescue assays, adults grown at 20°C were allowed to pulse lay eggs for 3-6 hr. Eggs were placed at 25°C for 45-48 hr, after which worm size was determined by COPAS Biosort time of flight measurements. In the case of *hsf-1(ok600)* rescue, balanced *ok6000/hT2* worms were allowed to lay eggs for approximately 4 hr before removing adults and leaving plates at 20°C for three days. All worms ≥ L4 were scored for presence of the balancer (pharyngeal GFP).

Microscopy

Worms were anesthetized in 1 mM levamisole in M9 and imaged on 2% agarose pads. Images for Figure 4-13 were collected as Z-stacks on a Leica DMI4000 with a 63X lens and deconvolved (10 iterations, 16-bit, blind, with background removed) using Leica software. Heat shock of these worms was performed by placing the slide on a 35°C heat block. Images of *hsp-16.2p::GFP* expression were collected at with a 10X lens on the same microscope and not deconvolved, heat shocks as described in "RNAi screen" section. Worms in Figure 4-13 were grown at 20°C and were L4 the day before imaging. *hsp-16.2p::GFP* worms were grown 4 days at 16°C from arrested L1.

qRT-PCR

RNA isolation and qRT-PCR were carried out as described in Morton and Lamitina, 2013, with the following changes: worms were grown for 4 days at 16°C (from synchronized L1s) on RNAi, plates were heat shocked and recovered as described in the "RNAi screen" section above, 125 worms were collected for each sample, and no DNase treatment step was included. Directly after the phase separation procedure in the Trizol (Ambion, Cat. no. 15596-018) RNA extraction protocol, an equal volume 70% ethanol was added and the RNAeasy purification protocol (Qiagen, Cat. no. 74106) was implemented. Quadruplicate technical replicates were run.

Heat stoke preconditioning

Preconditioning assays were modeled after published protocols (Kourtis et al., 2012), with some changes made. Young adult worms (grown from synchronized L1s at 20°C for three days) were washed off plates with 20°C M9 and split into two aliquots in 1.5 mL tubes, in a final volume of 200 μL. One tube for each strain was placed in a 34-35°C

water bath for 30 min, while the other (control) was placed in a 20°C incubator for the same time. Worms were transferred to 3 cm plates and left to recover at 20°C for 6 hr. Short recovery periods (10 min or 20 min) were not found to increase survival in preconditioned worms and in many cases actually decreased survival. After recovery, worms were washed off again with 20°C M9, placed into 1.5 mL tubes (200 μL final volume), and heat stroked in a 39°C water bath for 15 min. Worms were placed on 6 cm plates and left 20°C until the next day (16-20 hr). Plates were scored blindly for percent survival. Worms were considered alive if they moved in response to a plate tap.

Statistical analysis

Survival studies were analyzed using the Kaplan-Meier log rank function (GraphPad Software). Comparison of three or more samples used one-way ANOVA with Bonferroni post-tests analysis.

Acknowledgements

We thank Chris Link for the HSP-16.2 antibody, Krysta Brown for performing the *smo-1* RNAi lifespan analysis (Figure 4-11D), and Tim Chaya for plate preparation and OG119 screening during the RNAi screen. This work was supported by NIH training grant T32 GM07229 (E.A.M.) and by NIH grant R01AA017580 (T.L.). Some nematode strains used in this work were provided by the Caenorhabditis Genetics Center, which is funded by the NIH National Center for Research Resources (NCRR).

Chr I		Chr II		Chr III	
Name†	Score	Name†	Score	Name†	Score
F56C11.1	-1	F23F1.5	-1	T17A3.10	-2
rpl-7	-1	*rpt-4*	-1	F40G9.1	-2
smo-1	3	*etr-1*	-1	*btb-1*	-1
tub-2	3	*ubxn-3*	-1	F40G9.5	-1
inx-13	-1	II-1I11	-1	F40G9.6	-1
rpl-13	-1	B0432.1	-1	*mxl-2*	-1
F55C7.2	3	C24H12.5	3	*mat-3*	3
rpn-8	-1	C24H12.6	-1	*dac-1*	-2
D1007.3	-1	*mlt-8*	-1	*rps-29*	-2
rpl-24.1	-1	*clec-118*	-1	K02F3.12	-1
pde-5	-1	F46F5.6	-1	*fbxa-51*	-1
T19B4.1	-2	F28A10.10	-1	*fbxa-55*	-1
ari-1	-1	*fbxc-27*	-1	M01E10.3	-2
T08B2.11	3	*fbxb-16*	-1	Y39A3A.2	-1
C10G11.1	-1	F52C6.12	-1	*fbxa-7*	-2
C10G11.6	-1	*fbsb-36*	-1	*fbxa-43*	-1
ZC328.1	-1	T16A1.2	-1	*gip-1*	-1
knl-2	-1	K09F6.5	-1	H14E04.2	-2
let-607	-1	F09D1.1	-2	W04B5.4	-1
dad-1	-2	F08D12.1	-1	W04B5.5	-2
R06C7.2	-1	K12H6.2	-1	W04B5.6	-2
hint-1	-1	*nhr-88*	-1	E02H9.7	-2
dylt-1	-1	T10D4.1	-1	T20B6.2	-1
I-3J10	-1	*sri-56*	-1	***ubl-1***	-2
K04G2.4	-1	T10D4.7	-1	*fipr-29*	-1
rpl-25.2	-1	T10D4.11	-1	*gei-1*	-2
mfap-1	-1	ZC239.4	-1	F59A2.5	-2
pbs-7	-1	F14D2.2	-1	*spe-41*	-1
pas-4	-1	T06D4.4	-1	C34C12.2	-1
gei-17	-2	C16C8.10	-1	*hmit-1.3*	-2
lim-9	-1	C01F1.1	-1	M01F1.7	-1
F25H5.3	-1	*ntl-2*	-2	C54C6.5	-1
eft-2	-1	*fkh-6*	-1	*unc-93*	-1
rpl-14	-1	*sra-33*	-1	C46F11.2	-2
tag-179	-1	*sre-39*	-1	C46F11.3	-2
1-5B17 (seq T23D8.3)‡	-2	*rpn-5*	-1	T27D1.3	-1
Y106G6E.1	-1	R05F9.12	-1	*pdi-1*	-2
wts-1	-1	*mdt-4*	-1	C14B1.2	-1
F25D7.4	3	ZK546.14	-1	F34D10.7	-1
Y106G6H.4	-1	*pbs-3*	-1	*cyp-25A3*	-1
Y106G6H.10	-1	*rpl-22*	-2	C36A4.4	-1
I-5C14	3	C34F11.3	-1	*brc-1*	-1
B0511.6	-1	*pho-1*	-1	*pat-3*	-1
lrk-1	-1	EEED8.2	3	C03C10.4	-2
I-5H23	-1	C17C3.3	-1	*unc-79*	-1
F56G4.6	-1	C25H3.6	-1	C16C10.2	-1
hsf-1	-2	F55C12.4	-1	*glod-4*	-1
gly-16	-1	II-4D05	-1	R74.2	-1
gly-17	-1	*fbf-1*	-1	*dnj-16*	-2
F08A8.2	-1	F21H12.1	3	*tag-131*	3
pbs-2	-1	C30B5.4	-2	B0284.4	3
W05B5.2	-1	*phb-2*	-1	*prdx-3*	-1
clec-107	-1	F13H8.2	-2	*rnp-4*	-2

ZK1225.5	3
F44F1.3	-1
vrs-2	-1
W09G3.6	-1
W04A8.2	-1
clec-113	-1
rps-20	-1
pbs-5	-1
Y39G10AR.8	-1
Y39G10AR.7	-1
Y39G10AR.7	-1
Y47G6A.9	3
rpl-17	-1
wwp-1	-1
deps-1	-1
I-8C23	-1
*cdk-7**	-1
*mis-12**	-1
F53B6.5*	-1
F55A12.10*	-1
*sst-20**	-1
*crs-2**	-1

F13H8.3	-1
rpl-10	-2
cct-1	-2
ifg-1	-2
nst-1	-1
cct-4	-2
hel-1	-1
acp-2	-1
frs-2	-1
T13H5.4	-1
rpl-5	-1
rpl-26	-2
C18E9.7	-1
jun-1	-1
let-23	-1
pqn-95	-1
gst-13	-1
Y51B9A.5	-1
M176.3	-1
mex-6	-1
zfp-2	-1
ZK1307.7	-1
nlp-11	-1
ZK1321.1	-1
R53.4	-1
F54B3.3	-1
let-858	3
rpl-41	-1
nuo-1	-1
mat-2	-1
***rps-9* (seq *crn-3*)**	-1
age-1	-1
clec-144	-1
top-2	-1
npp-3	-1
Y57A10A.13	-1
Y57A10C.9	-1
clec-64	-1
Y81G3A.4	3
his-9	-1
ZK131.11	3
Y39G8B.9	-1
hot-7	-1
Y48B6A.10	-2
srh-41	-1
btb-20	3
nspb-10	-1
tps-2	-1
tag-297	-1
ZC101.1	-1
C09F9.1	3
Y54E2A.1	-1
Y54E2A.1	-1
eif-3.B	-1
Y53F4B.23	-1
Y46G5A.4	-1
abcx-1	-1

cct-5	-2
clec-151	-2
rps-0	-2
pal-1	-1
C35D10.11	3
C27F2.1	-1
nca-2	-1
C45G9.10	-1
grs-1	-2
III-2F08	-1
R02F2.7	-1
F01F1.2	-2
C28H8.3	-1
F25B5.6	3
srg-6	-1
srg-2	-2
srg-3	-2
gar-2	-1
F47D12.3	-1
hmg-1.2	-1
F47D12.9	-2
Y102E9.6	-2
lim-8	-1
III-3P01	-1
rpl-36	-1
prs-1	-1
T20B12.5	-1
cup-5	3
rpl-9	-1
lpd-7	-1
lpd-7	-1
ZK686.3	3
C14B9.3	-1
rpl-21	-1
C14B9.8	-1
bath-42	-1
rfp-1	3
C06E1.1	3
R08D7.2	-1
eif-3.D	-2
F59B2.9	-2
emb-9	3
cbp-1	-1
K11H3.3	-2
cyld-1	-1
cyld-1	-2
ttr-2	-1
K03H1.5	-1
T16G12.6	-1
bath-43	3
T20G5.4	-1
cor-1	-2
M03C11.3	-2
Y39A1A.18	-1
Y39A1A.21	-1
mrt-2	-1
mdt-21	-1

		vps-32.1	-1	Y49E10.23	-2
		icd-1	-1	Y49E10.24	-1
		krs-1	-1	Y111B2A.5	-2
		rpl-33	-1	III-6G18	3
		F07F6.8*	-1	ZK1010.8	-1
		ZK666.2*	-1	*snf-7*	-2
		T05C1.1*	-1	F56A8.3	-1
		*ash-2**	3	*klp-19*	-2
		*sec-5**	-1	T27E9.2	-2
		*srh-99**	-1	T28A8.5	-2
		Y48C3A.20*	-1	Y66D12A.1	-1
		*fut-1**	-1	III-7I09	1
				Y53G8AR.5	-2
				Y53G8AR.2	-2
				H06I04.3	-1
				ubl-1	-1
				nlp-32	-1
				Y71H2AM.5	-1
				*trf-1**	-1
				Y53G8AM.4*	-1
				Y69F12A.1*	-1
				Y39A1A.1*	-2
				H14E04.1*	-1
				*gpr-1**	-1
				*trxr-2**	-2
				Y39E4B.2*	-2
Chr IV		Ch V		Chr X	
Name†	Score	Name†	Score	Name†	Score
R02D3.8	3	*egl-8*	-1	*sor-3*	3
col-101	-1	B0348.5	-1	F13C5.2	-1
dsc-4	-2	***rps-27***	-1	T19D7.3	-1
F56B3.2	-1	*nhr-252*	-1	*daf-3*	-1
F56B3.8	-1	ZK6.7	-1	*cutl-21*	-1
F38A1.8	-1	B0554.3	-1	T13G4.1	-1
pbs-1	-1	R11G11.6	3	C36C9.5	-1
hrp-1	-1	*srh-246*	-1	F07G6.8	-1
elks-1	-1	*rab-1*	-1	Y75D11A.2	-1
F58E2.4	-1	*fbxa-195*	-1	F53B1.8	-1
F58E2.5	-1	F53E2.1	-2	F53B3.5	-1
srz-23	-1	*sru-28*	-2	Y71H10A.1	3
F56D6.6	-1	C38C3.3	-1	F40F4.6	-1
F47C12.1	-2	K02H11.4	-1	F11D5.1	-1
hlh-30	-2	*srw-96*	-1	C04F6.2	-1
F49F1.6	-2	*sri-27*	-2	F47F2.1	3
Y51H4A.13	3	*str-160*	-1	C16B8.4	-1
Y24D9A.5	-1	F59A7.9	-2	R02E12.4	-1
rpl-7A	-1	*clec-208*	-1	F09F9.2	-1
ZK185.3	-2	*cyp-33C1*	-1	ZK470.2	-1
F28E10.1	-1	*nhr-134*	-1	F14H12.7	3
F29B9.10	-1	*cyp-33C7*	-1	*spr-3*	-1
E04A4.5	-1	*cyp-33C5*	-1	R08E3.2	-1
E03H12.5	-1	W02H5.3	3	K05B2.5	-1
ssq-4	-1	V-2J04	-1	ZC8.6	-2
nspd-3	-1	*lag-2*	-1	*pnk-4*	-2
ZK354.2	-1	T28A11.4	-2	T03G11.3	3
Y4C6B.2	-1	T28A11.5	-1	T03G11.4	-2

elo-6	-2	T28A11.16	-1	T03G11.5	-2
F41H10.9	-1	T28A11.17	-1	*kin-2*	-1
H35B03.2	-1	F35F10.7	-1	T07H6.3	-1
H32C10.1	-1	C17B7.3	-2	C03B1.12	-1
K02B2.3	-1	C17B7.4	-1	K04E7.1	-1
rps-25	-1	*srbc-36*	-2	T07H6.3	-1
pqn-22	-2	*grl-27*	-1	C03B1.12	-1
nspb-4	-1	*cyp-35A3*	-1	K04E7.1	-1
F38A5.11	-1	*srh-8*	-1	*pgp-10*	-2
nspb-2	-2	*cyp-35A4*	-2	ZK867.2	-1
C01B10.7	-2	F38H12.5	-2	*unc-10*	-1
C01B10.8	-2	T05B4.12	-1	*sng-1*	-1
C01B10.9	-1	***ugt-12***	-2	*spp-5*	-2
Y73B6A.2	-1	*srh-22*	-1	C07D8.5	-1
IV-3E20	-1	*srh-23*	-2	C07D8.6	-2
spd-3	-1	*srd-22*	-1	F45E1.2	3
H34C03.2	-1	F14F9.4	-1	F45E1.4	-1
dyci-1	-1	*sago-1*	-1	F45E1.5	-1
C17H12.5	-1	F13H6.5	-1	C02B8.5	-1
C17H12.6	-1	*atp-4*	-2	M60.5	3
C25A8.1	-2	*gad-1*	-1	F08F1.8	-1
R13A1.5	-1	W02F12.5	-1	F08F1.9	-1
R13A1.7	-2	*bbs-8*	-1	F16F9.3	3
plk-3	-1	T15B7.6	-2	***sdha-1***	-1
R05G6.5	-1	*lgc-54*	-1	C24A3.4	-1
glt-6	-2	*srg-31*	-1	*tsp-11*	-1
F49E8.2	-1	F20A1.1	-2	*tmbi-4*	-1
F49E8.7	-1	*srsx-32*	-1	F36G3.1	3
nol-10	-2	*mys-1*	-1	*fip-5*	-1
C46A5.4	3	*nhr-286*	-1	*fipr-21*	-1
C06A6.2	3	*cpsf-2*	-2	C39B10.5	-2
nhr-258	-2	F09G2.9	-1	*elt-2*	-1
D2096.8	-1	C05C8.5	-1	F59F5.4	-2
spp-10	-2	**C05C8.6**	-2	F59F5.5	-2
C53B4.6	-1	C13A2.9	-1	*syd-2*	-1
vps-26	-2	*cyp-35A1*	-2	F13E6.3	-1
dct-15	-1	**F19F10.9**	-2	*pgp-8*	-1
fat-3	-1	*nhr-94*	-1	F47B10.6	-1
C47E12.7	-2	***rpl-39***	-2	F38B2.3	3
C04G2.9	-1	*his-7*	-1	*cutl-11*	-2
gst-2	-1	*str-85*	3	F46F2.4	-1
rack-1	-1	V-6D23	3	*glb-28*	-1
F01G10.1	3	*rbx-1*	-1	Y15E3A.3	-2
Y43C5A.3	-1	F46B6.6	-1	H13N06.4	-1
T07G12.2	-1	**C08B6.5**	-1	*hke-4.2*	-1
ugt-54	-1	**ZK856.12 (seq F32D1.2.2)**	-1	ZK1073.2	-1
hrs-1	-1	*pap-1*	-2	Y13C8A.1	-2
Y69E1A.3	-1	***lpd-9***	-1	K09E3.6	-1
cyb-2.1	-1	H09F14.1	-1	T23C6.5	-1
F13H10.4	-1	*ocr-1*	3	X-7B24	-1
F13H10.5	-2	D1054.14	-1	T24D5.2	-2
rps-5	-1	T04C12.3	-1	*nhr-17*	-1
imp-2	-1	*glb-3*	-1	C02B4.3	-1
nhr-7	-1	*gpa-1*	-1	*ugt-50*	-2
his-63	1	R13H4.7	-2	*nhr-272*	-1
mbf-1	-1	F58H1.7	-1	*pgp-15*	-1
twk-25	-1	*add-2*	-1	F22E10.5	-2

sec-24.1	-2
F12F6.7	-2
F12F6.8	-1
rps-11	-2
cutl-27	-1
nhr-43	-2
ZK822.5	-1
ZK829.1	-1
unc-22	-1
K08E4.7	-1
lex-1	3
B0001.7	3
F20B10.3	-1
Y39C12A.9	-1
rps-23	-1
F08G5.1	-1
C25G4.6	-1
T04A11.3	-1
sru-19	-1
rbd-1	-1
K10D11.4	3
scl-7	3
col-132	-1
C08F11.10	-2
rpl-18	-1
noah-2	-1
nuo-3	-1
Y40H7A.4	3
sra-30	3
Y73F8A.13	-1
Y105C5A.15	-2
Y116A8C.10	-1
hsp-1	-1
sru-15	-1
Y38F2AR.10	3
rps-28	-1
clec-174	-1
IV-8J02	-1
nhr-242	-1
F35F11.1*	-1
C08F11.14*	-1
ZK616.2*	-1
W08E12.8*	-1
Y59E9AR.8*	-1
Y67A10A.7*	-1

C27A7.6	3
F55C5.8	-1
K01D12.15	-1
ttr-27	-1
T16G1.7	-2
R186.3	-2
F57B1.7	-1
***somi-1* (seq *bir-2*)**	-1
F53F4.11	-1
str-165	-1
D1086.5	3
srd-26	3
T16A9.4	3
T16A9.5	-1
rrbs-1	-1
F23B12.7	-2
C53A5.6	-2
unc-112	-1
H12D21.7	3
dnj-3	3
C01G10.4	3
Y75B12A.2	-1
cyn-3	3
ech-1	3
T06E6.1	-1
F35E8.9	-1
F36G9.13	-1
fbxa-99	-1
his-3	3
F44G3.7	-1
F21H7.3	-1
srw-29	-1
str-15	-2
F36D3.8	-1
cand-1	-1
phy-3	3
fbxa-110	-1
srh-206	-2
srz-54	-1
srh-118	-1
F16H6.4	-2
F16H6.9	-1
srh-207	-1
srh-209	-1
V-12I05	-1
V-12E04	-1
emb-4	-1
fbxb-63	-2
fbxb-65	-2
C25F9.6 (seq *emb-4*)	-1
Y43F8B.10	-2
Y113G7B.17	-1
mdt-17	-1
K02E2.6	-1
rpl-2	-1
Y44A6D.5	-1
Y61A9LA.10	-1

T14G8.4	-1
F11C1.2	-1
K08H2.3	-1
K08H2.4	-1
col-44	-1
Y12A6A.2	-1
gck-4	-1
F55F3.2	3
F19D8.2	-2
M03B6.1	-2
meg-2	-1
X-6F07	-1
dsl-4	-1
F28H6.4	-1
F28H6.6	-1
F28H6.7	-1
D1025.2	-1
unc-3	-2
dmd-4	-1
dpf-2	-1
*jkk-1**	-1
T21H8.5*	-1

		Y97E10AL.2	-1		
		*rpt-2**	-1		
		Y39B6A.42*	-1		
		*ztf-7**	-1		
		*srt-1**	3		
		F31D4.2*	-1		
		*scpl-4**	-1		
		*srj-15**	-1		
		B0462.1*	-1		
		*grl-9**	-1		

Table 4-1. Primary screen hits

Genes in the final hit list are highlighted in gray. If sequencing revealed a mistake in library clone annotation, it is indicated by the sequenced gene name in parentheses.
Score values are:
-1 = Post-heat shock GFP expression slightly less than empty vector
-2 = Post-heat shock GFP expression much less than empty vector
3 = Post-heat shock GFP expression much greater than empty vector
1= Slight pre-heat shock GFP expression

* Clone from ORF RNAi library. All other clones are from the MRC library.
† Wells that did not have a library-annotated sequence name are designated by their MRC library geneservice location
‡ MRC library location lists this well as empty, but it grew a clone sequenced as T23D8.3

Secondary hit list	Reason for elimination	Final sequenced hit list (44)
F53F4.11		F53F4.11
rpl-33	Reduced *gpdh-1p::GFP*/TOF	
rpl-36	COPAS >0.6 of EV	
ubl-1		*ubl-1*
hel-1	Reduced *gpdh-1p::GFP*/TOF	
smo-1		*smo-1*
rps-5	Reduced *gpdh-1p::GFP*/TOF	
F19F10.9		F19F10.9
bli-3	COPAS >0.6 of EV	
rpl-7	COPAS >0.6 of EV	
rpl-21	COPAS >0.6 of EV	
F58E2.5	COPAS >0.6 of EV	
abcx-1		*abcx-1*
symk-1	Reduced *gpdh-1p::GFP*/TOF	
T23D8.3	Reported empty well sequenced as T23D8.3	T23D8.3
cct-5	Reduced *gpdh-1p::GFP*/TOF	
npp-3		*npp-3*
rpl-26		*rpl-26*
rps-29	Reduced *gpdh-1p::GFP*/TOF	
lpd-9		*lpd-9*
lpd-7	COPAS >0.6 of EV	
noah-2	Too small to sort, culture could not be recovered	
atp-4	COPAS >0.6 of EV	
cpsf-2	Reduced *gpdh-1p::GFP*/TOF	
hsp-1		*hsp-1*
T06E6.1		T06E6.1
rps-9	Sequenced as *crn-3*	*crn-3*
rps-27		*rps-27*
rpl-17	Reduced *gpdh-1p::GFP*/TOF	
gei-17		*gei-17*
Y39G10AR.8		Y39G10AR.8
B0511.6		B0511.6
T13H5.4		T13H5.4
eif-3.B		*eif-3.B*
cbp-1	COPAS >0.6 of EV	
Y24D9A.5	COPAS >0.6 of EV	
rpl-7A	COPAS >0.6 of EV	
rpl-14		*rpl-14*
clec-107		*clec-107*
clec-113		*clec-113*
wwp-1		*wwp-1*
ifg-1		*ifg-1*

R53.4	Reduced *gpdh-1p::GFP*/TOF	
Y39G10AR.7		Y39G10AR.7
somi-1	Sequenced as *bir-2*	*bir-2*
sec-24.1		*sec-24.1*
rpl-39		*rpl-39*
rps-11	Reduced *gpdh-1p::GFP*/TOF	
rpl-18		*rpl-18*
rps-28		*rps-28*
nuo-3		*nuo-3*
rpl-2		*rpl-2*
sdha-1		*sdha-1*
his-63		*his-63*
rps-23		*rps-23*
Y61A9LA.10		Y61A9LA.10
C47E12.7		C47E12.7
ugt-12		*ugt-12*
C08B6.5		C08B6.5
ZK856.12	Sequenced as F32D1.2.2	F32D1.2.2
D1054.14	Reduced *gpdh-1p::GFP*/TOF	
unc-112	Reduced *gpdh-1p::GFP*/TOF	
col-44		*col-44*
Y12A6A.2		Y12A6A.2
C53B4.6		C53B4.6
C05C8.6		C05C8.6
F55C5.8	Reduced *gpdh-1p::GFP*/TOF	
C53A5.6	Reduced *gpdh-1p::GFP*/TOF	
C25F9.6	Sequenced as *emb-4*	*emb-4*
srd-26	COPAS >0.6 of EV	

Table 4-2. Secondary and final hit lists

Oligo Name	Oligo Sequence	Purpose
TL118	GAGTCAGTGAGCGAGGAAGC	Sequencing RNAi clones
OG130	TCCGGGTACTGTTGCTCATT	Reverse primer for sequencing *hsf-1(sy441)*
OG535	CCCAATCCAAGAGAGGTATCCTT	qRT-PCR primer for *act-2*, forward
OG536	GAAGCTCGTTGTAGAAAGTGTGATG	qRT-PCR primer for *act-2*, reverse
OG615	GAAAGGTTGAAATCCTCGCG	qRT-PCR primer for *hsp-70* (C12C8.1), forward
OG616	TCGAAAACTGTATTCTCCGGATTAC	qRT-PCR primer for *hsp-70* (C12C8.1), reverse
OG1029	ACAAGGACGTCCCGAATTACTATCACAGATTCGTAG AAAGCAATCGGCA	Mutagenesis primer K192R
OG1054	AAGCAAGCTCCGCCCATTTATTGGCT	Forward primer for sequencing *hsf-1(sy441)* (intronic)
OG1095	GCTCCAGAAACTGAAACTTCTTGACGCGGAACACGC ATTATCAGTTGTT	Mutagenesis primer K24R
OG1096	CATTTGTGTCCACATATCGCGATTTTCACGTGTAAGC TTATTCATCTTATCCTCCAT	Mutagensis primer K239R
OG1097	AGCACCCTGATAATCCCGACGCAGCGCAGAAATCCC ACG	Mutagenesis primer K434R
OG1098	TTCTTGACGCGGGACACGCATTATCAGTTGTTGCTG	Re-inserting silent Val-Val mutation

Table 4-3. Primers

Category	Gene	Description
Protein folding	*hsp-1*	HSP70A, a member of the heat shock family of proteins
Ribosomal	*rpl-2*	Large ribosomal subunit L8 protein
	rpl-18	Large ribosomal subunit L18 protein
	rpl-14	Large ribosomal subunit L14 protein
	rps-28	Small ribosomal subunit S28 protein
	rps-23	Small ribosomal subunit S23 protein
	rpl-26	Large ribosomal subunit L26 protein
	rpl-39	Large ribosomal subunit L39 protein
	rps-27	Small ribosomal subunit S27 protein
	F53F4.11	Uncharacterized conserved protein. Predicted ribosomal.
Translation	*eif-3.B*	Eukaryotic initiation factor
	Y39G10AR.8	Translation initiation factor
	ifg-1	Ortholog of the translation initiation factor 4F
	ubl-1	Similar to *Drosophila* ubiquitin/ ribosomal protein S27a
	C47E12.7	Predicted to be involved in rRNA processing
	Y61A9LA.10	BLAST homolgy to human ribosome biogenesis BMS1 protein
Post-Translational Modification	*gei-17*	BLAST homology to *S. cerevisiae* SUMO ligase
	smo-1	SUMO, a small ubiquitin-like post-translational modification
	wwp-1	Putative E3 ubiquitin ligase
Transcription/mRNA processing	T13H5.4	KOG splicing factor 3a
	F19F10.9	Homolog of the human SART1 gene, which may be involved in mRNA splicing
Mitochondrial	*nuo-3*	Locus encodes two proteins: an homolog of the WAVE1 complex and a putative NADH-ubiquinone oxidoreductase alpha subunit
	F32D1.2.2	Mitochondrial F1F0-ATP synthase subunit
	sdha-1	Ortholog of human succinate dehydrogenase complex subunit A
Membrane	C08B6.5	Glutamate-gated kainate-type ion channel receptor subunit
	clec-113	C-type lectin

	clec-107	C-type lectin
Apoptosis	*bir-2*	Protein with two BIR domains that may be involved in apoptosis.
	crn-3	Cell death-related nuclease
Transporter	*abcx-1*	ABC transporter
	C53B4.6	UDP N-acetylgulcosamine transporter
Growth and Development	B0511.6	DEAD-box helicase; loss via RNAi indicates required for larval development
	Y39G10AR.7	Involved in growth
	lpd-9	RNAi indicates required for fat storage and for larval growth and development
	T23D8.3	RNAi indicates required for embryonic and larval development
	emb-4	Required for normal embryonic and postembryonic development
Other/Unknown	*his-63*	H3 histone
	col-44	Cuticle collagen.
	ugt-12	UDP-glucuronosyl transferase
	npp-3	Nucleoporin
	sec-24.1	One of two *C. elegans* Sec24 homologs
	C05C8.6	Contains BTB domain (protein-protein interaction)
	T06E6.1	Uncharacterized conserved protein
	Y12A6A.2	

Table 4-4. Predicted hit gene functions

Gene	GFP/TOF mean	GFP/TOF SD	N	TOF mean	TOF SD
smo-1	2.7997	0.9768	71	0.9880	0.1280
EV	1	0.4265	97	1.0000	0.1106
ubl-1	0.5984	0.3448	155	0.7818	0.1988
C53B4.6	0.5853	0.4007	23	0.8867	0.0927
sdha-1	0.4588	0.2303	72	1.0021	0.1525
hsp-1	0.4455	0.1811	29	0.8621	0.1042
gei-17	0.4452	0.2248	59	0.9512	0.1253
C47E12.7	0.4105	0.1944	76	0.8946	0.1281
rps-28	0.4054	0.1973	59	0.7794	0.0951
rps-27	0.3982	0.1842	43	0.7941	0.1069
GFP	0.3975	0.2226	84	1.0249	0.1570
hsf-1	0.3973	0.2116	75	0.9362	0.1688
col-44	0.3880	0.1400	206	1.0642	0.2366
emb-4	0.3530	0.2259	103	1.0216	0.2060
lpd-9	0.3225	0.1297	110	0.9137	0.1446
clec-107	0.3212	0.1590	28	0.9535	0.1923
sec-24.1	0.3193	0.2796	29	0.7714	0.0891
ifg-1	0.3114	0.2032	92	0.8637	0.2014
crn-3	0.3036	0.2058	39	0.8173	0.0800
nuo-3	0.2624	0.1536	41	0.8936	0.1326
T06E6.1	0.2580	0.1176	100	1.0039	0.1589
Y39G10AR.8	0.2519	0.2259	110	0.7683	0.2457
T23D8.3	0.2740	0.1691	56	0.8353	0.1055
npp-3	0.2457	0.1873	42	0.8347	0.1292
Y39G10AR.7	0.2352	0.2098	84	0.6379	0.1767
rpl-18	0.2303	0.1413	47	0.8270	0.1040
clec-113	0.2190	0.1440	20	0.9418	0.1250
B0511.6	0.2057	0.2904	42	0.5548	0.1068
ugt-12	0.2032	0.1293	80	0.9283	0.1807
rpl-39	0.1962	0.1823	60	0.5982	0.1110
F19F10.9	0.1916	0.0983	71	0.9091	0.1215
C08B6.5	0.1862	0.1160	64	1.0070	0.1773
F32D1.2.2	0.1828	0.0890	63	0.9836	0.1141
bir-2	0.1705	0.2272	84	0.8880	0.1131
Y12A6A.2	0.1702	0.0648	220	1.0365	0.2265
eif-3.B	0.1679	0.1243	62	0.9158	0.1518
wwp-1	0.1678	0.1847	34	0.9336	0.1578
T13H5.4	0.1644	0.1280	21	0.8476	0.0745
rpl-2	0.1572	0.1340	22	0.8421	0.1351
Y61A9LA.10	0.1519	0.1138	44	0.8405	0.1114
rpl-14	0.1317	0.5026	37	0.5587	0.1809
rpl-26	0.1280	0.1002	62	0.5630	0.1423
rps-23	0.1048	0.0666	24	0.4516	0.0677
abcx-1	0.0890	0.0621	95	0.7063	0.1658
F53F4.11	0.0755	0.0368	31	0.8032	0.0811
C05C8.6	0.0646	0.0544	74	0.5215	0.1109

Table 4-5. COPAS quantification of screen hits

Both GFP/TOF and TOF are normalized to empty vector (EV) values.

		No HS			
	Gene	16°C§	20°C‡	25°C†	HS
ORF Library	*hsp-12.3*			***	****
	hsp-12.6			**	****
	hsp-16.2			*	**
	hsp-16.41			**	****
	hsp-25			**	**
	Y55F3BR.6			**	****
	ZK1128.7			*	****
	F08H9.3			*	****
	F08H9.4			*	****
	hsp-1			**	****
	hsp-3			*	****
	hsp-4			***	***
	C49H3.8			**	****
	C30C11.4			***	****
	cct-1			**	***
	cct-6			*	***
	cct-8		**	**	**
	pfd-2			*	****
	pfd-3			*	****
	pfd-4			*	**
	pfd-5			***	***
	dnj-7			*	****
	dnj-13			***	****
	dnj-16			***	****
	dnj-23			**	****
	F54F2.9			**	****
	cnx-1			**	****
	T05E11.3		*		****
	asfl-1			*	****
	C01G10.10			**	****
	unc-23			**	****
	ZC395.10			*	****
	C17G10.2			*	****
MRC Library	*hsp-16.2*			**	****
	hsp-43			*	****
	hsp-1	*	**	***	****
	hsp-6			**	***
	F44E5.4			**	****
	cct-2		**		****
	cct-3			*	****
	cct-6		*		****
	cct-7		**		****
	cct-8		**	*	****
	dnj-13			**	****
	dnj-24			*	****
	F54F2.9			*	****
	cuc-1			*	****

Table 4-6. Chaperone RNAi library screen without heat shock

§ Scored after 4 and 5 days 16°C

‡ Scored after 3 and 4 days 20°C

† Scored after 2 and 3 days 25°C
* Weak GFP expression in one worm
** Weak GFP expression in multiple worms
*** Moderate GFP expression in multiple worms
**** Strong GFP expression in nearly all worms
HS = Expression after heat shock of 25°C worms.

Trial	Strain	Mean lifespan* (Days ± SEM)	Number of worms	p-value vs. N2	p-value vs. h*sf-1(sy441)*	p-value *hsf-1(sy441); drSi13* vs. *hsf-1(sy441); drSi27*
1†	N2	10.6 ± 0.5	49/50			
	hsf-1(sy441)	4.1 ± 0.4	36/50	p<0.0001		
	hsf-1(sy441); drSi13[hsf-1::GFP]	9.4 ± 0.3	43/50	0.0028	p<0.0001	
	hsf1-(sy441);drSi27 [hsf-1(K4xR)::GFP]	8.6 ± 0.3	50/50	p<0.0001	p<0.0001	0.1473
2†	N2	9.1 ± 0.3	48/50			
	hsf-1(sy441)	3.6 ± 0.3	37/49	p<0.0001		
	hsf-1(sy441); drSi13[hsf-1::GFP]	8.8 ± 0.3	38/50	0.0572	p<0.0001	
	hsf1-(sy441);drSi27 [hsf-1(K4xR)::GFP]	8.7 ± 0.2	39/50	0.006	p<0.0001	0.0749
RNAi	N2 (EV RNAi)	9.2 ± 0.4	60/110			
	N2 (*smo-1* RNAi)	5.4 ± 0.2	57/100	p<0.0001		

Table 4-7. Statistics of *hsf-1(sy441):hsf-1(K4xR)::GFP* and *smo-1* RNAi lifespans
Lifespans were conducted at 25°C. p-values determined using Kaplan-Meier log rank tests.
†Performed on plates containing 50 μM FUdR.
*Excludes censored worms.

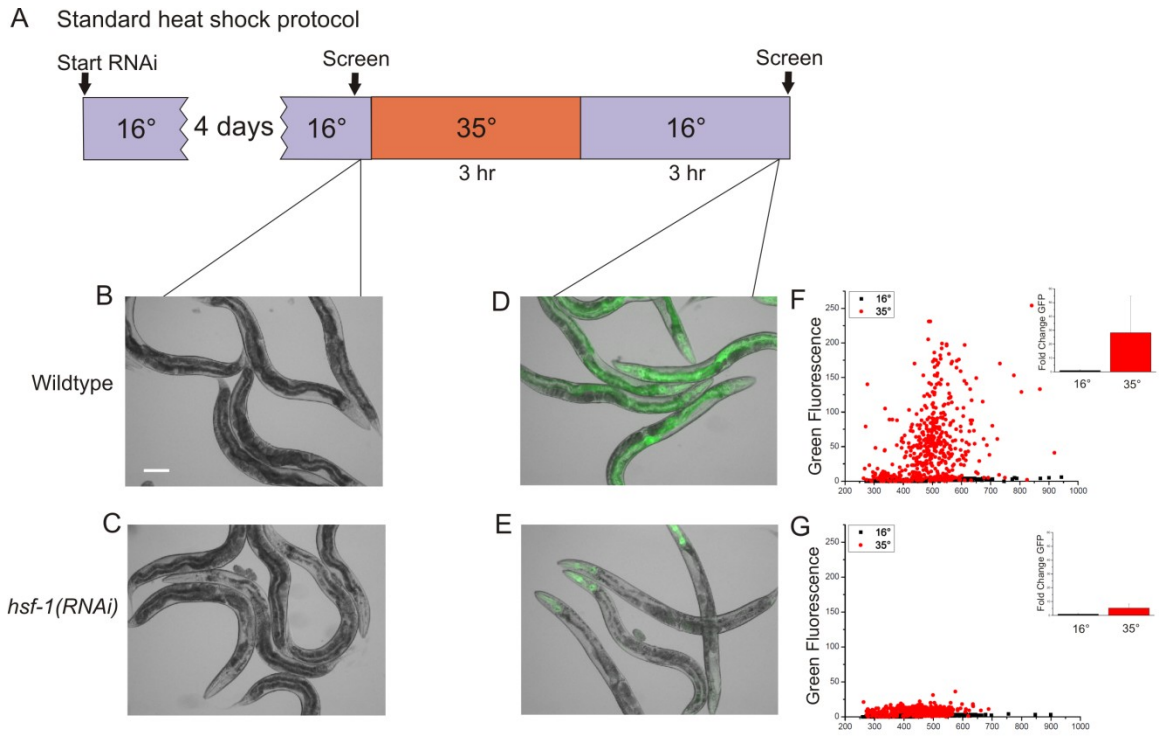

Figure 4-1. Screening strategy for regulators of *hsp-16.2p::GFP* expression

(A) L1 *hsp-16.2p::GFP* worms were placed on RNAi and grown at 16°C for four days. Adult worms were visually screened before and after heat shock (three hours at 35°C followed by three hours of recovery at 16°C). Image of wild-type worms before (B) or after (D) heat shock, or *hsf-1(RNAi)* worms before (C) and after (E) heat shock. Scale bar = 100µm. Fluorescence of worms before (16°C) and after (35°C) heat shock was quantified with a COPAS Biosort for wild type (F) and *hsf-1(RNAi)* (G) and plotted versus time of flight (TOF). Scale bar = 100µm. (Inset: mean of scatterplot ± SD. N ≥ 432 worms.)

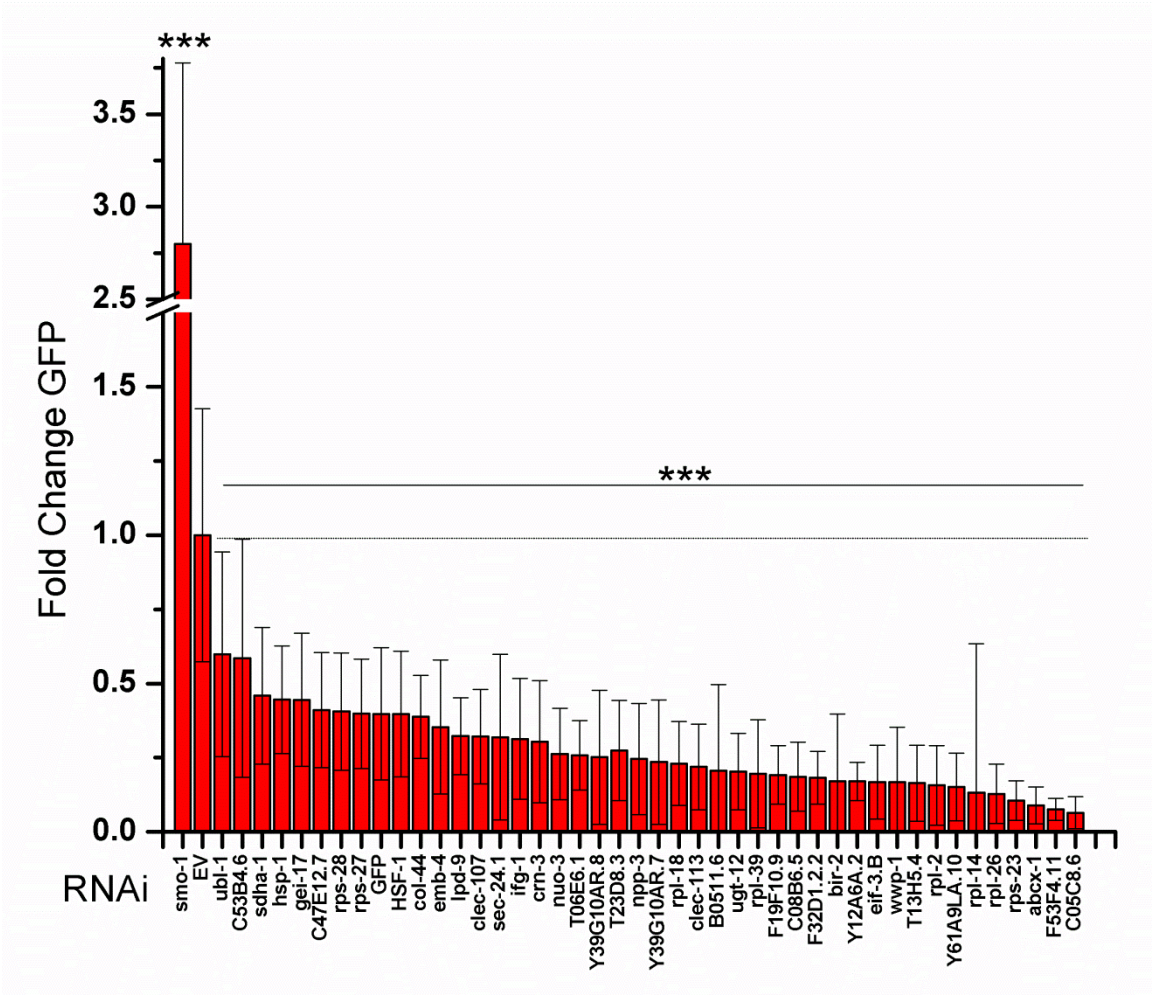

Figure 4-2. GFP quantification of screen hits

Worms were grown on RNAi, heat shocked as described, and measured for GFP expression using a COPAS Biosort. Plotted are wild type (EV), *hsf-1(RNAi)*, and the 43 other RNAi clones that affected post-heat shock GFP expression. Bars represent mean fluorescence ± SD after heat shock, corrected for worm size (time of flight) and normalized to the EV sample heat shocked at the same time (though only one EV sample is graphed). (N ≥ 20 worms for each sample. See Table 4-5 for N values of each sample.) One-way ANOVA was used to analyze data – all hits were significant compared to EV by Bonferroni post test, *** - $p < 0.001$.

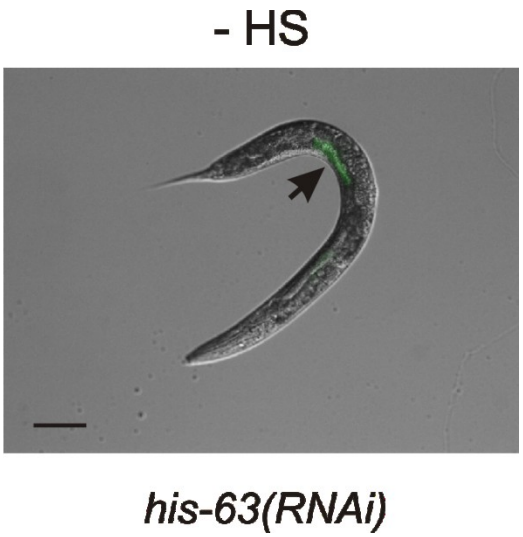

Figure 4-3. *his-63* RNAi induces weak GFP expression before heat shock

DIC and fluorescence images are overlain for *hsp-16.2p::GFP* worms grown on *his-63* RNAi at 16°C. Some GFP expression is seen without heat shock (arrow). Scale bar = 100 μm.

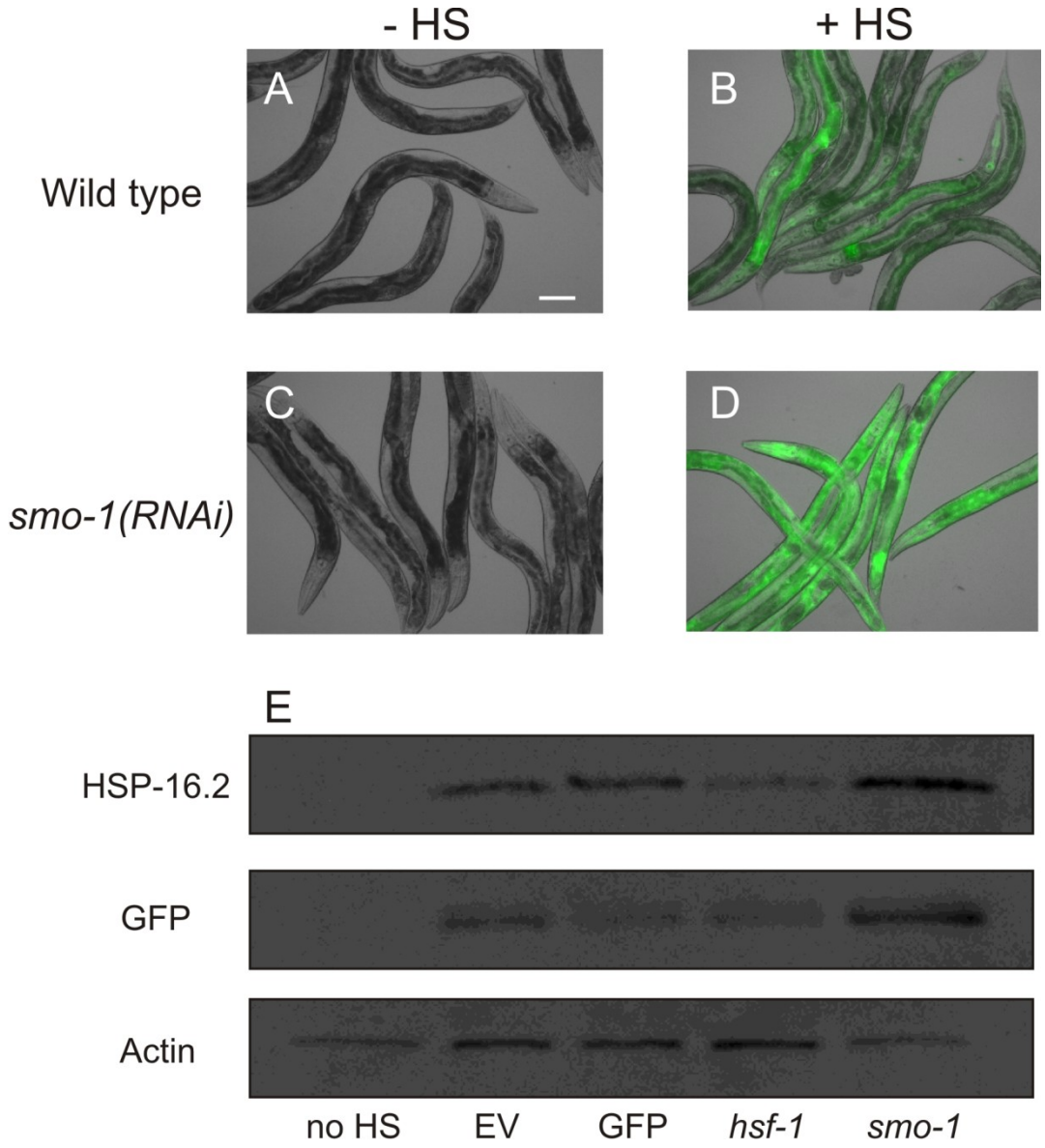

Figure 4-4. HSP-16.2 expression is increased on *smo-1* RNAi

DIC and fluorescence images are overlain for *hsp-16.2p::GFP* worms on empty vector (A, B) or *smo-1* RNAi (C, D) with (+HS) and without (-HS) standard heat shock. Scale bar = 100µm. (E) Western blot for HSP-16.2, GFP and β-actin on *hsp-16.2p::GFP* worms grown on empty vector without heat shock (no HS) or with heat shock on empty vector (EV), GFP RNAi, *hsf-1* RNAi or *smo-1* RNAi. The fold increases of HSP-16.2/actin intensity on *smo-1* RNAi relative to on EV in three replicates were 2.4, 4.7, and 1.8.

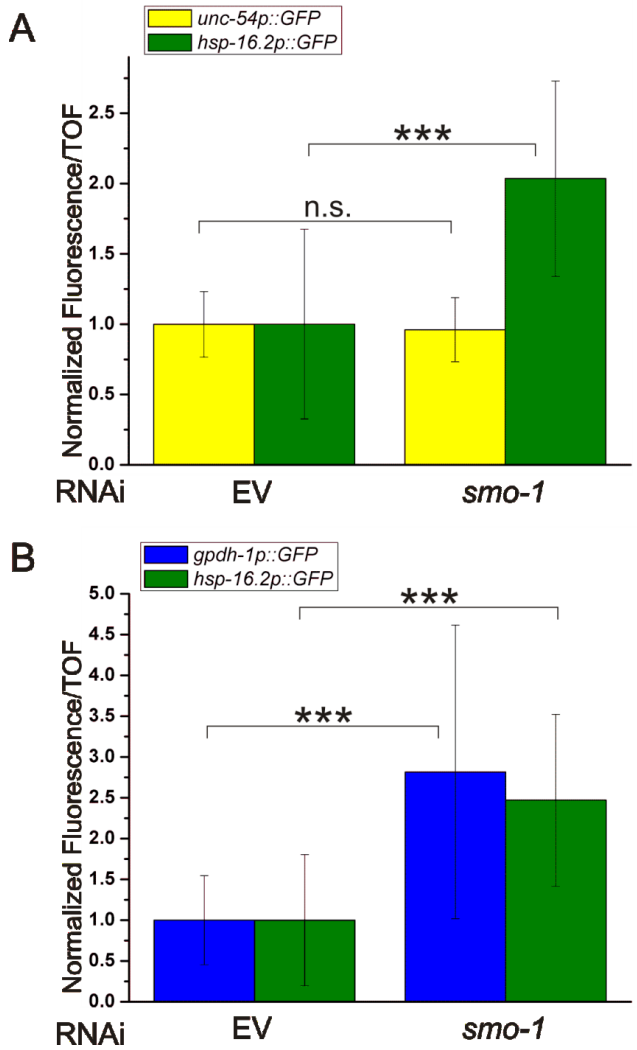

Figure 4-5. Effect of *smo-1* RNAi on other reporters

Heat shock-induced *hsp-16.2p::GFP* expression was compared to constitutively expressed *unc-54p::YFP* (A) or salt-induced *gpdh-1::GFP* expression (B) on empty vector and *smo-1* RNAi. Salt induction used 200 mM NaCl. GFP/TOF or YFP/TOF values were normalized to the mean value of EV for that strain. Bars represent mean ± SD. ($N \geq 167$. n.s. – not significant, *** - $p < 0.001$ by one-way ANOVA with Bonferroni post test.) In this trial, the fold change on *smo-1* RNAi over EV was 2.82-fold for *gpdh-1p::GFP* expression and 2.47-fold for *hsp-16.2P::GFP* expression. In a previous trial, the fold change on *smo-1* RNAi was 1.71-fold for *gpdh-1p::GFP* expression and 4.42-fold for *hsp-16.2P::GFP* expression. ($N \geq 72$ worms.)

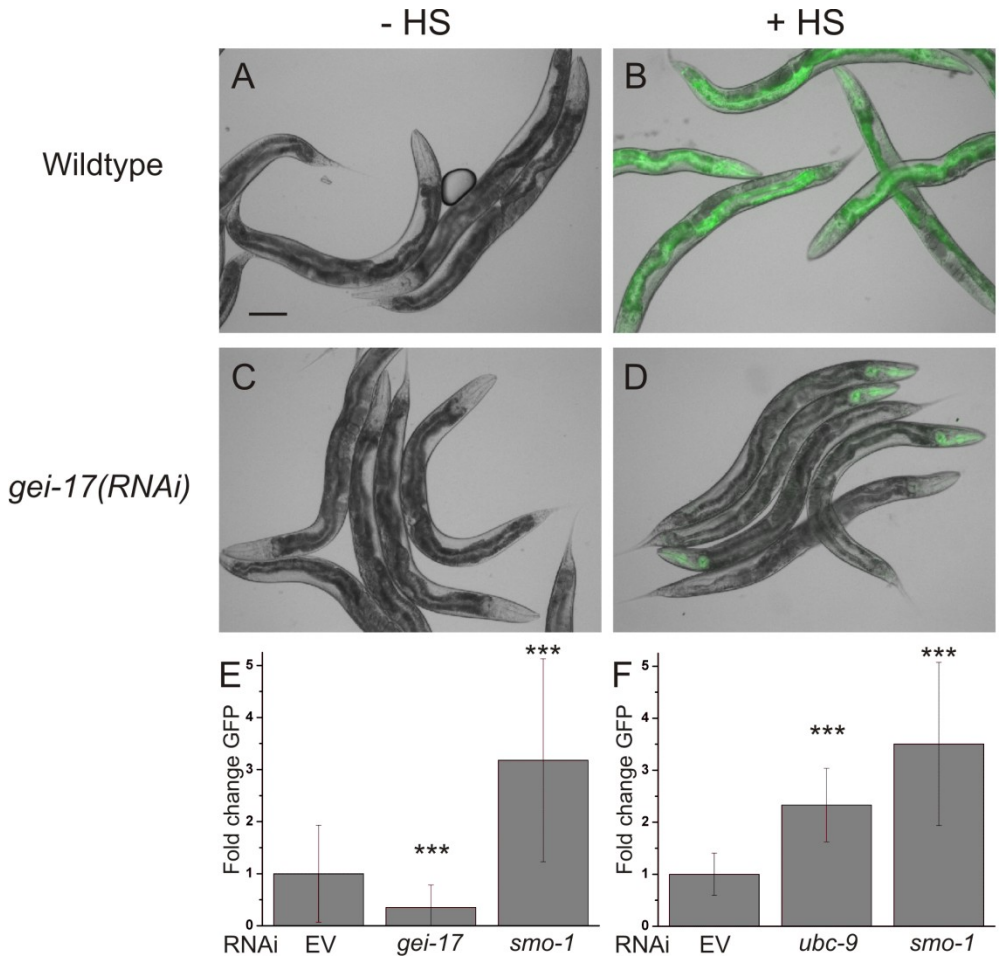

Figure 4-6. *hsp-16.2p::GFP* expression is reduced on RNAi against the putative SUMO E3 ligase *gei-17* and increased on RNAi against the E2 enzyme *ubc-9*.

DIC and fluorescence images are overlain for *hsp-16.2p::GFP* worms on empty vector (A,B) or *gei-17* (C,D) RNAi, with (+HS) and without (-HS) standard heat shock. Scale bar = 100µm. (E) Mean fluorescence ± SD after heat shock of *hsp-16.2p::GFP* worms grown on empty vector (EV), *gei-17*, or *smo-1* RNAi. Fluorescence is corrected for worm size and normalized to expression on EV. (N ≥ 287 worms for each sample). (F) Mean fluorescence ± SD 24 hr after standard heat shock protocol of *hsp-16.2p::GFP* worms grown on empty vector (EV), *ubc-9*, or *smo-1* RNAi. Fluorescence is corrected for worm size and normalized to expression on EV. (N ≥ 92 worms for each sample). UBC-9 and GEI-17 are predicted to be, respectively, the E2 and E3 enzymes involved in SUMO conjugation. (*** - $p < 0.001$ relative to EV by one-way ANOVA with Bonferroni post test.)

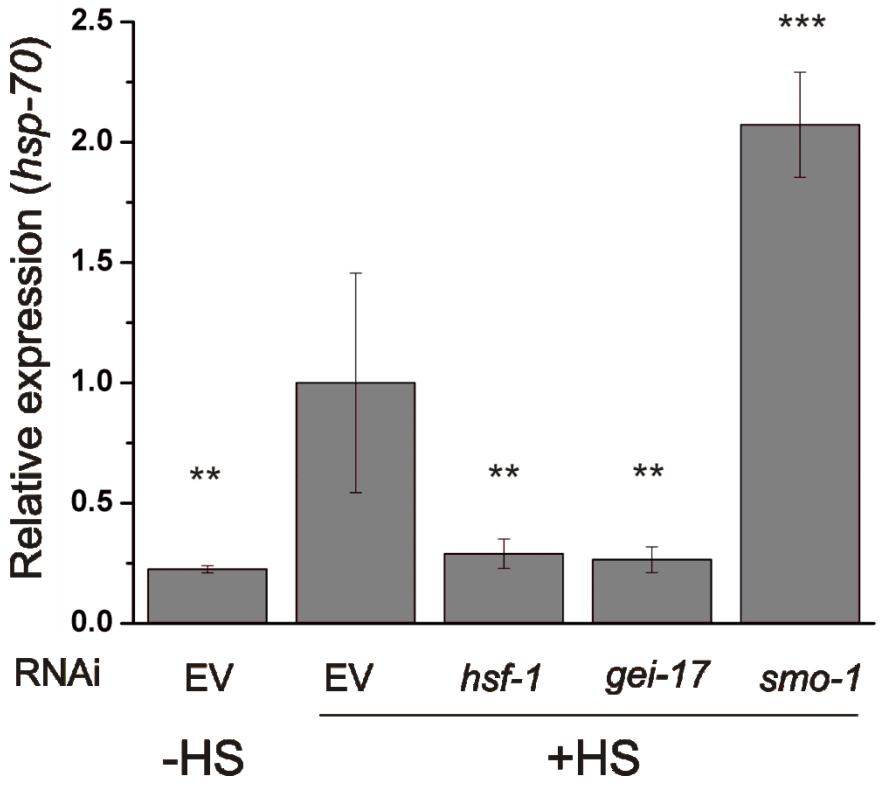

Figure 4-7. Another HSF-1 target gene also shows decreased expression on *gei-17* and increased expression on *smo-1* RNAi after heat shock

RT-PCR was used to determine *hsp-70* (C12C8.1) mRNA expression in non-heat shocked worms (-HS) or heat shocked (+HS) worms grown on empty vector (EV), *hsf-1*, *gei-17* or *smo-1* RNAi, 16°C. Bars represent mean of 3-4 technical replicates ± SD, normalized to EV +HS. (** - $p < 0.01$, *** - $p < 0.001$ by one-way ANOVA with Bonferroni post test.)

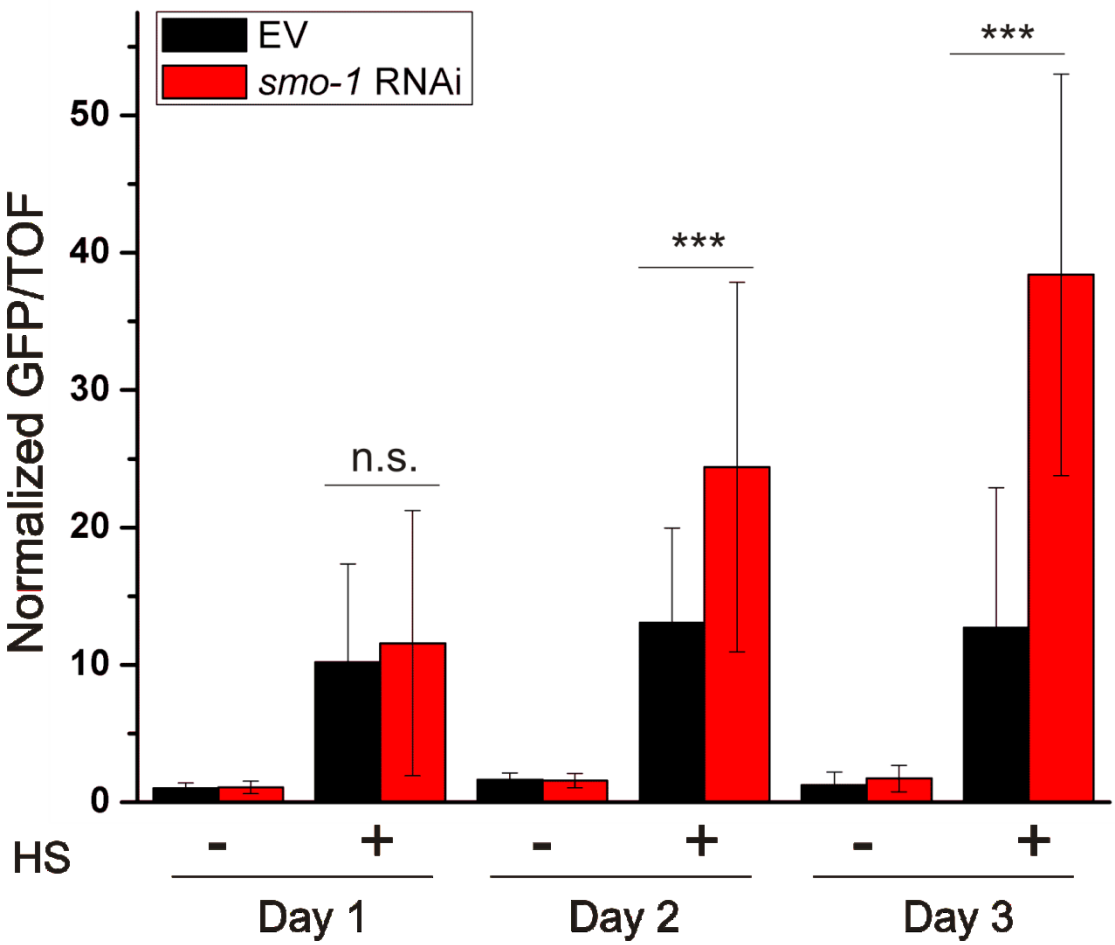

Figure 4-8. Post-developmental *smo-1* RNAi increases *hsp-16.2p::GFP* expression

hsp-16.2p::GFP worms were grown from synchronized L1s to adulthood at 16°C on OP50, and then transferred to empty vector (EV) or *smo-1* RNAi. Fluorescence was quantified for samples with and without heat shock (HS) using the COPAS Biosort after one, two or three days on RNAi at 16°C. Bars represent mean GFP/TOF normalized to the no HS EV sample on day 1, ± SD. (N ≥ 42 worms. n.s. – not significant, *** - $p < 0.001$ by one-way ANOVA with Bonferroni post test.)

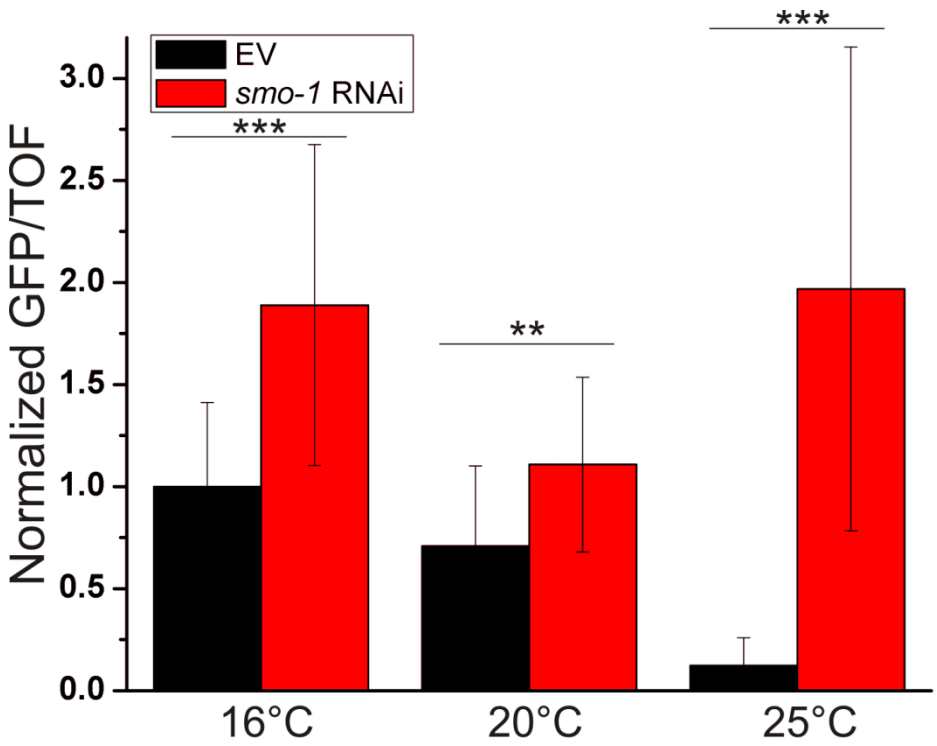

Figure 4-9. *smo-1* RNAi affects *hsp-16.2p::GFP* after heat shock of worms grown at various temperatures

Quantification of GFP fluorescence after heat shock for *hsp-16.2p::GFP* worms grown on empty vector (EV) or *smo-1* RNAi at 16°C (4 days), 20°C (3 days), or 25°C (2 days). All bars show heat shocked worms. GFP was normalized to worm size (TOF) and GFP/TOF normalized to EV heat shocked worms grown at 16°C, bars represent mean ± SD. ($N \geq 48$ worms. ** - $p < 0.01$, *** - $p < 0.001$ by one-way ANOVA with Bonferroni post test.)

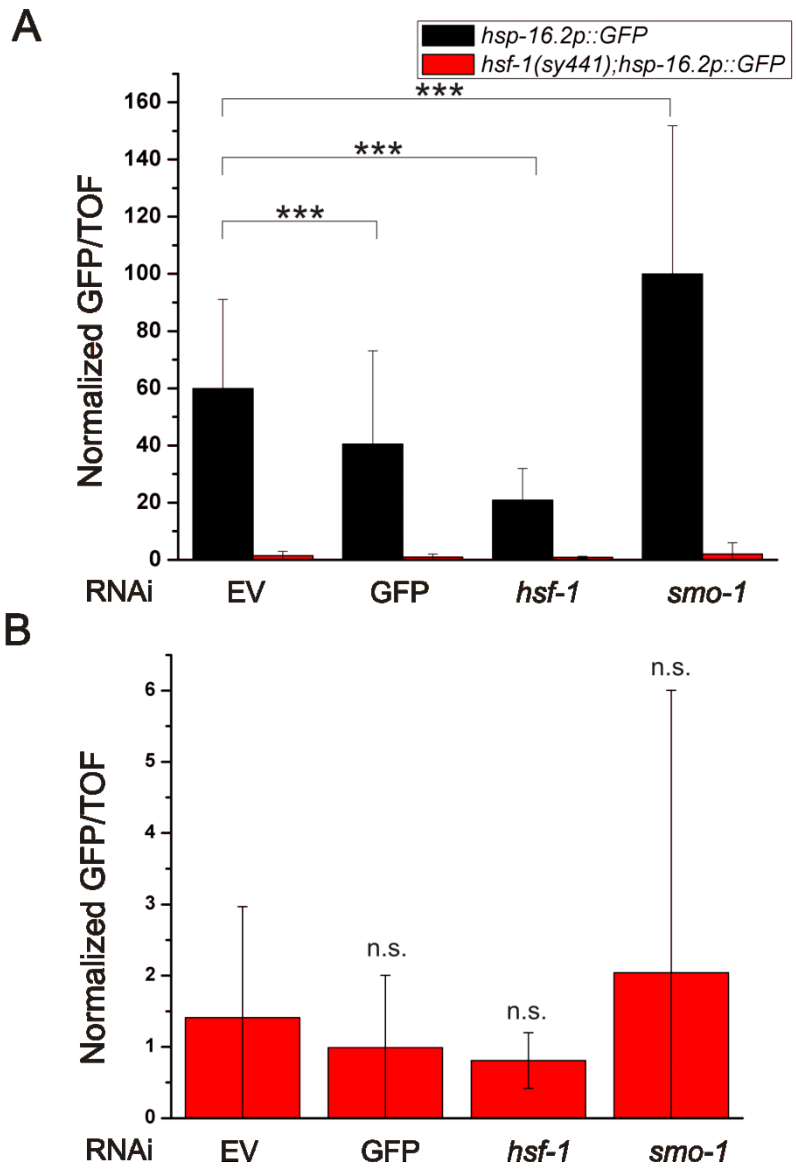

Figure 4-10. HSF-1 is necessary for *hsp-16.2p::GFP* overexpression on *smo-1* RNAi

(A) Heat shocked *hsp-16.2p::GFP* (black) and *hsf-1(sy441);hsp-16.2p::GFP* (red) worms grown at 16°C on RNAi, fluorescence was quantified by COPAS Biosort. Relative to *hsp-16.2p::GFP* EV, all black bars were *** - $p < 0.001$ by one-way ANOVA and Bonferroni post-test. Bars represent mean GFP/TOF normalized to the no HS empty vector control for that strain, ± SD. (B) Enlarged *hsf-1(sy441);hsp-16.2p::GFP* data from (A). Relative to EV, all samples in (B) were not significant (n.s.) by one-way ANOVA with Bonferroni post-test. ($N \geq 105$ worms.)

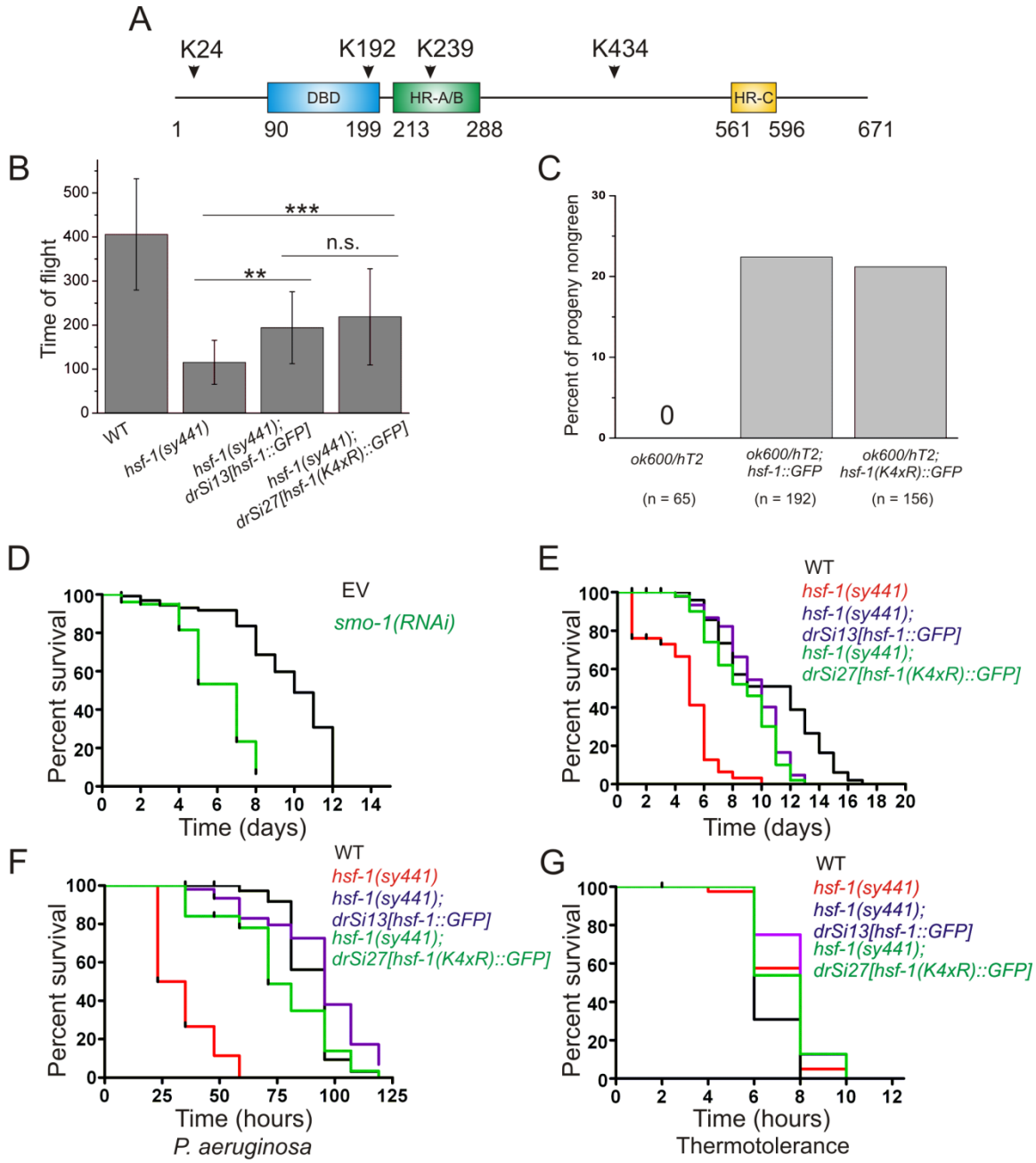

Figure 4-11. HSF-1(K4xR)::GFP is functional

(A) *C. elegans* HSF-1 with potentially sumoylated lysines marked. (B) N2 (WT), *hsf-1(sy441)*, *hsf-1(sy441);drSi13[hsf-1::GFP]*, and *hsf-1(sy441);drSi27[hsf-1(K4xR)::GFP]* at 25°C after 48 hrs were analyzed for size (time of flight) by COPAS Biosort (N ≥ 26 animals. Mean ± SD, *** - $p < 0.001$, ** - $p < 0.01$, n.s. – not significant by one-way ANOVA with Bonferroni post test). Note that of three trials, *hsf-1(sy441);hsf-1::GFP*

vs. *hsf-1(sy441);hsf-1(K4xR)::GFP* was not significant in two trials, but had $p < 0.001$ for increased growth of K4xR-rescued line in one trial. (C) Percent of total L4 or older progeny (after 3 days at 20°C) that are nongreen. Parents were *hsf-1(ok600)/hT2[GFP]*. Nongreen progeny are homozygous for *ok600,* exhibiting HSF-1::GFP or HSF-1(K4xR)::GFP rescue. Total number of progeny is listed below the graph. (D) Lifespan of N2 on empty vector (EV) or *smo-1* RNAi at 25°C. ($N \geq 100$ worms, p-value of < 0.0001). (E) Lifespan of young adult WT, *hsf-1(sy441)*, *hsf-1(sy441);hsf-1::GFP*, and *hsf-1(sy441); hsf-1(K4xR)::GFP* at 25°C. ($N = 50$ worms for each strain. p-value between *hsf-1(sy441);hsf-1::GFP* and *hsf-1(sy441);hsf-1(K4xR)::GFP* was 0.1473 in this trial, 0.0749 in a second trial.) (F) Survival of young adults on *Pseudomonas aeruginosa* PA14 at 25°C. ($N \geq 50$ worms. p-value between *hsf-1(sy441);hsf-1::GFP* and *hsf-1(sy441);hsf-1(K4xR)::GFP* is 0.0024.) (G) Thermotolerance of young adults at 35°C. ($N = 40$ worms per strain. In this trial, p-value between *hsf-1(sy441);hsf-1::GFP* and *hsf-1(sy441);hsf-1(K4xR)::GFP* is 0.1984. In three other trials, p-values were 0.4490, 0.0136 (K4xR shorter), and 0.0003(K4xR longer).) Survival assays used Kaplan-Meier log rank test.

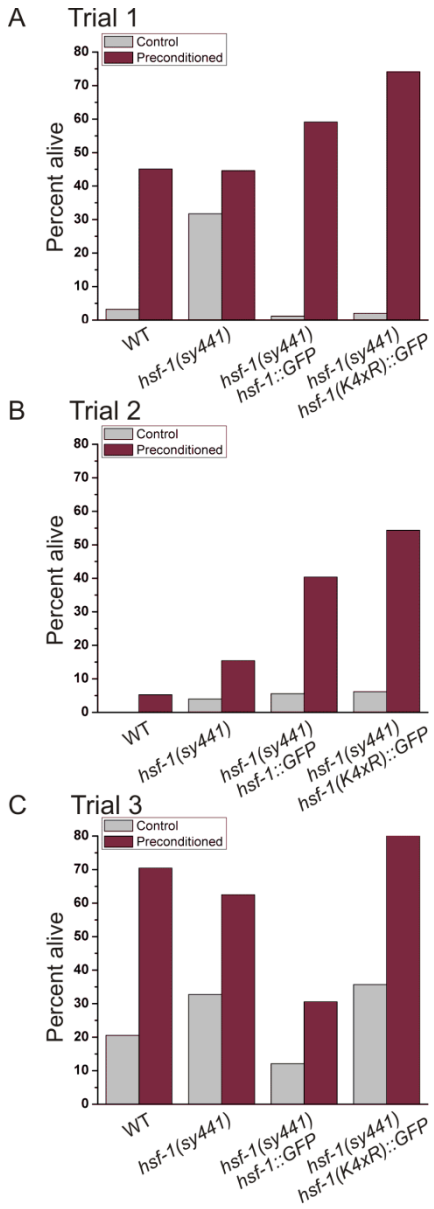

Figure 4-12. Preconditioning survival against heat shock shows a trend for increased HSF-1(K4xR)::GFP survival

Adult N2 (WT), *hsf-1(sy441)*, *hsf-1(sy441);drSi13[hsf-1::GFP]*, and *hsf-1(sy441):drSi27[hsf-1(K4xR)::GFP]* grown at 20°C were either preconditioned (35°C 30 min) or not (20°C 30 min, control), allowed to recover at 20°C for 6 hr, and then given a heat stroke of 39°C for 15 min. Worms were placed on plates at 20°C and scored as alive or dead the next day. Percent survival in three biological replicates is presented here. ((A) N ≥ 104, (B) N ≥ 127, and (C) N ≥ 84 worms.)

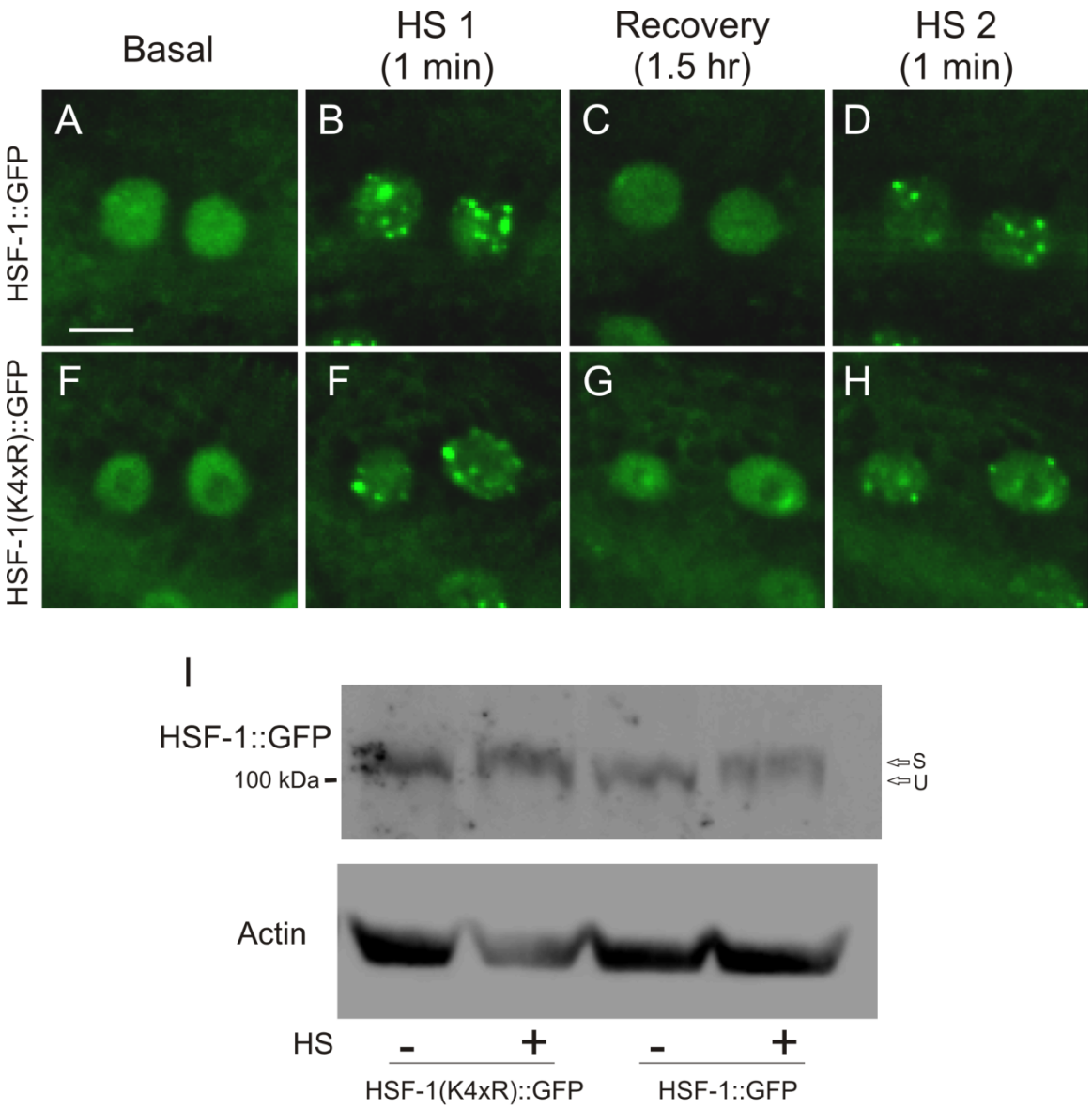

Figure 4-13. HSF-1(K4xR)::GFP localizes to the nucleus, forms heat shock granules and undergoes heat-induced molecular weight shift

Young adult *drSi13[hsf-1::GFP]* (A-D) and *drSi27[hsf-1(K4xR)::GFP]* (E-H) were imaged before heat shock (20°C), after 1 min 35°C (HS 1), after recovery (1.5 hr 20°C), and after a second heat shock of 1 min 35°C (HS 2). Scale bar = 5µm. (I) Immunoblot with anti-GFP and anti-β-actin antibodies against young adults worms expressing *drSi13* HSF-1::GFP or *drSi27* HSF-1(K4xR)::GFP. Worms were subject to 16°C (-HS) or 35°C (+HS) for 20 min. Arrows point to shifted (S) or unshifted (U) HSF-1::GFP.

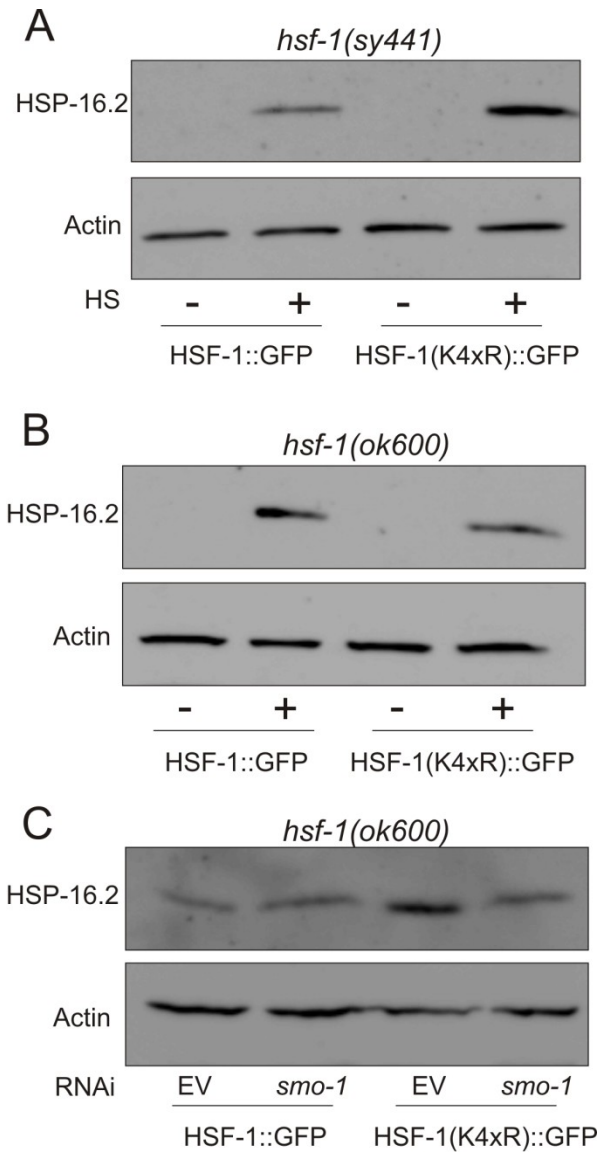

Figure 4-14. HSF-1(K4xR)::GFP induced enhanced HSP-16.2 expression in *hsf-1(sy441)* hypomorphic background but not consistently in null background.

Western blots against HSP-16.2 (top panel) and β-actin (bottom panel) with or without a 35°C 3hr heat shock (HS) followed by 3 hr recovery at 16°C. (A) *drSi13[hsf-1::GFP]* and *drSi27[hsf-1(K4xR)::GFP]* in *hsf-1(sy441)* background, grown on OP50. N = 3 (biological replicates). (B) *drSi13[hsf-1::GFP]* and *drSi27[hsf-1(K4xR)::GFP]* in *hsf-1(ok600)* background, grown on OP50. N = 2 (biological replicates). (C) *drSi13[hsf-1::GFP]* and *drSi27[hsf-1(K4xR)::GFP]* in *hsf-1(ok600)* background, grown on RNAi bacteria for empty vector (EV) or *smo-1*. N = 2 (biological replicates).

5. Discussion

HSF1 is a critical transcription factor in the eukaryotic cellular response to heat stress, as well as a factor relevant in a variety of other processes. Attempts to understand the many steps in its activation and the relative importance of each level of regulation are long-standing, and many aspects of HSF1 biology have been plagued by contradictory results or lack of appropriate tools. In this work, I have developed new tools for use in the study of HSF-1 in *C. elegans*, and I address some of the current discrepancies in the dogma of HSF-1 behavior using this model system. I observed that in *C. elegans*, HSF-1 localizes predominantly to the nucleus, even in the absence of heat shock. *C. elegans* HSF-1 collects into dynamic, reversible, stress-induced, subnuclear structures that share many characteristics with human HSF1 stress granules (including indications of transcriptional activity). Activation of HSF-1 by heat shock leads to HSP gene expression, and I performed a genome-wide screen for genes involved in regulation of this expression. HSF-1 target HSP genes appear to be tightly repressed at 16°C and have many positive regulators needed for full expression after induction.

Nuclear granule conservation and function

We propose here that the nuclear puncta of HSF-1 observed in worms are equivalent to human HSF1 granules. This is a surprising suggestion because the field of HSF1 granule study has long believed granules to be human-specific. The presence of true HSF-1 granules in worms would open up new tools for determining the function of this structure and present the opportunity to study the role of granules in different tissues within a whole organism and across the lifetime of an animal. Given the evolutionary distance between *C. elegans* and humans, conservation between them would also argue

that granule function has an important cellular function. One obvious question must first be raised, though: if granule formation is truly an evolutionarily conserved property of HSF1, why have granules not been observed in other species?

Most of the evidence for human-specific granules comes from the failure to detect them in mouse or hamster cell lines (Denegri et al., 2002; Sarge et al., 1993). This is not due to divergence of the HSF1 molecule: mouse and hamster HSF1s are both capable of forming granules in the presence of amenable DNA sequences. Mouse HSF1 tagged with either GFP or FLAG formed granules when expressed in HeLa cells (Cotto et al., 1997), and hamster HSF1 formed granules when human chromosomes were expressed in hamster cells (Denegri et al., 2002). Thus, the ability of the HSF1 protein to form granules is conserved among mammals. This suggests that something about the genomic substrate and not the protein accounts for the lack of granules in murine cells. It is known that cell lines such as mouse 3T3 cells have chromosomal abnormalities. Imaging live cells in their native organismal context allowed us to get a more accurate picture of HSF-1 behavior. More extensive studies on murine HSF1 localization (such as in primary cells or tissue) may be warranted. It is also worth noting that one group has reported granule formation of human HSF1 when expressed in *Hsf1*$^{-/-}$ mouse embryonic fibroblasts (Hong et al., 2001), though another group failed to observe this (Hietakangas et al., 2003). It is possible that further study might reveal that certain mouse cells do have the genomic architecture to support granule formation.

Other HSF structures – that do not show the human-like properties that we see with *C. elegans* HSF-1 but that may nevertheless have similar function – have been observed in other organisms. In response to stress, HSF binds to HSE repeats in

telomeres of the midge *Chironomus thummi* (Martinez et al., 2001). HSF3, which has been proposed to be a major enactor of the heat shock response in birds (Kawazoe et al., 1999), exhibits a punctate nuclear staining pattern after heat shock in chicken embryo fibroblasts (Nakai et al., 1995). In *Drosophila* cells, large clusters of non-coding RNA (ncRNA) transcripts termed omega speckles form with heat shock, to which hnRNPs are recruited (Prasanth et al., 2000). The above structures have not been as well characterized as human HSF1 granules, so further investigation (such as we have done and are continuing to do on *C. elegans* granules) is needed to determine how unique human stress granules really are.

HSF-1 granule formation in worms was promoted by DNA binding and, in a subset of granules, associated with marks of active transcription. Interestingly, we observed that human HSF1 expressed in worms appeared capable (after extended stress) of forming granules as well (Figure 2-9), suggesting that there are DNA sequences in the worm that can support human granules. The true test of worm HSF-1 granules will be to determine the DNA sequences at which binding occurs. We have not ruled out the possibility that worm granules are sites of *hsp* target genes, but analogy to human granules would predict that these sites are non-protein coding repeat regions and produce long ncRNAs. Human granule binding sites are transcribed; if the same is true for *C. elegans* granules, RNA-seq techniques could be employed to search for long ncRNAs induced with heat shock.

Human satellite II and III repeats, at which granules form, are rich in GAA repeats, reminiscent of (though not exactly reproducing) HSF1 binding sites (HSEs) (Prosser et al., 1986). Sat II and III repeats are specific to humans and primates

(respectively) (Jarmuz et al., 2007; Mitchell et al., 1981), but if, as is speculated, HSF1 in human cells is binding to the "pseudo-HSEs," it is possible that worm HSF-1 may have a different GAA-rich target DNA sequence. A search of the genome for GAA enrichment revealed several large regions in worms that appear to have high GAA content (data not shown). Some of these sites could possibly be used in a candidate approach to investigate colocalization with HSF-1 worm granules.

What is the function of human HSF1 granules? Many hypotheses have been proposed since their discovery. Early investigators suggested granules might be compartments for HSF1 regulation, controlling post-translational modification or oligomerization (Jolly et al., 1999). The discovery that non-coding RNAs are transcribed from granules has steered models away from the idea that granules function to affect HSF1 activity specifically. One proposed alternative explanation is that these ncRNAs have a role in chromatin organization, such as heterochromatin assembly at repetitive regions (Biamonti, 2004; Jolly et al., 2004), or even protection of rearrangement-prone chromatin during stress (Jolly et al., 2002). HAP, a protein that associates with human HSF1 granules, has also been reported to play a part in chromatin structure (Renz and Fackelmayer, 1996). Another current popular hypothesis is that granules are sights of storage or sequestration. RNPs and splicing factors may be recruited to granules in order to keep them from other targets, perhaps even promoting alternative splicing of some gene products (Biamonti and Vourc'h, 2010; Weighardt et al., 1999). Consistent with this model, heat shock inhibits pre-mRNA splicing and disassembles the nucleolus (Bond, 1988; Liu et al., 1996; Yost and Lindquist, 1986, 1991). We have yet to confirm if splicing factors colocalize with the granules that form in *C. elegans* nuclei, but genes

predicted to be involved in mRNA splicing were identified in our RNAi screen (Table 4-4), linking splicing factors with the heat shock response in *C. elegans*.

Basal activity of HSF1

Our observation of constitutively nuclear HSF-1 localization is consistent with HSF-1 having transcriptional roles outside of acute heat stress. The involvement of HSF-1 in development and aging suggests that it has a basal function, contrary to the simplistic model of total inactivity and cytoplasmic sequestration under non-stress conditions. Though large-scale HSF1 DNA binding only occurs with stress (with the exception of the constitutive binding in *S. cerevisiae*), there does appear to be a low level of basal HSF1 DNA binding in mammals (Fiorenza et al., 1995; Rabindran et al., 1993). We have started to explore this issue by performing microarray analysis on the worm *hsf-1* hypomorph *sy441* and comparing to wild type, both grown at 16°C. Surprisingly, we found hundreds of genes upregulated in *hsf-1(sy441)* mutants under basal conditions (data not shown), suggesting HSF-1 might act as a genetic repressor in the absence of stress. It has already been demonstrated that mammalian HSF1 represses cytokine genes during exposure to bacterial lipopolysaccharide or fever temperatures (Cahill et al., 1996; Singh et al., 2000; Xiao et al., 1999). Our data regarding the ability of a DNA-binding domain mutant (R145A) of HSF-1 to rescue only some *sy441* phenotypes suggested to us that the mechanisms of HSF-1 activity under basal conditions are different from those under heat shock (Chapter 2). The model of differential regulation between various functions of HSF1 has also been proposed by others (Jedlicka et al., 1997; Xiao et al., 1999).

The role of chaperones in HSF1 regulation

The activation of HSF1 is affected by its cellular environment. Human HSF1 expressed in *Drosophila* or *Xenopus* becomes activated at lower temperatures than it does in human cells (Baler et al., 1993; Clos et al., 1993; Zuo et al., 1994). Thirty-seven degrees, while not stressful to human cells, is capable of inducing activity of hHSF1 in a cell that perceives 37°C as a stress (such as flies and frogs). Our own observations of human HSF1 in *C. elegans* reinforce this. Although hHSF1 did not rescue function of worm HSF-1, granule formation did occur after an extended heat shock exposure. This was equally true for heat shocks of 35°C (a worm-stressful temperature) or 42°C (a human-stressful temperature). Moreover, the threshold temperature at which *C. elegans* HSF-1 forms granules is determined by the growth temperature (Figure 2-6). These observations argue against a model of the HSF1 protein itself being a sensor of temperature; one specific temperature does not seem to be intrinsically stressful to the protein. Instead, this dependence on cell environment lends credence to the model of the proteostasis state of the cell being in some way the trigger for HSF1 activation.

A widely held mechanism for this latter model is the direct binding of cytoplasmic chaperones to HSF1, keeping it inactive. This explanation is attractive for its intuitiveness: stress induces protein misfolding, which occupies chaperones, releasing HSF1 from repression and activating the heat shock response pathway. At first, HSP70 was proposed as the major repressor of basal HSF1 (Baler et al., 1996; Mosser et al., 1993). Enough subsequent evidence contradicted this that this model has been mostly dismissed in favor of HSP90 being the primary regulator (Rabindran et al., 1994; Shamovsky and Nudler, 2008; Voellmy, 2004; Voellmy and Boellmann, 2007). Most

support for the HSP90 model comes from reports that changes in HSP90 activity (overexpression, depletion, or chemical inhibition) affect HSF1 (Duina et al., 1998; Zou et al., 1998). It seems plausible that these results may be a sign that interference with HSP90 function (maintaining protein homeostasis) influences HSF1 activity, and not necessarily evidence of direct HSP90 repression of HSF1. There are reports of direct interaction between the two (Ali et al., 1998; Guo et al., 2001; Knowlton and Sun, 2001; Zou et al., 1998), but evidence of the type of dynamics predicted by the model is generally lacking. Some have described the interaction as unstable (Zou et al., 1998) or observed that HSP90 interacts equally with stressed and un-stressed HSF1 (Ali et al., 1998), a result hard to reconcile with its release being a factor in activation. A recent study in the yeast *Candida albicans* reported that Hsp90 interaction with Hsf1 increases with heat shock rather than decreasing as predicted (Leach et al., 2012).

Our own observations led us to doubt the model of HSF-1 activation by release from cytoplasmic chaperones. First, we found that *in vivo*, HSF-1 is predominantly nuclear (Chapter 2). Though shuttling of small quantities of HSF-1 into and out of the nucleus is certainly possible (in fact, likely (Vujanac et al., 2005)), the presence of the bulk of HSF-1 in the nucleus does not suggest that it is being held inactive by cytoplasmic chaperones. Second, in our genome-wide RNAi screen, we failed to pull out any chaperones whose knockdown resulted in activation of HSF-1, making it likely that there are other regulators involved (or perhaps that chaperone activity in regards to HSF-1 is redundant), although we did observe activation on chaperone RNAi in conjunction with high growth temperature (Chapter 4). If the protein folding balance in the cell is affected by disruption of HSP90 or introduction of misfolded proteins, HSF1 could be

activated through signals that don't depend on direct chaperone interaction. Translation-associated proteins and RNA are one such possibility (Shamovsky et al., 2006), and indeed, many ribosomal proteins were selected in our screen for their effects on HSF-1-dependent gene transcription.

Others have calculated that the rate of HSF1 activation is much faster *in vivo* than predicted based on release from inhibition, arguing for involvement of positive regulators (Shamovsky et al., 2006). We identified many potential positive regulators in our screen. These genes appear to be involved in activation of heat-induced gene transcription and fall into a wide variety of functional classes. These hits have not yet been determined to act upstream of HSF-1, but they were heat stress-specific in their effects (in that they did not similarly affect an osmotic stress reporter) and are promising candidates for HSF-1 regulators.

Post-translational modification of HSF1

Most sumoylation targets are nuclear proteins, and the function of sumoylation of transcription factors is most often repressive (Gill, 2005; Johnson, 2004). SUMO can affect proteins through several different mechanisms, such as regulation of nucleocytoplasmic or subnuclear localization (Dobreva et al., 2003; Ross et al., 2002; Stade et al., 2002), interaction with co-repressors (Lin et al., 2006), or binding to DNA (Anckar et al., 2006). SUMO itself may have some ability to repress transcription, as artificially recruiting SUMO to a promoter (by GAL4-SUMO-1 fusion) represses expression (Ross et al., 2002; Yang et al., 2003).

In organisms with multiple SUMOs, heat shock has been shown to promote conjugation of certain SUMOs to targets. Of the three mammalian SUMOs, SUMO-2

and SUMO-3, but not SUMO-1, show a large increase in protein conjugation with stress in mammalian cells (Saitoh and Hinchey, 2000). In *Arabidopsis*, heat shock also induces conjugation of two of its eight SUMOs (these two SUMOs are equally related to all three human SUMOs) (Kurepa et al., 2003). Mammalian SUMO-1 shares 48% and 46% identity with SUMO-2 and 3, respectively, while SUMO-2 and 3 share 95% identity with each other (Saitoh and Hinchey, 2000). One important facet of this sequence difference is that SUMO-1 lacks a lysine in the N-terminus that is present in SUMO-2/3. This SUMO-2/3-specific lysine is itself a target for sumoylation, allowing polymeric chain formation (Tatham et al., 2001). The single SUMO in *C. elegans* is more closely related to human SUMO-1 than it is SUMO-2/3 and lacks the lysine used for chain formation. It is unclear whether the heat shock-induced global upregulation of sumoylation seen in other systems is applicable to the single-SUMO system of *C. elegans*.

Kaminsky *et al*. catalogued the SUMO conjugate proteins in mixed-stage populations of worms (Kaminsky et al., 2009). HSF-1 was among these proteins. Our own observations of RNAi knockdown of SUMO expression suggest that sumoylation may be involved in downregulation of the heat shock response pathway. In human cells, HSF1 is a known SUMO target, but controversy exists as to the outcome of this modification. Our results support the work of Hietakangas *et al*. (Hietakangas et al., 2003; Hietakangas et al., 2006), asserting that sumoylation is a mechanism for downregulation of HSF1 activity after stress-induced activation (and implying that this method of regulation is conserved). We mutated four potential sumoylation sites in worm HSF-1 but failed to definitively phenocopy the effect of *smo-1* RNAi, leaving open the possibilities that HSF-1 may be sumoylated on a different site, that SUMO's role in

the heat shock response may be through a different target, or that downregulation of SUMO may simply be disrupting to the overall protein folding state of the cell. Clarification of the effect of sumoylation is needed, but the worm remains a promising tool for furthering our understanding of the mechanism of interaction between SUMO and the heat shock response.

The involvement of other post-translational modifications in *C. elegans* HSF-1 regulation is also yet to be determined. Chiang *et al*. report worm HSF-1 is inducibly phosphorylated (Chiang et al., 2012), and our own data also suggest post-translational modification with stress (Figure 2-12), but the residues and function of these modifications are unknown. *sir-2.1* (a predicted deacetylase) mutants had decreased HSP-16.2 expression after heat shock compared to wild type (data not shown), suggesting worm HSF-1 may also be acetylated, like human HSF1. Human HSF1 is reportedly acetylated only with stress, and SIRT1 (deacetylase) siRNA caused reduced HSF1 DNA binding at every time-point in heat shock (0.5 hr through 6 hr) (Westerheide et al., 2009). This modification seems especially important in the early regulation of HSF1 DNA binding after heat shock, since binding compared to control was reduced the most at 30 min, but at 4 hr and 6 hr binding was nearly the same (Westerheide et al., 2009). SIRT1 is reduced with age (late passage of cells), and this correlates with decreased HSF1 DNA binding, perhaps linking lifespan and the post-translational modification of HSF1 (Westerheide et al., 2009). Worms are an excellent model system for longevity studies, so they may yet prove valuable in exploring this potential connection.

In summary, our studies in *C. elegans* have made valuable contributions to the field of HSF-1 research. We have determined the *in vivo* localization of HSF-1, and

characterized post-heat shock behavior, post-translational modification, and potential HSF-1 interactors mediating repression, activation, and attenuation. The strains we developed have been requested by many other labs and are now deposited at the Caenorhabditis Genetics Center for use by others in the study of HSF-1 behavior. Our research provides tools and groundwork for many avenues for future work on elucidating the mechanisms behind the complex regulation of this transcription factor.

BIBLIOGRAPHY

Abravaya, K., Myers, M.P., Murphy, S.P., and Morimoto, R.I. (1992). The human heat shock protein hsp70 interacts with HSF, the transcription factor that regulates heat shock gene expression. Genes & development *6*, 1153-1164.

Ahn, S.G., Liu, P.C., Klyachko, K., Morimoto, R.I., and Thiele, D.J. (2001). The loop domain of heat shock transcription factor 1 dictates DNA-binding specificity and responses to heat stress. Genes & development *15*, 2134-2145.

Åkerfelt, M., Morimoto, R.I., and Sistonen, L. (2010). Heat shock factors: integrators of cell stress, development and lifespan. Nature reviews Molecular cell biology *11*, 545-555.

Alastalo, T.P., Hellesuo, M., Sandqvist, A., Hietakangas, V., Kallio, M., and Sistonen, L. (2003). Formation of nuclear stress granules involves HSF2 and coincides with the nucleolar localization of Hsp70. Journal of cell science *116*, 3557-3570.

Alavez, S., Vantipalli, M.C., Zucker, D.J., Klang, I.M., and Lithgow, G.J. (2011). Amyloid-binding compounds maintain protein homeostasis during ageing and extend lifespan. Nature *472*, 226-229.

Ali, A., Bharadwaj, S., O'Carroll, R., and Ovsenek, N. (1998). HSP90 interacts with and regulates the activity of heat shock factor 1 in *Xenopus* oocytes. Molecular and cellular biology *18*, 4949-4960.

Amin, J., Ananthan, J., and Voellmy, R. (1988). Key features of heat shock regulatory elements. Molecular and cellular biology *8*, 3761-3769.

Ananthan, J., Goldberg, A.L., and Voellmy, R. (1986). Abnormal proteins serve as eukaryotic stress signals and trigger the activation of heat shock genes. Science (New York, NY) *232*, 522-524.

Anckar, J., Hietakangas, V., Denessiouk, K., Thiele, D.J., Johnson, M.S., and Sistonen, L. (2006). Inhibition of DNA binding by differential sumoylation of heat shock factors. Molecular and cellular biology *26*, 955-964.

Anckar, J., and Sistonen, L. (2007). SUMO: getting it on. Biochemical Society transactions *35*, 1409-1413.

Anckar, J., and Sistonen, L. (2011). Regulation of HSF1 function in the heat stress response: implications in aging and disease. Annual review of biochemistry *80*, 1089-1115.

Baler, R., Dahl, G., and Voellmy, R. (1993). Activation of human heat shock genes is accompanied by oligomerization, modification, and rapid translocation of heat shock transcription factor HSF1. Molecular and cellular biology *13*, 2486-2496.

Baler, R., Zou, J., and Voellmy, R. (1996). Evidence for a role of Hsp70 in the regulation of the heat shock response in mammalian cells. Cell stress & chaperones *1*, 33-39.

Bard, F., Casano, L., Mallabiabarrena, A., Wallace, E., Saito, K., Kitayama, H., Guizzunti, G., Hu, Y., Wendler, F., Dasgupta, R.*, et al.* (2006). Functional genomics reveals genes involved in protein secretion and Golgi organization. Nature *439*, 604-607.

Barna, J., Princz, A., Kosztelnik, M., Hargitai, B., Takacs-Vellai, K., and Vellai, T. (2012). Heat shock factor-1 intertwines insulin/IGF-1, TGF-beta and cGMP signaling to control development and aging. BMC developmental biology *12*, 32.

Beckmann, R.P., Mizzen, L.E., and Welch, W.J. (1990). Interaction of Hsp 70 with newly synthesized proteins: implications for protein folding and assembly. Science (New York, NY) *248*, 850-854.

Ben-Zvi, A., Miller, E.A., and Morimoto, R.I. (2009). Collapse of proteostasis represents an early molecular event in *Caenorhabditis elegans* aging. Proceedings of the National Academy of Sciences of the United States of America *106*, 14914-14919.

Bharadwaj, S., Ali, A., and Ovsenek, N. (1999). Multiple components of the HSP90 chaperone complex function in regulation of heat shock factor 1 *in vivo*. Molecular and cellular biology *19*, 8033-8041.

Bhowmick, B.K., Takahata, N., Watanabe, M., and Satta, Y. (2006). Comparative analysis of human masculinity. Genetics and molecular research : GMR *5*, 696-712.

Biamonti, G. (2004). Nuclear stress bodies: a heterochromatin affair? Nature reviews Molecular cell biology *5*, 493-498.

Biamonti, G., and Vourc'h, C. (2010). Nuclear stress bodies. Cold Spring Harbor perspectives in biology *2*, a000695.

Bienz, M., and Pelham, H.R. (1982). Expression of a *Drosophila* heat-shock protein in *Xenopus* oocytes: conserved and divergent regulatory signals. The EMBO journal *1*, 1583-1588.

Bierkamp, C., Luxey, M., Metchat, A., Audouard, C., Dumollard, R., and Christians, E. (2010). Lack of maternal Heat Shock Factor 1 results in multiple cellular and developmental defects, including mitochondrial damage and altered redox homeostasis, and leads to reduced survival of mammalian oocytes and embryos. Developmental biology *339*, 338-353.

Bies, J., Markus, J., and Wolff, L. (2002). Covalent attachment of the SUMO-1 protein to the negative regulatory domain of the c-Myb transcription factor modifies its stability and transactivation capacity. The Journal of biological chemistry *277*, 8999-9009.

Biggin, M.D. (2011). Animal transcription networks as highly connected, quantitative continua. Developmental cell *21*, 611-626.

Birmingham, A., Selfors, L.M., Forster, T., Wrobel, D., Kennedy, C.J., Shanks, E., Santoyo-Lopez, J., Dunican, D.J., Long, A., Kelleher, D.*, et al.* (2009). Statistical methods for analysis of high-throughput RNA interference screens. Nature methods *6*, 569-575.

Bluher, M., Kahn, B.B., and Kahn, C.R. (2003). Extended longevity in mice lacking the insulin receptor in adipose tissue. Science (New York, NY) *299*, 572-574.

Bond, U. (1988). Heat shock but not other stress inducers leads to the disruption of a sub-set of snRNPs and inhibition of *in vitro* splicing in HeLa cells. The EMBO journal *7*, 3509-3518.

Bonner, J.J., Ballou, C., and Fackenthal, D.L. (1994). Interactions between DNA-bound trimers of the yeast heat shock factor. Molecular and cellular biology *14*, 501-508.

Bouras, T., Fu, M., Sauve, A.A., Wang, F., Quong, A.A., Perkins, N.D., Hay, R.T., Gu, W., and Pestell, R.G. (2005). SIRT1 deacetylation and repression of p300 involves lysine residues 1020/1024 within the cell cycle regulatory domain 1. The Journal of biological chemistry *280*, 10264-10276.

Boyd, W.A., Smith, M.V., Kissling, G.E., and Freedman, J.H. (2010). Medium- and high-throughput screening of neurotoxicants using *C. elegans*. Neurotoxicology and teratology *32*, 68-73.

Boyd, W.A., Smith, M.V., Kissling, G.E., Rice, J.R., Snyder, D.W., Portier, C.J., and Freedman, J.H. (2009). Application of a mathematical model to describe the effects of chlorpyrifos on *Caenorhabditis elegans* development. PloS one *4*, e7024.

Brandman, O., Stewart-Ornstein, J., Wong, D., Larson, A., Williams, C.C., Li, G.W., Zhou, S., King, D., Shen, P.S., Weibezahn, J.*, et al.* (2012). A ribosome-bound quality control complex triggers degradation of nascent peptides and signals translation stress. Cell *151*, 1042-1054.

Brenner, S. (1974). The genetics of *Caenorhabditis elegans*. Genetics *77*, 71-94.

Broday, L., Kolotuev, I., Didier, C., Bhoumik, A., Gupta, B.P., Sternberg, P.W., Podbilewicz, B., and Ronai, Z. (2004). The small ubiquitin-like modifier (SUMO) is required for gonadal and uterine-vulval morphogenesis in *Caenorhabditis elegans*. Genes & development *18*, 2380-2391.

Burns, A.R., Kwok, T.C., Howard, A., Houston, E., Johanson, K., Chan, A., Cutler, S.R., McCourt, P., and Roy, P.J. (2006). High-throughput screening of small molecules for bioactivity and target identification in *Caenorhabditis elegans*. Nature protocols *1*, 1906-1914.

Buschmann, T., Lerner, D., Lee, C.G., and Ronai, Z. (2001). The Mdm-2 amino terminus is required for Mdm2 binding and SUMO-1 conjugation by the E2 SUMO-1 conjugating enzyme Ubc9. The Journal of biological chemistry *276*, 40389-40395.

Cahill, C.M., Waterman, W.R., Xie, Y., Auron, P.E., and Calderwood, S.K. (1996). Transcriptional repression of the prointerleukin 1beta gene by heat shock factor 1. The Journal of biological chemistry *271*, 24874-24879.

Chen, W., Syldath, U., Bellmann, K., Burkart, V., and Kolb, H. (1999). Human 60-kDa heat-shock protein: a danger signal to the innate immune system. Journal of immunology (Baltimore, Md : 1950) *162*, 3212-3219.

Chen, Y., Barlev, N.A., Westergaard, O., and Jakobsen, B.K. (1993). Identification of the C-terminal activator domain in yeast heat shock factor: independent control of transient and sustained transcriptional activity. The EMBO journal *12*, 5007-5018.

Chiang, W.C., Ching, T.T., Lee, H.C., Mousigian, C., and Hsu, A.L. (2012). HSF-1 regulators DDL-1/2 link insulin-like signaling to heat-shock responses and modulation of longevity. Cell *148*, 322-334.

Chiodi, I., Biggiogera, M., Denegri, M., Corioni, M., Weighardt, F., Cobianchi, F., Riva, S., and Biamonti, G. (2000). Structure and dynamics of hnRNP-labelled nuclear bodies induced by stress treatments. Journal of cell science *113 (Pt 22)*, 4043-4053.

Chiodi, I., Corioni, M., Giordano, M., Valgardsdottir, R., Ghigna, C., Cobianchi, F., Xu, R.M., Riva, S., and Biamonti, G. (2004). RNA recognition motif 2 directs the recruitment of SF2/ASF to nuclear stress bodies. Nucleic acids research *32*, 4127-4136.

Chou, S.D., Prince, T., Gong, J., and Calderwood, S.K. (2012). mTOR is essential for the proteotoxic stress response, HSF1 activation and heat shock protein synthesis. PloS one *7*, e39679.

Christians, E., Davis, A.A., Thomas, S.D., and Benjamin, I.J. (2000). Maternal effect of Hsf1 on reproductive success. Nature *407*, 693-694.

Christians, E., Michel, E., Adenot, P., Mezger, V., Rallu, M., Morange, M., and Renard, J.P. (1997). Evidence for the involvement of mouse heat shock factor 1 in the atypical expression of the HSP70.1 heat shock gene during mouse zygotic genome activation. Molecular and cellular biology *17*, 778-788.

Chu, B., Zhong, R., Soncin, F., Stevenson, M.A., and Calderwood, S.K. (1998). Transcriptional activity of heat shock factor 1 at 37°C is repressed through phosphorylation on two distinct serine residues by glycogen synthase kinase 3 and protein kinases Cα and Cζ. The Journal of biological chemistry *273*, 18640-18646.

Chung, N., Zhang, X.D., Kreamer, A., Locco, L., Kuan, P.F., Bartz, S., Linsley, P.S., Ferrer, M., and Strulovici, B. (2008). Median absolute deviation to improve hit selection for genome-scale RNAi screens. Journal of biomolecular screening *13*, 149-158.

Clancy, D.J., Gems, D., Harshman, L.G., Oldham, S., Stocker, H., Hafen, E., Leevers, S.J., and Partridge, L. (2001). Extension of life-span by loss of CHICO, a *Drosophila* insulin receptor substrate protein. Science (New York, NY) *292*, 104-106.

Clos, J., Rabindran, S., Wisniewski, J., and Wu, C. (1993). Induction temperature of human heat shock factor is reprogrammed in a *Drosophila* cell environment. Nature *364*, 252-255.

Clos, J., Westwood, J.T., Becker, P.B., Wilson, S., Lambert, K., and Wu, C. (1990). Molecular cloning and expression of a hexameric *Drosophila* heat shock factor subject to negative regulation. Cell *63*, 1085-1097.

Cohen, E., Bieschke, J., Perciavalle, R.M., Kelly, J.W., and Dillin, A. (2006). Opposing activities protect against age-onset proteotoxicity. Science (New York, NY) *313*, 1604-1610.

Cotto, J., Fox, S., and Morimoto, R. (1997). HSF1 granules: a novel stress-induced nuclear compartment of human cells. Journal of cell science *110 (Pt 23)*, 2925-2934.

Cotto, J.J., Kline, M., and Morimoto, R.I. (1996). Activation of heat shock factor 1 DNA binding precedes stress-induced serine phosphorylation. Evidence for a multistep pathway of regulation. The Journal of biological chemistry *271*, 3355-3358.

Dai, C., Santagata, S., Tang, Z., Shi, J., Cao, J., Kwon, H., Bronson, R.T., Whitesell, L., and Lindquist, S. (2012). Loss of tumor suppressor NF1 activates HSF1 to promote carcinogenesis. The Journal of clinical investigation *122*, 3742-3754.

Dai, C., Whitesell, L., Rogers, A.B., and Lindquist, S. (2007). Heat shock factor 1 is a powerful multifaceted modifier of carcinogenesis. Cell *130*, 1005-1018.

Dai, R., Frejtag, W., He, B., Zhang, Y., and Mivechi, N.F. (2000). c-Jun NH2-terminal kinase targeting and phosphorylation of heat shock factor-1 suppress its transcriptional activity. The Journal of biological chemistry *275*, 18210-18218.

DasGupta, R., Kaykas, A., Moon, R.T., and Perrimon, N. (2005). Functional genomic analysis of the Wnt-wingless signaling pathway. Science (New York, NY) *308*, 826-833.

De Maio, A., Santoro, M.G., Tanguay, R.M., and Hightower, L.E. (2012). Ferruccio Ritossa's scientific legacy 50 years after his discovery of the heat shock response: a new view of biology, a new society, and a new journal. Cell stress & chaperones *17*, 139-143.

Denegri, M., Chiodi, I., Corioni, M., Cobianchi, F., Riva, S., and Biamonti, G. (2001). Stress-induced nuclear bodies are sites of accumulation of pre-mRNA processing factors. Molecular biology of the cell *12*, 3502-3514.

Denegri, M., Moralli, D., Rocchi, M., Biggiogera, M., Raimondi, E., Cobianchi, F., De Carli, L., Riva, S., and Biamonti, G. (2002). Human chromosomes 9, 12, and 15 contain the nucleation sites of stress-induced nuclear bodies. Molecular biology of the cell *13*, 2069-2079.

Desterro, J.M., Rodriguez, M.S., and Hay, R.T. (1998). SUMO-1 modification of IkappaBalpha inhibits NF-kappaB activation. Molecular cell *2*, 233-239.

Dobreva, G., Dambacher, J., and Grosschedl, R. (2003). SUMO modification of a novel MAR-binding protein, SATB2, modulates immunoglobulin mu gene expression. Genes & development *17*, 3048-3061.

Doitsidou, M., Flames, N., Lee, A.C., Boyanov, A., and Hobert, O. (2008). Automated screening for mutants affecting dopaminergic-neuron specification in *C. elegans*. Nature methods *5*, 869-872.

Dorman, J.B., Albinder, B., Shroyer, T., and Kenyon, C. (1995). The *age-1* and *daf-2* genes function in a common pathway to control the lifespan of *Caenorhabditis elegans*. Genetics *141*, 1399-1406.

Duina, A.A., Kalton, H.M., and Gaber, R.F. (1998). Requirement for Hsp90 and a CyP-40-type cyclophilin in negative regulation of the heat shock response. The Journal of biological chemistry *273*, 18974-18978.

Duprez, E., Saurin, A.J., Desterro, J.M., Lallemand-Breitenbach, V., Howe, K., Boddy, M.N., Solomon, E., de The, H., Hay, R.T., and Freemont, P.S. (1999). SUMO-1 modification of the acute promyelocytic leukaemia protein PML: implications for nuclear localisation. Journal of cell science *112 (Pt 3)*, 381-393.

Dye, B.T., and Schulman, B.A. (2007). Structural mechanisms underlying posttranslational modification by ubiquitin-like proteins. Annual review of biophysics and biomolecular structure *36*, 131-150.

Ellis, R.J. (1993). The general concept of molecular chaperones. Philosophical transactions of the Royal Society of London Series B, Biological sciences *339*, 257-261.

Emmons, S.W., Rosenzweig, B., and Hirsh, D. (1980). Arrangement of repeated sequences in the DNA of the nematode *Caenorhabditis elegans*. Journal of molecular biology *144*, 481-500.

Eymery, A., Souchier, C., Vourc'h, C., and Jolly, C. (2010). Heat shock factor 1 binds to and transcribes satellite II and III sequences at several pericentromeric regions in heat-shocked cells. Experimental cell research *316*, 1845-1855.

Fargnoli, J., Kunisada, T., Fornace, A.J., Jr., Schneider, E.L., and Holbrook, N.J. (1990). Decreased expression of heat shock protein 70 mRNA and protein after heat treatment in cells of aged rats. Proceedings of the National Academy of Sciences of the United States of America *87*, 846-850.

Farkas, T., Kutskova, Y.A., and Zimarino, V. (1998). Intramolecular repression of mouse heat shock factor 1. Molecular and cellular biology *18*, 906-918.

Ferrarini, M., Heltai, S., Zocchi, M.R., and Rugarli, C. (1992). Unusual expression and localization of heat-shock proteins in human tumor cells. International journal of cancer Journal international du cancer *51*, 613-619.

Fiorenza, M.T., Farkas, T., Dissing, M., Kolding, D., and Zimarino, V. (1995). Complex expression of murine heat shock transcription factors. Nucleic acids research *23*, 467-474.

Friedman, D.B., and Johnson, T.E. (1988). Three mutants that extend both mean and maximum life span of the nematode, *Caenorhabditis elegans*, define the *age-1* gene. Journal of gerontology *43*, B102-109.

Fritsch, M., and Wu, C. (1999). Phosphorylation of *Drosophila* heat shock transcription factor. Cell stress & chaperones *4*, 102-117.

Frøkjær-Jensen, C., Davis, M.W., Hopkins, C.E., Newman, B.J., Thummel, J.M., Olesen, S.P., Grunnet, M., and Jorgensen, E.M. (2008). Single-copy insertion of transgenes in *Caenorhabditis elegans*. Nature genetics *40*, 1375-1383.

Fujimoto, M., Hayashida, N., Katoh, T., Oshima, K., Shinkawa, T., Prakasam, R., Tan, K., Inouye, S., Takii, R., and Nakai, A. (2010). A novel mouse HSF3 has the potential to activate nonclassical heat-shock genes during heat shock. Molecular biology of the cell *21*, 106-116.

Fujimoto, M., Izu, H., Seki, K., Fukuda, K., Nishida, T., Yamada, S., Kato, K., Yonemura, S., Inouye, S., and Nakai, A. (2004). HSF4 is required for normal cell growth and differentiation during mouse lens development. The EMBO journal *23*, 4297-4306.

Gallo, G.J., Prentice, H., and Kingston, R.E. (1993). Heat shock factor is required for growth at normal temperatures in the fission yeast *Schizosaccharomyces pombe*. Molecular and cellular biology *13*, 749-761.

Gallo, G.J., Schuetz, T.J., and Kingston, R.E. (1991). Regulation of heat shock factor in *Schizosaccharomyces pombe* more closely resembles regulation in mammals than in *Saccharomyces cerevisiae*. Molecular and cellular biology *11*, 281-288.

Garigan, D., Hsu, A.L., Fraser, A.G., Kamath, R.S., Ahringer, J., and Kenyon, C. (2002). Genetic analysis of tissue aging in *Caenorhabditis elegans*: a role for heat-shock factor and bacterial proliferation. Genetics *161*, 1101-1112.

Giannakou, M.E., Goss, M., Junger, M.A., Hafen, E., Leevers, S.J., and Partridge, L. (2004). Long-lived *Drosophila* with overexpressed dFOXO in adult fat body. Science (New York, NY) *305*, 361.

Gill, G. (2005). Something about SUMO inhibits transcription. Current opinion in genetics & development *15*, 536-541.

Goodson, M.L., Hong, Y., Rogers, R., Matunis, M.J., Park-Sarge, O.K., and Sarge, K.D. (2001). Sumo-1 modification regulates the DNA binding activity of heat shock transcription factor 2, a promyelocytic leukemia nuclear body associated transcription factor. The Journal of biological chemistry *276*, 18513-18518.

Grady, D.L., Ratliff, R.L., Robinson, D.L., McCanlies, E.C., Meyne, J., and Moyzis, R.K. (1992). Highly conserved repetitive DNA sequences are present at human centromeres. Proceedings of the National Academy of Sciences of the United States of America *89*, 1695-1699.

Green, M., Schuetz, T.J., Sullivan, E.K., and Kingston, R.E. (1995). A heat shock-responsive domain of human HSF1 that regulates transcription activation domain function. Molecular and cellular biology *15*, 3354-3362.

Guan, Q., Wen, C., Zeng, H., and Zhu, J. (2012). A KH domain-containing putative RNA-binding protein is critical for heat stress-responsive gene regulation and thermotolerance in *Arabidopsis*. Molecular plant.

Guettouche, T., Boellmann, F., Lane, W.S., and Voellmy, R. (2005). Analysis of phosphorylation of human heat shock factor 1 in cells experiencing a stress. BMC biochemistry *6*, 4.

Guo, Y., Guettouche, T., Fenna, M., Boellmann, F., Pratt, W.B., Toft, D.O., Smith, D.F., and Voellmy, R. (2001). Evidence for a mechanism of repression of heat shock factor 1 transcriptional activity by a multichaperone complex. The Journal of biological chemistry *276*, 45791-45799.

Hahn, J.S., and Thiele, D.J. (2004). Activation of the *Saccharomyces cerevisiae* heat shock transcription factor under glucose starvation conditions by Snf1 protein kinase. The Journal of biological chemistry *279*, 5169-5176.

Hajdu-Cronin, Y.M., Chen, W.J., and Sternberg, P.W. (2004). The L-type cyclin CYL-1 and the heat-shock-factor HSF-1 are required for heat-shock-induced protein expression in *Caenorhabditis elegans*. Genetics *168*, 1937-1949.

Harrison, C.J., Bohm, A.A., and Nelson, H.C. (1994). Crystal structure of the DNA binding domain of the heat shock transcription factor. Science (New York, NY) *263*, 224-227.

He, B., Meng, Y.H., and Mivechi, N.F. (1998). Glycogen synthase kinase 3β and extracellular signal-regulated kinase inactivate heat shock transcription factor 1 by facilitating the disappearance of transcriptionally active granules after heat shock. Molecular and cellular biology *18*, 6624-6633.

Hietakangas, V., Ahlskog, J.K., Jakobsson, A.M., Hellesuo, M., Sahlberg, N.M., Holmberg, C.I., Mikhailov, A., Palvimo, J.J., Pirkkala, L., and Sistonen, L. (2003). Phosphorylation of serine 303 is a prerequisite for the stress-inducible SUMO modification of heat shock factor 1. Molecular and cellular biology *23*, 2953-2968.

Hietakangas, V., Anckar, J., Blomster, H.A., Fujimoto, M., Palvimo, J.J., Nakai, A., and Sistonen, L. (2006). PDSM, a motif for phosphorylation-dependent SUMO modification. Proceedings of the National Academy of Sciences of the United States of America *103*, 45-50.

Hilgarth, R.S., Murphy, L.A., O'Connor, C.M., Clark, J.A., Park-Sarge, O.K., and Sarge, K.D. (2004). Identification of *Xenopus* heat shock transcription factor-2: conserved role of sumoylation in regulating deoxyribonucleic acid-binding activity of heat shock transcription factor-2 proteins. Cell stress & chaperones *9*, 214-220.

Hirano, Y., Murata, S., Tanaka, K., Shimizu, M., and Sato, R. (2003). Sterol regulatory element-binding proteins are negatively regulated through SUMO-1 modification independent of the ubiquitin/26 S proteasome pathway. The Journal of biological chemistry *278*, 16809-16819.

Høj, A., and Jakobsen, B.K. (1994). A short element required for turning off heat shock transcription factor: evidence that phosphorylation enhances deactivation. The EMBO journal *13*, 2617-2624.

Holmberg, C.I., Hietakangas, V., Mikhailov, A., Rantanen, J.O., Kallio, M., Meinander, A., Hellman, J., Morrice, N., MacKintosh, C., Morimoto, R.I.*, et al.* (2001). Phosphorylation of

serine 230 promotes inducible transcriptional activity of heat shock factor 1. The EMBO journal *20*, 3800-3810.

Holmberg, C.I., Illman, S.A., Kallio, M., Mikhailov, A., and Sistonen, L. (2000). Formation of nuclear HSF1 granules varies depending on stress stimuli. Cell stress & chaperones *5*, 219-228.

Holway, A.H., Hung, C., and Michael, W.M. (2005). Systematic, RNA-interference-mediated identification of mus-101 modifier genes in *Caenorhabditis elegans*. Genetics *169*, 1451-1460.

Holzenberger, M., Dupont, J., Ducos, B., Leneuve, P., Geloen, A., Even, P.C., Cervera, P., and Le Bouc, Y. (2003). IGF-1 receptor regulates lifespan and resistance to oxidative stress in mice. Nature *421*, 182-187.

Hong, Y., Rogers, R., Matunis, M.J., Mayhew, C.N., Goodson, M.L., Park-Sarge, O.K., and Sarge, K.D. (2001). Regulation of heat shock transcription factor 1 by stress-induced SUMO-1 modification. The Journal of biological chemistry *276*, 40263-40267.

Hsu, A.L., Murphy, C.T., and Kenyon, C. (2003). Regulation of aging and age-related disease by DAF-16 and heat-shock factor. Science (New York, NY) *300*, 1142-1145.

Huot, J., Roy, G., Lambert, H., Chretien, P., and Landry, J. (1991). Increased survival after treatments with anticancer agents of Chinese hamster cells expressing the human Mr 27,000 heat shock protein. Cancer research *51*, 5245-5252.

Inouye, S., Izu, H., Takaki, E., Suzuki, H., Shirai, M., Yokota, Y., Ichikawa, H., Fujimoto, M., and Nakai, A. (2004). Impaired IgG production in mice deficient for heat shock transcription factor 1. The Journal of biological chemistry *279*, 38701-38709.

Jacquier-Sarlin, M.R., and Polla, B.S. (1996). Dual regulation of heat-shock transcription factor (HSF) activation and DNA-binding activity by H2O2: role of thioredoxin. The Biochemical journal *318 (Pt 1)*, 187-193.

Jakobsen, B.K., and Pelham, H.R. (1988). Constitutive binding of yeast heat shock factor to DNA *in vivo*. Molecular and cellular biology *8*, 5040-5042.

Jameel, A., Skilton, R.A., Campbell, T.A., Chander, S.K., Coombes, R.C., and Luqmani, Y.A. (1992). Clinical and biological significance of HSP89 alpha in human breast cancer. International journal of cancer Journal international du cancer *50*, 409-415.

Jarmuz, M., Glotzbach, C.D., Bailey, K.A., Bandyopadhyay, R., and Shaffer, L.G. (2007). The evolution of satellite III DNA subfamilies among primates. American journal of human genetics *80*, 495-501.

Jedlicka, P., Mortin, M.A., and Wu, C. (1997). Multiple functions of *Drosophila* heat shock transcription factor in vivo. The EMBO journal *16*, 2452-2462.

Jin, X., Moskophidis, D., and Mivechi, N.F. (2011). Heat shock transcription factor 1 is a key determinant of HCC development by regulating hepatic steatosis and metabolic syndrome. Cell metabolism *14*, 91-103.

Johnson, E.S. (2004). Protein modification by SUMO. Annual review of biochemistry *73*, 355-382.

Johnson, E.S., Schwienhorst, I., Dohmen, R.J., and Blobel, G. (1997). The ubiquitin-like protein Smt3p is activated for conjugation to other proteins by an Aos1p/Uba2p heterodimer. The EMBO journal *16*, 5509-5519.

Johnson, P.R., and Hochstrasser, M. (1997). SUMO-1: Ubiquitin gains weight. Trends in cell biology *7*, 408-413.

Jolly, C., Konecny, L., Grady, D.L., Kutskova, Y.A., Cotto, J.J., Morimoto, R.I., and Vourc'h, C. (2002). *In vivo* binding of active heat shock transcription factor 1 to human chromosome 9 heterochromatin during stress. The Journal of cell biology *156*, 775-781.

Jolly, C., Metz, A., Govin, J., Vigneron, M., Turner, B.M., Khochbin, S., and Vourc'h, C. (2004). Stress-induced transcription of satellite III repeats. The Journal of cell biology *164*, 25-33.

Jolly, C., Morimoto, R., Robert-Nicoud, M., and Vourc'h, C. (1997). HSF1 transcription factor concentrates in nuclear foci during heat shock: relationship with transcription sites. Journal of cell science *110 (Pt 23)*, 2935-2941.

Jolly, C., and Morimoto, R.I. (2000). Role of the heat shock response and molecular chaperones in oncogenesis and cell death. Journal of the National Cancer Institute *92*, 1564-1572.

Jolly, C., Usson, Y., and Morimoto, R.I. (1999). Rapid and reversible relocalization of heat shock factor 1 within seconds to nuclear stress granules. Proceedings of the National Academy of Sciences of the United States of America *96*, 6769-6774.

Jones, D., Crowe, E., Stevens, T.A., and Candido, E.P. (2002). Functional and phylogenetic analysis of the ubiquitylation system in *Caenorhabditis elegans*: ubiquitin-conjugating enzymes, ubiquitin-activating enzymes, and ubiquitin-like proteins. Genome biology *3*, RESEARCH0002.

Jurivich, D.A., Pachetti, C., Qiu, L., and Welk, J.F. (1995). Salicylate triggers heat shock factor differently than heat. The Journal of biological chemistry *270*, 24489-24495.

Kaminsky, R., Denison, C., Bening-Abu-Shach, U., Chisholm, A.D., Gygi, S.P., and Broday, L. (2009). SUMO regulates the assembly and function of a cytoplasmic intermediate filament protein in *C. elegans*. Developmental cell *17*, 724-735.

Kang, P.J., Ostermann, J., Shilling, J., Neupert, W., Craig, E.A., and Pfanner, N. (1990). Requirement for hsp70 in the mitochondrial matrix for translocation and folding of precursor proteins. Nature *348*, 137-143.

Kaur, J., and Ralhan, R. (1995). Differential expression of 70-kDa heat shock-protein in human oral tumorigenesis. International journal of cancer Journal international du cancer *63*, 774-779.

Kawazoe, Y., Tanabe, M., Sasai, N., Nagata, K., and Nakai, A. (1999). HSF3 is a major heat shock responsive factor during chicken embryonic development. European journal of biochemistry / FEBS *265*, 688-697.

Kelley, P.M., and Schlesinger, M.J. (1978). The effect of amino acid analogues and heat shock on gene expression in chicken embryo fibroblasts. Cell *15*, 1277-1286.

Kenyon, C., Chang, J., Gensch, E., Rudner, A., and Tabtiang, R. (1993). A *C. elegans* mutant that lives twice as long as wild type. Nature *366*, 461-464.

Khazaeli, A.A., Tatar, M., Pletcher, S.D., and Curtsinger, J.W. (1997). Heat-induced longevity extension in *Drosophila*. I. Heat treatment, mortality, and thermotolerance. The journals of gerontology Series A, Biological sciences and medical sciences *52*, B48-52.

Kim, J., Cantwell, C.A., Johnson, P.F., Pfarr, C.M., and Williams, S.C. (2002). Transcriptional activity of CCAAT/enhancer-binding proteins is controlled by a conserved inhibitory domain that is a target for sumoylation. The Journal of biological chemistry *277*, 38037-38044.

Kim, S.A., Yoon, J.H., Lee, S.H., and Ahn, S.G. (2005). Polo-like kinase 1 phosphorylates heat shock transcription factor 1 and mediates its nuclear translocation during heat stress. The Journal of biological chemistry *280*, 12653-12657.

Kim, S.J., Tsukiyama, T., Lewis, M.S., and Wu, C. (1994). Interaction of the DNA-binding domain of *Drosophila* heat shock factor with its cognate DNA site: a thermodynamic analysis using analytical ultracentrifugation. Protein science : a publication of the Protein Society *3*, 1040-1051.

Kingston, R.E., Schuetz, T.J., and Larin, Z. (1987). Heat-inducible human factor that binds to a human hsp70 promoter. Molecular and cellular biology *7*, 1530-1534.

Kline, M.P., and Morimoto, R.I. (1997). Repression of the heat shock factor 1 transcriptional activation domain is modulated by constitutive phosphorylation. Molecular and cellular biology *17*, 2107-2115.

Knowlton, A.A., and Sun, L. (2001). Heat-shock factor-1, steroid hormones, and regulation of heat-shock protein expression in the heart. American journal of physiology Heart and circulatory physiology *280*, H455-464.

Kourtis, N., Nikoletopoulou, V., and Tavernarakis, N. (2012). Small heat-shock proteins protect from heat-stroke-associated neurodegeneration. Nature *490*, 213-218.

Kregel, K.C., Moseley, P.L., Skidmore, R., Gutierrez, J.A., and Guerriero, V., Jr. (1995). HSP70 accumulation in tissues of heat-stressed rats is blunted with advancing age. Journal of applied physiology (Bethesda, Md : 1985) *79*, 1673-1678.

Kurepa, J., Walker, J.M., Smalle, J., Gosink, M.M., Davis, S.J., Durham, T.L., Sung, D.Y., and Vierstra, R.D. (2003). The small ubiquitin-like modifier (SUMO) protein modification system in *Arabidopsis.* Accumulation of SUMO1 and -2 conjugates is increased by stress. The Journal of biological chemistry *278*, 6862-6872.

Lamitina, T., Huang, C.G., and Strange, K. (2006). Genome-wide RNAi screening identifies protein damage as a regulator of osmoprotective gene expression. Proceedings of the National Academy of Sciences of the United States of America *103*, 12173-12178.

Larson, J.S., Schuetz, T.J., and Kingston, R.E. (1995). *In vitro* activation of purified human heat shock factor by heat. Biochemistry *34*, 1902-1911.

LaRue, B.L., and Padilla, P.A. (2011). Environmental and genetic preconditioning for long-term anoxia responses requires AMPK in *Caenorhabditis elegans*. PloS one *6*, e16790.

Leach, M.D., Budge, S., Walker, L., Munro, C., Cowen, L.E., and Brown, A.J. (2012). Hsp90 orchestrates transcriptional regulation by Hsf1 and cell wall remodelling by MAPK signalling during thermal adaptation in a pathogenic yeast. PLoS pathogens *8*, e1003069.

Lee, Y.J., Kim, E.H., Lee, J.S., Jeoung, D., Bae, S., Kwon, S.H., and Lee, Y.S. (2008). HSF1 as a mitotic regulator: phosphorylation of HSF1 by Plk1 is essential for mitotic progression. Cancer research *68*, 7550-7560.

Li, W., Bengtson, M.H., Ulbrich, A., Matsuda, A., Reddy, V.A., Orth, A., Chanda, S.K., Batalov, S., and Joazeiro, C.A. (2008). Genome-wide and functional annotation of human E3 ubiquitin ligases identifies MULAN, a mitochondrial E3 that regulates the organelle's dynamics and signaling. PloS one *3*, e1487.

Lin, D.Y., Huang, Y.S., Jeng, J.C., Kuo, H.Y., Chang, C.C., Chao, T.T., Ho, C.C., Chen, Y.C., Lin, T.P., Fang, H.I.*, et al.* (2006). Role of SUMO-interacting motif in Daxx SUMO modification, subnuclear localization, and repression of sumoylated transcription factors. Molecular cell *24*, 341-354.

Lindquist, S. (1986). The heat-shock response. Annual review of biochemistry *55*, 1151-1191.

Link, C.D., Cypser, J.R., Johnson, C.J., and Johnson, T.E. (1999). Direct observation of stress response in *Caenorhabditis elegans* using a reporter transgene. Cell stress & chaperones *4*, 235-242.

Lithgow, G.J., White, T.M., Melov, S., and Johnson, T.E. (1995). Thermotolerance and extended life-span conferred by single-gene mutations and induced by thermal stress. Proceedings of the National Academy of Sciences of the United States of America *92*, 7540-7544.

Littlefield, O., and Nelson, H.C. (1999). A new use for the 'wing' of the 'winged' helix-turn-helix motif in the HSF-DNA cocrystal. Nature structural biology *6*, 464-470.

Liu, A.Y., Lin, Z., Choi, H.S., Sorhage, F., and Li, B. (1989). Attenuated induction of heat shock gene expression in aging diploid fibroblasts. The Journal of biological chemistry *264*, 12037-12045.

Liu, X.D., Liu, P.C., Santoro, N., and Thiele, D.J. (1997). Conservation of a stress response: human heat shock transcription factors functionally substitute for yeast HSF. The EMBO journal *16*, 6466-6477.

Liu, Y., Liang, S., and Tartakoff, A.M. (1996). Heat shock disassembles the nucleolus and inhibits nuclear protein import and poly(A)+ RNA export. The EMBO journal *15*, 6750-6757.

Long, J.C., and Caceres, J.F. (2009). The SR protein family of splicing factors: master regulators of gene expression. The Biochemical journal *417*, 15-27.

Mahajan, R., Delphin, C., Guan, T., Gerace, L., and Melchior, F. (1997). A small ubiquitin-related polypeptide involved in targeting RanGAP1 to nuclear pore complex protein RanBP2. Cell *88*, 97-107.

Manuel, M., Rallu, M., Loones, M.T., Zimarino, V., Mezger, V., and Morange, M. (2002). Determination of the consensus binding sequence for the purified embryonic heat shock factor 2. European journal of biochemistry / FEBS *269*, 2527-2537.

Martinez-Balbas, M.A., Dey, A., Rabindran, S.K., Ozato, K., and Wu, C. (1995). Displacement of sequence-specific transcription factors from mitotic chromatin. Cell *83*, 29-38.

Martinez, J.L., Sanchez-Elsner, T., Morcillo, G., and Diez, J.L. (2001). Heat shock regulatory elements are present in telomeric repeats of *Chironomus thummi*. Nucleic acids research *29*, 4760-4766.

Massie, M.R., Lapoczka, E.M., Boggs, K.D., Stine, K.E., and White, G.E. (2003). Exposure to the metabolic inhibitor sodium azide induces stress protein expression and thermotolerance in the nematode *Caenorhabditis elegans*. Cell stress & chaperones *8*, 1-7.

Matunis, M.J., Coutavas, E., and Blobel, G. (1996). A novel ubiquitin-like modification modulates the partitioning of the Ran-GTPase-activating protein RanGAP1 between the cytosol and the nuclear pore complex. The Journal of cell biology *135*, 1457-1470.

Mayya, V., Lundgren, D.H., Hwang, S.I., Rezaul, K., Wu, L., Eng, J.K., Rodionov, V., and Han, D.K. (2009). Quantitative phosphoproteomic analysis of T cell receptor signaling reveals system-wide modulation of protein-protein interactions. Science signaling *2*, ra46.

McColl, G., Rogers, A.N., Alavez, S., Hubbard, A.E., Melov, S., Link, C.D., Bush, A.I., Kapahi, P., and Lithgow, G.J. (2010). Insulin-like signaling determines survival during stress via posttranscriptional mechanisms in *C. elegans*. Cell metabolism *12*, 260-272.

McKenzie, S.L., Henikoff, S., and Meselson, M. (1975). Localization of RNA from heat-induced polysomes at puff sites in *Drosophila melanogaster*. Proceedings of the National Academy of Sciences of the United States of America *72*, 1117-1121.

McMillan, D.R., Xiao, X., Shao, L., Graves, K., and Benjamin, I.J. (1998). Targeted disruption of heat shock transcription factor 1 abolishes thermotolerance and protection against heat-inducible apoptosis. The Journal of biological chemistry *273*, 7523-7528.

Mendillo, M.L., Santagata, S., Koeva, M., Bell, G.W., Hu, R., Tamimi, R.M., Fraenkel, E., Ince, T.A., Whitesell, L., and Lindquist, S. (2012). HSF1 drives a transcriptional program distinct from heat shock to support highly malignant human cancers. Cell *150*, 549-562.

Meng, L., Gabai, V.L., and Sherman, M.Y. (2010). Heat-shock transcription factor HSF1 has a critical role in human epidermal growth factor receptor-2-induced cellular transformation and tumorigenesis. Oncogene *29*, 5204-5213.

Mercier, P.A., Winegarden, N.A., and Westwood, J.T. (1999). Human heat shock factor 1 is predominantly a nuclear protein before and after heat stress. Journal of cell science *112 (Pt 16)*, 2765-2774.

Metchat, A., Akerfelt, M., Bierkamp, C., Delsinne, V., Sistonen, L., Alexandre, H., and Christians, E.S. (2009). Mammalian heat shock factor 1 is essential for oocyte meiosis and directly regulates Hsp90alpha expression. The Journal of biological chemistry *284*, 9521-9528.

Metz, A., Soret, J., Vourc'h, C., Tazi, J., and Jolly, C. (2004). A key role for stress-induced satellite III transcripts in the relocalization of splicing factors into nuclear stress granules. Journal of cell science *117*, 4551-4558.

Mezger, V., Rallu, M., Morimoto, R.I., Morange, M., and Renard, J.P. (1994). Heat shock factor 2-like activity in mouse blastocysts. Developmental biology *166*, 819-822.

Mifflin, L.C., and Cohen, R.E. (1994). Characterization of denatured protein inducers of the heat shock (stress) response in *Xenopus laevis* oocytes. The Journal of biological chemistry *269*, 15710-15717.

Mirault, M.E., Southgate, R., and Delwart, E. (1982). Regulation of heat-shock genes: a DNA sequence upstream of *Drosophila* hsp70 genes is essential for their induction in monkey cells. The EMBO journal *1*, 1279-1285.

Mitchell, A.R., Gosden, J.R., and Ryder, O.A. (1981). Satellite DNA relationships in man and the primates. Nucleic acids research *9*, 3235-3249.

Mivechi, N.F., Koong, A.C., Giaccia, A.J., and Hahn, G.M. (1994a). Analysis of HSF-1 phosphorylation in A549 cells treated with a variety of stresses. International journal of hyperthermia : the official journal of European Society for Hyperthermic Oncology, North American Hyperthermia Group *10*, 371-379.

Mivechi, N.F., Murai, T., and Hahn, G.M. (1994b). Inhibitors of tyrosine and Ser/Thr phosphatases modulate the heat shock response. Journal of cellular biochemistry *54*, 186-197.

Mohri-Shiomi, A., and Garsin, D.A. (2008). Insulin signaling and the heat shock response modulate protein homeostasis in the *Caenorhabditis elegans* intestine during infection. The Journal of biological chemistry *283*, 194-201.

Morita, M.T., Tanaka, Y., Kodama, T.S., Kyogoku, Y., Yanagi, H., and Yura, T. (1999). Translational induction of heat shock transcription factor sigma32: evidence for a built-in RNA thermosensor. Genes & development *13*, 655-665.

Morley, J.F., and Morimoto, R.I. (2004). Regulation of longevity in *Caenorhabditis elegans* by heat shock factor and molecular chaperones. Molecular biology of the cell *15*, 657-664.

Moronetti Mazzeo, L.E., Dersh, D., Boccitto, M., Kalb, R.G., and Lamitina, T. (2012). Stress and aging induce distinct polyQ protein aggregation states. Proceedings of the National Academy of Sciences of the United States of America *109*, 10587-10592.

Morton, E., and Lamitina, T. (2010). A suite of MATLAB-based computational tools for automated analysis of COPAS Biosort data. BioTechniques *48*, xxv-xxx.

Morton, E.A., and Lamitina, T. (2013). *Caenorhabditis elegans* HSF-1 is an essential nuclear protein that forms stress granule-like structures following heat shock. Aging cell *12*, 112-120.

Mosser, D.D., Duchaine, J., and Massie, B. (1993). The DNA-binding activity of the human heat shock transcription factor is regulated in vivo by hsp70. Molecular and cellular biology *13*, 5427-5438.

Mosser, D.D., Kotzbauer, P.T., Sarge, K.D., and Morimoto, R.I. (1990). In vitro activation of heat shock transcription factor DNA-binding by calcium and biochemical conditions that affect protein conformation. Proceedings of the National Academy of Sciences of the United States of America *87*, 3748-3752.

Mosser, D.D., Theodorakis, N.G., and Morimoto, R.I. (1988). Coordinate changes in heat shock element-binding activity and HSP70 gene transcription rates in human cells. Molecular and cellular biology *8*, 4736-4744.

Muller, S., Berger, M., Lehembre, F., Seeler, J.S., Haupt, Y., and Dejean, A. (2000). c-Jun and p53 activity is modulated by SUMO-1 modification. The Journal of biological chemistry *275*, 13321-13329.

Murphy, S.P., Gorzowski, J.J., Sarge, K.D., and Phillips, B. (1994). Characterization of constitutive HSF2 DNA-binding activity in mouse embryonal carcinoma cells. Molecular and cellular biology *14*, 5309-5317.

Murshid, A., Chou, S.D., Prince, T., Zhang, Y., Bharti, A., and Calderwood, S.K. (2010). Protein kinase A binds and activates heat shock factor 1. PloS one *5*, e13830.

Nakai, A., Kawazoe, Y., Tanabe, M., Nagata, K., and Morimoto, R.I. (1995). The DNA-binding properties of two heat shock factors, HSF1 and HSF3, are induced in the avian erythroblast cell line HD6. Molecular and cellular biology *15*, 5268-5278.

Nakai, A., and Morimoto, R.I. (1993). Characterization of a novel chicken heat shock transcription factor, heat shock factor 3, suggests a new regulatory pathway. Molecular and cellular biology *13*, 1983-1997.

Nakai, A., Tanabe, M., Kawazoe, Y., Inazawa, J., Morimoto, R.I., and Nagata, K. (1997). HSF4, a new member of the human heat shock factor family which lacks properties of a transcriptional activator. Molecular and cellular biology *17*, 469-481.

Nollen, E.A., Garcia, S.M., van Haaften, G., Kim, S., Chavez, A., Morimoto, R.I., and Plasterk, R.H. (2004). Genome-wide RNA interference screen identifies previously undescribed regulators of polyglutamine aggregation. Proceedings of the National Academy of Sciences of the United States of America *101*, 6403-6408.

Nover, L., Bharti, K., Doring, P., Mishra, S.K., Ganguli, A., and Scharf, K.D. (2001). *Arabidopsis* and the heat stress transcription factor world: how many heat stress transcription factors do we need? Cell stress & chaperones *6*, 177-189.

Okuma, T., Honda, R., Ichikawa, G., Tsumagari, N., and Yasuda, H. (1999). In vitro SUMO-1 modification requires two enzymatic steps, E1 and E2. Biochemical and biophysical research communications *254*, 693-698.

Olsen, J.V., Vermeulen, M., Santamaria, A., Kumar, C., Miller, M.L., Jensen, L.J., Gnad, F., Cox, J., Jensen, T.S., Nigg, E.A.*, et al.* (2010). Quantitative phosphoproteomics reveals widespread full phosphorylation site occupancy during mitosis. Science signaling *3*, ra3.

Orosz, A., Wisniewski, J., and Wu, C. (1996). Regulation of *Drosophila* heat shock factor trimerization: global sequence requirements and independence of nuclear localization. Molecular and cellular biology *16*, 7018-7030.

Östling, P., Björk, J.K., Roos-Mattjus, P., Mezger, V., and Sistonen, L. (2007). Heat shock factor 2 (HSF2) contributes to inducible expression of *hsp* genes through interplay with HSF1. The Journal of biological chemistry *282*, 7077-7086.

Parker, C.S., and Topol, J. (1984). A *Drosophila* RNA polymerase II transcription factor binds to the regulatory site of an hsp 70 gene. Cell *37*, 273-283.

Parsell, D.A., and Lindquist, S. (1993). The function of heat-shock proteins in stress tolerance: degradation and reactivation of damaged proteins. Annual review of genetics *27*, 437-496.

Pelham, H.R. (1982). A regulatory upstream promoter element in the *Drosophila* hsp 70 heat-shock gene. Cell *30*, 517-528.

Pelham, H.R. (1986). Speculations on the functions of the major heat shock and glucose-regulated proteins. Cell *46*, 959-961.

Pelham, H.R., and Bienz, M. (1982). A synthetic heat-shock promoter element confers heat-inducibility on the herpes simplex virus thymidine kinase gene. The EMBO journal *1*, 1473-1477.

Pelisch, F., Gerez, J., Druker, J., Schor, I.E., Munoz, M.J., Risso, G., Petrillo, E., Westman, B.J., Lamond, A.I., Arzt, E.*, et al.* (2010). The serine/arginine-rich protein SF2/ASF regulates protein sumoylation. Proceedings of the National Academy of Sciences of the United States of America *107*, 16119-16124.

Peteranderl, R., and Nelson, H.C. (1992). Trimerization of the heat shock transcription factor by a triple-stranded alpha-helical coiled-coil. Biochemistry *31*, 12272-12276.

Pirkkala, L., Nykanen, P., and Sistonen, L. (2001). Roles of the heat shock transcription factors in regulation of the heat shock response and beyond. FASEB journal : official publication of the Federation of American Societies for Experimental Biology *15*, 1118-1131.

Prahlad, V., Cornelius, T., and Morimoto, R.I. (2008). Regulation of the cellular heat shock response in *Caenorhabditis elegans* by thermosensory neurons. Science (New York, NY) *320*, 811-814.

Prahlad, V., and Morimoto, R.I. (2011). Neuronal circuitry regulates the response of *Caenorhabditis elegans* to misfolded proteins. Proceedings of the National Academy of Sciences of the United States of America *108*, 14204-14209.

Prasanth, K.V., Rajendra, T.K., Lal, A.K., and Lakhotia, S.C. (2000). Omega speckles - a novel class of nuclear speckles containing hnRNPs associated with noncoding hsr-omega RNA in *Drosophila*. Journal of cell science *113 Pt 19*, 3485-3497.

Prosser, J., Frommer, M., Paul, C., and Vincent, P.C. (1986). Sequence relationships of three human satellite DNAs. Journal of molecular biology *187*, 145-155.

Pujol, N., Zugasti, O., Wong, D., Couillault, C., Kurz, C.L., Schulenburg, H., and Ewbank, J.J. (2008). Anti-fungal innate immunity in *C. elegans* is enhanced by evolutionary diversification of antimicrobial peptides. PLoS pathogens *4*, e1000105.

Rabindran, S.K., Giorgi, G., Clos, J., and Wu, C. (1991). Molecular cloning and expression of a human heat shock factor, HSF1. Proceedings of the National Academy of Sciences of the United States of America *88*, 6906-6910.

Rabindran, S.K., Haroun, R.I., Clos, J., Wisniewski, J., and Wu, C. (1993). Regulation of heat shock factor trimer formation: role of a conserved leucine zipper. Science (New York, NY) *259*, 230-234.

Rabindran, S.K., Wisniewski, J., Li, L., Li, G.C., and Wu, C. (1994). Interaction between heat shock factor and hsp70 is insufficient to suppress induction of DNA-binding activity in vivo. Molecular and cellular biology *14*, 6552-6560.

Ralhan, R., and Kaur, J. (1995). Differential expression of Mr 70,000 heat shock protein in normal, premalignant, and malignant human uterine cervix. Clinical cancer research : an official journal of the American Association for Cancer Research *1*, 1217-1222.

Rallu, M., Loones, M., Lallemand, Y., Morimoto, R., Morange, M., and Mezger, V. (1997). Function and regulation of heat shock factor 2 during mouse embryogenesis. Proceedings of the National Academy of Sciences of the United States of America *94*, 2392-2397.

Rea, S.L., Wu, D., Cypser, J.R., Vaupel, J.W., and Johnson, T.E. (2005). A stress-sensitive reporter predicts longevity in isogenic populations of *Caenorhabditis elegans*. Nature genetics *37*, 894-898.

Reindle, A., Belichenko, I., Bylebyl, G.R., Chen, X.L., Gandhi, N., and Johnson, E.S. (2006). Multiple domains in Siz SUMO ligases contribute to substrate selectivity. Journal of cell science *119*, 4749-4757.

Ren, J., Gao, X., Jin, C., Zhu, M., Wang, X., Shaw, A., Wen, L., Yao, X., and Xue, Y. (2009). Systematic study of protein sumoylation: Development of a site-specific predictor of SUMOsp 2.0. Proteomics *9*, 3409-3412.

Renz, A., and Fackelmayer, F.O. (1996). Purification and molecular cloning of the scaffold attachment factor B (SAF-B), a novel human nuclear protein that specifically binds to S/MAR-DNA. Nucleic acids research *24*, 843-849.

Ritossa, F. (1962). A new puffing pattern induced by temperature shock and DNP in *Drosophila*. Experientia *18*, 571-557.

Ritossa, F. (1996). Discovery of the heat shock response. Cell stress & chaperones *1*, 97-98.

Ritossa, F.M. (1964). Behaviour of RNA and DNA synthesis at the puff level in salivary gland chromosomes of *Drosophila*. Experimental cell research *36*, 515-523.

Rizzi, N., Denegri, M., Chiodi, I., Corioni, M., Valgardsdottir, R., Cobianchi, F., Riva, S., and Biamonti, G. (2004). Transcriptional activation of a constitutive heterochromatic domain of the human genome in response to heat shock. Molecular biology of the cell *15*, 543-551.

Rodriguez, M.S., Dargemont, C., and Hay, R.T. (2001). SUMO-1 conjugation in vivo requires both a consensus modification motif and nuclear targeting. The Journal of biological chemistry *276*, 12654-12659.

Ross, S., Best, J.L., Zon, L.I., and Gill, G. (2002). SUMO-1 modification represses Sp3 transcriptional activation and modulates its subnuclear localization. Molecular cell *10*, 831-842.

Rossi, A., Elia, G., and Santoro, M.G. (1998). Activation of the heat shock factor 1 by serine protease inhibitors. An effect associated with nuclear factor-kappaB inhibition. The Journal of biological chemistry *273*, 16446-16452.

Rytinki, M.M., Lakso, M., Pehkonen, P., Aarnio, V., Reisner, K., Perakyla, M., Wong, G., and Palvimo, J.J. (2011). Overexpression of SUMO perturbs the growth and development of *Caenorhabditis elegans*. Cellular and molecular life sciences : CMLS *68*, 3219-3232.

Saitoh, H., and Hinchey, J. (2000). Functional heterogeneity of small ubiquitin-related protein modifiers SUMO-1 versus SUMO-2/3. The Journal of biological chemistry *275*, 6252-6258.

Sampson, D.A., Wang, M., and Matunis, M.J. (2001). The small ubiquitin-like modifier-1 (SUMO-1) consensus sequence mediates Ubc9 binding and is essential for SUMO-1 modification. The Journal of biological chemistry *276*, 21664-21669.

Sandqvist, A., Bjork, J.K., Akerfelt, M., Chitikova, Z., Grichine, A., Vourc'h, C., Jolly, C., Salminen, T.A., Nymalm, Y., and Sistonen, L. (2009). Heterotrimerization of heat-shock factors 1 and 2 provides a transcriptional switch in response to distinct stimuli. Molecular biology of the cell *20*, 1340-1347.

Santagata, S., Hu, R., Lin, N.U., Mendillo, M.L., Collins, L.C., Hankinson, S.E., Schnitt, S.J., Whitesell, L., Tamimi, R.M., Lindquist, S.*, et al.* (2011). High levels of nuclear heat-shock factor

1 (HSF1) are associated with poor prognosis in breast cancer. Proceedings of the National Academy of Sciences of the United States of America *108*, 18378-18383.

Sarge, K.D., Murphy, S.P., and Morimoto, R.I. (1993). Activation of heat shock gene transcription by heat shock factor 1 involves oligomerization, acquisition of DNA-binding activity, and nuclear localization and can occur in the absence of stress. Molecular and cellular biology *13*, 1392-1407.

Sarge, K.D., Park-Sarge, O.K., Kirby, J.D., Mayo, K.E., and Morimoto, R.I. (1994). Expression of heat shock factor 2 in mouse testis: potential role as a regulator of heat-shock protein gene expression during spermatogenesis. Biology of reproduction *50*, 1334-1343.

Sarge, K.D., Zimarino, V., Holm, K., Wu, C., and Morimoto, R.I. (1991). Cloning and characterization of two mouse heat shock factors with distinct inducible and constitutive DNA-binding ability. Genes & development *5*, 1902-1911.

Sato, A., Asano, T., Ito, K., and Asano, T. (2012). 17-Allylamino-17-demethoxygeldanamycin and ritonavir inhibit renal cancer growth by inhibiting the expression of heat shock factor-1. International journal of oncology *41*, 46-52.

Schedl, P., Artavanis-Tsakonas, S., Steward, R., Gehring, W.J., Mirault, M.E., Goldschmidt-Clermont, M., Moran, L., and Tissieres, A. (1978). Two hybrid plasmids with *D. melanogaster* DNA sequences complementary to mRNA coding for the major heat shock protein. Cell *14*, 921-929.

Schuetz, T.J., Gallo, G.J., Sheldon, L., Tempst, P., and Kingston, R.E. (1991). Isolation of a cDNA for HSF2: evidence for two heat shock factor genes in humans. Proceedings of the National Academy of Sciences of the United States of America *88*, 6911-6915.

Sentis, S., Le Romancer, M., Bianchin, C., Rostan, M.C., and Corbo, L. (2005). Sumoylation of the estrogen receptor alpha hinge region regulates its transcriptional activity. Molecular endocrinology (Baltimore, Md) *19*, 2671-2684.

Shalizi, A., Gaudilliere, B., Yuan, Z., Stegmuller, J., Shirogane, T., Ge, Q., Tan, Y., Schulman, B., Harper, J.W., and Bonni, A. (2006). A calcium-regulated MEF2 sumoylation switch controls postsynaptic differentiation. Science (New York, NY) *311*, 1012-1017.

Shamovsky, I., Ivannikov, M., Kandel, E.S., Gershon, D., and Nudler, E. (2006). RNA-mediated response to heat shock in mammalian cells. Nature *440*, 556-560.

Shamovsky, I., and Nudler, E. (2008). New insights into the mechanism of heat shock response activation. Cellular and molecular life sciences : CMLS *65*, 855-861.

Shi, Y., Mosser, D.D., and Morimoto, R.I. (1998). Molecular chaperones as HSF1-specific transcriptional repressors. Genes & development *12*, 654-666.

Shinka, T., Sato, Y., Chen, G., Naroda, T., Kinoshita, K., Unemi, Y., Tsuji, K., Toida, K., Iwamoto, T., and Nakahori, Y. (2004). Molecular characterization of heat shock-like factor

encoded on the human Y chromosome, and implications for male infertility. Biology of reproduction *71*, 297-306.

Shuey, D.J., and Parker, C.S. (1986). Binding of *Drosophila* heat-shock gene transcription factor to the hsp 70 promoter. Evidence for symmetric and dynamic interactions. The Journal of biological chemistry *261*, 7934-7940.

Singh, I.S., Viscardi, R.M., Kalvakolanu, I., Calderwood, S., and Hasday, J.D. (2000). Inhibition of tumor necrosis factor-alpha transcription in macrophages exposed to febrile range temperature. A possible role for heat shock factor-1 as a negative transcriptional regulator. The Journal of biological chemistry *275*, 9841-9848.

Singh, V., and Aballay, A. (2006a). Heat-shock transcription factor (HSF)-1 pathway required for *Caenorhabditis elegans* immunity. Proceedings of the National Academy of Sciences of the United States of America *103*, 13092-13097.

Singh, V., and Aballay, A. (2006b). Heat shock and genetic activation of HSF-1 enhance immunity to bacteria. Cell cycle (Georgetown, Tex) *5*, 2443-2446.

Sistonen, L., Sarge, K.D., and Morimoto, R.I. (1994). Human heat shock factors 1 and 2 are differentially activated and can synergistically induce hsp70 gene transcription. Molecular and cellular biology *14*, 2087-2099.

Sistonen, L., Sarge, K.D., Phillips, B., Abravaya, K., and Morimoto, R.I. (1992). Activation of heat shock factor 2 during hemin-induced differentiation of human erythroleukemia cells. Molecular and cellular biology *12*, 4104-4111.

Smith, B.J., and Yaffe, M.P. (1991). A mutation in the yeast heat-shock factor gene causes temperature-sensitive defects in both mitochondrial protein import and the cell cycle. Molecular and cellular biology *11*, 2647-2655.

Smith, M.V., Boyd, W.A., Kissling, G.E., Rice, J.R., Snyder, D.W., Portier, C.J., and Freedman, J.H. (2009). A discrete time model for the analysis of medium-throughput *C. elegans* growth data. PloS one *4*, e7018.

Somasundaram, T., and Bhat, S.P. (2004). Developmentally dictated expression of heat shock factors: exclusive expression of HSF4 in the postnatal lens and its specific interaction with alphaB-crystallin heat shock promoter. The Journal of biological chemistry *279*, 44497-44503.

Soncin, F., Zhang, X., Chu, B., Wang, X., Asea, A., Ann Stevenson, M., Sacks, D.B., and Calderwood, S.K. (2003). Transcriptional activity and DNA binding of heat shock factor-1 involve phosphorylation on threonine 142 by CK2. Biochemical and biophysical research communications *303*, 700-706.

Sorger, P.K. (1990). Yeast heat shock factor contains separable transient and sustained response transcriptional activators. Cell *62*, 793-805.

Sorger, P.K., Lewis, M.J., and Pelham, H.R. (1987). Heat shock factor is regulated differently in yeast and HeLa cells. Nature *329*, 81-84.

Sorger, P.K., and Nelson, H.C. (1989). Trimerization of a yeast transcriptional activator via a coiled-coil motif. Cell *59*, 807-813.

Sorger, P.K., and Pelham, H.R. (1988). Yeast heat shock factor is an essential DNA-binding protein that exhibits temperature-dependent phosphorylation. Cell *54*, 855-864.

Spradling, A., Pardue, M.L., and Penman, S. (1977). Messenger RNA in heat-shocked *Drosophila* cells. Journal of molecular biology *109*, 559-587.

Sprando, R.L., Olejnik, N., Cinar, H.N., and Ferguson, M. (2009). A method to rank order water soluble compounds according to their toxicity using *Caenorhabditis elegans*, a Complex Object Parametric Analyzer and Sorter, and axenic liquid media. Food and chemical toxicology : an international journal published for the British Industrial Biological Research Association *47*, 722-728.

Stade, K., Vogel, F., Schwienhorst, I., Meusser, B., Volkwein, C., Nentwig, B., Dohmen, R.J., and Sommer, T. (2002). A lack of SUMO conjugation affects cNLS-dependent nuclear protein import in yeast. The Journal of biological chemistry *277*, 49554-49561.

Steinacher, R., and Schar, P. (2005). Functionality of human thymine DNA glycosylase requires SUMO-regulated changes in protein conformation. Current biology : CB *15*, 616-623.

Steinkraus, K.A., Smith, E.D., Davis, C., Carr, D., Pendergrass, W.R., Sutphin, G.L., Kennedy, B.K., and Kaeberlein, M. (2008). Dietary restriction suppresses proteotoxicity and enhances longevity by an hsf-1-dependent mechanism in *Caenorhabditis elegans*. Aging cell *7*, 394-404.

Subramanian, L., Benson, M.D., and Iniguez-Lluhi, J.A. (2003). A synergy control motif within the attenuator domain of CCAAT/enhancer-binding protein alpha inhibits transcriptional synergy through its PIASy-enhanced modification by SUMO-1 or SUMO-3. The Journal of biological chemistry *278*, 9134-9141.

Sulston, J.E., and Brenner, S. (1974). The DNA of *Caenorhabditis elegans*. Genetics *77*, 95-104.

Sulston, J.E., and Hodgkin, J. (1988). Methods. In *The Nematode Caenorhabditis elegans* (Cold Spring Harbor, NY: Cold Spring Harbor Laboratory Press).

Tagarro, I., Fernandez-Peralta, A.M., and Gonzalez-Aguilera, J.J. (1994). Chromosomal localization of human satellites 2 and 3 by a FISH method using oligonucleotides as probes. Human genetics *93*, 383-388.

Takemori, Y., Enoki, Y., Yamamoto, N., Fukai, Y., Adachi, K., and Sakurai, H. (2009). Mutational analysis of human heat-shock transcription factor 1 reveals a regulatory role for oligomerization in DNA-binding specificity. The Biochemical journal *424*, 253-261.

Talamillo, A., Sanchez, J., Cantera, R., Perez, C., Martin, D., Caminero, E., and Barrio, R. (2008). Smt3 is required for *Drosophila melanogaster* metamorphosis. Development (Cambridge, England) *135*, 1659-1668.

Tatar, M., Khazaeli, A.A., and Curtsinger, J.W. (1997). Chaperoning extended life. Nature *390*, 30.

Tatham, M.H., Jaffray, E., Vaughan, O.A., Desterro, J.M., Botting, C.H., Naismith, J.H., and Hay, R.T. (2001). Polymeric chains of SUMO-2 and SUMO-3 are conjugated to protein substrates by SAE1/SAE2 and Ubc9. The Journal of biological chemistry *276*, 35368-35374.

Teixeira-Castro, A., Ailion, M., Jalles, A., Brignull, H.R., Vilaca, J.L., Dias, N., Rodrigues, P., Oliveira, J.F., Neves-Carvalho, A., Morimoto, R.I., *et al.* (2011). Neuron-specific proteotoxicity of mutant ataxin-3 in *C. elegans*: rescue by the DAF-16 and HSF-1 pathways. Human molecular genetics *20*, 2996-3009.

Tessari, A., Salata, E., Ferlin, A., Bartoloni, L., Slongo, M.L., and Foresta, C. (2004). Characterization of *HSFY*, a novel *AZFb* gene on the Y chromosome with a possible role in human spermatogenesis. Molecular human reproduction *10*, 253-258.

Timmons, L., and Fire, A. (1998). Specific interference by ingested dsRNA. Nature *395*, 854.

Tissieres, A., Mitchell, H.K., and Tracy, U.M. (1974). Protein synthesis in salivary glands of *Drosophila melanogaster*: relation to chromosome puffs. Journal of molecular biology *84*, 389-398.

Udelsman, R., Blake, M.J., Stagg, C.A., Li, D.G., Putney, D.J., and Holbrook, N.J. (1993). Vascular heat shock protein expression in response to stress. Endocrine and autonomic regulation of this age-dependent response. The Journal of clinical investigation *91*, 465-473.

Ullrich, S.J., Robinson, E.A., Law, L.W., Willingham, M., and Appella, E. (1986). A mouse tumor-specific transplantation antigen is a heat shock-related protein. Proceedings of the National Academy of Sciences of the United States of America *83*, 3121-3125.

Voellmy, R. (2004). On mechanisms that control heat shock transcription factor activity in metazoan cells. Cell stress & chaperones *9*, 122-133.

Voellmy, R., and Boellmann, F. (2007). Chaperone regulation of the heat shock protein response. Advances in experimental medicine and biology *594*, 89-99.

Volovik, Y., Maman, M., Dubnikov, T., Bejerano-Sagie, M., Joyce, D., Kapernick, E.A., Cohen, E., and Dillin, A. (2012). Temporal requirements of heat shock factor-1 for longevity assurance. Aging cell *11*, 491-499.

Vuister, G.W., Kim, S.J., Orosz, A., Marquardt, J., Wu, C., and Bax, A. (1994). Solution structure of the DNA-binding domain of *Drosophila* heat shock transcription factor. Nature structural biology *1*, 605-614.

Vujanac, M., Fenaroli, A., and Zimarino, V. (2005). Constitutive nuclear import and stress-regulated nucleocytoplasmic shuttling of mammalian heat-shock factor 1. Traffic (Copenhagen, Denmark) *6*, 214-229.

Walker, G.A., and Lithgow, G.J. (2003). Lifespan extension in *C. elegans* by a molecular chaperone dependent upon insulin-like signals. Aging cell *2*, 131-139.

Walker, G.A., Thompson, F.J., Brawley, A., Scanlon, T., and Devaney, E. (2003). Heat shock factor functions at the convergence of the stress response and developmental pathways in *Caenorhabditis elegans*. FASEB journal : official publication of the Federation of American Societies for Experimental Biology *17*, 1960-1962.

Wang, X., Khaleque, M.A., Zhao, M.J., Zhong, R., Gaestel, M., and Calderwood, S.K. (2006). Phosphorylation of HSF1 by MAPK-activated protein kinase 2 on serine 121, inhibits transcriptional activity and promotes HSP90 binding. The Journal of biological chemistry *281*, 782-791.

Wang, Y., and Dasso, M. (2009). SUMOylation and deSUMOylation at a glance. Journal of cell science *122*, 4249-4252.

Weighardt, F., Cobianchi, F., Cartegni, L., Chiodi, I., Villa, A., Riva, S., and Biamonti, G. (1999). A novel hnRNP protein (HAP/SAF-B) enters a subset of hnRNP complexes and relocates in nuclear granules in response to heat shock. Journal of cell science *112 (Pt 10)*, 1465-1476.

Westerheide, S.D., Anckar, J., Stevens, S.M., Jr., Sistonen, L., and Morimoto, R.I. (2009). Stress-inducible regulation of heat shock factor 1 by the deacetylase SIRT1. Science (New York, NY) *323*, 1063-1066.

Westerheide, S.D., and Morimoto, R.I. (2005). Heat shock response modulators as therapeutic tools for diseases of protein conformation. The Journal of biological chemistry *280*, 33097-33100.

Westerheide, S.D., Raynes, R., Powell, C., Xue, B., and Uversky, V.N. (2012). HSF transcription factor family, heat shock response, and protein intrinsic disorder. Current protein & peptide science *13*, 86-103.

Westwood, J.T., Clos, J., and Wu, C. (1991). Stress-induced oligomerization and chromosomal relocalization of heat-shock factor. Nature *353*, 822-827.

Westwood, J.T., and Wu, C. (1993). Activation of *Drosophila* heat shock factor: conformational change associated with a monomer-to-trimer transition. Molecular and cellular biology *13*, 3481-3486.

Wisniewski, J., Orosz, A., Allada, R., and Wu, C. (1996). The C-terminal region of *Drosophila* heat shock factor (HSF) contains a constitutively functional transactivation domain. Nucleic acids research *24*, 367-374.

Wu, C. (1984a). Activating protein factor binds *in vitro* to upstream control sequences in heat shock gene chromatin. Nature *311*, 81-84.

Wu, C. (1984b). Two protein-binding sites in chromatin implicated in the activation of heat-shock genes. Nature *309*, 229-234.

Wu, C., Wilson, S., Walker, B., Dawid, I., Paisley, T., Zimarino, V., and Ueda, H. (1987). Purification and properties of *Drosophila* heat shock activator protein. Science (New York, NY) *238*, 1247-1253.

Xiao, H., and Lis, J.T. (1988). Germline transformation used to define key features of heat-shock response elements. Science (New York, NY) *239*, 1139-1142.

Xiao, H., Perisic, O., and Lis, J.T. (1991). Cooperative binding of *Drosophila* heat shock factor to arrays of a conserved 5 bp unit. Cell *64*, 585-593.

Xiao, X., Zuo, X., Davis, A.A., McMillan, D.R., Curry, B.B., Richardson, J.A., and Benjamin, I.J. (1999). HSF1 is required for extra-embryonic development, postnatal growth and protection during inflammatory responses in mice. The EMBO journal *18*, 5943-5952.

Yang, S.H., Jaffray, E., Hay, R.T., and Sharrocks, A.D. (2003). Dynamic interplay of the SUMO and ERK pathways in regulating Elk-1 transcriptional activity. Molecular cell *12*, 63-74.

Yao, J., Munson, K.M., Webb, W.W., and Lis, J.T. (2006). Dynamics of heat shock factor association with native gene loci in living cells. Nature *442*, 1050-1053.

Yokoyama, K., Fukumoto, K., Murakami, T., Harada, S., Hosono, R., Wadhwa, R., Mitsui, Y., and Ohkuma, S. (2002). Extended longevity of *Caenorhabditis elegans* by knocking in extra copies of hsp70F, a homolog of mot-2 (mortalin)/mthsp70/Grp75. FEBS letters *516*, 53-57.

Yost, H.J., and Lindquist, S. (1986). RNA splicing is interrupted by heat shock and is rescued by heat shock protein synthesis. Cell *45*, 185-193.

Yost, H.J., and Lindquist, S. (1991). Heat shock proteins affect RNA processing during the heat shock response of Saccharomyces cerevisiae. Molecular and cellular biology *11*, 1062-1068.

Yuan, C.X., Czarnecka-Verner, E., and Gurley, W.B. (1997). Expression of human heat shock transcription factors 1 and 2 in HeLa cells and yeast. Cell stress & chaperones *2*, 263-275.

Zandi, E., Tran, T.N., Chamberlain, W., and Parker, C.S. (1997). Nuclear entry, oligomerization, and DNA binding of the *Drosophila* heat shock transcription factor are regulated by a unique nuclear localization sequence. Genes & development *11*, 1299-1314.

Zhong, M., Orosz, A., and Wu, C. (1998). Direct sensing of heat and oxidation by *Drosophila* heat shock transcription factor. Molecular cell *2*, 101-108.

Zimarino, V., Wilson, S., and Wu, C. (1990). Antibody-mediated activation of *Drosophila* heat shock factor in vitro. Science (New York, NY) *249*, 546-549.

Zou, J., Guo, Y., Guettouche, T., Smith, D.F., and Voellmy, R. (1998). Repression of heat shock transcription factor HSF1 activation by HSP90 (HSP90 complex) that forms a stress-sensitive complex with HSF1. Cell *94*, 471-480.

Zuo, J., Baler, R., Dahl, G., and Voellmy, R. (1994). Activation of the DNA-binding ability of human heat shock transcription factor 1 may involve the transition from an intramolecular to an

intermolecular triple-stranded coiled-coil structure. Molecular and cellular biology *14*, 7557-7568.